UNCLASSIFIED CONTRACTOR

AFAPL-TR-71-20

BRUSHLESS DC STARTER GENERATOR

PREPARED BY

LEAR SIEGLER, INC.

POWER EQUIPMENT DIVISION

MAPLE HEIGHTS, OHIO

Cleveland

FINAL REPORT

AFAPL -TR- 71-20

January 1971

APPROVED FOR PUBLIC RELEASE, DISTRIBUTION UNLIMITED

United States Air Force

Air Force Aero Propulsion Laboratory

Wright-Patterson Air Force Base, Ohio

270

NOTICE

When Government drawings, specifications, or other data are used for any purpose other than in connection with a definitely related Government procurement operation, the United States Government thereby incurs no responsibility nor any obligation whatsoever; and the fact that the Government may have formulated, furnished, or in any way supplied the said drawings, specifications, or other data, is not to be regarded by implication or otherwise as in any manner licensing the holder or any other person or corporation, or conveying any rights or permission to manufacture, use or sell any patented invention that may in any way be related thereto.

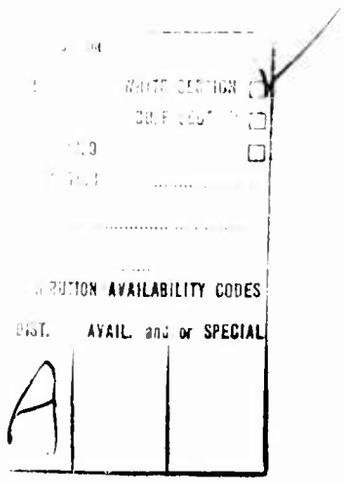

Unclassified

Security Classification

DOCUMENT CONTROL DATA - R & D

(Security classification of title, body of abstract and indexing annotation must be entered when the overall report is classified)

1 ORIGINATING ACTIVITY *(Corporate author)*

Lear Siegler, Inc.
Power Equipment Division
~~Maple Heights~~ Cleveland, Ohio 44137

2a. REPORT SECURITY CLASSIFICATION

Unclassified

2b. GROUP

3 REPORT TITLE

Brushless DC Starter Generator

4 DESCRIPTIVE NOTES *(Type of report and inclusive dates)*

Final June, 1966 through August, 1970

5 AUTHOR(S) *(First name, middle initial, last name)*

Vytautas F. Janonis

6 REPORT DATE	7a. TOTAL NO. OF PAGES	7b. NO. OF REFS
January, 1971	~~230~~ 252	5

8a. CONTRACT OR GRANT NO	9a. ORIGINATOR'S REPORT NUMBER(S)
AF33(615)3625	TR-132
b. PROJECT NO 812808	
c. BPSN 6(638128 62405214)	9b. OTHER REPORT NO(S) *(Any other numbers that may be assigned this report)* AFAPL-TR-71-20
d.	

10 DISTRIBUTION STATEMENT

Distribution of this Document is Unlimited

11 SUPPLEMENTARY NOTES	12 SPONSORING MILITARY ACTIVITY
None	Air Force Aero Propulsion Laboratory Wright-Patterson Air Force Base, Ohio

13 ABSTRACT

This report covers work performed on Contract #AF33(615)3625, Design and Development of a Brushless DC Starter Generator System and its testing. The unit was built and tested as a DC power generator and aircraft engine starter. In the generating mode the unit produced 200 amperes at 28-30 VDC within + 0.5V regulation. The AC ripple component was below specification requirements of 1.5V peak. The unit was tested over the full speed range of 7700-12,000 RPM utilizing blast air cooling per MIL-G-6162(2). In the engine starting mode the unit was tested only at half rated conditions and 22 lb. ft. starting torque at 385 amp input current. The required starting torque of 40 lb. ft. with 800 amp input was projected as possible with this machine design, but only with static commutator solid state switches which meet full current requirements. Since the specially developed static commutator hardware was capable of achieving only half its required current rating; the full contract objectives of the starting mode were not met. The recommendations in this report suggest the necessary improvements in the solid state commutator hardware in order to fulfill the starting mode requirements as stated by the objectives of this contract.

DD FORM 1 NOV 65 1473

Unclassified

Security Classification

UNCLASSIFIED CONTRACTOR
-TR-

BRUSHLESS DC STARTER GENERATOR

Prepared By

LEAR SIEGLER, INC.
Power Equipment Division
~~Maple Heights~~ Cleveland, Ohio

FINAL REPORT
AFAPL-TR-71-20

January 1971

United States Air Force
Air Force Aero Propulsion Laboratory
Wright-Patterson Air Force Base, Ohio

FOREWORD

This report covers research and development work conducted for the United States Air Force, Air Force Aero Propulsion Laboratory, Wright-Patterson Air Force Base, Ohio, by Lear Siegler, Inc., Power Equipment Division, Maple Heights, Ohio, in accordance with the requirements of Contract Number AF33(615)3625. Work was conducted under Air Force Project Number 812808, Budget Program Sequence Number 6(638128 62405214) and was monitored by Mr. P. R. Bertheaud, AFAPL/POP-1. The research period was June, 1966 through August, 1970.

This report contains no classified information extracted from other classified documents. The restriction legend appearing on the top of all pages within Appendix II of this report is not valid and is hereby rescinded.

Publication of this report does not constitute Air Force approval of the report's findings or conclusions. It is published only for the exchange and simulation of ideas.

Richard G. Leiby, Major, USAF
Chief, Propulsion and Power Branch
Air Force Aero Propulsion Laboratory

ABSTRACT

This report covers work performed on Contract #AF33(615)3625, Design and Development of a Brushless DC Starter-Generator System and its testing. The unit was built and tested as a DC power generator and aircraft engine starter. In the generating mode the unit produced 200 amperes at 28-30 VDC within ±0.5V regulation. The AC ripple component was below specification requirements of 1.5V peak. The unit was tested over the full speed range of 7700-12,000 RPM utilizing blast air cooling per MIL-G-6162(2). In the engine starting mode the unit was tested only at half rated conditions and 22 lb.ft. starting torque at 385 amp input current. The required starting torque of 40 lb.ft. with 800 amp input was projected as possible with this machine design, but only with static commutator solid state switches which meet full current requirements. Since the specially developed static commutator hardware was capable of achieving only half its required current rating; the full contract objectives of the starting mode were not met. The recommendations in this report suggest the necessary improvements in the solid state commutator hardware in order to fulfill the starting mode requirements as stated by the objectives of this contract.

TABLE OF CONTENTS

TABLE OF CONTENTS (contd)

TABLE OF CONTENTS (contd)

LIST OF ILLUSTRATIONS

LIST OF ILLUSTRATIONS (contd)

LIST OF ILLUSTRATIONS (contd)

TABLES

SECTION I

1.0 OBJECTIVE

The program objectives and brushless DC starter-generator requirements are stated in Exhibit A as a part of the overall U. S. Air Force Contract No. 33(615)-3625. For the sake of clarity and ease of reference, the requirements of Exhibit "A" are presented below.

EXHIBIT "A"
Statement of Work
Brushless DC Starter-Generator

I. Objective: The objective of this program is to increase the reliability and life of DC starter-generators by designing brushless machines in lieu of the brush type machines.

II. Scope: The Contractor will design, fabricate and evaluate a brushless starter-generator (SG) to the following design objectives:

A. The SG shall be designed for minimum dimensions and weight. However, it shall not exceed the over-all dimensions of 11"x5-1/2"x5-1/2" and a weight of 30 lbs.

B. The SG shall operate over the speed range of 7700 to 12000 RPM and mount on a Type XIID drive conforming to standard AND 20002.

C. The generator portion of the starter-generator shall use as a guide the applicable sections of MIL-G-6162 and be capable of delivering full rated load at rated voltage continuously. The generator shall be designed to meet the following parameters:

1. Rating: 6 kw
2. Output Voltage: 30 volts DC
3. Output Current: 200 amperes

D. With an 800 ampere input, the motor portion of the starter-generator shall have a minimum cranking torque of 40 lb.ft. and be capable of an inertia load of 25 lb.ft.^{2} from 0 to 500 RPM within 10 seconds.

E. The starter-generator shall be capable of operating in the 25% overspeed condition for five minutes without damage.

F. The overhung moment of the starter-generator shall not be greater than 160 inch pounds.

G. The cooling requirement of the starter-generator shall be minimum. For altitude operation, blast cooling shall be provided in accordance with the requirements of MIL-G-6162.

III. Environment: The starter-generator shall be capable of operation under all the following environmental conditions:

A.	Ambient Temperature:	-65° to 125°
B.	Altitude:	0 to 50,000 ft.
C.	Humidity:	0 to 100%
D.	Vibration:	20g - 80 to 2,000 cps
E.	Shock:	50g
F.	Acceleration:	10g

The operation of the starter-generator shall not be impaired by salt spray, fungus, sand or dust. These requirements are in accordance with applicable sections of MIL-G-6162.

IV. Evaluation: The Contractor shall demonstrate the ability of the starter-generator to operate under all environmental conditions. The starter-generator shall maintain its mechanical and electrical integrity and deliver rated load after each environmental test. The Contractor shall demonstrate the endurance of the starter-generator by operating the starter-generator as follows:

	Ambient Temp.	Altitude	Load	Time
A.	-65°F	SL	50 lb.ft.^{2}	Start and stop starter-Generator three times (2 min.wait between starts)
B.	-65°F	SL	100 amperes	1 hour
C.	-65°F	50,000 ft.	200 amperes	20 hours
D.	Repeat Tests A, B and C for 10 cycles			
E.	125°F	SL	50 lb.ft.^{2}	Start and stop starter-generator three times (2 min.wait between starts)
F.	125°F	SL	200 amperes	10 hours
G.	Repeat Tests E and F for 10 cycles.			

It was understood that the successful achievement of the required objectives set by this contract will require technical advancements in the field of semiconductor technology and packaging techniques. Funding was allocated to provide this program with solid state commutator components. With this in mind the program was organized to meet the objectives and technical requirements as stated in Exhibit "A".

Although the requirements of Exhibit "A" resemble those of the conventional starter-generator system, the start torque requirement is greater than that for a conventional unit of the same size and weight.

SECTION II

2.0 INTRODUCTION

2.1 DEFINITION OF BSG SYSTEM

The technical requirements of the brushless starter-generator system are quite similar to those existing and used for conventional DC systems. They are, however, more demanding in performance when compared with the allowable size and weight of the unit. The similarity to a conventional system in end operation allows easier understanding of this more complex hardware. In general, a starter generator system is an electrical installation of DC machine and associated system components so that dual modes of operation are achieved from one set of hardware. These two modes of operation are as follows:

a) The system performs as electrical to mechanical energy converter and provides mechanical energy necessary to start a given aircraft engine. This mode of operation will be referred to in this report as the starting mode.

b) The system performs as mechanical to electrical energy converter necessary to provide the electrical DC power on the aircraft. This mode of operation will be referred to in this report as the generating mode.

The typical conventional starter generator system is shown in block diagram Figure 2.1.A. It is immediately apparent that the most essential system component in Figure 2.1.A is the starter-generator. The conventional DC starter-generator is an electrical DC machine using a mechanical commutator for current commutation

between machine windings in a manner consistent with starting and generating modes as defined above.

The brushless starter-generator (B.S.G.) is an electrical machine where the mechanical commutator is replaced by solid state devices, thus eliminating the mechanical contacts carrying electrical currents. The unit also provides both the starting and generating modes of operation.

Since this contract is concerned mainly with brushless starter-generator hardware, a more detailed introductory concept of this hardware is presented below.

2.2 DESCRIPTION OF BSG SYSTEM COMPONENTS AND THEIR OPERATION

Figure 2.1.B shows a pictorial view of the brushless starter generator hardware using a Lundell type electromechanical converter. This type of electromechanical converter (electrical machine) consists of a solid rotor-rotational member and a wound multiphase stator-stationary member. The machine is excited through the stationary exciter coils mounted to the stator and concentric with the rotor assembly. The steady state continuous flux pattern must be established between the rotor and the stator. This is achieved by the DC excitation current in the stationary exciter coils. A static commutator assembly is attached to this electromechanical converter, as seen in Figure 2.1.B. This subassembly is shown in concentric ring construction. In this model, the necessary cooling is provided through finned heat sink shown in the static commutator assembly. This assembly is stationary and is mounted to the stator housing of the machine. The rotor

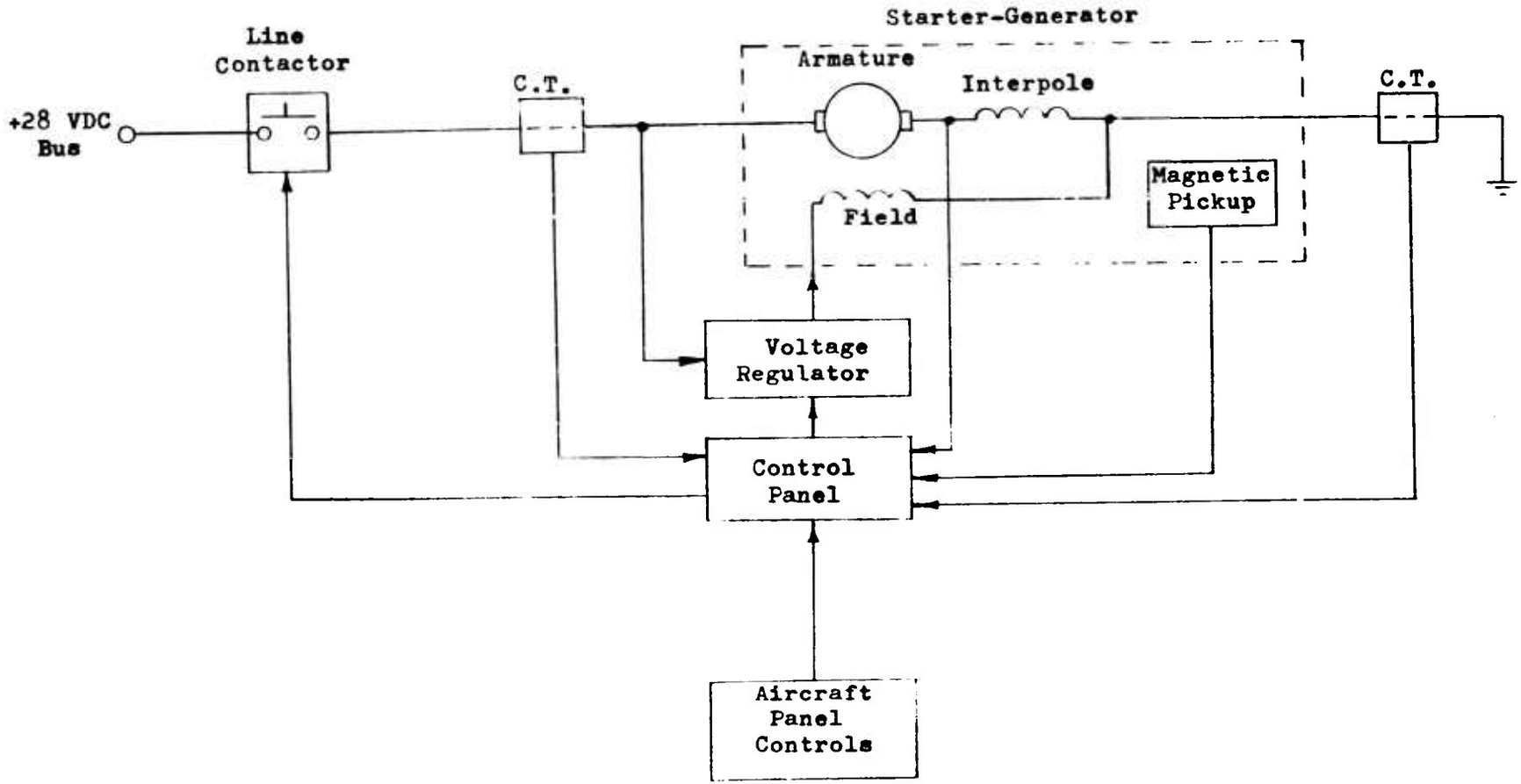

FIGURE 2.1A BLOCK DIAGRAM OF A CONVENTIONAL STARTER-GENERATOR SYSTEM

BRUSHLESS STARTER GENERATOR

using

LUNDELL TYPE ELECTROMECHANICAL CONVERTER

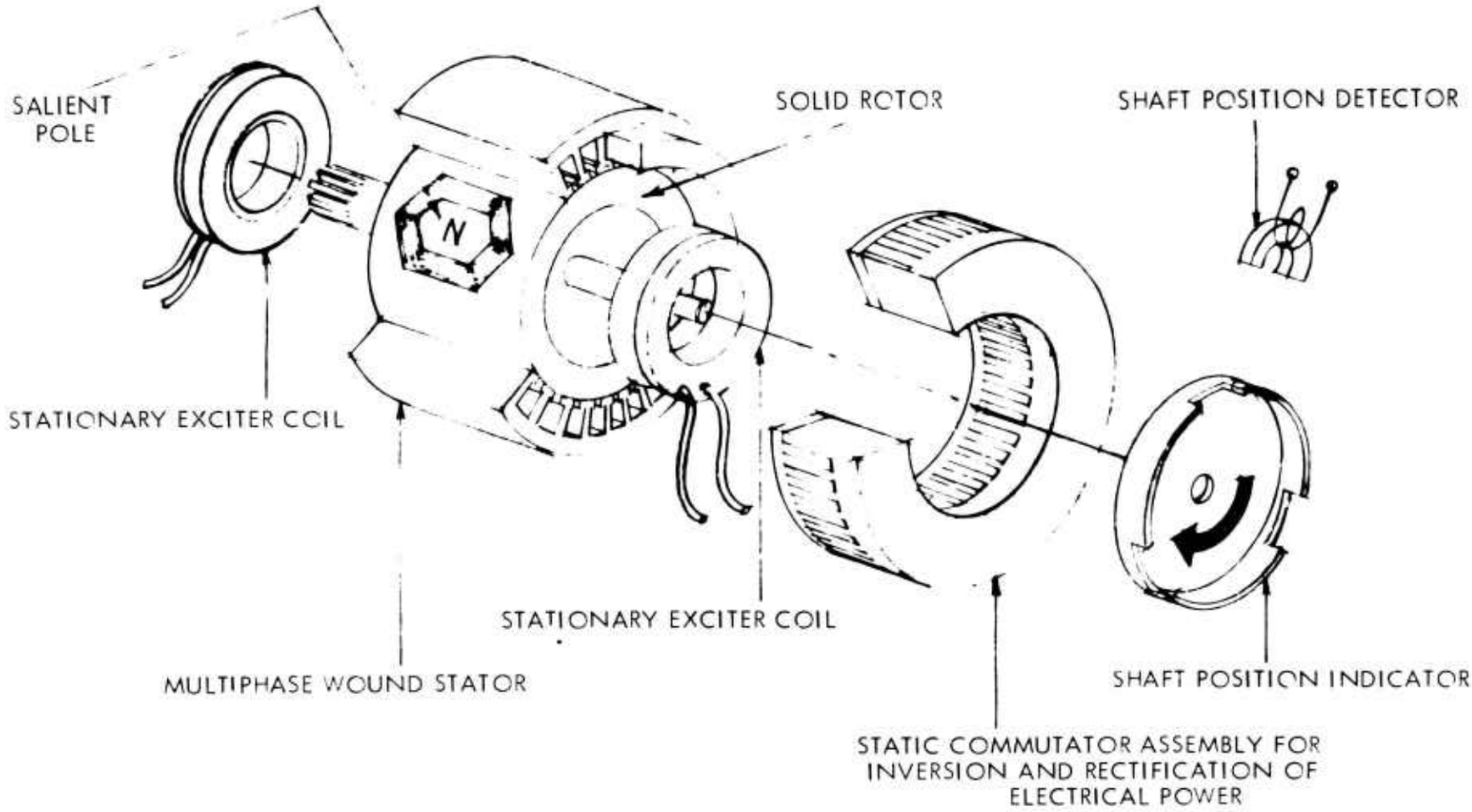

FIGURE 2.1B BRUSHLESS STARTER-GENERATOR USING A LUNDELL TYPE OF ELECTROMECHANICAL CONVERTER

assembly has the shaft position indicator mounted to the shaft. This device provides a means of determining relative position of the rotor to the stator. This position is necessary for timed, synchronous excitation of the stator winding by the solid state commutator. The shaft position sensing device is pictorially represented by the stationary electro-magnet. The variation of the effective permeability of the electro-magnet pickup produces variation in its excitation current. This variation is detected and the appropriate static commutator solid state switches are energized. This connects the machine windings to the DC electrical power source developing a torque couple. Once the torque is developed on the rotor, rotational movement of the rotor assembly is achieved. With it, the position indicating device is advanced. The rotation of position indicating device provides information necessary to energize other segments of the solid state commutator. The other segments of the solid state commutator energize other windings of the machine. This continuous advancement of the current conduction in various machine windings provides necessary torque to spin the rotor assembly and the attached load. In this B.S.G. application the attached load is a jet or turbine engine. The torque developed by the machine therefore would accelerate the engine from its standstill position to ignition speed and beyond.

During the initial rotor revolutions, the machine back EMF is practically zero; therefore, the DC power source would provide ohmic magnitude of the inrush current to the motor windings.

Since this inrush current must flow through the solid state commutator, it is apparent that commutator current handling capability must be matched accordingly. To restrict this excessive current flow through the static commutator, it is necessary to exercise some means of current limiting. The exact method of current limiting during the start-up mode of this brushless starter-generator was postponed until a better definition of solid state static commutator could be achieved.

Once the machine reaches a speed so that its back EMF controls the input current magnitude of the machine, the input current limiting is not needed. The final rotor speed at the given machine excitation is primarily controlled by the DC power source voltage magnitude. At this time the aircraft engine, previously ignited, has reached the self-sustained operation at its minimum speed. Beyond this point the brushless starter-generator is not required to operate in its starting mode. The machine now can be used as a DC power generator. DC power generation is achieved by rectifying the machine's output with solid state rectifiers. The output of the machine must be smooth, ripple-free DC of the required voltage magnitude and provided through the complete range of engine speeds as specified in Exhibit "A".

Through both modes of operation this machine field excitation is achieved by providing an appropriate amount of DC current in the machine's exciter coils. During the starting mode, the excitation is at the highest, therefore a maximum amount of DC current is required in the exciter coils. During the generating

mode, the excitation coils are energized by the current magnitude compatible with the output voltage regulation as established by the voltage regulator.

SECTION III

3.0 ELECTROMECHANICAL CONVERTER

3.1 DEFINITION OF ELECTROMECHANICAL CONVERTER

The electromechanical converter in the brushless starter-generator assembly provides the means of a bidirectional electromechanical energy conversion. For example, during the starting mode the electromechanical converter provides electrical to mechanical energy conversion. The mechanical output of the brushless starter-generator shaft is used to accelerate a jet or turbine engine. The opposite is true during the generating mode. The mechanical shaft power from the engine is used by the brushless starter-generator converter to produce DC electrical output. The electromechanical converter in this case is an incomplete electrical machine. The incompleteness of the electromechanical converter is evident since the converter can not be connected directly to the DC electrical power source. The missing subassembly to make the electromechanical converter operational is the commutator. In the brushless starter-generator the commutator is made up of solid state devices.

3.1.1 Review of Converter Types

In selecting an electromechanical converter it was important to realize that the solid state commutator is a stationary device and therefore it must be mounted to the frame of the over-all assembly. With this, the stator windings must also be stationary. This alone immediately restricts the choice of an electromechanical converter. For example, the DC machine uses a mechanical

commutator which is rotating on the shaft together with the armature. In the B.S.G. case the direct replacement of the commutator with the solid state commutator is not possible. It becomes evident that the electromechanical converter for this application must be of the type that has rotating pole pieces and stationary stator windings. A review of this type of electromechanical converter was performed at the beginning of this program. The important highlights are presented below.

3.1.1.1 Permanent Magnet Machines

One type of electromechanical converters fitting the inverted machine requirements is a permanent magnet machine. The rotor of this machine is made of a permanent magnet and stator is wound to suit the solid state commutator requirements. An investigation immediately revealed the deficiencies of this approach to the brushless starter-generator electromechanical converter.

a) The unit operates with low air gap flux densities; therefore, its weight and size is greater than that of other machines.

b) The unit requires special excitation controls in order to meet the required output voltage control while in the generating mode.

c) The permanent magnet integrity at high peripheral speeds is doubtful where the maximum machine diameter and length is as specified in Exhibit "A".

d) Demagnetizing effects by heavy stator currents are detrimental to the permanent magnet characteristics. Heavy currents in stator windings are needed during the starting mode of the brushless starter generator so that 40 lb.ft. starting torque is achieved from the small size machine.

Any one of the above mentioned deficiencies is severe enough to reject the permanent magnet machine from this application; therefore, this type of electromechanical converter was excluded from further design study.

3.1.1.2 Homopolar Machines

Since homopolar machines are true DC machines, it would appear they are most suitable for DC generators. It isn't so. First, they use slip rings, mercury wetted contacts or similar devices in providing output current flow. The output terminal voltage of these devices is very low and a direct application to this program is not suitable. Because of slip rings, any other combination of homopolar compound machines were excluded from this program.

3.1.1.3 Lundell Type Machines

Initially, the Lundell type machines appear to be suited to this application since they comply with inverted machine geometry previously designed. The geometry of the rotor shapes the pole piece design and the poles are excited from stationary, excitation coils mounted firmly to the stator housing of this machine. Figure 3.1.1.3A shows a typical outline of stationary coil Lundell

INSIDE-COIL, STATIONARY, TWO COIL
LUNDELL A. C. GENERATOR (BECKY-ROBINSON)

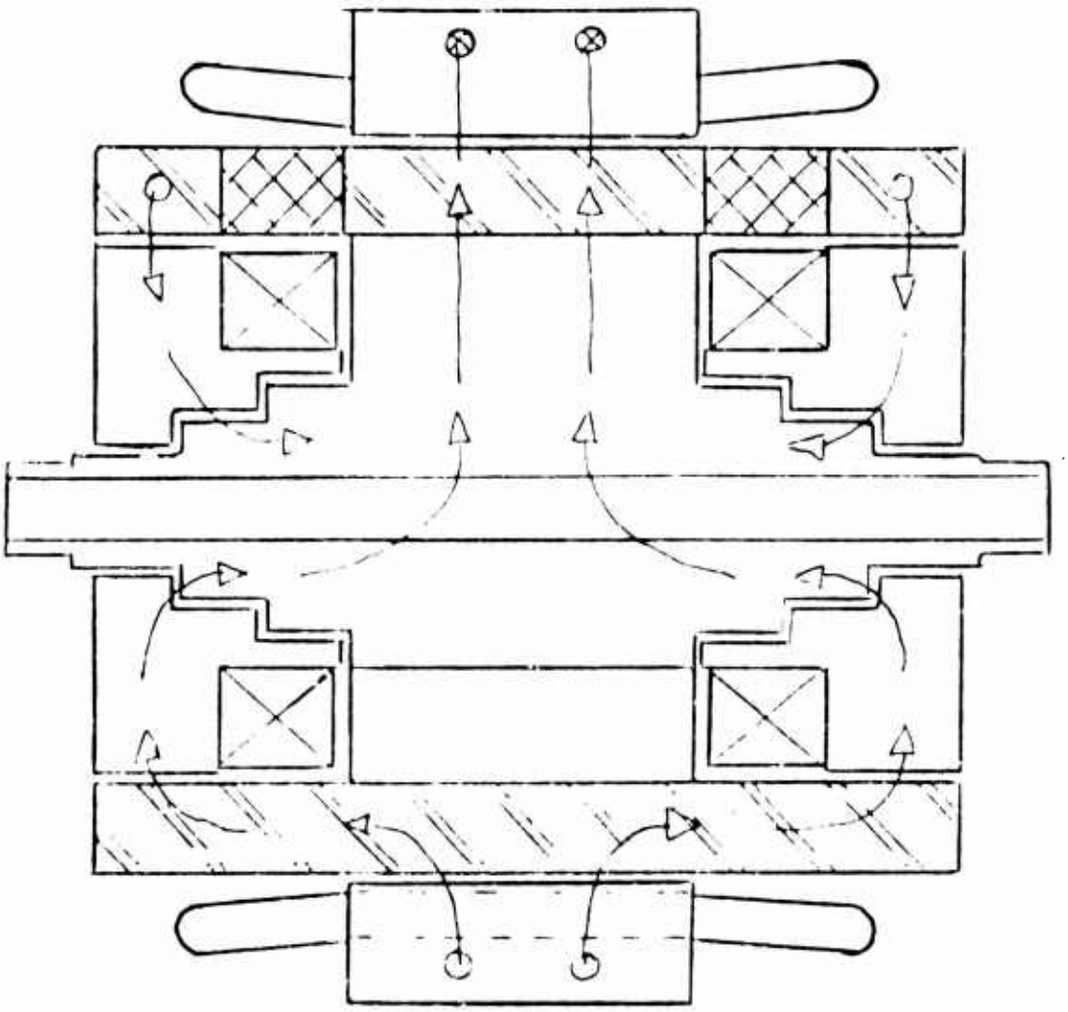

A brushless, stationary-coil Lundell-type generator that uses two exciting coils is described in U. S. Patent 2,796,542 issued to A. Becky.

Figure 3.1.1 3A

type machine. The arrows depict magnetic flux distribution in the machine. Since the flux pattern is provided by stationary coils energized with DC, the concept of somewhat more conventional voltage regulators to be used with this electromechanical converter appears quite suitable. The integrity of the rotor to operate at 15,000 RPM as required by the overspeed specification, is quite satisfactory since these types of machines are designed for operational speeds substantially beyond that requirement. Some variations of rotor and stator geometries fitting under the general description of Lundell type machines were also considered but were not suited for this application. For example, the rotational coil Lundell type machine would require its excitation through the slip rings. This is objectionable to the brushless concept of this program. The pancake type machine geometries were reviewed and rejected since their over-all diameter did not fit within the specification requirements. Since the most suited machine for this application was one shown in Figure 3.1.1.3A, an initial design study was conducted. The following input current conditions were considered -- 800, 600 and 400 amps. Also, the design was evaluated for the starting mode providing starting torque capabilities of 28 lb.ft. and 40 lb.ft. The weight and the size of the machine were carefully monitored. The magnetic materials for the stator utilized Hyperco 50 and the rotor was made out of H130 electrical steel. The ideal electromechanical weight of machine was used as criteria for comparison. The results of this study are plotted in Figure 3.1.1.3B. This weight does not include stationary excitation

Figure 3.1.1.3B

coils necessary to provide the flux and its distribution in the rotor. It was found during the study that 28 lb. ft. was the maximum possible torque from this machine without favoring the starting or generating mode. A higher torque than 28 lb. ft. starting capability would require a larger and heavier machine. The design conclusions were plotted in Figure 3.1.1.3B. It is noticeable that 28 lb.ft. torque capabilities of this machine during its initial starting would put the electro-mechanical weight of this machine just below 30 lbs. Since this weight is ideal electromechanical weight of the machine, the housing and end bells and additional commutator weight would make the brushless starter generator over-all weight beyond 30 lb. Since 30 lbs. is the specified maximum weight of this hardware, the Lundell type machine, as pictured in Figure 3.1.1.3A, producing the required torque of 40 lb.ft., is not suitable for this application. Figure 3.1.1.3B shows plot of electromechanical weight vs. input currents of this machine at 40 lb.ft. requirements. The curve exceeds 30 lb. weight limit. Beyond that the diameter of the brushless starter-generator would also be violated by the use of a secsyn type of electro-mechanical converter. These machines require certain length to diameter ratios in order to establish useful flux pattern in the rotor. The machine diameter was established to be between 6 and 6-1/2 inches which is in excess of specification require-ments. From the above data, the Lundell type of machine, al-though it is very attractive in its physical construction, was found to be unsuitable for a brushless starter-generator where

weight and starting torque requirements are of the values specified in Exhibit "A".

3.1.1.4 Wound Rotor Machine

A review was made on wound rotor type machines. These machines use windings on the rotor to establish magnetic pole pieces. It was previously established that the solid state commutator will energize stationary windings in the stator and the rotational member will provide the necessary pole pieces mounted on a machine shaft. This is the important criteria in selecting the machine's geometry. This criteria is met by wound rotor machines. Figure 3.1.1.4A shows the typical geometry involved in providing the over-all machine operation using a salient pole wound rotor design. The rotor excitation is achieved by the small exciter and the rotating rectifiers so that DC current is made available for the main rotor pole pieces. The stator is conventional and can be designed to suit a solid state commutator. The flux pattern of this machine is shown in Figure 3.1.1.4B for a 4 pole machine design. This type of machine geometry is quite suited to fulfill the requirements of the brushless starter generator in its generating mode. In the starting mode, two possibilities of machine utilization exist. One, the machine could be started as a synchronous induction motor by shorting the field windings and providing damper bars in the field pole periphery. The second mode of starting utilizes the field at its maximum capacity of excitation and provides necessary electronics for synchronous starting mode of this machine configuration. The design showed

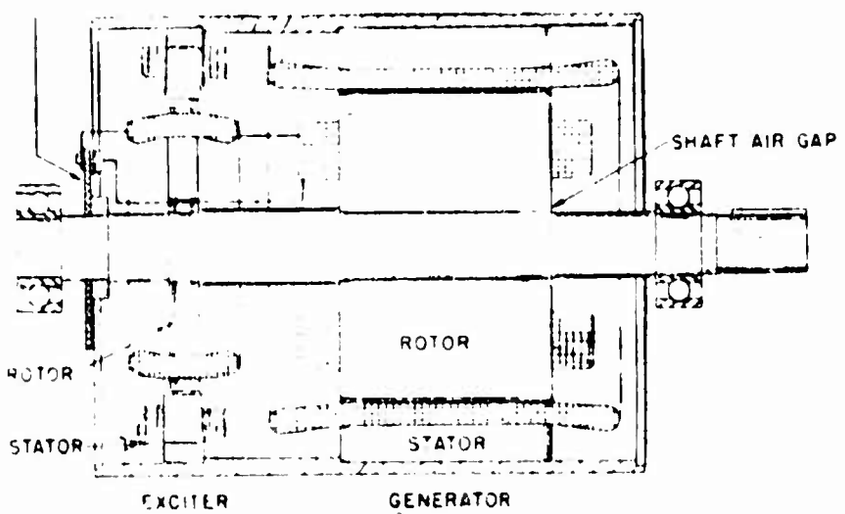

A-C Generator

SCHEMATIC SHOWING THE ARRANGEMENT USED TO MAKE THE WOUND-POLE GENERATORS BRUSHLESS. THE A-C CURRENT IN THE EXCITER ROTOR IS RECTIFIED BY THE ROTATING RECTIFIERS AND THE D-C OUTPUT OF THE RECTIFIERS IS FED INTO THE MAIN GENERATOR FIELD WINDINGS

Figure 3.1.1.4A

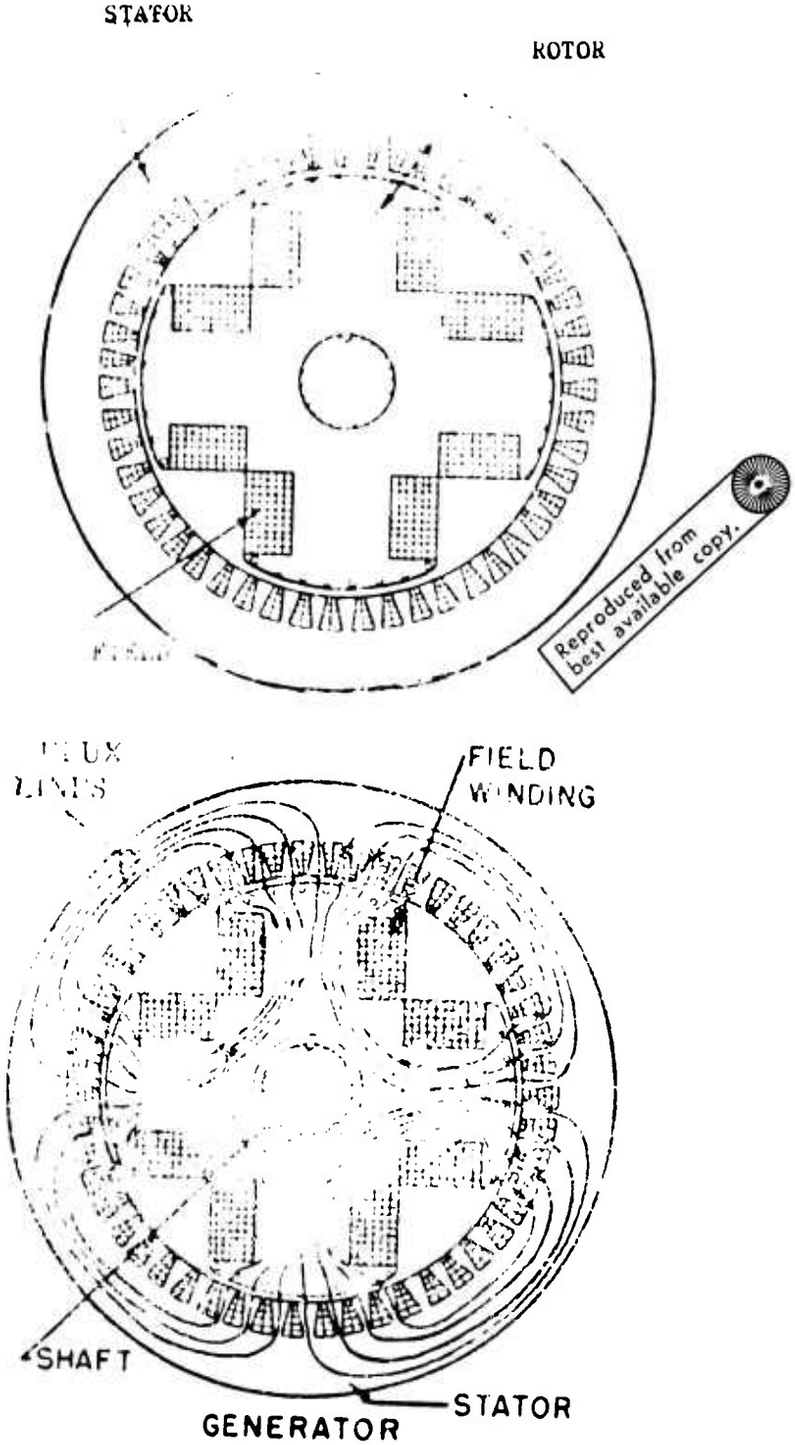

SECTION VIEWS OF A WOUND-POLE, SYNCHRONOUS GENERATOR SHOWING THE ARRANGEMENT OF THE WINDINGS AND THE PATH OF THE MAGNETIC FLUX

Figure 3.1.1.4B

this synchronous start produced more shaft torque than an induction start. This finding principally dictated the machine design to be a synchronous motor during the starting mode and a synchronous generator during the generating mode for this brushless starter-generator system. Several designs of this type of machine were carried out for comparison with solid rotor Lundell type machines. The ideal electromagnetic weight of this machine was plotted against input current. Again, 28 lb.ft. torque was indicated, depicting the machine weight ranging from 15 to 20 pounds. The torque over 28 lb.ft. was dictating the size of the machine, as shown by the second plot in the same Figure 3.1.1.4C. The materials used were Hyperco 50. The 40 lb.ft. starting torque requirements put the electromagnetic weight of the machine in the range of 20 to 27 lbs. with input current ranges of 400 to 800 amps.

3.1.2 Selection of Suitable Converter

The summary of the design, as plotted in Figure 3.1.1.3B gives us direct comparison between the two possible machines for this application. The first is the Lundell type solid rotor machine; the second is the wound pole rotor. Since the specification requirements can be met with the wound pole synchronous machine, it was selected as the final approach. It will operate during the starting mode as a synchronous converter producing 40 lb.ft. torque at 600 amp input into the stator windings. It was projected that the complete housed machine will weigh 25 lbs., leaving 5 lbs. for the solid state commutator. The machine length is projected to be approximately 9 inches.

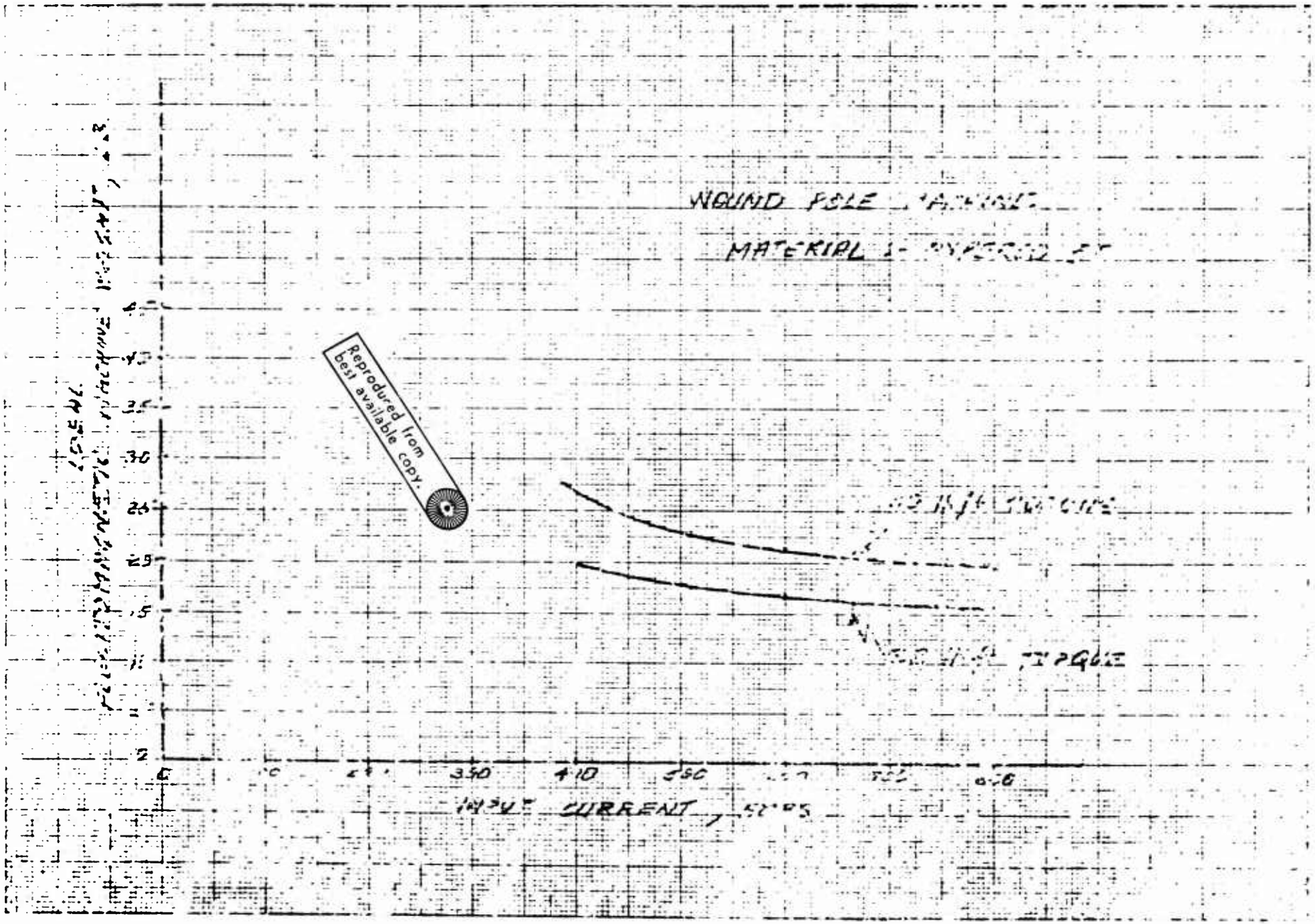

3.1.3 Converter Design

During the comparative design study of electromechanical converters, one of solid rotor Lundell type, the second a wound pole synchronous generator, the emphasis was placed on the magnitude of the commutating inductance as exhibited by both machines at their terminals. It was found that the wound rotor machine can achieve a commutating inductance figure equal to 15 to 20 microhenries per phase of the machine output terminals. Contrary to this, the solid rotor machine, Lundell type, always had several times higher commutating inductance at its terminals. The magnitude of commutating inductance was determined by calculating the subtransient reactance of the wound pole machine. To verify this value the tests were performed during the generating mode and the commutating inductance magnitude was established from oscilloscope data. (The agreement between two magnitudes was within 10%).

The knowledge specification of the direct axis sub-transient reactance or commutating reactance is very essential in predicting the quality of output power of this machine during its generating mode, especially AC ripple magnitude. The generating mode of this brushless starter-generator involves rectifiers. In performing the normal function of AC to DC power rectification they depend on the commutating reactance of a given AC source. During the commutation of current from one winding to the next, the two rectifiers temporarily short their respective windings of the machine. The duration of this

short circuit is dependent on the magnitude of the current and the subsequent commutating reactance value. Figure 3.1.3A clearly shows the commutating reactance effect on the output voltage VL. During the commucation period the output voltage VL follows the mean voltage of two instantaneous phase voltages. This mean voltage is lower than instantaneous value of voltage in the next phase E_b. This reduction in output voltage VL not only produces lower output value of VL, but also upsets the theoretical magnitude of the output ripple voltage. Since the output ripple magnitude is specified, the rectification during the current commutating interval must be contained so that the AC ripple magnitude can meet the specifications with minimum filtering. The magnitude of the commutating inductance was established during the design of this machine to be approximately 15 microhenries per phase. The simple three phase bridge type rectification of this electromechanical converter output produced DC output with AC ripple magnitude above specified acceptable limits of 1.5 volts peak. This rectification was felt deficient to do the job. It became apparent that, to reduce the output ripple magnitude, it was necessary to reduce the magnitude of the commutating current. This was accomplished by using two sets of 3 phase output windings designed in the machine positioned 30 electrical degrees apart. In conjunction with two sets of three phase, bridge type rectifier assemblies. These assemblies are connected to a common two terminal output through the interphase reactor. Since this type of geometry was required during the generating mode of the brushless starter-generator, it

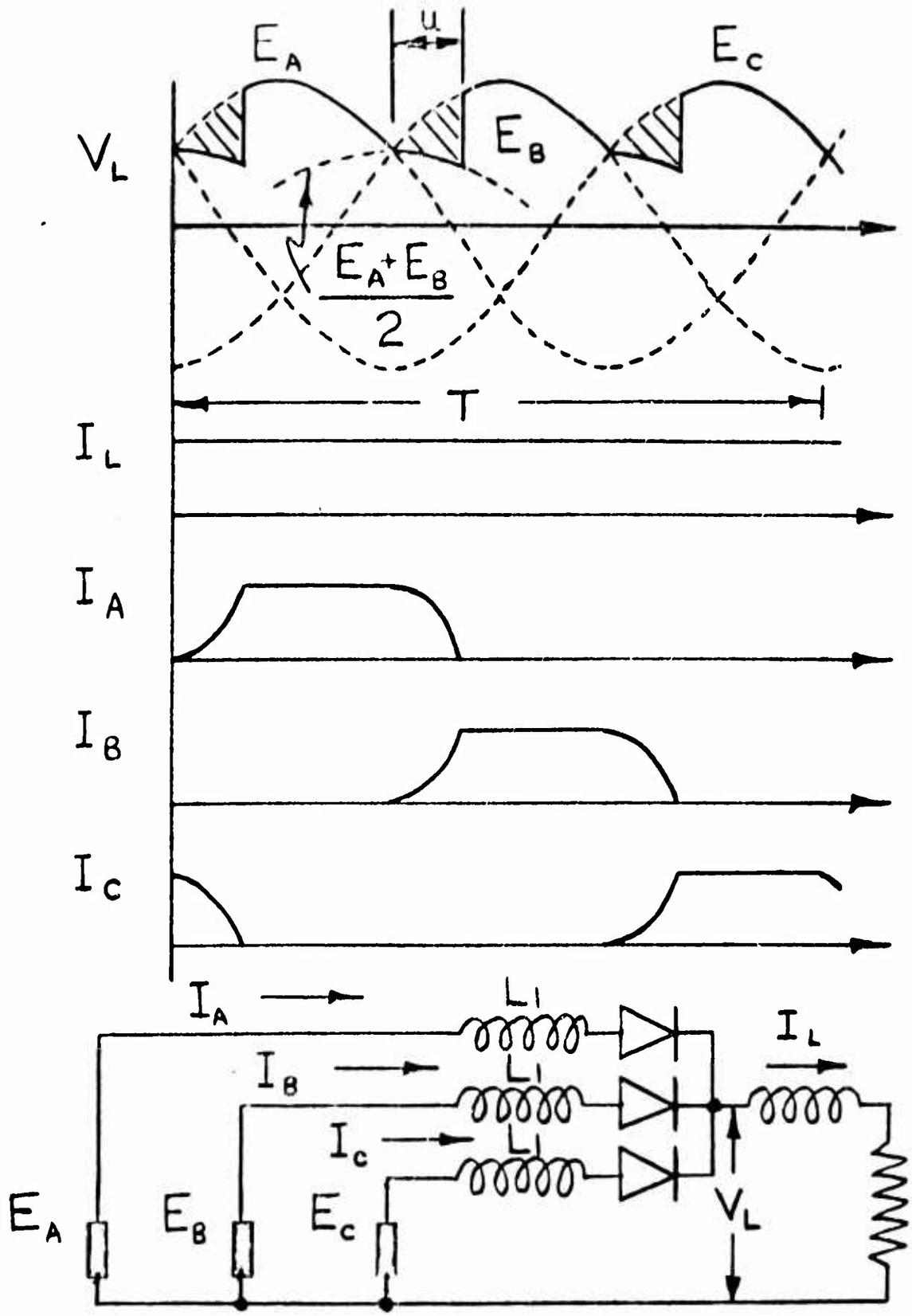

Figure 3.1.3A

was also found that the same geometry is complimentary during the starting mode of this machine. During the starting mode two sets of solid state commutator switches could be utilized to provide current flow into the stator windings simultaneously. Now, each winding in the stator will handle one half of the total input current which was limited to 800 amperes. At the same time, each solid state commutator switch will handle only one half amps of the required input current of 800 amps. This reduction in solid state commutator current handling capacity is also quite helpful in procuring the solid state switches for the commutator assembly.

3.1.3.1 Choice of Geometry

Once the machine commutating reactance and winding configuration has been established, the geometry of the machine was specified as follows. The machine will be no more than 9 inches in length, 5-1/2 inches by 5-1/2 inches square and will weigh, with the excitation device mounted inside, no more than 25 pounds. During the generating mode, the machine will be capable of delivering the required output of 30 volts and 200 amps at the minimum speed of 7,700 RPM. Since the machine design requiring 40 lb. ft. starting torque capability involved excessive electromagnetics, the output power of 30 volts and 200 amps was possible at a speed of 4,000 RPM. This over-design is unavoidable.

Although the electromechanical converter assumes round tube geometry, the square corners on the housing will be used for mounting the necessary power rectifiers used in the generating

mode of this machine. These rectifiers in the four corners shall leave enough clearance to allow the necessary air flow for cooling the entire machine in its generating mode. The air flow in the machine assembly will be as follows. First, the cooling air will come into the commutator end of the machine, will disperse to the four corners where the rectifiers are mounted. The air flow will be equally divided through the four openings and provide cooling to the rectifiers. After the necessary heat removal is achieved in the rectifier assemblies mounted in the corners, the four streams of cooling air will be diverted into the front of the machine where the heat removal will be provided for the inside of the machine. The cooling air will flow through the rotor subassembly and the machine air gap. The allowable pressure drop was calculated to be sufficient to do the necessary cooling in the steady state generating mode of the brushless starter-generator. The exhaust of the cooling air is provided through the four openings at the end of the machine. The typical view of the housing indicating provisions for the air flow is shown in Figure 3.1.3.1A. The front of the housing has the necessary provisions for mounting the unit on a type XIID drive, conforming to standard AND20002. The intake and exhaust openings in the housing are clearly seen with reference to the previous description. The cooling air pressure drop from the input into the machine assembly to the output was designed to meet the specification requirements of 6 inches of water. This makes the brushless starter-generator compatible with the cooling provisions of the conventional DC starter-generators.

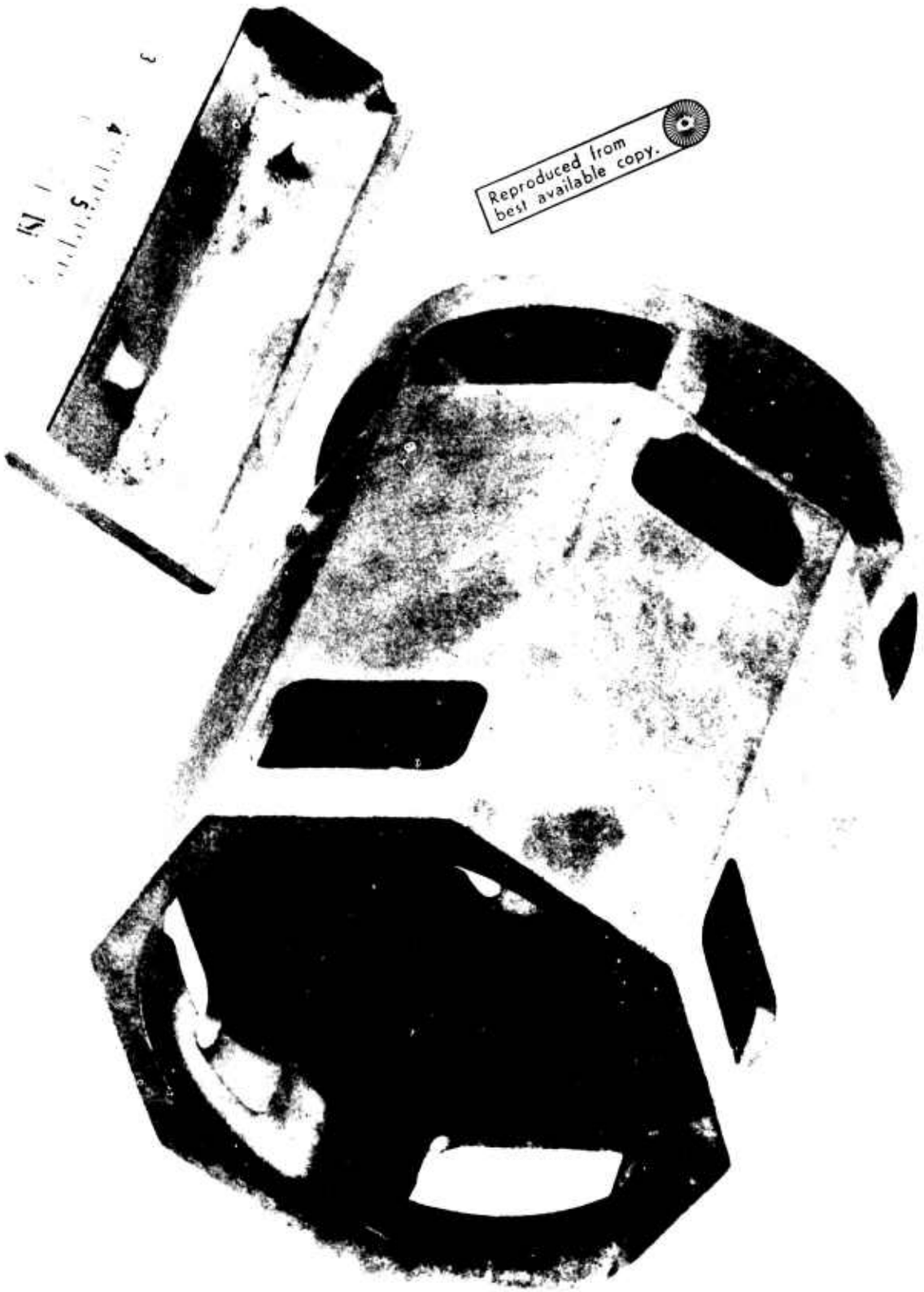

Figure 3.1.3.1-

3.1.3.2 Stator

Because of ripple requirements and the quality of the output DC power required during the generating mode of this brushless starter-generator system, the stator of the machine was wound with a multi-phase windin, arrangement. Actually, the arrangement consists of two, three phase wye connected windings electrically shifted by 30°. A typical winding diagram or layout is shown in Figure 3.1.3.2A. The stator has 42 slots with winding A placed at the bottom of a slot and winding B at the top. The stator lamination material is Hyperco 50. This choice was made to conserve the size and weight of the machine. Each coil has 2 turns of 4 #20 round wires in parallel. A high temperature insulation system was used throughout. The wire insulation was HML and the varnish was Doryl, using high temperature curing cycle.

3.1.3.3 Rotor

In order to insure the machine's commutating inductance at 15 microhenries per phase, the design of the machine had to be carefully conducted so that the required parameter would be attainable in the given geometry. To provide these characteristics a 6 pole rotor design was required. The typical display of rotor geometry with its pole pieces is shown in Figure 3.1.3.3A. The material of rotor laminations is Hyperco 50. Damper bars in the pole piece were used and are clearly visible in Figure 3.1.3.3A. The heavier damper bar construction can not be used in this geometry since integrity of the rotor at

STATOR WIRING DIAGRAM

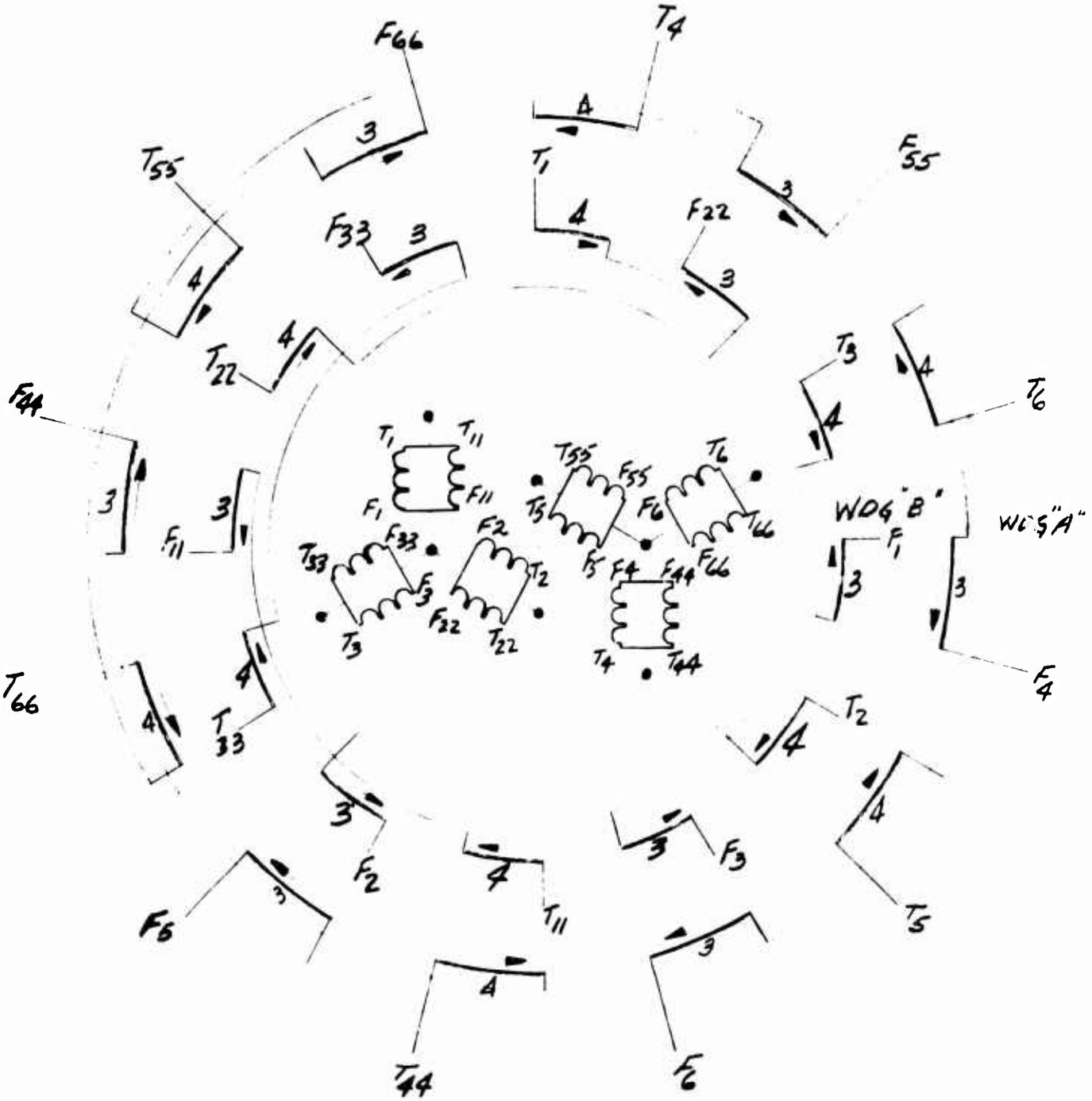

Figure 3.1.3.2a

15,000 RPM overspeed would be impaired. The winding design on the rotor pole pieces is compatible with the required air flow. The pole pieces were wound of edge type rectangular insulated wire to achieve the required excitation together with the proper flow of cooling air around each pole piece. It was predicted that adequate heat storage conditions would exist in the pole piece hardware during the operation of the machine as a starter. This is another factor indicating that the starting torque requirements dictate the size, the weight and the cooling procedure of this starter generator. In this design approximately 20:1 increase in pole piece excitation will be needed during the starting mode, in contrast with low level excitation requirements during the generating mode. The rotor diameter was set to be 3.875 inches. This provided the machine assembly with the air gap of .025 inches.

3.1.3.4 Shaft and Bearings

Because of additional subassemblies to be mounted on the rotor assembly, the shaft utilized in this electromechanical converter had to be designed adapting a quill shaft configuration. The shaft critical speed was recalculated and found to be well above the over-all requirements of this machine. The damper from the shaft assembly was removed. Shaft modifications had to be made in order that a shaft position indicating device, a set of rotary rectifiers and a subassembly of rotating transformer can be accomodated on the over-all rotor assembly. The shaft is shown on Drawing #23068-1100.

DWG NO 23068-1100

REVISIONS				
ZONE	LTR	DESCRIPTION	DATE	APPROVED

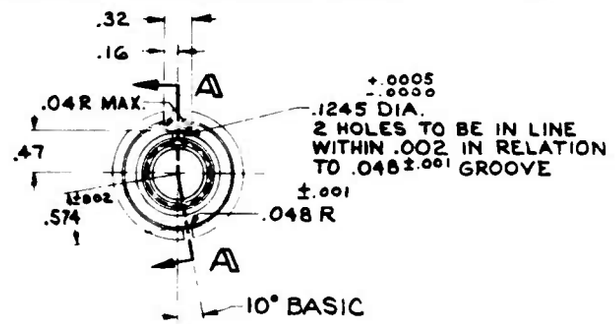

VIEW B-B

#8 BROWN & SHARPE TAPER APPROX. .50 IN. TAPER PER FT.
SURFACE ROUGHNESS 63

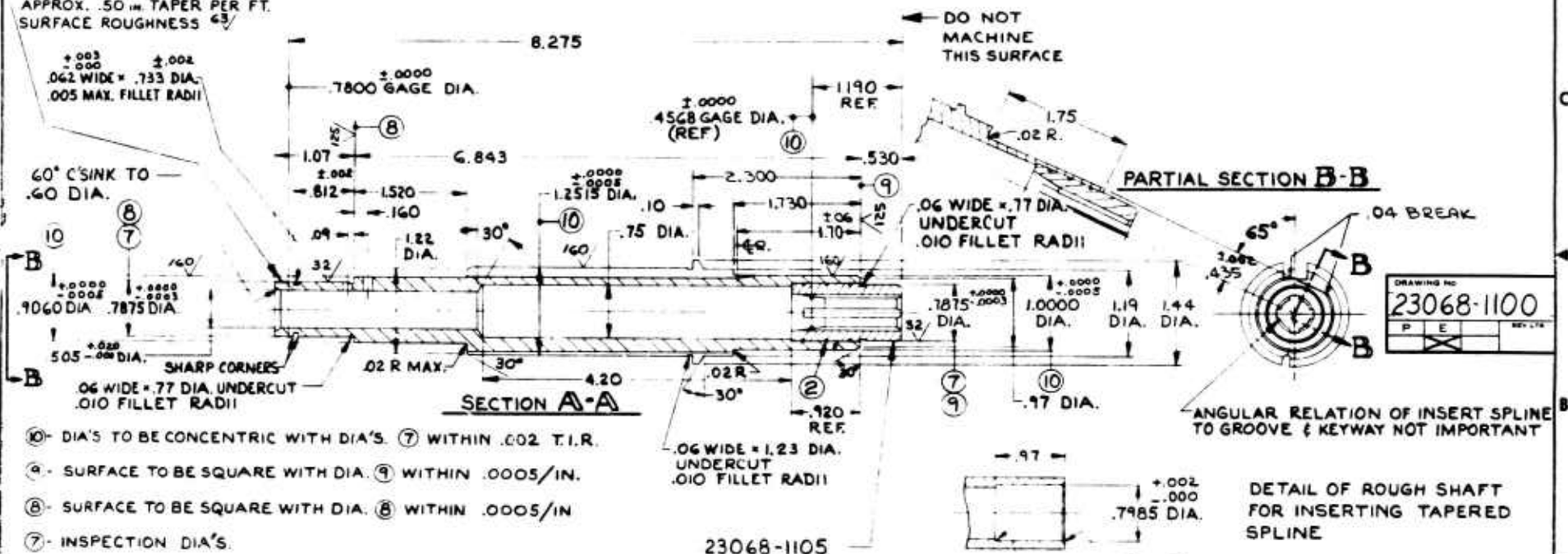

DRAWING NO 23068-1100 P E

⑩- DIA'S TO BE CONCENTRIC WITH DIA'S. ⑦ WITHIN .002 T.I.R.

⑨- SURFACE TO BE SQUARE WITH DIA. ⑨ WITHIN .0005/IN.

⑧- SURFACE TO BE SQUARE WITH DIA. ⑧ WITHIN .0005/IN

⑦- INSPECTION DIA'S.

6 - MAGNAFLUX PER MIL-I-6868

5 - BREAK EDGES .015 MAX.

4 - 250 FINISH ALL OVER EXCEPT AS NOTED

3 - HARDEN & TEMPER PER MIL-H-6875 (16-010005) HARDNESS RC 28-32

②- COPPER BRAZE PER MIL-B-7883 (PS 1700) USING FILLER METAL PER QQ-W-341 (05-566253)

1 - ~~PART MARK PER 16-045005~~

NOTES:

23068-310	23068-000
NEXT ASSY	USED ON
FIRST APPLICATION	

UNLESS OTHERWISE SPECIFIED, DIMENSIONS ARE IN INCHES. TOLERANCES ON: DECIMALS XX ± .01 XXX ± .005 ANGLES ± 0° 30'

DO NOT SCALE THIS DRAWING

MATERIAL
STEEL
QQ-S-624
COMP. 4130

DRAWN BY	C D HENDRICKSON	9-13-67
CHECKED BY	P URQUERT	10-29-67
MATL APPROVED	E Crawford	11-6-67
PROJECT ENGR	R Yeat	11-3-67
CONTRACT NO		

LEAR SIEGLER, INC / POWER EQUIPMENT DIVISION

SHAFT, ROTOR

SIZE	CODE IDENT NO	DRAWING NO
C	31435	23068-1100

SCALE 1:1 SHEET 1 OF 1

AF N A CUST. PTI ASSIGNED

40

3.1.4 CONVERTER FABRICATION

3.1.4.1 Stator Assembly

The stator was wound per previously described specification and is shown in Figure 3.1.4.1A. The unit assembled into the housing is shown in Figure 3.1.4.1B. This figure shows the stator mounted in the finished housing with a clear indication of air exhaust ports. Also, it is important to note that the windings, two sets of three phase wye connected, are brought out with leads and externally connected to make up two sets of three phase outputs as shown in Figure 3.1.3.2A. The stator end turns and lead connections are shown in their respective positions before the end bell of the machine is secured. Figure 3.1.4.1A not only shows the close-up of the stator winding assembly placed in the housing, but also displays two sets of shaft position pick-ups which are used in the over-all brushless starter-generator system to be explained later.

3.1.4.2 Rotor Assembly

As was explained previously, the rotor pole pieces were edge wound with rectangular magnet wire. The pictorial view of rotor wound pole piece assembly is shown in Figure 3.1.4.2A. Again 6 pole construction is clearly visible and the construction of the rotor to sustain overspeeds of 15,000 RPM are displayed. The ends of edge wound copper are supported by insert and ring assemblies as shown in Figure 3.1.4.2A. In this manner the rigidity of the rotor winding is maintained through the range of operating speed. The rotor insulation is HML coated with Doryl high temperature

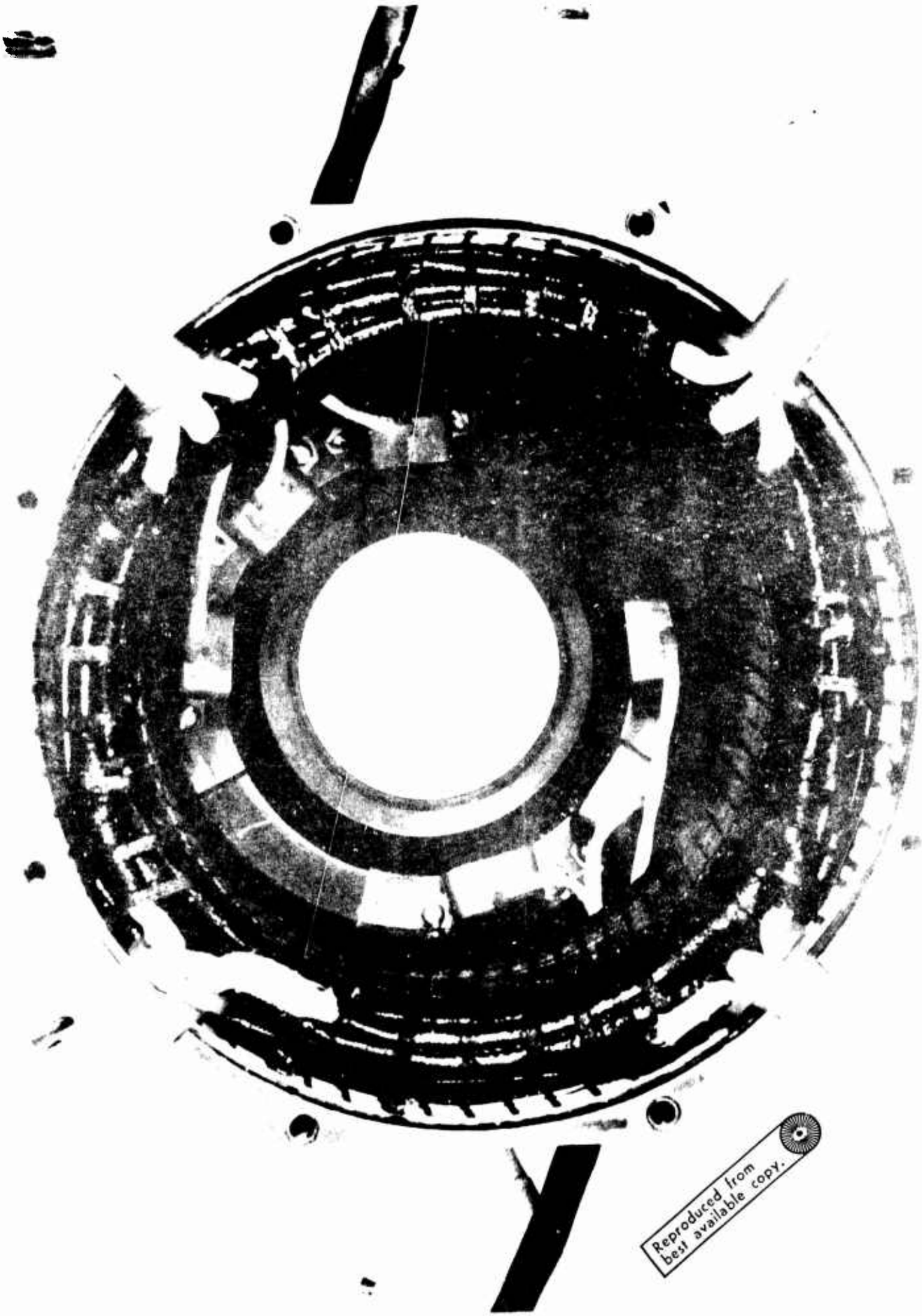

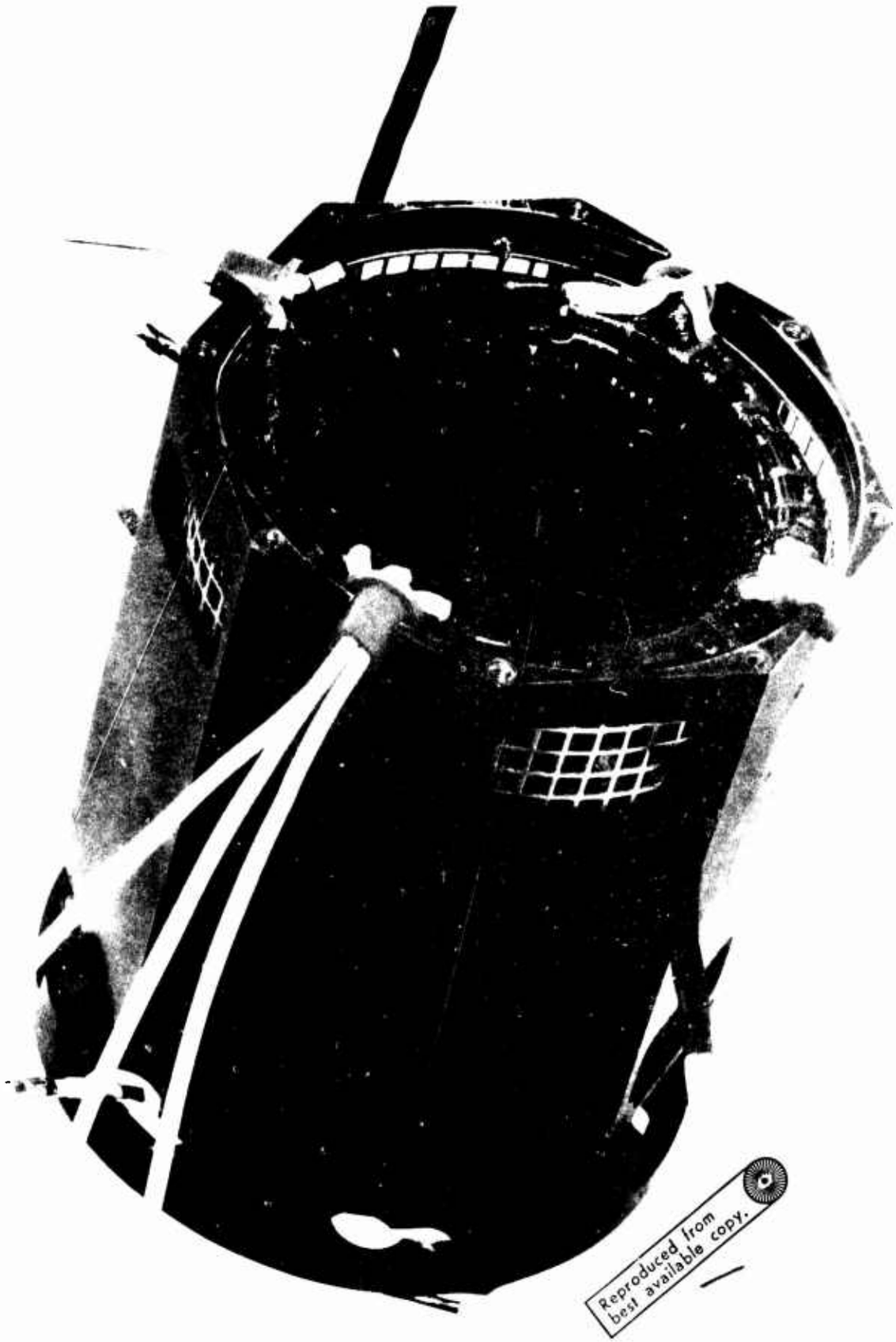

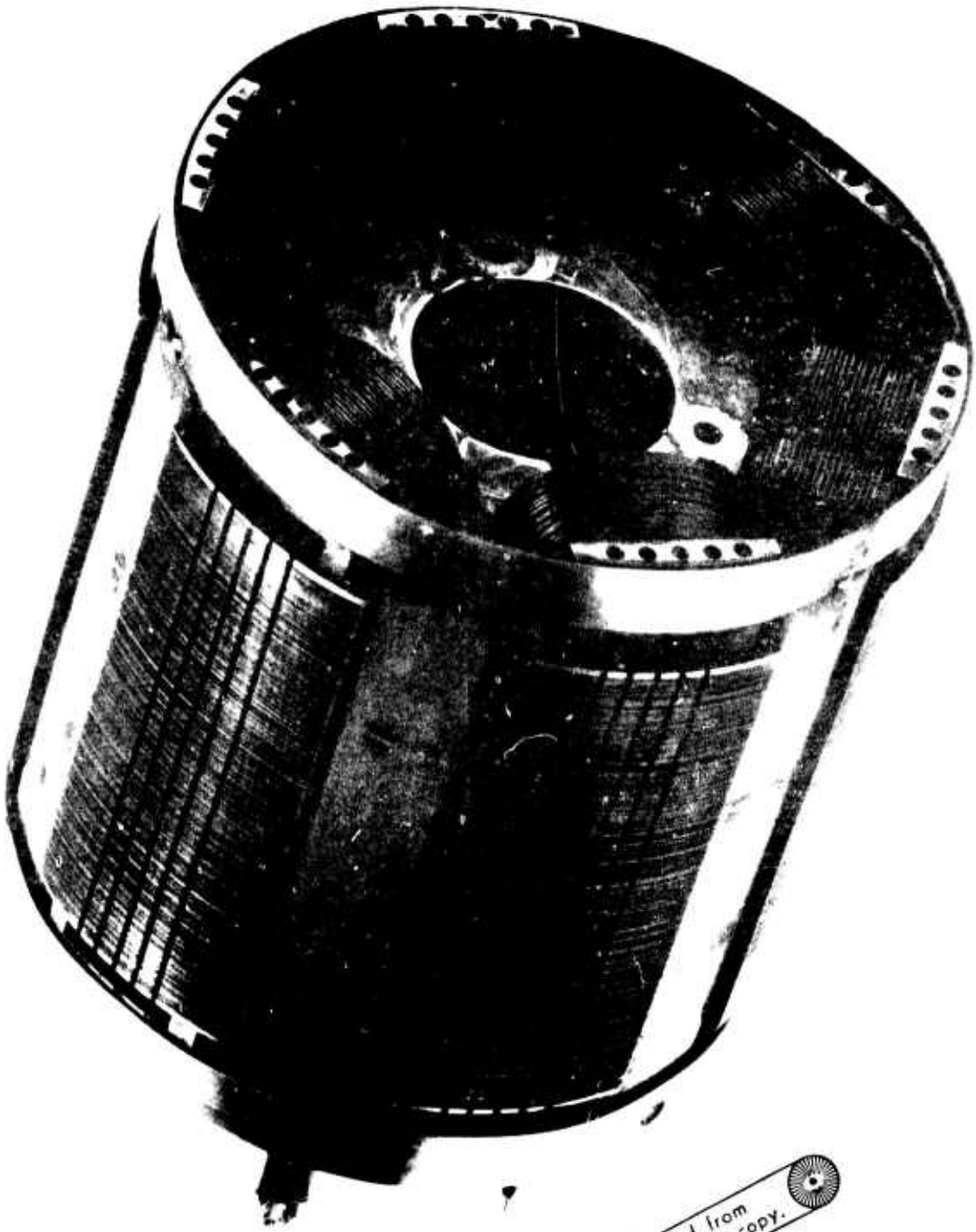

curing cycle varnish. The pole pieces were series interconnected for six pole design and the excitation leads are shown on the far side of the rotor assembly. The completed rotor assembly is shown in Figure 3.1.4.2 . As previously mentioned, in addition to the pole pieces of the machine, on the same shaft one can see the additional systems components mounted for operation of this electromechanical converter as a DC starter-generator. These additional components will be described later.

3.2 ADDITIONAL CONVERTER COMPONENTS

3.2.1 Shaft Position Sensor

Before the electromechanical converter can be used as a DC machine, the solid state commutator must be matched to the converter. Earlier, it was pointed out that the brushless starter-generator will operate as a DC electrical machine in the mode of synchronous starting and generating. The synchronous starting mode requires synchronous means to control solid state commutator switches. They, in turn, control currents in the stator windings which are always in a fixed position with respect to the rotor pole pieces. With this in mind, it is apparent that some means must be devised to detect the relative position of the stator windings with respect to the position of the pole pieces. In the conventional machine, this is automatically achieved by mounting the mechanical commutator rigidly to the armature assembly. In the brushless starter-generator arrangement this position detection is

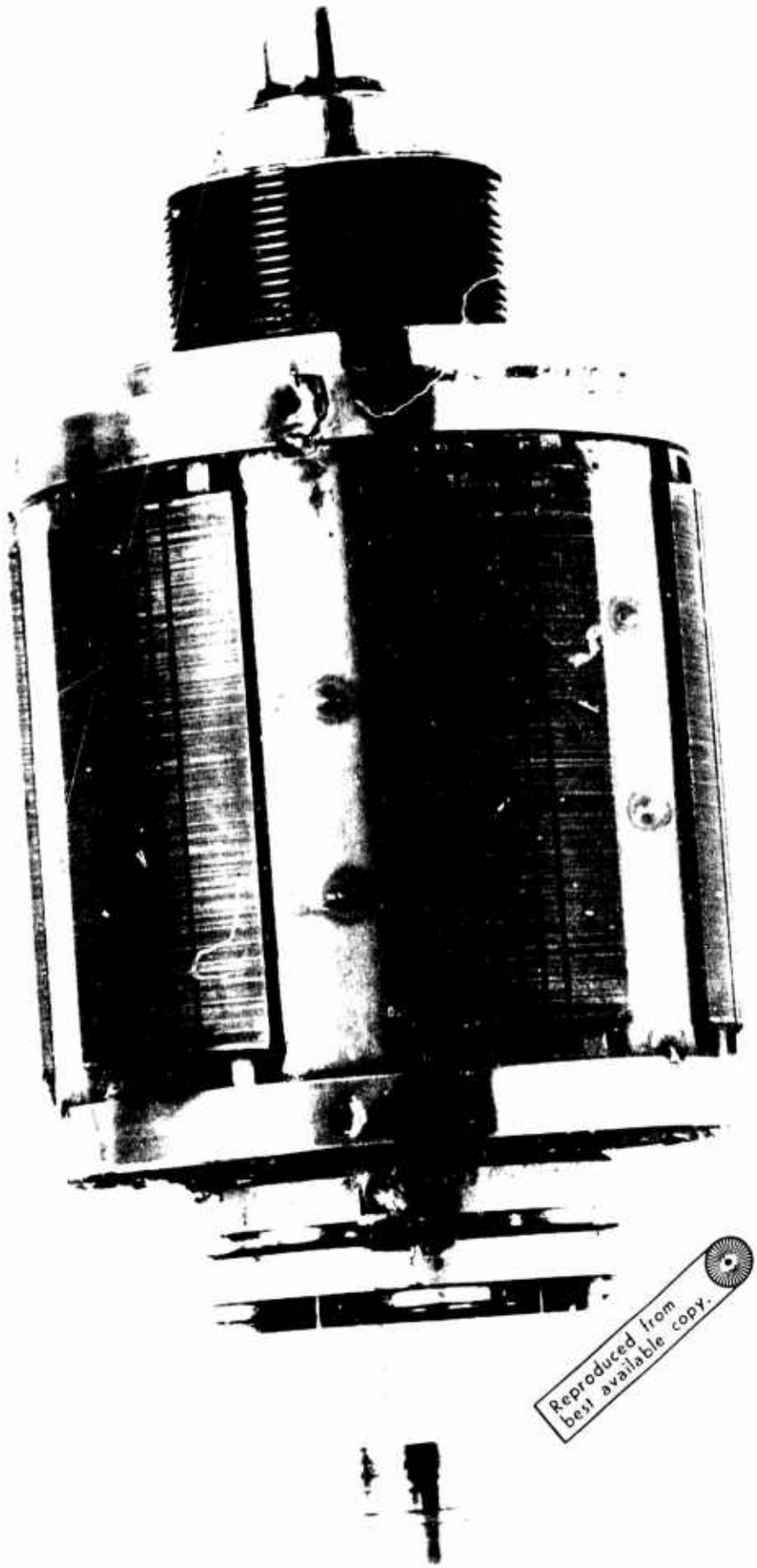

accomplished by sensing of the position on the rotor assembly. Since the pole pieces are mechanically secured to the shaft of the machine, sensing machine's shaft position is synonomous to the rotor pole piece position detection. A number of detection schemes were analyzed for this application. Some involved the use of Hall effect semiconductor devices; others used light or even atomic radiation. Because of the simplicity of the circuitry and inherent capability to work in the environment encountered in this machine, the electromagnetic pick-up scheme was selected as the most suited to do this job. The principles of operation of an electromagnetic shaft position indicator are quite simple. The electromagnetic pick-up changes its magnetic reluctance depending upon the magnetic and non-magnetic material moving in proximity to the pick-up. This fundamental principle is utilized in constructing the shaft position sensing device. A number of pick-ups are mounted rigidly to the housing/stator assembly. The metallic wheel with fixed position is secured to the shaft of the machine. Alternating strips of magnetic and non-magnetic material are provided on the wheel surface. The rotating wheel with its different materials will pass by the air gap of the magnetic pick-up and thus allow the pick-up to distinguish the presence of magnetic or non-magnetic material. In order for this detection scheme to be useful in this brushless starter-generator application, it was necessary to provide zero speed shaft position detection so that the machine could produce initial starting torque at any shaft position at standstill. This zero speed detection is accomplished by providing the pick-up with fixed, high frequency

(16 KHz) carrier signal. The variation of the carrier signal current magnitude is a variable parameter proportional to the magnetic material presence or absence by the air gap of the pick-up. Figure 3.2.1.A shows a simplified electrical diagram and the output waveform available from the pick-up. The variation of an output signal due to the different materials in the air gap is approximately 2:1 which is ample to detect and command the solid state commutator switch.

3.2.1.1 Design

During the starting mode, especially in the repeated starts of a jet or turbine engine, the machine internal temperatures were predicted to reach over 400°F. These temperatures required the shaft position sensing components be capable of operation at high temperature levels. The high temperature requirements dictated the choice and placement of other electronic components required to do the wave shaping of the shaft position sensing device. It was necessary to mount the shaft position indicator and pick-ups in the machine assembly and leave the electronics outside of the machine and mount them to the housing. Figure 3.2.1.1A shows the shaft position detectors and position indicating wheel as it is used in this brushless starter-generator assembly. The electromagnetic pick-ups use 2 mil Hypercil magnetic core material and are wound with LMH insulated wire. The wound pick-ups are impregnated with Doryl high temperature impregnant and potted with a high temperature potting compound in μ metal shielded cans. The shields

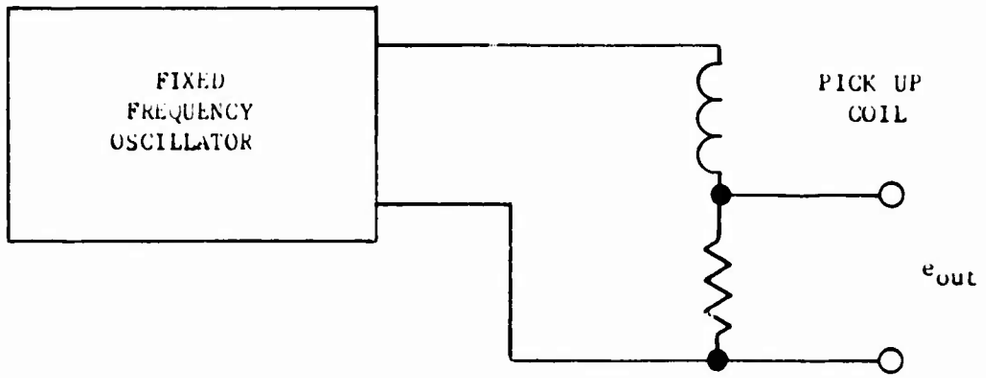

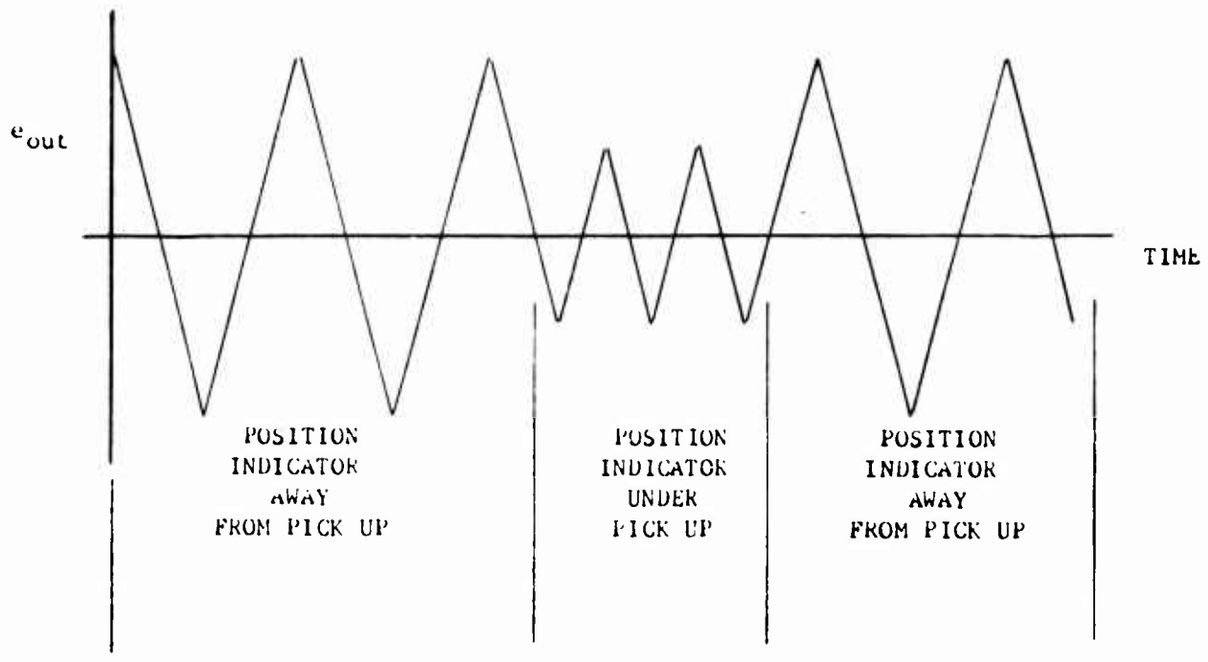

PICK UP OUTPUT WAVEFORM

Figure 3.2.1A

were necessary to eliminate possible electromagnetic interference between the rotating poll piece leakage flux and the information detected from the rotating wheel. The position indicating wheel is mechanically fixed to the shaft of the rotor. The electromagnetic pick-ups are mounted on the stator housing assembly of the machine and are made to be adjustable over approximately 20 mechanical degrees of the housing periphery. This physical adjustment is needed to insure the accuracy of detection of the pole piece relative position with respect to the stator winding placement in the actual hardware. A single wheel shaft position indicator is used together with six pick-ups. The quantity of the pick-ups came about primarily by the choice of stator windings to be used in this machine. As it was described previously, there are two, three-phase windings wound in the stator placed 30 electrical degrees from each other. Each phase of three phase windings will use one pick-up. The current flow in that phase winding will last for 120 electrical degrees in each half cycle of operation. Therefore, each three-phase winding will use three pick-ups. Since there are two sets of three phase windings, the six pick-up configuration was used. The shaft position indicating wheel was covered with μ Metal magnetic material for 60 mechanical degrees equally spaced in three areas of the wheel.

3.2.1.2 Fabrication

The shaft position indicating wheel was made of aluminum as shown in Figure 3.2.1.1A. The 60° required intervals were

covered with μ Metal. The pick-ups were Hypercil core material, 2 mils thick, with two coils of magnet wire and the whole sub-assembly was potted in the μ Metal can. Both of these devices are shown in Figure 3.2.1.1A. Figure 3.1.4.1A shows the actual mounting of the electromagnetic pick-ups in the stator housing assembly. The quantity of six pick-ups is evident. The electrical information is obtained through the shielded wires visible again in the machine assembly shown in Figure 3.1.4.1A . The placement of the position indicating wheel on the shaft is displayed in Figure 3.1.4.2B . The air gap between the wheel and the pick-ups is approximately .005". The mounting of the wheel and the pick-ups in the radial assembly is needed because the machine has considerable end play, which would increase the possibility of rubbing the wheel against the electromagnetic pick-ups. The radial accuracy of the machine air gap is good and established tolerances of an air gap will prevent a possibility of the wheel rubbing against the pick-up. The assembled hardware was tested for its performance. The modulation of peak excitation current between the presence and absence of magnetic material under the pick-up air gap was in agreement with the design providing approximately 2:1 amplitude modulation.

3.2.2 Rotary Transformer Rectifier Assembly

Since wound rotor machines require their pole piece field excitation on the rotor, the means of transmitting required excitation from the stationary point to the rotor were investigated next. Usually, the wound rotor machines are used with

rotary exciters. The rotary exciter is an auxiliary machine equipped with rotating rectifiers to provide DC current to the main machine pole pieces. The rotors of the machine and the exciter are mounted on a common shaft. The output power of the rotary exciter is controlled by the exciter stator. The stator is made of pole pieces which are acting as electromagnets controlling the exciter air gap flux. This compound machine assembly, in conjunction with the voltage regulator, provides the necessary controls of the main machine output. The above explained compound machine is satisfactory only for the generating mode of the brushless starter-generator hardware. During the starting mode where the machine's excitation must be at its maximum, the machine is at standstill and no rotary exciter output is possible. The rotor exciter is incapable of producing necessary excitation and the overall brushless starter-generator system would be useless as an engine starter. To remedy this situation during the starting mode of this brushless starter-generator machine, an AC excitation of the exciter stator poles must be incorporated so that the required main machine excitation power can be transmitted through the exciter air gap to the exciter rotor windings. In order to provide the exciter with necessary AC excitation, it is necessary to use a static inverter. The exciter field pole design must be altered and the inverter used in this system must be three-phase pulse width controlled device. This static inverter hardware would be used only during the starting mode of the brushless starter-generator system and will be left idle during the rest of the generating

mode. This approach was ruled out as cumbersome and introducing unnecessary weight to the over-all aircraft installation. Other means of wound pole machine excitation were investigated.

The most promising approach to the solution of this problem appeared in the use of a rotary transformer. The rotary transformer would be designed to provide necessary excitation during the start and the generating modes of the brushless starter-generator and it can be made to be a single phase device. Because of a single phase feature, the static inverter used to excite the rotary transformer can be designed as a single phase unit. This reduces starting mode circuit complexity. The rotary transformer secondary requires only single phase rectification in contrast to the rotary exciter where three-phase rectification normally would be used. Figure 3.2.2.A shows the magnetic flux path of a typical rotary transformer. The magnetic flux path, while encircling the primary and secondary windings in this transformer, also must cross two air gaps. These air gaps are kept at 0.005" each. Mechanically, the secondary windings on this transformer are free to rotate concentrically around the axis of a transformer which also is the axis of a mounting shaft of the machine assembly. The primary winding and its magnetic flux pattern is stationary and secured to the frame of the machine housing. To produce the required DC current for the main machine field excitation, the secondary winding of the rotary transformer is terminated in the single phase rectifier bridge arrangement. Single phase rectification

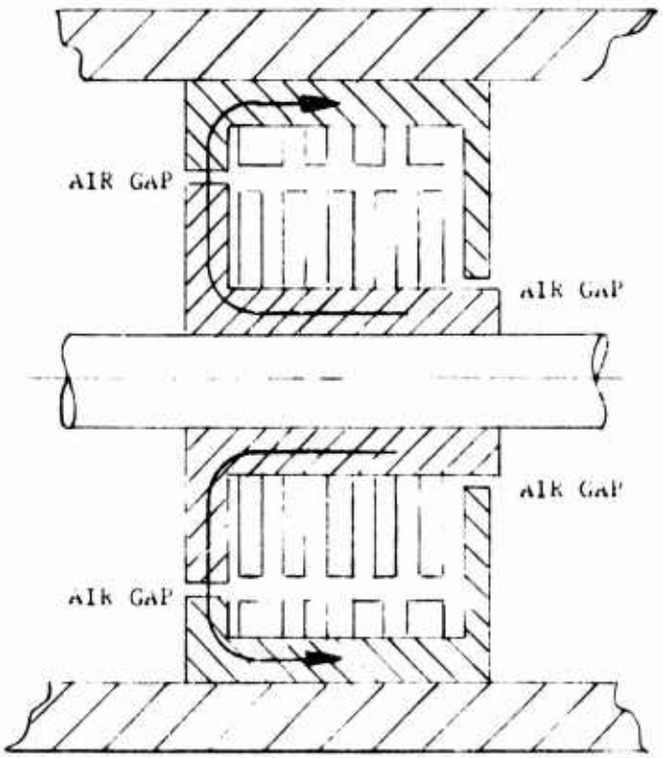

MAGNETIC FLUX PATTERN OF ROTARY TRANSFORMER

Figure 3.2.2A

provides AC to DC conversion. Since high frequency operation of the rotary transformer is possible, the design of this transformer and selection of magnetic materials together with magnetic geometry of the rotary transformer is very important. The high frequency operation allows this rotary transformer to be constructed in small size and weight configurations. The reduction of a rotary transformer weight and size is very important to the overall brushless starter-generator geometry and weight.

3.2.2.1 Design

Since the magnetic flux distribution of this rotary transformer, as shown in Figure 3.2.2A, includes two air gaps, the leakage inductance between the primary and secondary windings is of great importance. This leakage inductance controls the duration of the commutation overlap interval in the single phase bridge rectifier assembly. Since the main machine excitation current must cover the range of zero to 50 amperes, the commutating reactance controls the maximum output current magnitude and influences the selection of the operating frequency of this rotary transformer. In order to operate at high frequencies the commutating inductance value must be low. The geometry of the rotary transformer was selected to minimize the leakage inductance. The design goal of the leakage inductance was 10 microhenries. The operating frequency was selected to range from 2 kilohertz to 4 kilohertz. The low frequency range of this rotary transformer is used during the starting

mode of the brushless starter-generator and the high frequency operating point during the generator mode of the system. Because of multidirection of flux flow pattern in the rotary transformer magnetics, the choice of magnetic materials was carefully investigated. The following magnetic materials were considered for the rotary transformer application.

Silicon Iron (3%), Grain Oriented

Cubex Iron, Grain Oriented

47% Ortonol

Supermalloy

Ceramic pot-cores

The objective was set to select the magnetic material that exhibits easy axis of magnetization (1,0,0) along the direction of the magnetic flux flow in this rotary transformer. In practice, problems were encountered in providing workable samples of magnetic materials for this design. The magnetic material vendors were unyieldy in supplying us with necessary samples.

The ceramic pot-cores required special reinforcement in order to keep the integrity of magnetic materials under the fairly high peripheral speeds encountered in this rotary transformer design. Since this reinforcement required special dies and casts, the ceramic core manufacturers were reluctant to participate in this development.

Silicon iron (3%) was rejected because of an easy axis of magnetization being only along the one direction of magnetic flux path.

The pancake design of Cubex iron was made available and tested The bench tests were encouraging. The final machining of a transformer air gap damaged laminations and hardware was abandoned.

3.2.2.2 Fabrication

The 47 portinol magnetic material exhibiting mutually perpendicular easy axis of magnetization was procured. These laminations were 2 mils in thickness and were edge-stacked in the rotor and stator core assemblies. Retaining rings were used to maintain the integrity of the rotary transformer during high speed operation of the magnetic material. The rotary transformer was would with an edge type, HML insulated rectangular copper wire. The primary winding of this rotary transformer is center tapped. The secondary is wound on the rotating member of the transformer core. Its output is rectified by bridge-type, single phase rectifiers. Figure 3.2.2.2A shows disassembled hardware of the rotary transformer. The spin tests at elevated temperatures up to a speed of 15,000 RPM showed no movement of mechanical assembly indicating stable mechanical conditions of this rotary transformer.

The rectifier assembly is shown in Figure 3.2.1.1A. In this figure an assembly of two circular plates with swage type rectifiers pressed in their mounting holes are used for the rectification of the rotary transformer output. Once the rectifier hardware was made available and connected to the rotary trans-

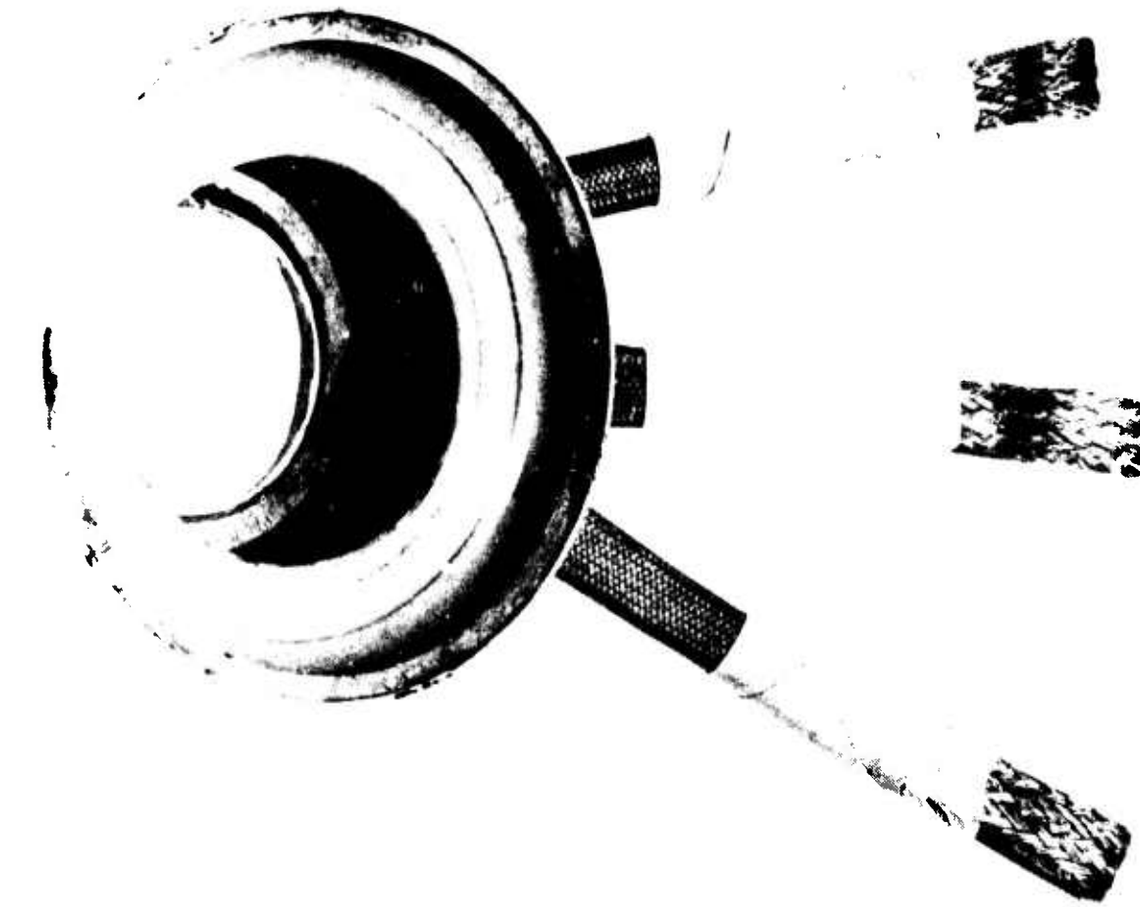

former and the AC voltage regulator, it was possible to check the complete rotary transformer excitation hardware while the machine was at standstill. This is quite an important factor. Normally, the rotary exciter has no output at standstill and cannot be tested or its operation investigated in its standstill mode. Contrary to the rotary exciter, this hardware allows a full electrical check-out and an electronic investigation of various transformer-rectifier parameters while the machine is at standstill. The commutation interval of the rectifying diodes, RF noise and other important parameters can be observed and analyzed with ease. Figure 3.2.2.1B shows an electrical schematic of the rotary transformer rectifier assembly. The tests of this excitation hardware were in full agreement with the design goals.

3.2.3 Rectifiers for Generating Mode

Since the required electrical power during the generating mode must be DC, it is necessary to rectify the AC output of the electromechanical converter. This rectification is performed with the help of multiphase rectifier hardware. To reduce the AC ripple component in the DC output, it was necessary to use two sets of three-phase rectifier bridge assemblies. To keep the best utilization of machine windings, the three-phase bridge circuitry was chosen. The machine housing was designed as a rectangular tube instead of a conventional cylinder shape. In each corner of the housing three rectifier assemblies of positive or negative polarity were mounted. As was explained

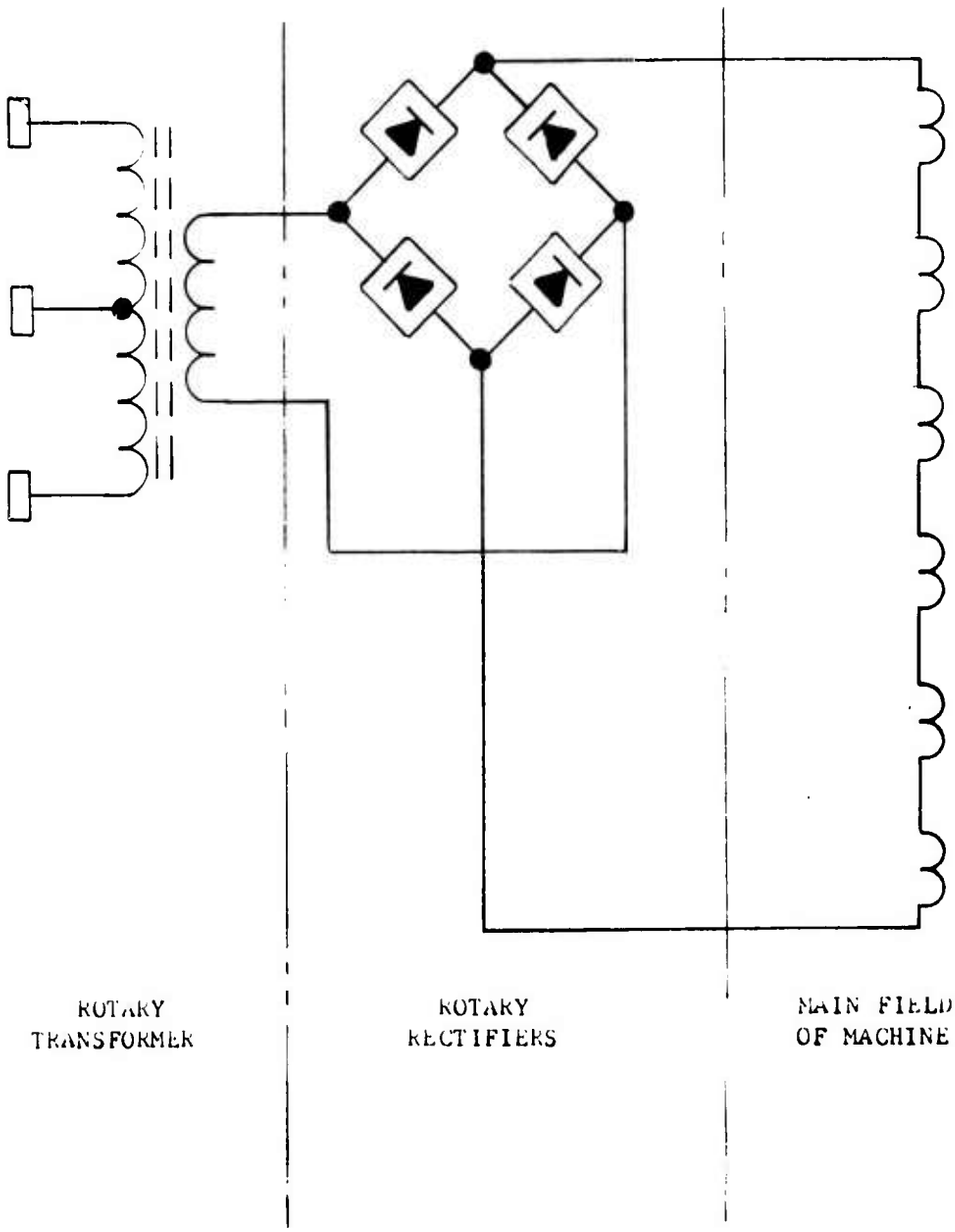

ROTARY TRANSFORMER-RECTIFIER ASSEMBLY
SCHEMATIC

54

Figure 3.2.2.1b

previously, the same corners in the machine housing are also used for carrying the machine's cooling air. The mounting of rectifiers in these corners required substantial care in choosing their geometry since very low air flow interference can be tolerated. The original choice was to use diodes mounted on common substrate so that minimum air flow interference is produced. The search for semiconductor vendors to supply these devices was made. After reviewing a number of semiconductor manufacturers, it was discovered that the necessary technology in hermetically sealing three rectifier assemblies on one heat sink is not readily available for direct utilization to this program. The hermetic seal against environmental conditions encountered in this brushless starter-generator application was the key in the requirements of the three-rectifier cell assembly.

Special fabrication effort was undertaken by Tarzian Manufacturing Co. to produce three rectifier junctions mounted on a common heat sink and being hermetically sealed.

Meanwhile, discrete components were evaluated for their capability to do this job. It appeared that conventional devices temporarily could be substituted in place of the three diode common heat sink assembly in each corner of the machine housing to provide the necessary multiphase rectification. The possible overvoltage on the DC bus and the machine voltage transients set the rectifier peak reverse voltage capability -- minimum 80, desirable 100 volts peak. The

average current rating was established to be 33 amps average and 57 amps RMS per rectifier. These values are derived from 200 amp output rating of the brushless starter generator. Each rectifier in this rectifier assembly is used for one third of its duty cycle. The nominal operating frequency is 400 Hertz. In each corner of the machine housing one quarter of a total machine cooling air is passed through the three rectifier assembly mounting. Figure 3.2.3A shows a typical rectifier set assembly. In selecting the heat sink design and the necessary hardware to mount the rectifiers, the cooling conditions at various altitudes were considered. The investigation confirmed the sufficient cooling of the rectifiers over the extreme environmental conditions of this brushless starter-generator system.

3.2.3.1 Integrated Rectifier Modules

The integrated package of three positive or negative polarity diodes is still considered as a best hardware approach for this machine's output rectification. The principle difficulty of obtaining these units is semiconductor manufacturers' willingness to produce the required modules meeting military requirements. A number of devices were investigated and all had problems with hermetic sealing. To produce devices with sound hermetic sealing requires development effort by the semiconductor manufacturers which will not be undertaken for this program. Figure 3.2.3.1A shows the typical construction of an integrated three-diode assembly. The units were installed in

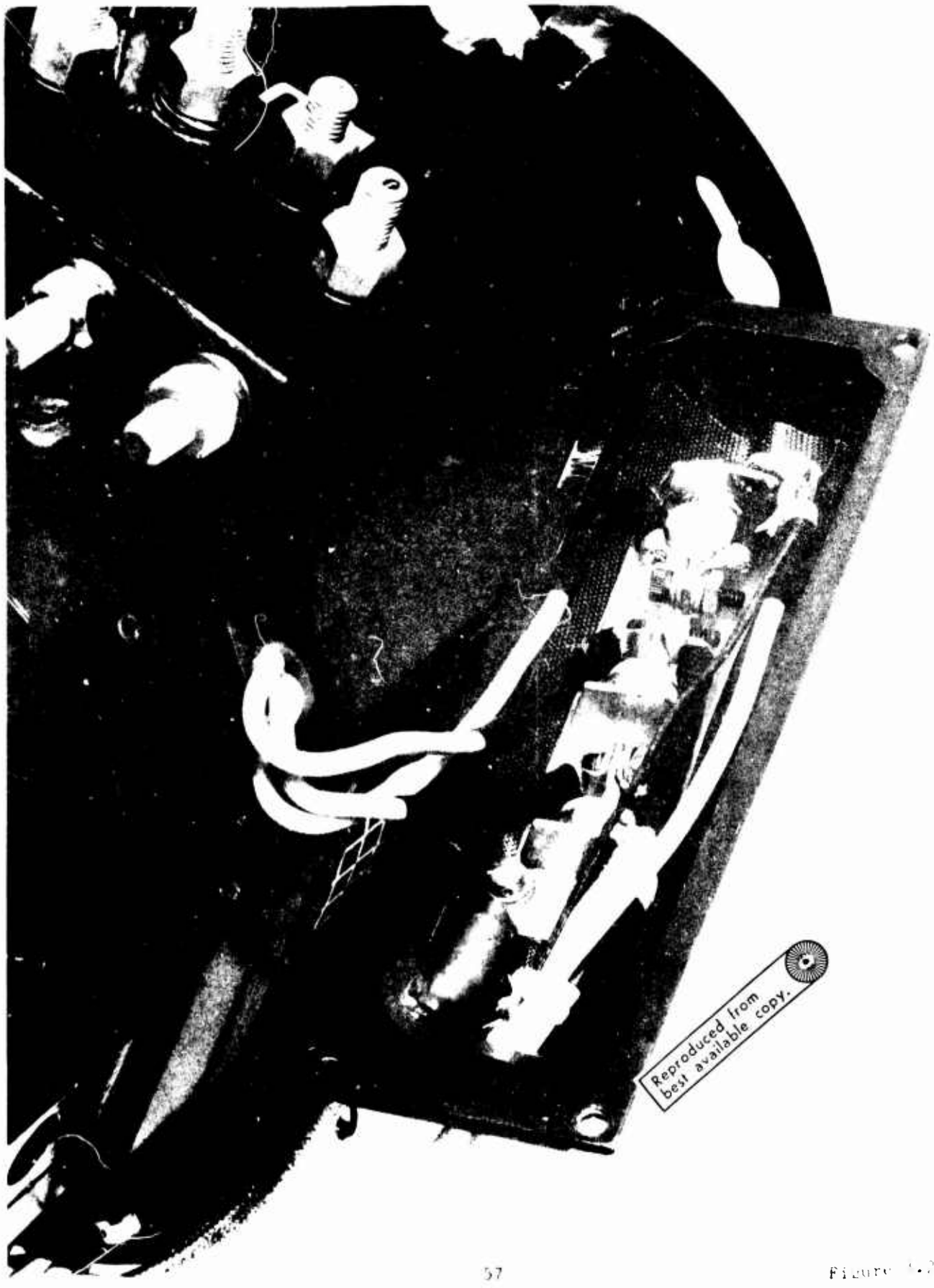

Figure 3.2.3A

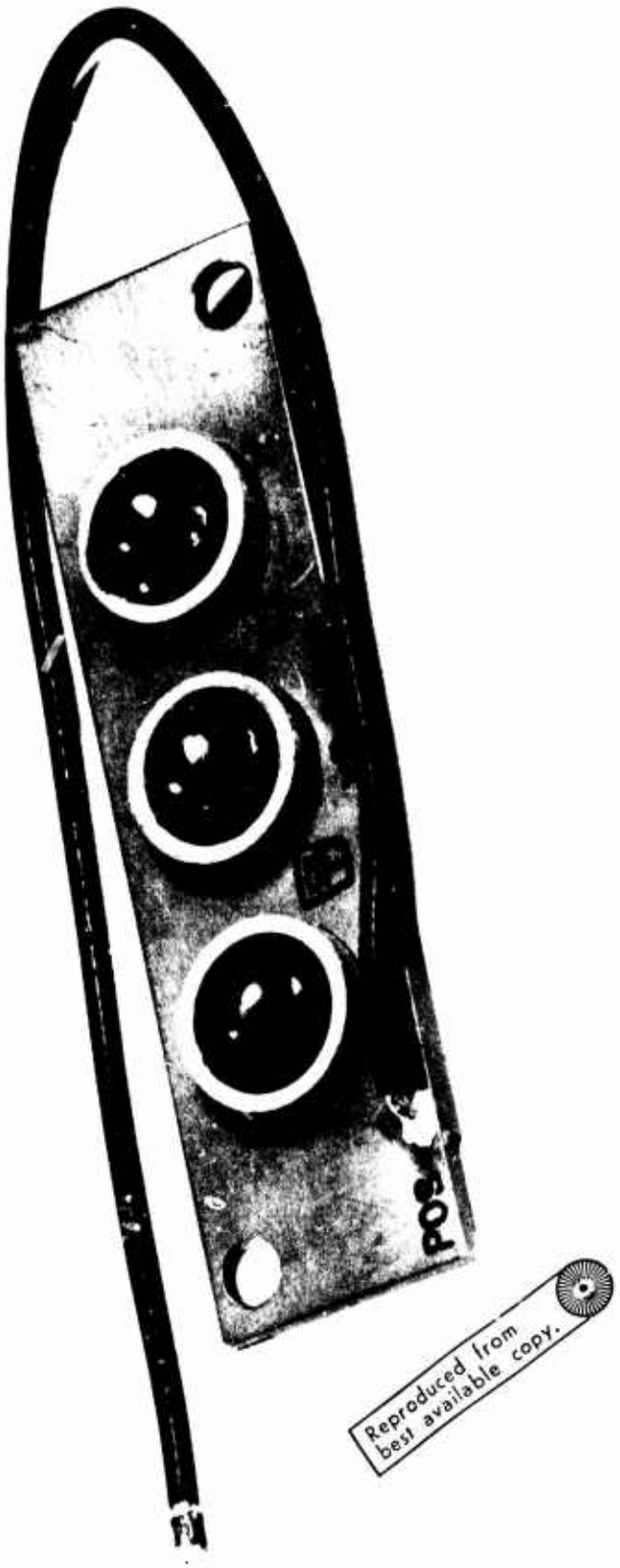

the machine and tested for electrical performance. The hermetic seal was considered very poor, therefore environmental testing was not conducted.

SECTION IV

4.0 STATIC COMMUTATOR

4.1 COMMUTATOR DEFINITION

In this brushless starter-generator system the static commutator is defined as an arrangement of the solid state switching devices capable of transferring electrical current between sets of machine windings upon application of low level command signal. This arrangement of solid state devices is actually achieved by assembling similar, individually packaged, semiconductor modules operating in their switching mode. The switching mode is needed to reduce the over-all losses of the solid state static commutator. The static commutator is the most important subassembly in this brushless starter-generator program. Its selection, definition and procurement took the largest portion of this program's effort. In the design of the electrical machine it was pointed out that the optimum electromagnetic weight of the machine is achieved with at least 800 ampere input current level. This high input current level happens in the starting mode of the brushless starter-generator system. Further machine analysis disclosed multiphase operation was needed. The multiphase operation was chosen to consist of two sets of three-phase windings. The two sets of windings disclosed the possibility of using 400 amps per each set of three phase machine windings. The choice of 400 amp current level per each three phase winding also is helpful in procurement of a solid state switch needed for the

static commutator. Further attempts of parallel machine windings showed increasing penalties in the machine size and weight and therefore was not recommended. The preliminary design of the machine disclosed its weight to be at 25 lbs. Since the specification requirement in Exhibit "A" sets the total weight at 30 lbs., this left only 5 lbs. for the static commutator hardware. The operating voltage on each commutator switch in the three-phase bridge arrangement is equal to the input voltage level set to be 30 volts DC. The voltage rating for the static commutator switch was set to be 80 volts peak minimum with preference for 100 volts peak. This choice came about from the requirements of MIL-STD-704 which is applicable to this hardware. Thermally, the static commutator switch must be capable of storing its losses during the starting cycles. It is important to note that no cooling provisions are available during the starting mode of the brushless starter-generator operation. Furthermore, the static commutator switch must operate in the environment as described by applicable military specifications covering the conventional starter-generator machines. From the above statements the crude definition of solid state commutator switch requirements was made available early in the program.

a)	Solid state switch current handling capability	400 amperes
b)	Solid switch sustaining voltage	80 volts peak
c)	Solid state switch weight	.4 to .5 (approx.)

d)	Number of switches required for static commutator	12
e)	Solid state switch control signal	5 volts, 10 mils compatible with I.C. outputs
f)	Static commutator geometry	A cylinder approximately 3" long, 5-1/2" diameter
g)	Solid state switch geometry	A wedge occupying 1/12th of the commutator cylinder.

The above definition of static commutator switch requirements provided a program with early information needed to investigate feasibility of the static commutator hardware. The feasibility of the static commutator was divided into two branches of research. One branch of research was dealing with silicon controlled rectifiers -- thyristors. The second group was investigating the transistor hybrid switches. The possibility of using silicon controlled rectifiers for this commutator was investigated in various details. A number of single SCR switches with forced commutation were investigated for applicability to this job. Some of them were built and tested to verify the design accuracies. For example, a single SCR switch capable of controlling 200 amps of DC current at 30 VDC was breadboarded and tested. It closely agreed with design predictions indicating its weight was in commutating capacitors and other auxiliary components; further weight reduction was not feasible. If the single switch weighs 2-1/2 pounds and 12 switches are required for the full solid state commutator as applicable to this program, it was

evident very quickly that this approach had to be abandoned.

The other approach of using SCR's for this solid state commutator was quite attractive at the beginning of this program. This approach was using SCR's in their natural commutation mode. (This mode of operation is possible when dealing with multiphase synchronous machines). Since the machine operates in synchronous start, the match of machine and SCR type commutator appeared to be quite feasible. In this inversion approach SCR's are used in their power inversion mode producing DC to AC power inversion with the aid of the machine's back EMF. The weight of this solid state switch was only 4 to 6 ounces and appeared quite suitable for this brushless starter commutator application where total weight of the commutator must not exceed 5 pounds. The problem encountered was in the initial starting of the machine. The total inertia of the machine, including its load, was too high to produce initial SCR current commutation as required. The back EMF produced for commutating the first SCR with the system heavily loaded with inertia type load was too low to provide natural commutation of current from one winding to the other. The machine's weight and size for the inertia values as specified by Exhibit "A" did not make this approach feasible.

The second branch of research in their study of solid state commutator feasibility was showing progress but only with the advancement in the "state-of-art" of power transistors. This

came about from the fact that 400 ampere current handling silicon transistors were not available, although this high amperage requirement could be met by parallel arrangement of transistors. The singular discrete transistors arranged to handle the 400 ampere current level could not be packaged in the required size and weight of previously defined single solid state switches. It became apparent that the solution for the small size, light weight, solid state commutator lies in the special packaging of solid state devices on a common substrate. By further investigation of this idea among the transistor manufacturers, it was decided to take this hybrid approach to fulfill the requirements of this solid state commutator. This approach verified the initial assumptions considered in the proposal stages of this contract.

4.1.1 Procurement

A detailed specification was written in order to procure the solid state commutator hardware. This document, LSI/PED specification No. 15-100011, was prepared and distributed to interested vendors. The instructions for bidding included a requirement for attendance at a Bidder's Conference prior to proposal submittal. This conference was held and all specification details were reviewed with the attending vendors. The following manufacturers were present at the Bidder's Conference.

Delco Division of GMC

Westinghouse

RCA

Solitron

Silicon Transistor Corporation (STC)

Motorola

Texas Instruments

General Electric

Technical Proposals were received from the following manufacturers:

RCA

Silicon Transistor Corporation (STC)

Solitron

Westinghouse

Proposal evaluation was made on technical content, design approachs, price and delivery.

A contract was subsequently awarded to RCA for Design and Development and fabrication of two sets of hardware (two commutators) on with delivery to be eight (8) months after receipt of order.

4.1.2 Description of Vendor Circuit Approach and Module Fabrication

The detailed circuit approach and module fabrication to be used in the static commutator is presented in RCA's technical proposal included in Appendix II of this report.

The proposed static commutator package mock-up was constructed by RCA early in the program so that thermal storage capabilities could be evaluated. The unit consisted of commutator housing (frame) and 12 wedges representing the solid state switches. The switches were held to the housing (frame) by the retainer brackets. Figure 4.1.2A shows this package assembly. The thermal tests were performed by heating the switch mock-up with internally mounted resistors. The weight of the assembly was approximately 3.5 lbs. The tests indicated insufficient thermal storage capability of the overall package and high thermal impedance paths. Therefore, the commutator package was redesigned. The new package distributed the available commutator material among the switches, thereby eliminating the original commutator housing. Figure 4.1.2B shows the new commutator package mock-up consisting of 12 switches. Each switch uses 1/1/12 of the commutator weight which was estimated to be approximately 5 lbs.

The individual switch hardware is shown in Figure 4.1.2C. The three pins shown in the front face of the switch are command signal inputs. The bolts are used to connect the main input power and the machine windings. One of the bolts is also used to mount the switch to the frame of the machine. The switch

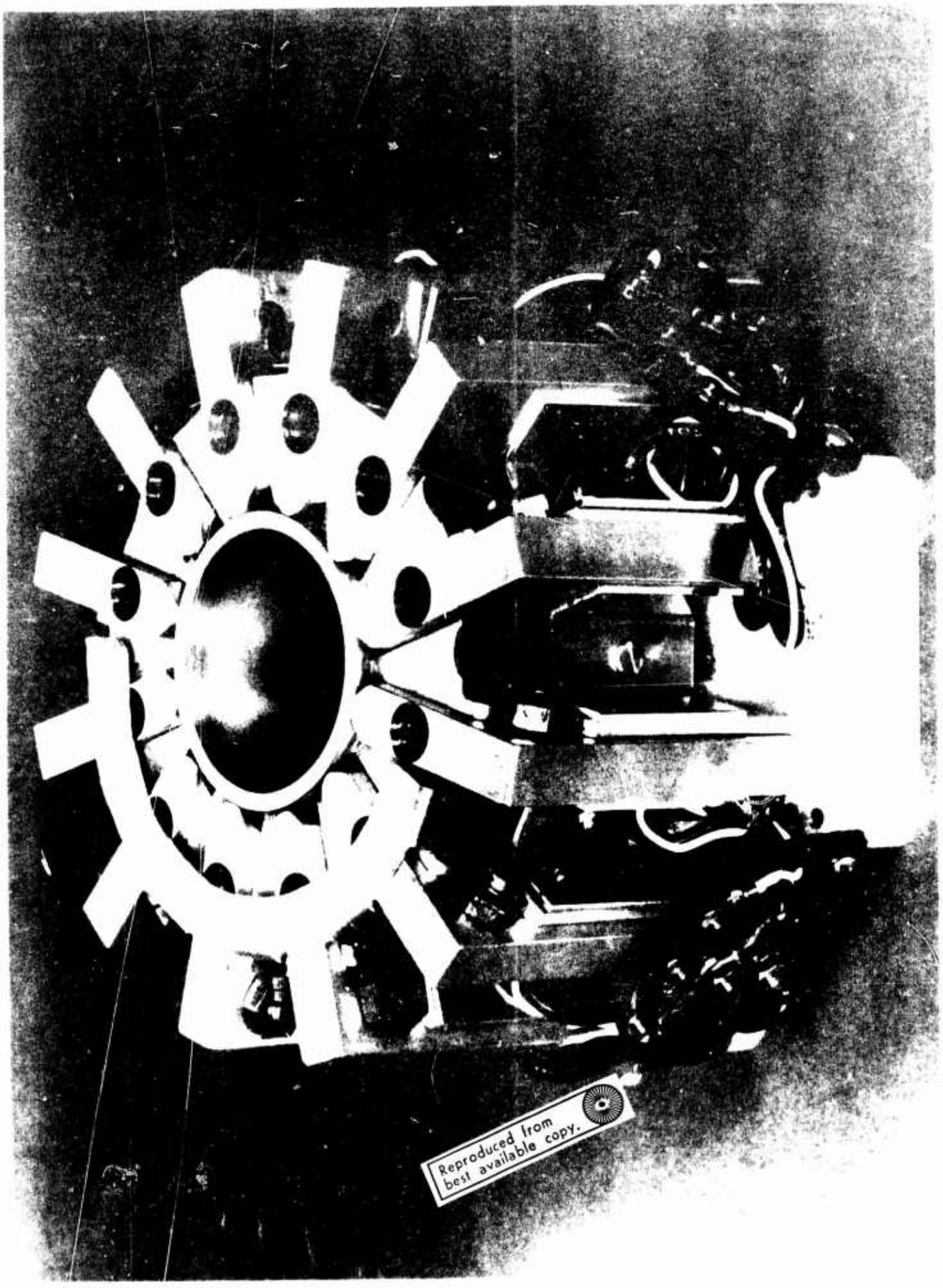

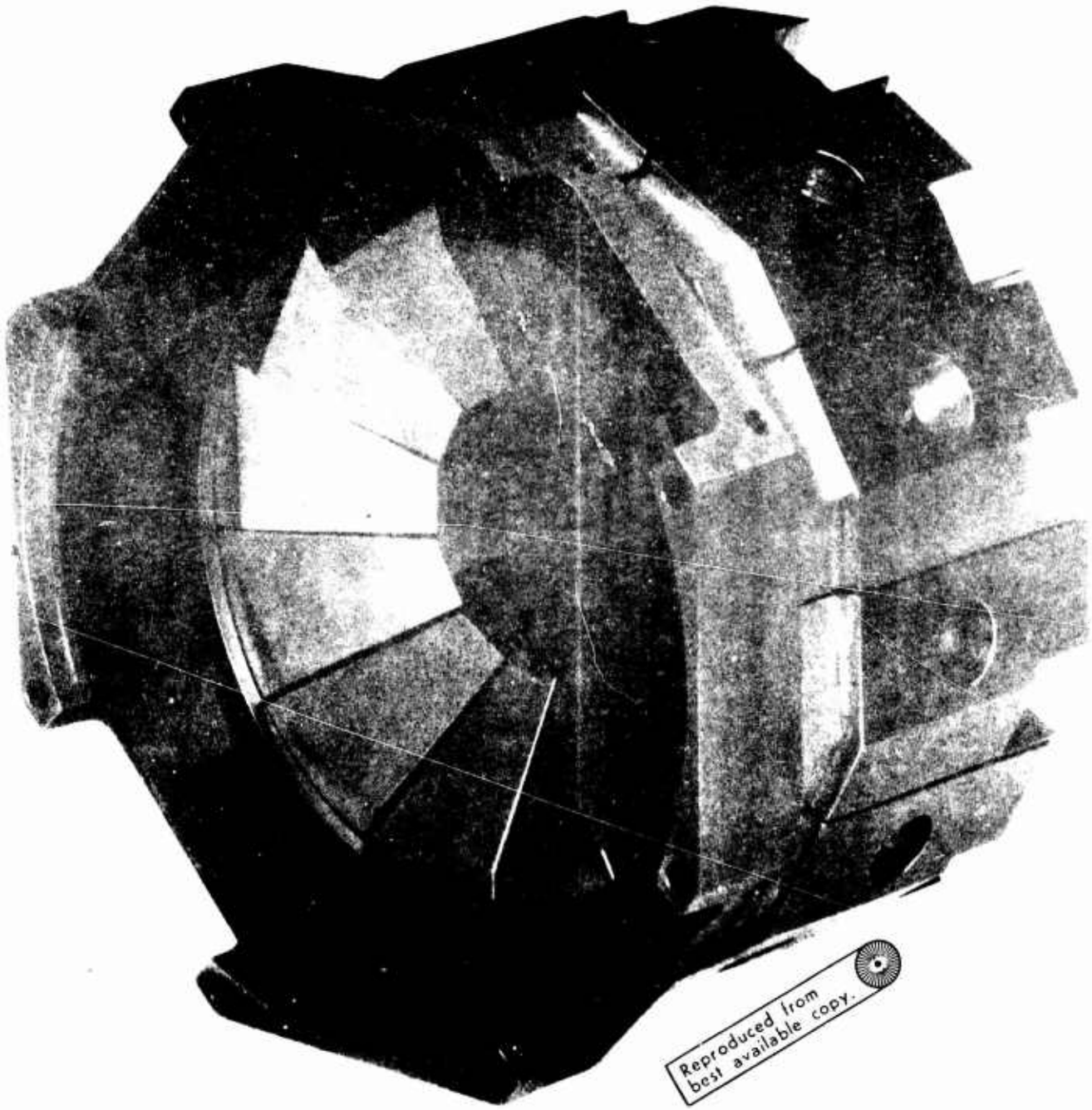

hardware is indexed so that positive and negative switches can not be accidentally interchanged.

The fabrication stages of the solid state switch modules are shown in the following series of photographs.

Stage 1 is a blank aluminum heat sink.

Stage 2 shows the molibdenum pedestals mounted for the positive and negative switch assemblies.

Stage 3 shows 6 power transistor modules mounted.

Stage 4 shows driver units mounted to the assembly.

Stage 5 displays power and driver transistor units completed.

Stage 6 shows preamplifier and pre-driver stages installed to positive and negative switch modules.

Stage 7 displays finished assembly with cover on.

The initial intent by RCA was to fabricate two sets of commutator hardware for this contract. Work was started with enough material for 100 switch modules. During the fabrication stages difficulties plagued the program and the yield of this pilot fabrication was very low. After various corrections in the fabrication equipment and procedures, enough modules were fabricated for one complete set of static commutator hardware.

4.1.3 Evaluation of Procured Devices

The final shipment of the static commutator switches was received during the month of February 1969. The total number of usable devices was 13, (6 positive modules and 7 negative modules). An order was placed for 2 additional positive switches. Their

STAGE-1

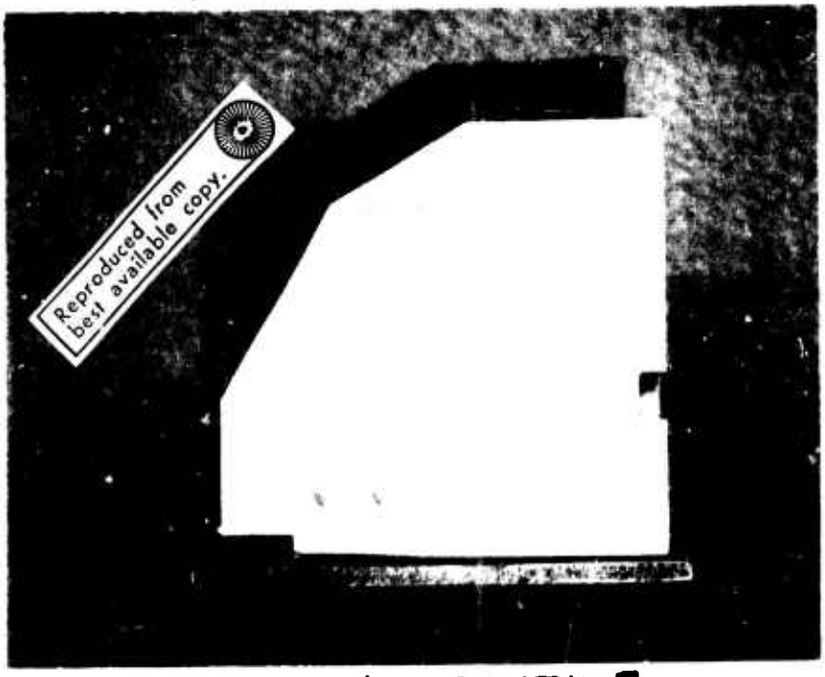

POSITIVE & NEGATIVE

/1

Figure 4.1.20

STAGE -2

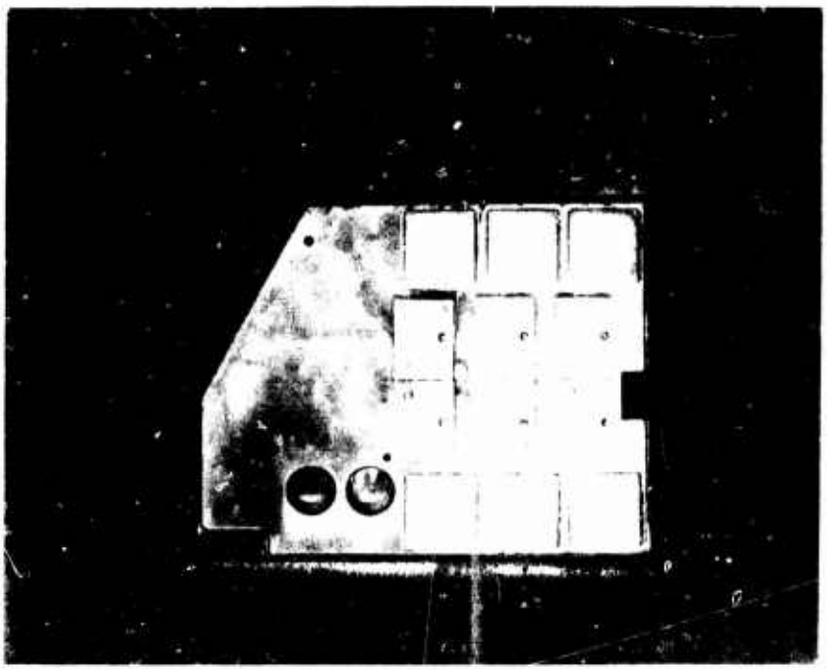

POSITIVE

STAGE -2

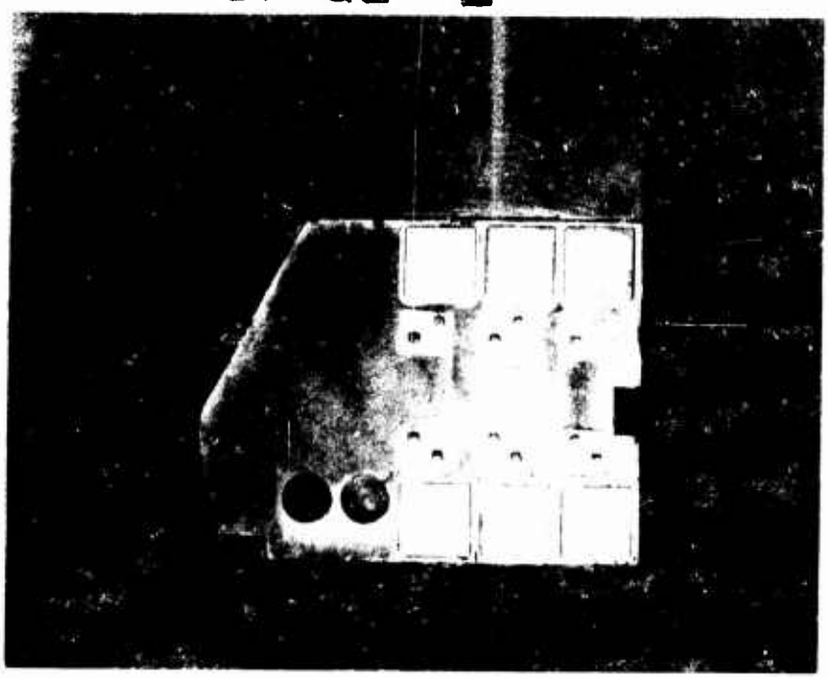

NEGATIVE

STAGE-3

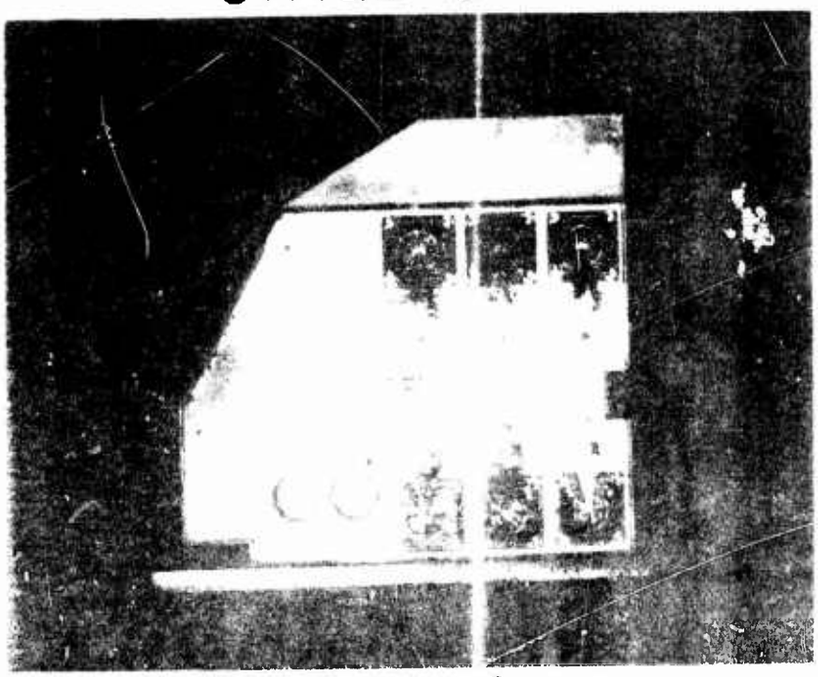

POSITIVE

STAGE-3

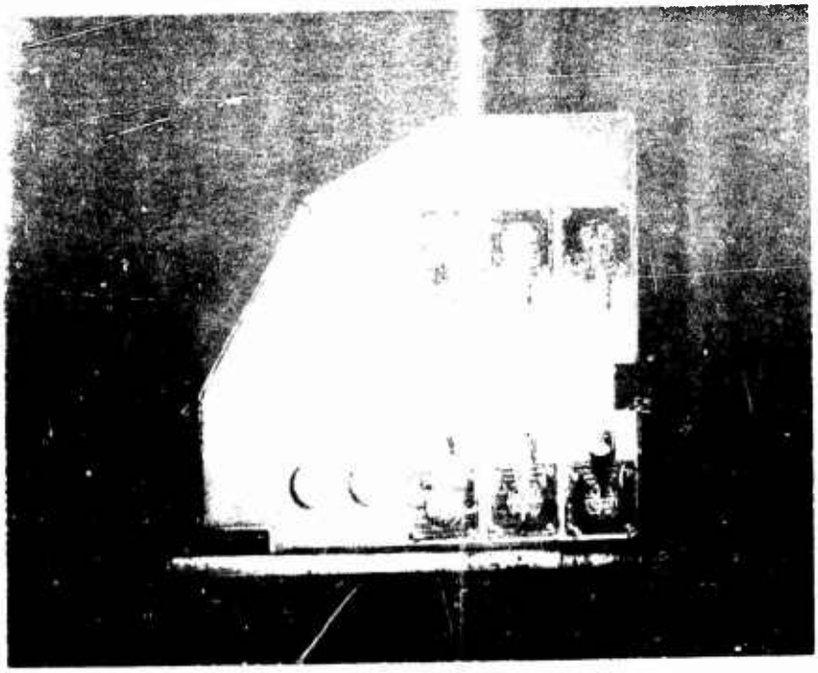

NEGATIVE

STAGE-4

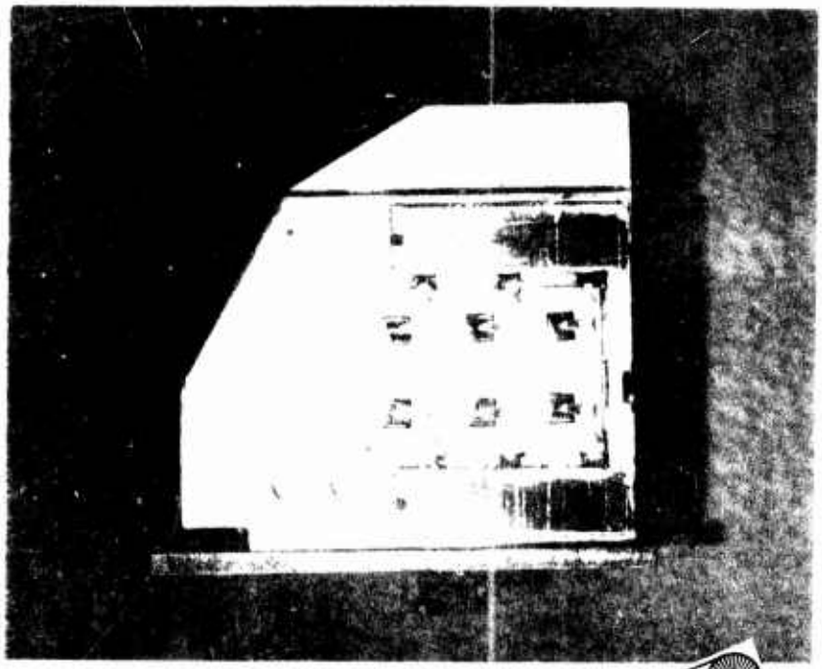

POSITIVE

STAGE-4

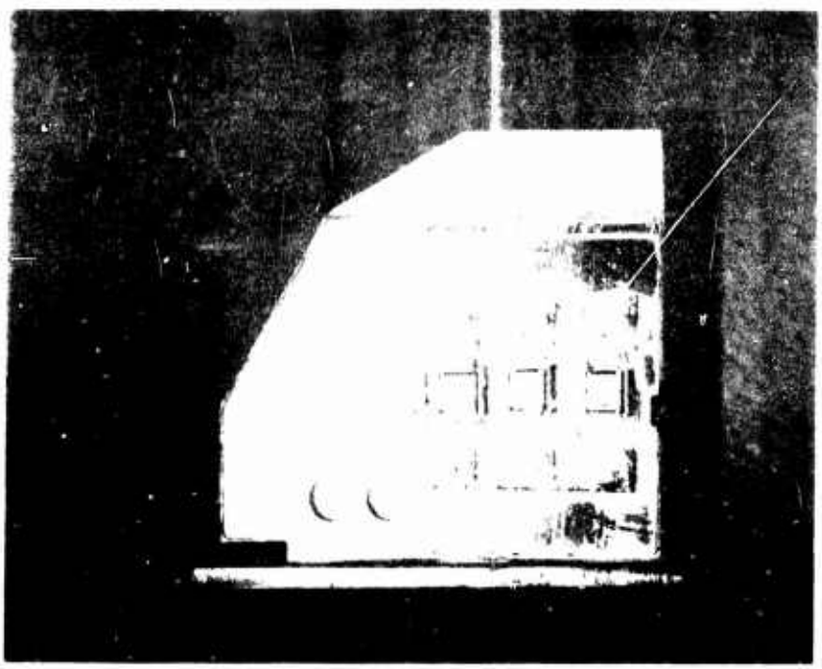

NEGATIVE

STAGE-5

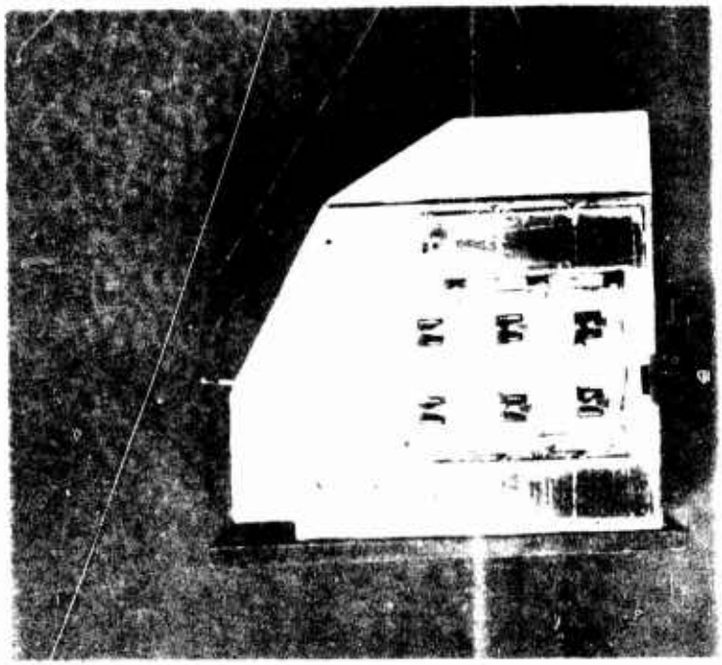

POSITIVE

STAGE-5

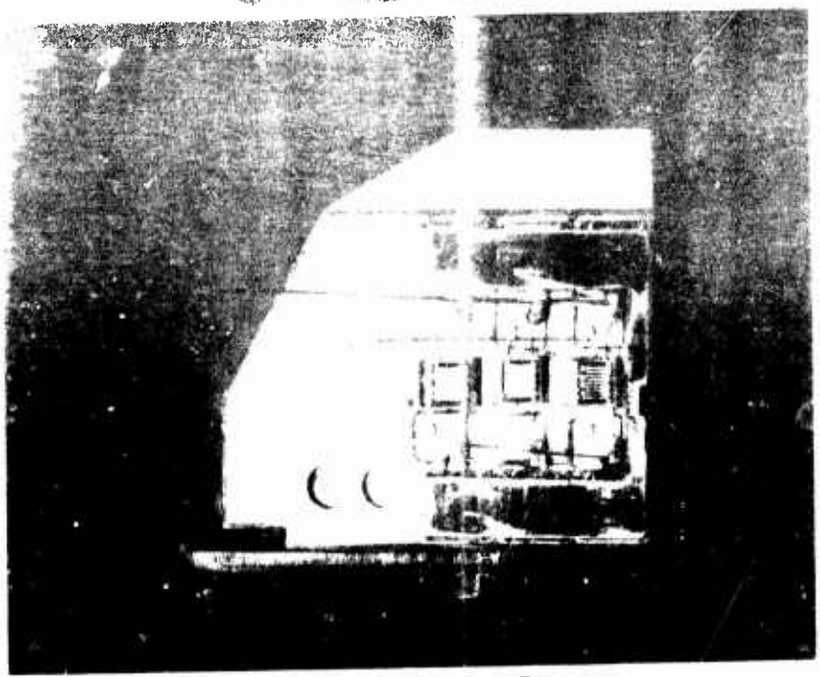

NEGATIVE

STAGE-6

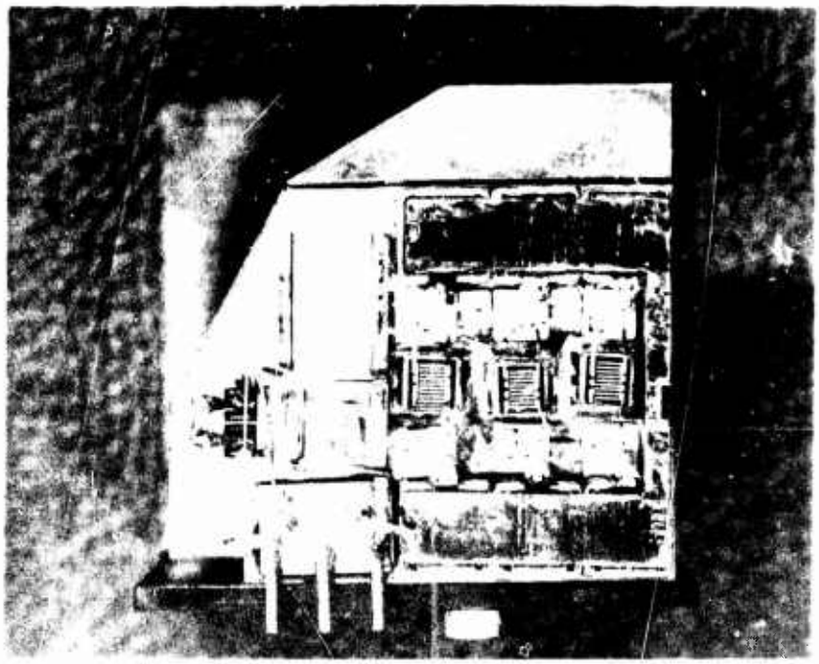

NEGATIVE

STAGE-6

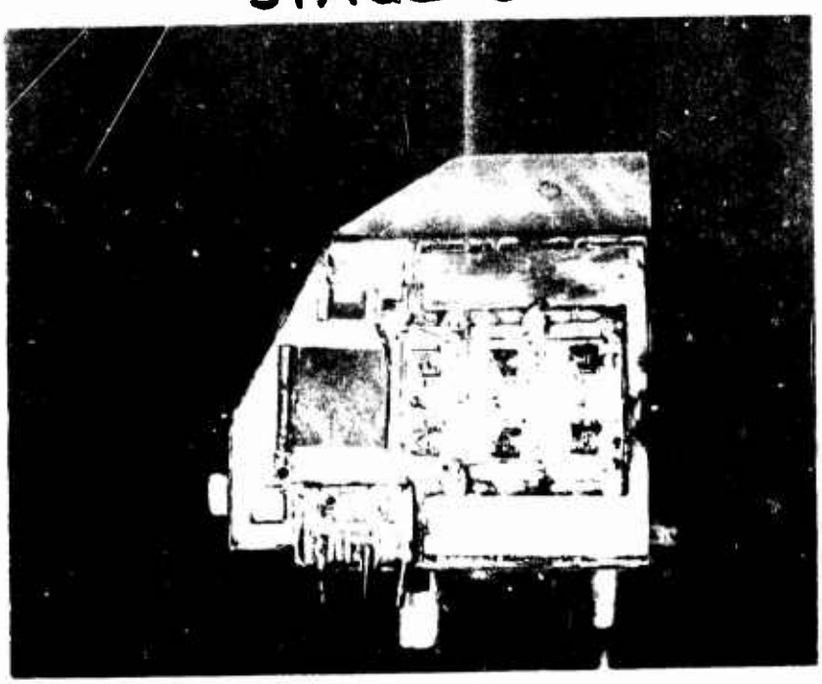

POSITIVE

STAGE-7

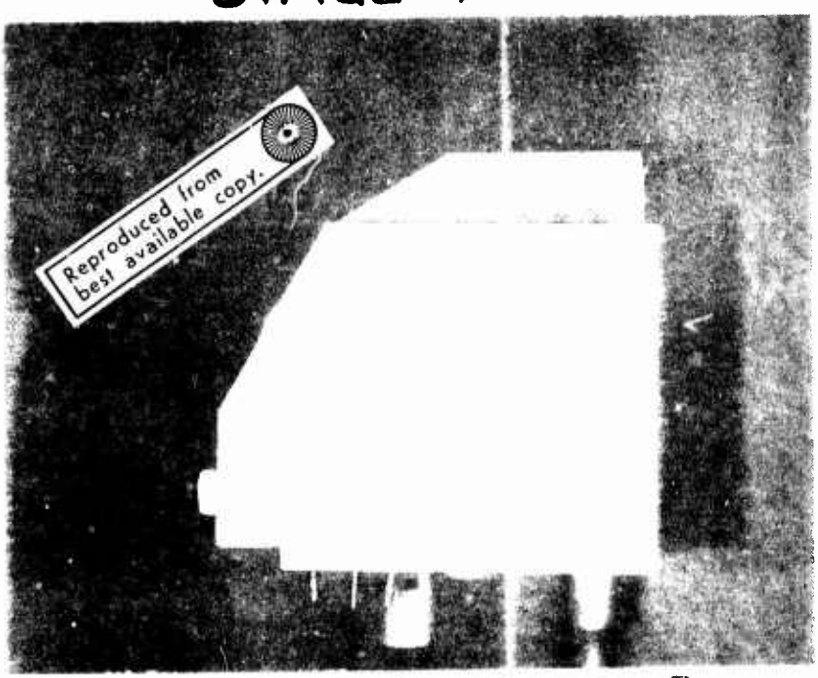

POSITIVE & NEGATIVE

delivery was set to be April 1969.

The units received were tested by RCA at 20 Hz and 200 Hz at 10% and 33% duty cycle. Tests were conducted for saturation, turn off time and leakage current at several temperatures up to 125°C.

The LSI/PED receiving inspection tests were performed on all the units and the findings were summarized in Table I.

During the acceptance tests at LSI/PED, negative switch #64 failed while operating at 100 amps. RCA tests show this unit operating at 400 amps.

Of the units delivered, several units were derated due to removal of either a driver or output transistor module. (This module failed during the fabrication stages of the switch and could not be salvaged). The workable delivered units and their associated ratings are given in Table II.

The commutator switches produced as a result of the RCA development program represent a best effort device and the state-of-the-art in power switching modules. However, they do not meet the requirements as outlined in the original specification for the static commutator. (LSI/PED specification No. 15-100011). They do, however, provide a commutator that can be evaluated with the machine to provide data on switch electrical performance and the performance of the machine with the static commutator within the performance limitations of the switch. Because of the lack of spare switches the test program had to be carried out in a more careful manner than would be necessary

TABLE I

	Switch No.	Type	Saturation Voltage 200A (Volts)	Saturation Voltage 300A (Volts)	Storage Time 200A (μsec)	Storage Time 300A (μsec)	Fall Time 200A (μsec)	Fall Time 300A (μsec)
	8	Pos.	1.85	2.75	11	14	10	15
	11	Pos.	2.25	3.4	12	16	10	18
	16	Pos.	2.1	2.85	9	14	8	15
	51	Neg.	1.4	2.0	12	17	10	20
	52	Neg.	1.2	1.5	10	20	8	22
	71	Neg.	1.6	2.2	9	16	8	17
	6	Pos.	1.9	2.4	11	10	10	12
(1)	11	Pos.	3.1	6.2	14	14	14	16
	12	Pos.	2.8	(2)	(9)	2	13	2
	19	Pos.	1.6	2.4	13	13	10	12
	100	Pos.	2.2	3.2	11	10	15	16
	50	Neg.	2.5	3.8	8	7	14	15
	62	Neg.	2.2	3.7	9	7	11	13
	64	Neg.	Failed during initial test @ 100 amps					
	65	Neg.	1.9	2.6	9	8	13	13
	70	Neg.	2.1	2.7	9	8	15	17
(1)	71	Neg.	2.0	2.7	8	7	12	13

(1) Readings after repair of switches.

(2) Readings not taken at 300 amps because of high saturation voltage (6V @ 250 amps).

TABLE II

Switch No.	Type	Functioning Output Transistors	Functioning Driver Transistors	Output Current Rating (amps)
6	Pos.	6	7	400
8	Pos.	6	5	334
11	Pos.	6	5	334
12	Pos.	6	6	400 *
19	Pos.	6	7	400
100	Pos.	5	7	334
50	Neg.	5	3	334
51	Neg.	6	3	400
52	Neg.	6	3	400
62	Neg.	6	3	400
65	Neg.	6	3	400
70	Neg.	6	3	400
71	Neg.	6	3	400

Units #16 and 64 are not included since they failed in tests at LSI/PED.

* Although switch #12 is rated at 400 amps by RCA, LSI/PED tests indicated the saturation voltage is too high to risk this operation in the circuit.

if more spares were available. The derating of some of the switches also imposed an upper limit of 200 amperes on the current at which the system could be tested. Although an attempt could have been made to operate at higher currents, the risk factor would have been very high.

The units were deficient as per requirements of LSI/PED specification 15-100011 in the following areas:

a) Current handling capacity

b) Thermal storage capacity

c) Hermetic seal

Beyond the above, RCA delivered only one set of the static commutator hardware without rectifying diode modules. The lack of spare parts imposed severe risks in testing the brushless starter-generator system during the starting mode. At the very beginning of these tests it was known that the full starting mode requirements would not be met. The testing was performed only to establish the feasibility of the starter-generator concept and the machine design. Commutator switches that meet the original specification would be required to assure the specified starter-generator performance.

The final report covering RCA's work on the static commutator switches is attached in Appendix III of this report.

4.2 Additional Electronic Components

4.2.1 Analog to Digital Converter for Shaft Position Indicator Signal

The shaft position indicators used in this brushless starter-generator system are electromechanical transducer devices whose electrical characteristics are changed by mechanical means. The hardware employed in this instance is a rotating wheel assembly which modulates the air gap flux of the electromagnetic pick-up while rotating a fixed proximity from it. Electrical output of the pick-up is shown in Figure 3.2.1.A. The output is amplitude modulated AC. In order to convert this output to the digital signal compatible with the static commutator input command, additional circuitry must be used to shape this analog modulated AC output. Figure 4.2.1A shows this additional circuitry necessary for pulse shaping. The input as shown in Figure 4.2.1A is an amplitude modulated AC signal derived from the magnetic pick-up. It must be demodulated so that the information stored in the magnitude variation of this signal could be used for commutator switch control. The demodulation is achieved by half wave rectification and RC filtering. The varying DC output from the RC filter is applied to the input of the voltage lever comparator. This is a simple analog to digital signal conversion. Integrated circuitry type voltage level comparator with hysteresis is used as the basic analog to digital converter. The output of A/D converter is a typical square wave signal. For each set of three phase machine output, three pick-ups are employed. The demodulation and A/D converter currents are identical for all

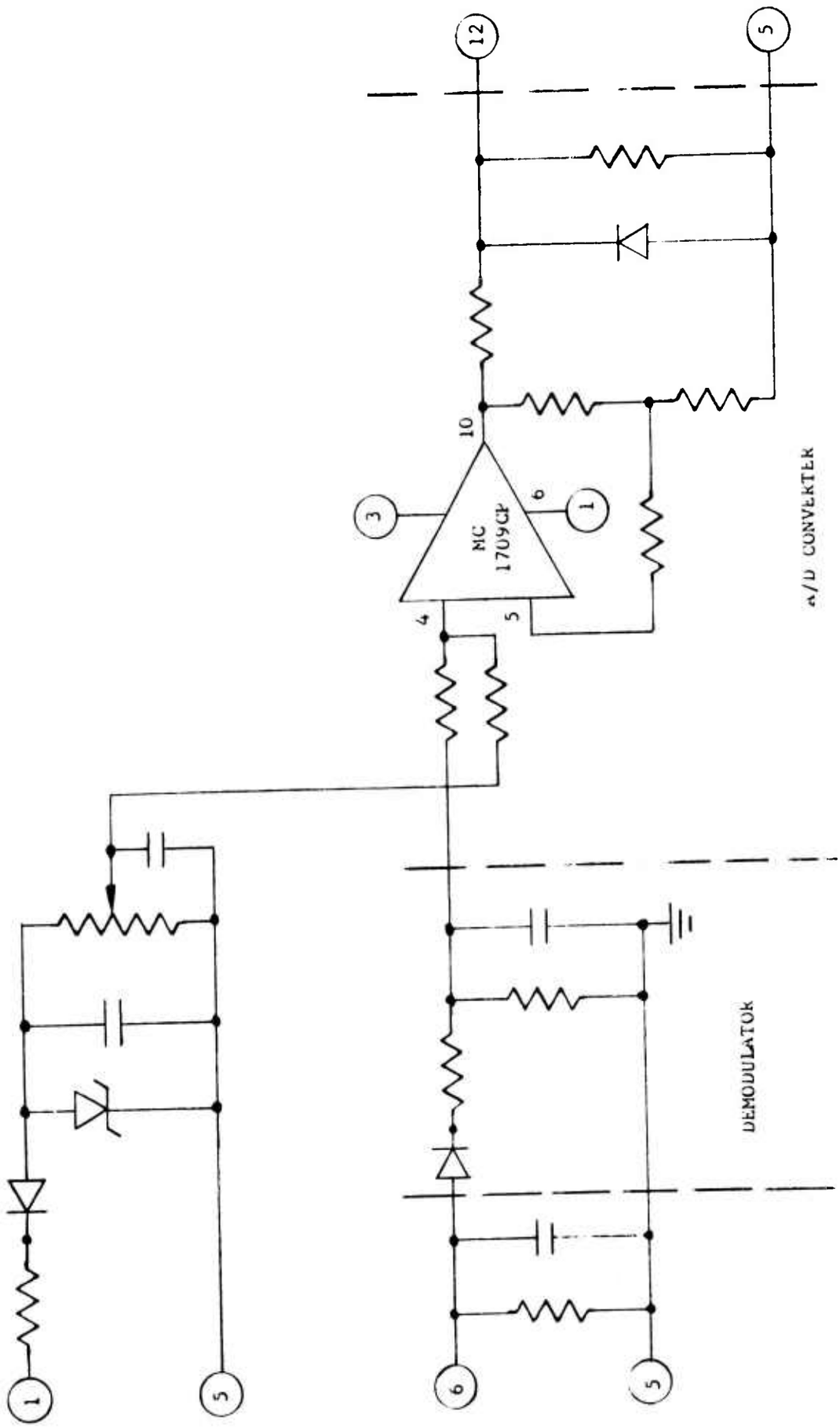

CIRCUIT SCHEMATIC FOR PULSE SHAPING

Figure 4.2.1A

pick-ups to one shown in Figure 4.2.1A. Therefore, for each set of three-phase machine windings the output is a set of three square waves. Since magnetic pick-ups are displaced approximately 120 electrical degrees from each other, the A/D converter output square waves are approximately 120° apart. By adjusting the pick-up positions an A/D converter level, symmetrical 120° phase shift among three A to D converter outputs is achieved. This set of symmetrical three-phase square waves is applied to the group of NAND gates shown in Figure 4.2.1B. The NAND gates are arranged in such a way that three-phase 120° stepped wave forms are produced by the NAND gates. These outputs are the exact digital wave forms needed to control the static commutator switches. Similar circuitry is used for the second set of three-phase machine windings and three pick-ups mounted in the housing of the machine. Their outputs are demodulated and A to D converters are used to produce digital square wave signal. The output, after the NAND gate stage, is another set of 120° stepped square wave, three-phase output. Between these two sets of outputs there is 30° phase shift. This phase shift is compatible with the 30° phase shift designed in the two sets of three-phase machine windings. During the starting operation, bot sets of machine windings are energized appropriately. Although the two sets of windings are energized, the 30° phase shift is maintained throughout the whole operation. This multi-phase arrangement is responsible for the smoother torque produced by the machine.

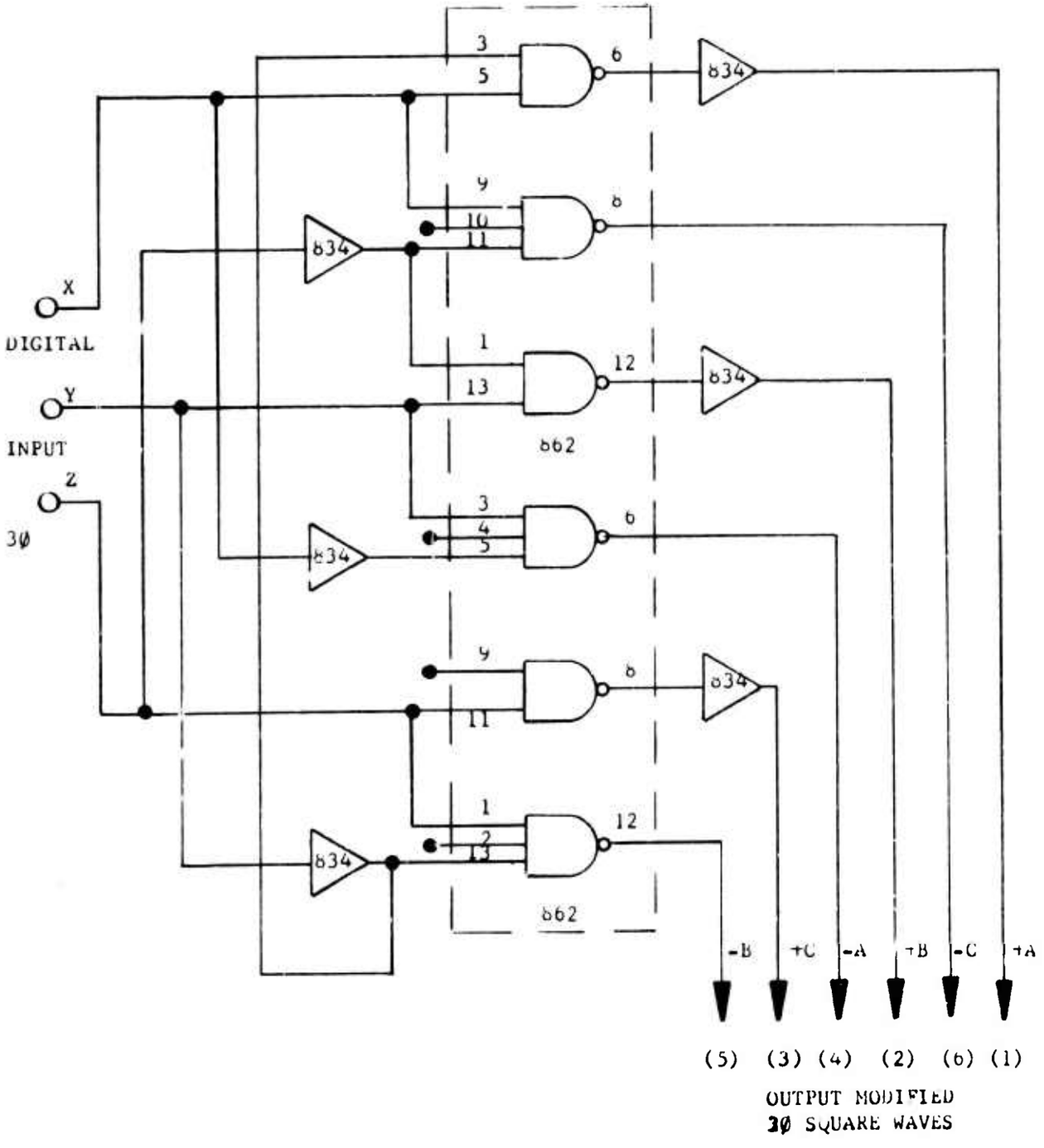

NAND GATE LOGIC FOR

3Ø WAVE SHAPING

Figure 4.2.1B

4.2.2 Auxiliary Power Supplies

To operate the static commutator switches it is necessary to provide them with auxiliary power supplies. The auxiliary power supplies are not physically located on the brushless starter-generator hardware. They are packaged in the voltage regulator assembly. The auxiliary power supplies shall maintain the output voltage of 11 volts $\pm$.5 volt and should be capable of providing current peaks up to 10 amps. Because of the positive and negative static commutator switches used, the power supplies must be common to plus and minus DC input busses. For example, an isolated power supply is needed to energize positive switches and an isolated power supply is needed to energize negative switches.

A number of circuitries were investigated to produce the necessary auxiliary power supplies. All the circuits used solid state devices in their switching mode. In this mode the efficiency of the power supply is highest and dissipation losses are minimized. A set of power supplies was breadboarded and tested under the required loading conditions compatible with solid state commutator hardware. Although electrically the power supplies performed satisfactorily, physically the size and weight of these power supplies was not suited for this program. Further investigations were made in reduction of size and weight of the power supplies. The conclusions indicated that similar solid state devices and packaging techniques are required for these power supplies as the devices used in the solid state commutator. It was decided to

postpone the packaging of power supplies until more technical data and a better understanding is gained on solid state switches used in the static commutator hardware.

SECTION V

5.0 BRUSHLESS STARTER GENERATOR SYSTEM HARDWARE

5.1 System Interconnections

Despite the deficiencies in the technical performance of the solid state commutator switches and very limited quantity of spare parts of the static commutator, it was agreed to continue this program and assemble the brushless starter-generator hardware for tests in the starting mode. The generating mode of this brushless starter-generator was accomplished independently of the solid state commutator. To simulate the identical air flow restrictions, a mock-up commutator assembly was made and attached to the machine housing. For the starting mode the brushless starter-generator system was interconnected with extended wiring leaving the commutator solid state switches mounted some 6 feet away from the electromechanical converter. This required careful placement of signal leads connecting the shaft sensing A and D converter and the input power leads of the solid state commutator.

5.1.1 Interconnections of Electromechanical Converter Hardware with Static Commutator Modules

The actual hardware interconnections between the static commutator modules and the machine are shown in Figures 5.1.1A, 5.1.1B and 5.1.1C. The figures A and B are displaying one half of the solid state commutator each. (The one half of the static commutator energizes one three-phase set of machine windings). Care was exercised in assembling and testing the solid state commutator switches. At that time, only three spare switches were available in the event of a failure. Figure 5.1.1C shows actual wiring coming out from

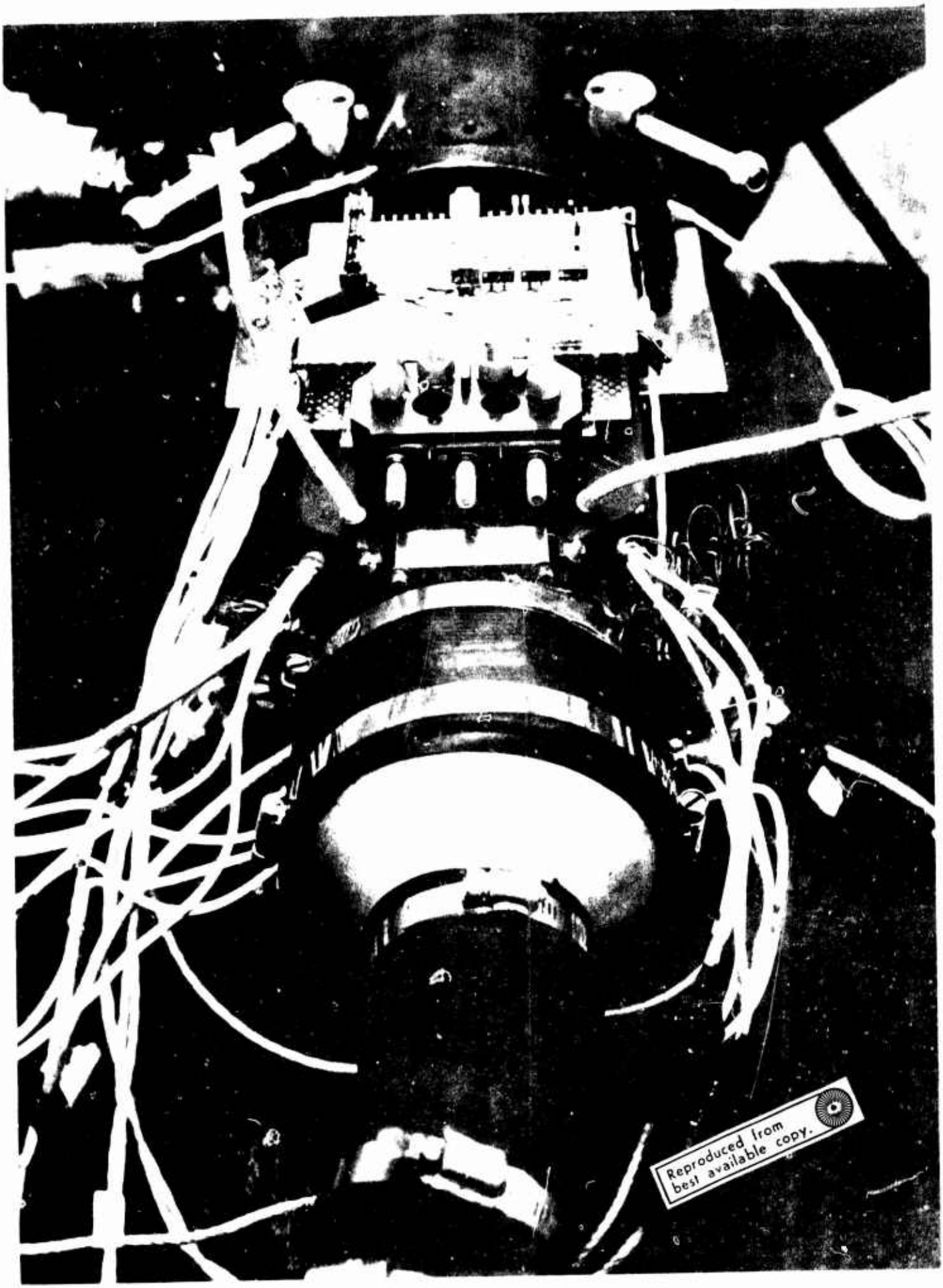

the machine. Figure 5.1.1D shows the electrical diagram for interwiring of static commutator modules in the machine. From the pictorial views of this hardware interconnections it is evident that ample room was left between each commutator solid state switch. This room is needed during various electrical tests and observations of a switch and machine operation. No attempt was made to mount solid state commutator to the required density and size. The main reason for constructing only the breadboard assembly of the commutator is in the understanding that the tests will be performed only within the limitations of the deficiencies of the solid state switches. Despite the commutator switch deficiencies, the commutator tests were performed in the actual system set-up at a maximum possible current handling capability of 400 amperes.

5.1.2 Interconnections Between Shaft Position Sensor and Static Commutator

Figure 5.1.1C also shows the vector board assembly of the analog to digital converter required for the conditioning of the shaft position signal. The shielded leads on the right hand side of the picture are coming from the machine housing and are terminated to the right hand side of the vector board. This shielded lead carries amplitude modulated magnetic pick-up information. A to D conversion and wave shaping is achieved on the vector board temporarily mounted on top of the machine. The left hand side of the vector board provides a group of shielded leads which carry the command signal to the commutator modules. The realistic hard-

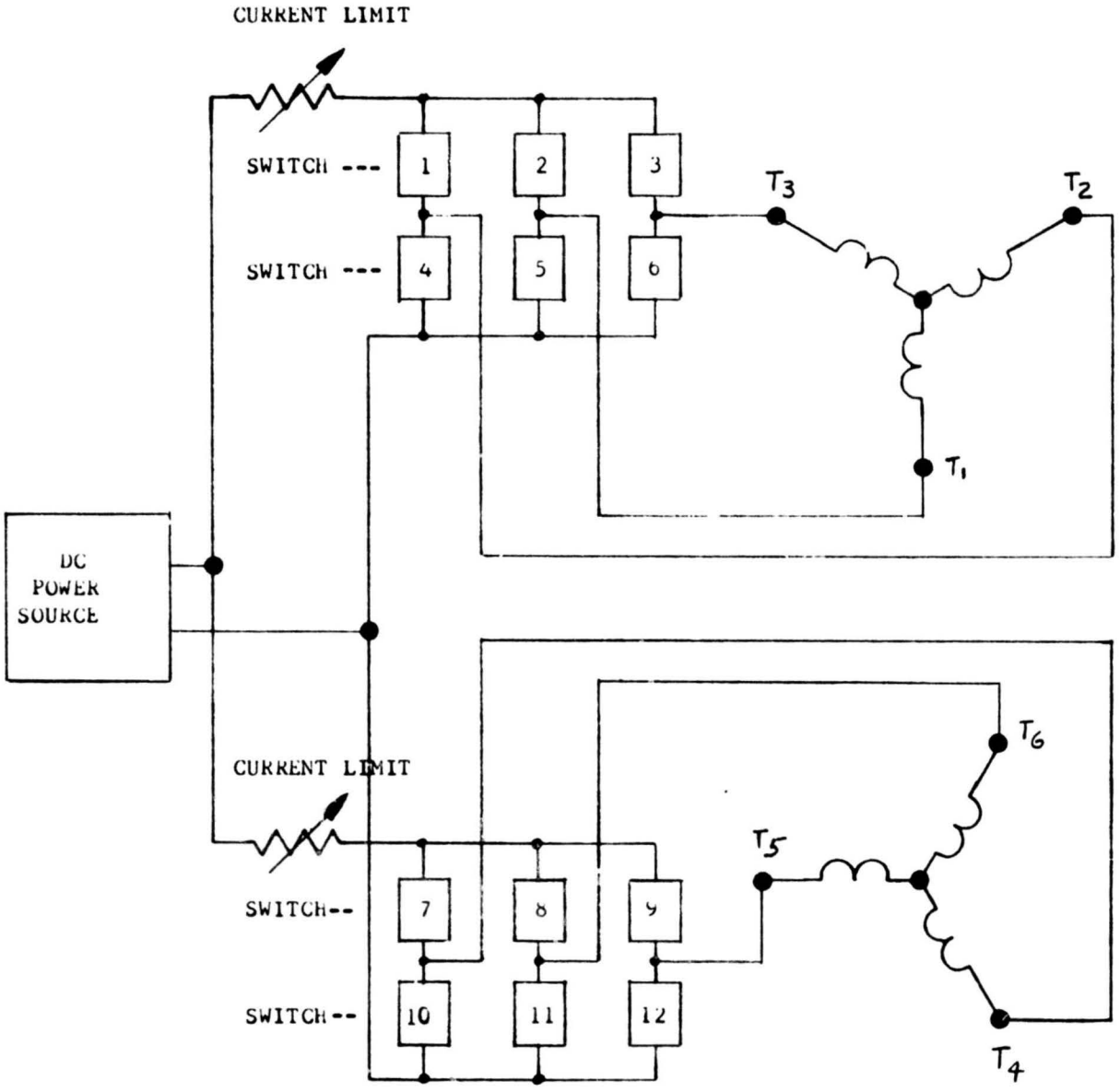

INTERWIRING OF STATIC COMMUTATOR ROTORS
TO MACHINE

Figure 5.1.1D

ware to accomplish this A to D conversion and pulse shaping can be achieved in much smaller size than shown in Figure 5.1.1C. The large scale integration circuit and new packaging techniques must be used to diminish the discrete component layout as shown on the vector boards. Figure 5.1.2A shows electrical schematic representing various connections between the shaft position sensing, A to D conversion and commutator module control. The machine hardware is also equipped with a forced air cooling system. This was needed so that repeated starts of flywheel acceleration during the starting mode of this brushless starter-generator system could be accomplished with minimum down time for cooling. In order to limit the current during this starting mode of this brushless starter generator set-up, carbon pile adjustable resistors were inserted between the DC voltage source and static commutator switches. This provided the test set-up with simple yet effective means for adjusting current levels within the safe magnitudes compatible with the solid state switches used in the breadboard mounted static commutator assembly.

5.2 System Excitation

In order to demonstrate the starting mode capability of this hardware it was necessary to provide system excitation within the brushless starter-generator assembly. This excitation was derived in the voltage regulator assembly board. A single oscillator was satisfactory to comply with different frequencies of excitation as needed by the machine and the shaft position inductors.

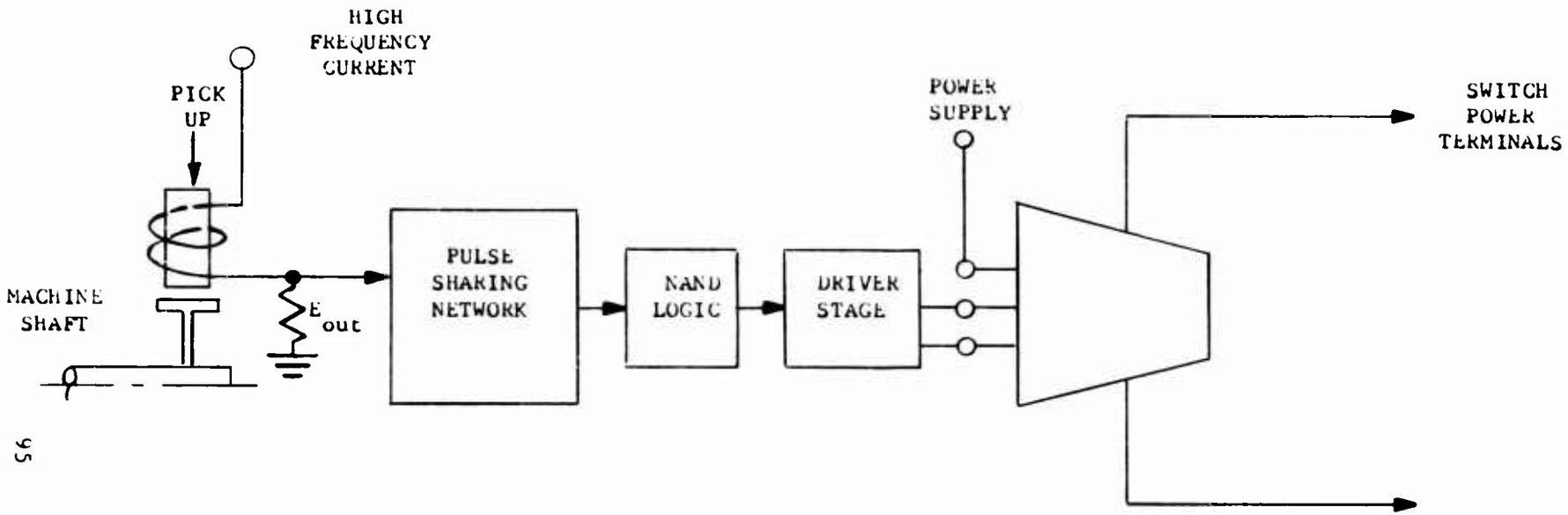

INTERWIRING OF SHAFT POSITION PICK-UP,
A/D CONVERTER AND STATIC COMMUTATOR MODULE

Figure 5.1.2A

5.2.1 Electromechanical Converter Excitation

The electromechanical converter excitation is achieved through the rotary transformer. Since the rotary transformer requires a controllable AC power, the AC type voltage regulator circuitry was designed and breadboarded.

The voltage regulator was operating as a single phase DC to AC inverter with pulse width control. By varying this pulse width, various amounts of machine excitation were achieved. One set of hardware covered both modes of the brushless starter-generator performance. During the generating mode excitation was quite low, contrary to that of the starting mode where excitation magnitudes were quite high, reaching to 50 and 60 ampere levels. To cover machine excitation over both generating and starting modes, variation in excitation frequency was necessary. This variation in frequency was achieved by the appropriate countdown using one high frequency oscillator. 2 to 4 KHz frequencies were used in the voltage regulator and the rotary transformer operation.

5.2.2 Shaft Position Indicator Excitation

The shaft position indicator excitation was derived from a common oscillator used in the voltage regulator. Its operating frequency was chosen to be at approximately 16 KHz. The isolated output provided a square wave voltage waveform capable of handling

highly inductive currents. This excitation channel is operated from a regulated DC voltage supply. The system transient voltage during the start-up, or otherwise, had practically no influence on the excitation output voltage magnitude; therefore, the transient interference was eliminated from the shaft position indicator channel.

5.2.3 Auxiliary Power Supplies

These supplies were substituted with 12 volt lead-acid type batteries. Where isolation was needed, a separate battery was used. The reason for this substitution was an expedience and contract cost savings since the system evaluation will be done only on what is possible to achieve with the limited capabilities of the static commutator. Again, this power supply substitution provided auxiliary power independent from the main power supply and its transients.

5.3 System Output Voltage Regulator

Since a rotary transformer is used for machine excitation, the voltage regulator circuitry must produce AC output to energize the transformer. The regulator circuitry assumed DC to AC, single phase inverter design. The input DC voltage was inverted into an AC square wave and in this case the square wave was pulse width controlled. The pulse width control allows variation in the output voltage of the voltage regulator; at the same time the rotary transformer will have variable output. With this the machine excitation will vary as required. To produce regulated

output voltage out of the brushless starter-generator system during the generating mode, the output voltage is being sensed and compared with the reference, the error actuates the width of the square wave pulse to be produced by the regulator circuitry to the rotary transformer which in turn varies the machine field excitation to regulate the output of the machine.

5.3.1 Design Approach

Figure 5.3.1A shows typical circuitry used in this AC voltage regulator design. Maximum current requirements during the starting mode reached 60 ampere levels. The circuitry required the choice of transistors capable of handling the required current. The input voltage to the regulator is 30 volts DC. Because of the push-pull switching transistor power stage and voltage doubling effect the power stage transistor voltages must be 60 volts minimum. The operating frequency of this DC to AC inverter is 2 to 4 KHz. During the starting mode, the lower frequency is being used; in the generating mode, higher frequency operation is incorporated. The square wave or digital type circuitry produced by the countdown IC's is amplified by several stages of switching transistor amplifiers. The driver stages provide the necessary width of pulse to energize the power transistors. The dynamic range of the control is from approximately 90% to zero output. The percentage of full "ON" condition is somewhat variable depending on frequency chosen for the operation

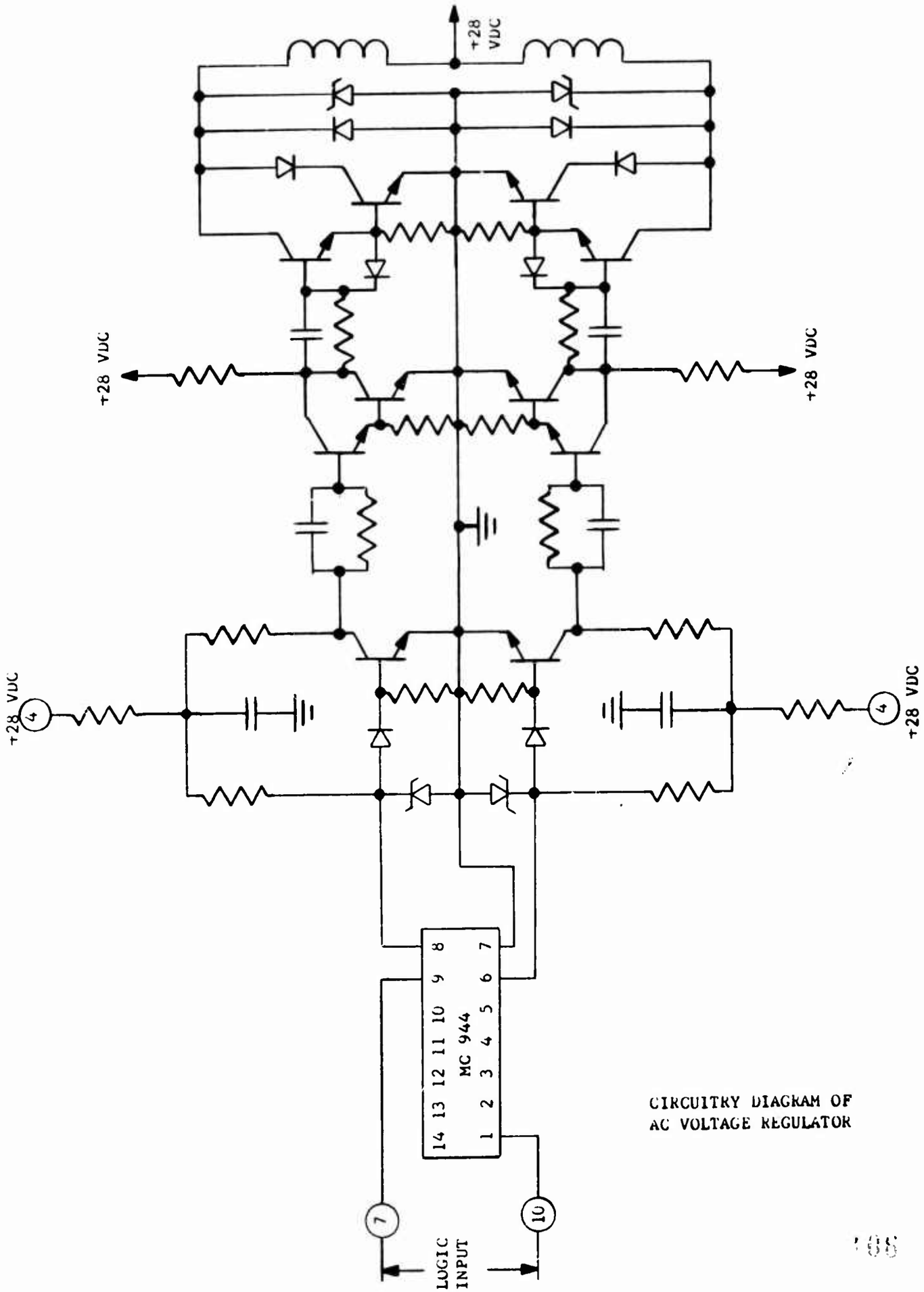

CIRCUITRY DIAGRAM OF
AC VOLTAGE REGULATOR

Figure 5.3.1A

of this voltage regulator. The rotary transformer winding, as seen in Figure 5.3.1A is center tapped so that only two power switching transistors are required to produce an AC output. Figure 5.3.1B shows an over-all view of the breadboarded AC voltage regulator. This breadboard assembly uses conventional discrete power transistor circuitry to achieve its end goal. The correct approach to this output voltage regulator package to be used on the aircraft would require similar packaging as that used in the static commutator circuit approach. Hardware of this nature was not contemplated to be procured for this program since the regulator is not a part of this contract.

5.3.2 Breadboard Evaluation

The designed voltage regulator breadboard was evaluated for its performance together with the rotary transformer mounted in the machine and loaded through rectification by the machine field windings. This made it possible to evaluate the performance of the rotary transformer. Figure 5.3.2A shows typical wave forms of output currents of the voltage regulator supplying the rotary transformer subassembly. The unit was capable of covering the full range of output control. The unit was tested at a variety of pulse width conditions and used in both generating and starting modes of this brushless starter-generator system operation. The regulator helped to establish that approximately 10 microhenries leakage inductance exists in the rotary transformer windings. It was shown that the leakage inductance of the rotary transformer controls the maximum available

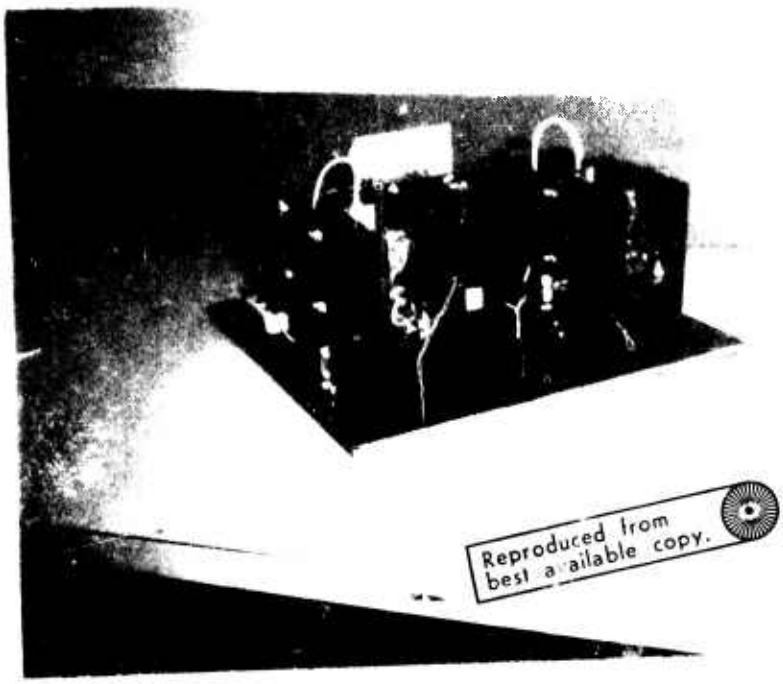
Reproduced from
best available copy.

STATIC VOLTAGE REGULATOR OUTPUT TRANSISTOR CURRENT
AT FULL LOAD FIELD EXCITATION

Transistor Q4

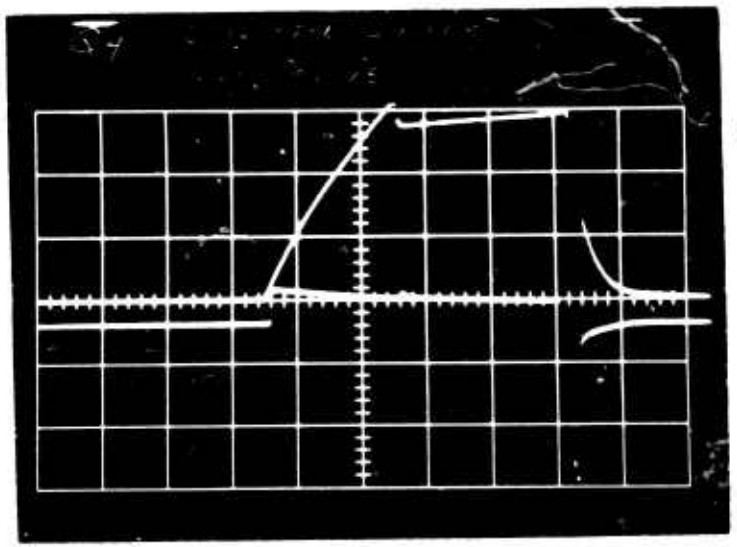

Top Trace - Collector Current - 25A/Div

Bottom Trace - Base Current - 4A/Div

Horizontal - 10 μsec/Div

Transistor Q8

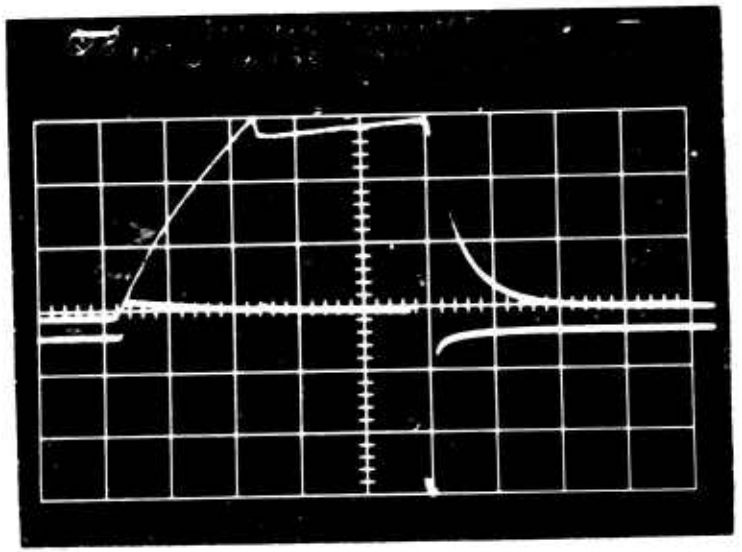

Top Trace - Collector Current - 25A/Div

Bottom Trace - Base Current - 4A/Div

Horizontal - 10 μsec/Div

Figure 5.3.2A

excitation to the machine.

The voltage regulator was connected into the system during the generating mode and proper stabilization and accuracy of output voltage control from the brushless starter-generator was achieved. The unit provided excitation for the low and high speed range just as well as no load to full load machine operating conditions.

SECTION VI

6.0 BRUSHLESS STARTER GENERATOR SYSTEM PERFORMANCE EVALUATION

Once all the necessary subassemblies to make up the brushless starter-generator system were fabricated, the system was put on test to evaluate the performance and compare it with the predicted values obtained during the design. The machine and its subassemblies, including all the auxiliary equipment necessary to operate a machine as a generator, was made available first, therefore the generating mode of this system was analyzed earlier in the program.

6.1 Generating Mode

For the tests in the generating mode, the brushless starter-generator was assembled to a complete package. In place of the static commutator, a mock-up static commutator assembly was made and attached to the machine. Figure 6.1A shows an assembled brushless starter-generator before the generating mode tests were performed. The initial generating mode tests were conducted to establish machine saturation voltage and verify the output ripple magnitude. Figure 6.1B shows typical machine saturation voltage versus machine field excitation. The tests were performed at 7,000, 9,000 and 12,000 RPM. The next set of generating mode tests were performed under the load conditions. The output of the machine was varied from zero to 200 amperes to obtain the measurements of the quality of the output voltage. Figures 6.1C and 6.1D show the output voltage ripple with and without the output filter. Figure 6.1C shows output

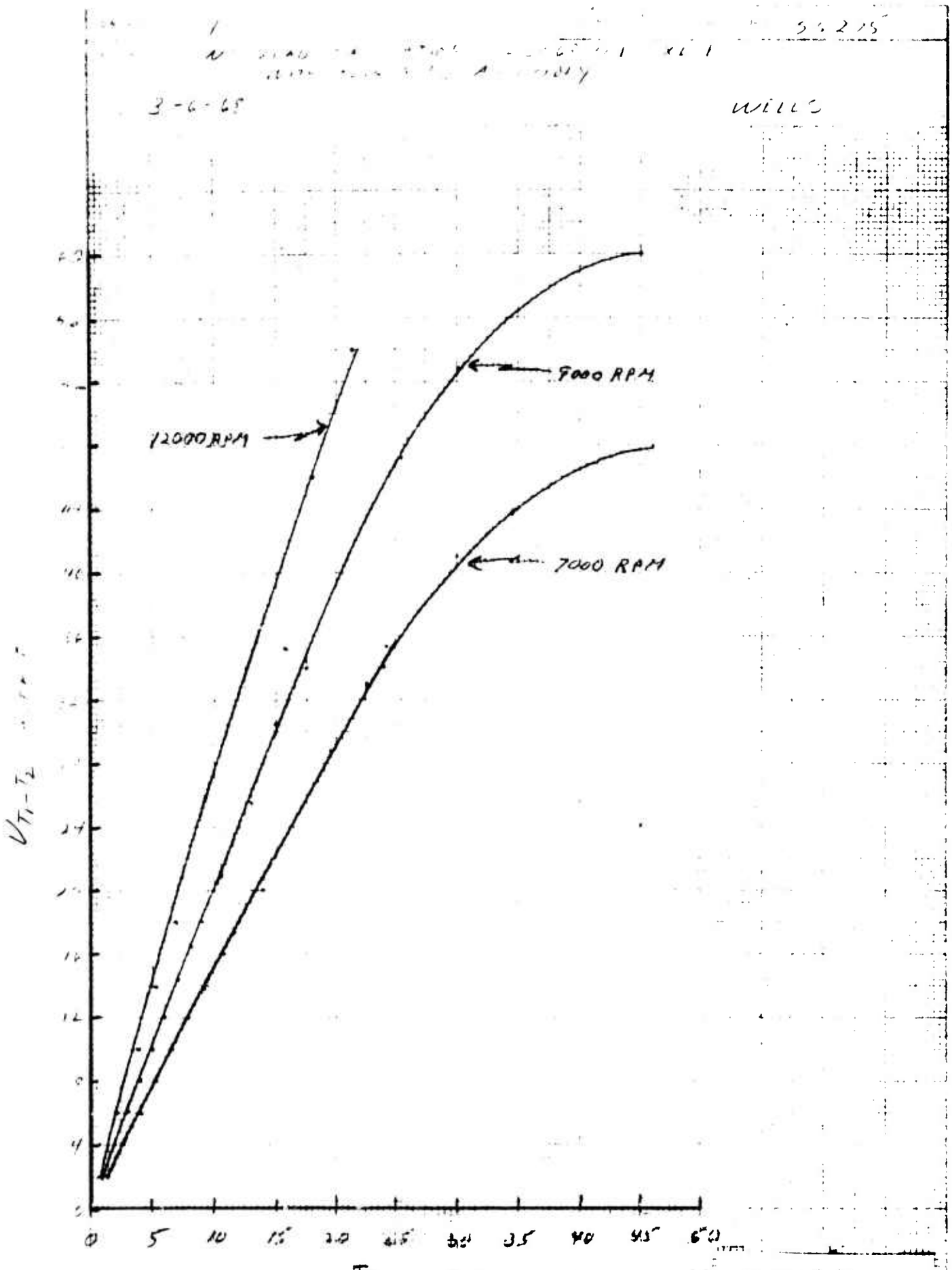
12000 RPM
9000 RPM
7000 RPM
$V_{T_1-T_2}$
0
5
10
15
20
25
30
35
40
45
50
I_{FLD} - D.C.

Figure 6.1B

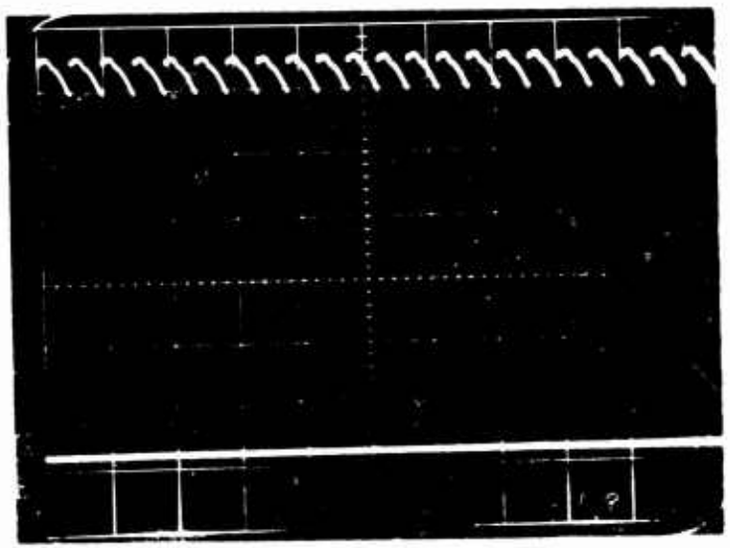

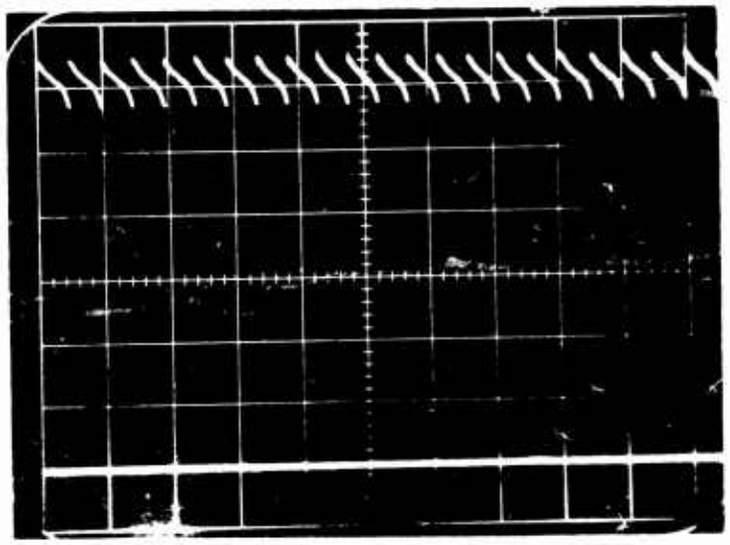

E_{load} = 30 V
I_{load} = 100 amp.
E_{field} = 6.6 V
I_{field} = 24 amp
Vertical = 5.0 V/Div.
Horizontal = 500 μsec./Div.
Machine Speed = 7000 RPM

E_{load} = 30 V
I_{load} = 200 amp.
E_{field} = 8.1 V
I_{field} = 31.0 amp.
Vertical = 5.0 V/Div.
Horizontal = 500 μsec./Div.
Machine Speed = 7000 RPM

Figure 6.1C

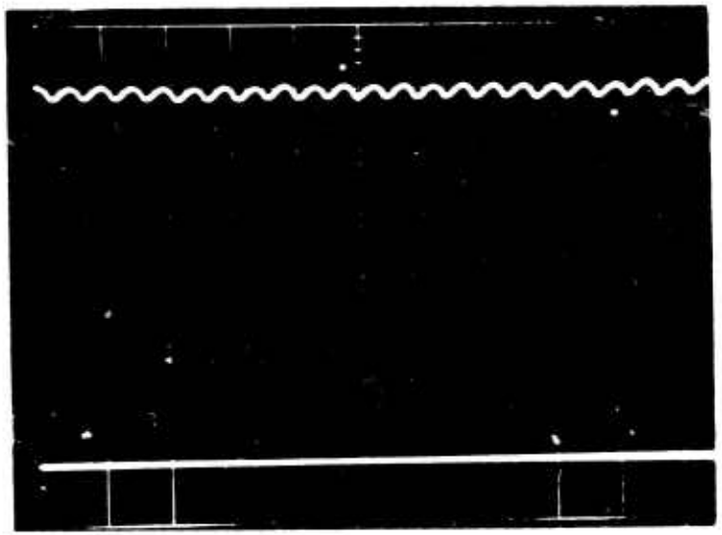

E_{load} = 30V

I_{load} = 100A

E_{field} = 6.2V

I_{field} = 22.5 amp

Vertical = 5.0 V/Div.

Horizontal = 500 usec./Div.

Machine Speed = 7000 RPM
with filter capacitor

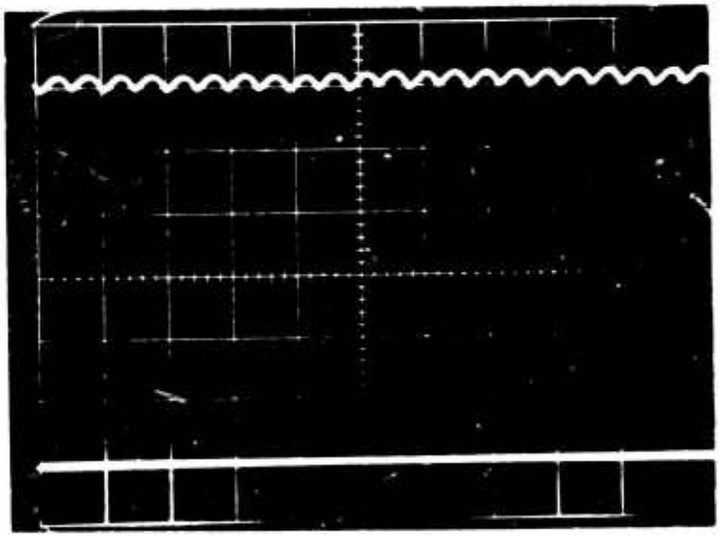

E_{load} = 30V

I_{load} = 200A

E_{field} = 7.8V

I_{field} = 31 amp

Vertical = 5.0 V/Div.

Horizontal = 500 usec./Div.

Machine Speed = 7000 RPM
with filter capacitor

Figure 6.10

voltage ripple without an output filter for half and full load conditions. From the information it becomes evident that unfiltered ripple voltage slightly exceeds peak to peak ripple requirements of the specification. Therefore, several simple filter configurations were investigated to reduce the output voltage ripple voltage to an acceptable value. Since the machine commutating reactance could be used as part of an inductive component of the LC filter, the single capacitor filter placed across the output terminals of the machine was satisfactory to reduce the ripple. The capacitor used was a 300 MFD tantalum. The output volt ripple utilizing the capacitor filter is shown in Figure 6.1D. Additional tests were run to determine the current balance in the windings and demonstrate the proper operation of a double bridge configuration, including two sets of three phase machine windings displaced 30 electrical degrees apart from each other. Figure 6.1E shows the rectifier current in one leg of each bridge and indicates a good balance between the currents. The next set of generating mode tests were performed to establish thermal capability of the machine and its rectifiers. During these tests the mechanical mock-up of commutator assembly was mounted on the machine to simulate the air flow conditions that will be present in the final assembly of the unit. Again, runs were made at 7,000 and 12,000 RPM, with full load current of 200 amperes. The air flow was adjusted to several different values and the effect on the machine and rectifier temperatures was monitored. The test data for these runs

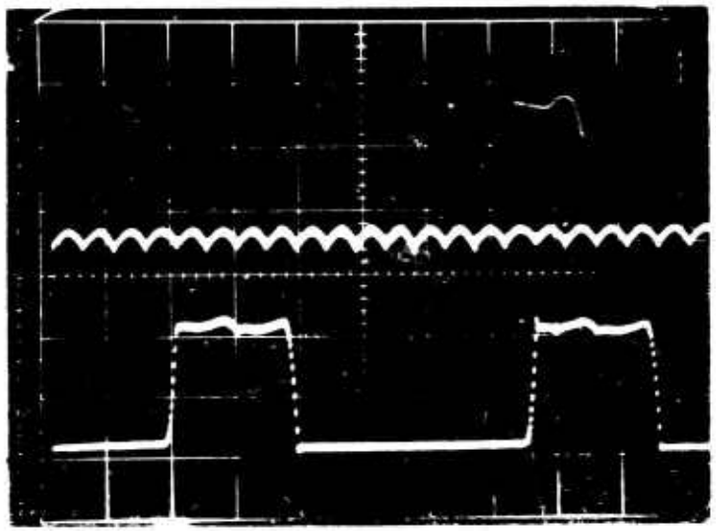

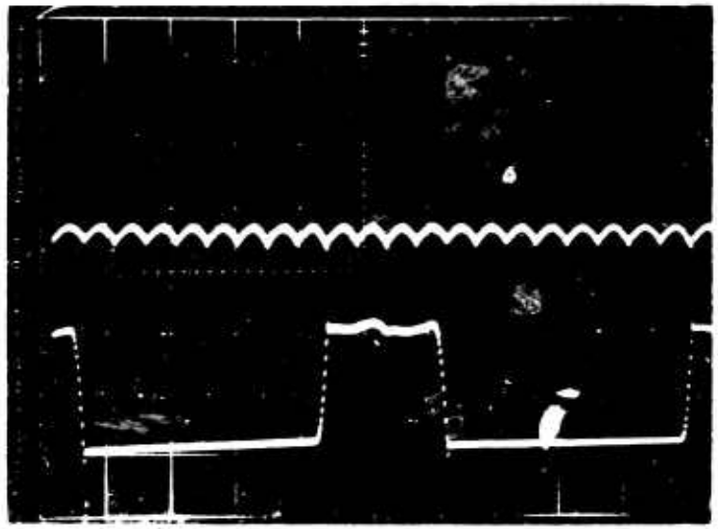

Top Trace - Total DC Current - 12.5A/DIV
Bottom Trace - 1/2 T2 Rectifier Current-6.2A/DIV
Horizontal - 500 μsec/DIV
Machine Speed - 7000 RPM

Top Trace - Total DC Current - 12.5A/DIV
Bottom Trace - 1/2 T5 Rectifier Current-6.2A/DIV
Horizontal - 500 μsec/DIV
Machine Speed - 7000 RPM

Figure 6.1E

is shown in Figures 6.1F and G. Curves of various machine temperatures and air flow are shown in Figures 6.1H and J. The rotor temperature was checked using temperature sensitive paints and indicated a maximum temperature of 425°F during these runs. The temperature ran slightly below the original temperatures predicted by the computer runs. This can be attributed to the difference in the exact air flow at various points in the unit, compared to the original values used in the computer calculations. All temperatures were well within the design limits for all conditions. During the thermal tests the commutator section was covered to prevent air leakage between the switch modules. A comparative run was made with the commutator section open. This required additional .45" of H_2O of inlet pressure to maintain the same air flow through the unit. This increase is fairly small and indicates that the unit could be run with this commutator section leakage open, if required. Finally, the starter-generator was tested under the full set of systems requirements, including AC voltage regulator and under the closed voltage loop conditions. Again, thermal tests were conducted at 7,000 RPM at full load of 200 amps for several volumes of inlet pressure and the effect of the unit temperature monitored. A thermal run was also conducted at 12,000 RPM and minimum inlet pressure and the temperatures at various points in the unit recorded. The test data for the various runs is shown in Figure 6.1K. A curve of air flow versus inlet pressure for 130°F inlet air is shown in Figure 6.1L. For an inlet

LEAR SIEGLER, IN
POWER EQUIPMENT DIVI
EXPERIMENTAL LABORATORY

E.W.O. 54024 MODEL NO. 23068-600 SERIAL NO. XL-1 DATE OF TEST 6-24-68

ROTOR NO. STATOR NO. BRUSH GRADE BAR PRESSURE

TITLE HEAT RUN - AIR FLOW

PARA NO.	TIME	E_L VOLT	I_L AMP	E_F VOLT	I_F AMP	SPEED RPM	AIR IN ←	AIR OUT	FRAME	A. DR. BRG.	#1 ELCT	#4 ELCT °F	#7 ELCT	#10 ELCT	STATOR WDG. END	STOR A.D. END
						7078	84									
						7078	82									
						7078	82									
						7078	82									
						7078	82									
						7078	82									
						7078	82									
	1540	30.0	200	7.32	32.0	7034	83	130	118	78	116	180	127	166	146	141
	1555	30.0	200	8.62	31.5	7035	87	161	144	114	122	185	135	176	173	181
	1610	30.0	200	8.65	31.5	7036	85	166	148	116	122	188	135	176	176	186
	1625	30.0	200	8.65	31.5	7035	84	166	148	116	122	186	136	177	176	188
6/25/68	1020	30.0	200	8.3	31.8	6974	130	164	145	137	153	204	162	194	178	181
	1035	30.0	200	9.0	31.8	7013	130	184	160	148	154	205	164	196	191	201
	1050	30.0	200	9.1	31.8	7015	130	187	164	150	154	206	164	197	193	203
	1105	30.0	200	9.1	32.0	7013	130	188	164	150	154	206	164	198	194	206
6/26/68	0900	30.0	200	8.5	30.5	7007	124	167	138	134	146	198	156	187	177	183
	0915	30.0	200	8.7	30.0	7010	130	180	148	146	153	205	163	194	188	196
	0930	30.0	200	8.75	30.5	7014	131	184	152	149	155	207	164	196	191	201
	0945	30.0	200	8.89	30.2	7017	130	184	152	148	154	206	164	196	191	201
	1010	30.0	200	8.6	30.2	7014	130	184	152	148	154	207	164	196	190	200
						7014	130									
						7014	130									
						7014	130									
						7014	130									
						7014	130									
						7014	130									

FORM 1349 A R 1 (6/65) PRECEEDING PAGE NO. FOLLOWING PAGE NO.

LEAR SIEGLER, INC.
POWER EQUIPMENT DIVISION
ENTAL LABORATORY TEST RECORD

EST 6-24-68 TEST LETTER: NO. 009673 TESTED BY WELLS

URE M.P. AIR GAP I.P. AIR GAP COG. ENGR. FAUCHT

PAGE OF

	#10 INLET	STATIC INLET DR. END	STATIC INLET ANTI DR. END	DR. DISC	#	STATIC INLET PRES. "H2O	FLOW MTR PRES. "H2O	INLET RECT. HOUSING "H2O	OUTLET RECT. HOUSING "H2O	BAR. PRES. "Hg.	FLOW MTR. FREQ. CPS	AIR FLOW CFM
					→	1.80	1.70	1.25	0.4	28.82	92	20.6
						2.0	2.0	1.49	0.5	28.82	102	22.2
						4.0	4.0	2.99	1.05	28.82	151	31.8
						8.0	8.0	6.01	2.06	28.82	225	47.9
						16.0	16.0	12.25	4.05	28.82	321	67.5
						26.0	26.01	20.05	6.49	28.82	409	80.7
						30.05	30.05	23.1	7.50	28.82	437	87.7
7	166	146	148	98	112	13.65	13.65	10.5	3.6	28.82	289	60.5
	176	173	183	113	126	13.9	13.9	10.75	3.7	28.82	290	60.5
	126	126	188	117	128	14.2	14.2	11.0	3.75	28.82	289	60.5
	122	126	188	118	129	14.1	14.1	10.9	3.75	28.82	290	60.5
	194	178	181	108	143	28.5	28.25	22.2	7.2	28.74	403	89.6
	196	191	201	119	149	29.3	29.55	22.9	7.45	28.74	406	89.6
1	192	193	205	124	151	29.2	29.4	22.8	7.4	28.74	405	89.6
1	198	194	206	126	152	29.1	29.2	22.7	7.4	28.74	406	89.6
	187	177	183	105	138	27.7	28.2	21.8	7.0	28.59	402	90
	174	188	176	114	146	28.1	28.35	21.9	7.1	28.59	405	90
1	196	191	201	120	150	28.1	28.3	21.85	7.05	28.59	404	90
1	196	191	201	122	150	28.0	28.2	21.8	7.05	28.59	404	90
1	196	190	200	124	150	28.0	28.2	21.8	7.05	28.59	406	90
						27.7	27.9	21.4	6.8	28.59	406	92.2
						22.0	22.1	16.9	5.4	28.59	360	81.0
						16.0	16.2	12.3	4.0	28.59	307	70.5
						8.0	8.15	6.1	2.05	28.59	215	50.2
						4.0	4.05	3.0	1.0	28.59	143	34.6
						2.0	2.05	1.5	0.45	28.59	100	23.7

FOLLOWING PAGE NO. A. F. SIC.

Figure 6.1F

SEP 16 19.

LEAR SIEGLER
POWER EQUIPMENT
EXPERIMENTAL LABORATO

E.W.O. 54024 MODEL NO. 23063-000 SERIAL NO. XL-1 DATE OF TEST 6-26-68

ROTOR NO. STATOR NO. BRUSH GRADE BAR PRESSURE

TITLE HEAT RUN - AIR FLOW

PARA NO.	TIME	E_L VOLT	I_L AMP	E_F VOLT	I_F AMP	SPEED RPM	AIR IN	AIR OUT	FRAME	AMB.	#1	#4	#7	#10	STATOR
							←					°F			
	1430	30.0	200	7.8	30.2	7004	126	172	148	138	156	214	169	205	186
	1445	30.0	200	8.35	30.2	7005	132	204	166	147	171	234	186	227	216
	1500	30.0	200	8.8	30.0	7008	129	207	169	160	169	232	184	225	216
	1515	30.0	200	8.88	30.1	7005	130	209	171	162	170	232	185	227	218
	1520	30.0	200	9.2	30.1	7004	127	218	178	166	178	247	196	244	232
	1530	30.0	200	9.2	30.1	7004	130	223	180	169	180	248	198	246	235
	1540	30.0	200	9.15	30.1	7002	130	226	183	172	182	250	200	248	238
	1550	30.0	200	9.15	30.1	7003	131	227	184	173	183	251	200	248	239
	1555	30.0	200	9.15	30.0	7001	130	233	189	177	192	263	212	264	248
	1605	30.0	200	9.31	30.1	7001	128	238	192	177	192	264	212	265	253
	1615	30.0	200	9.32	30.1	6997	131	242	194	178	195	267	216	268	257
	1625	30.0	200	9.32	30.1	7001	131	243	195	178	195	267	216	269	258
6/28/68	0950	30.0	200	7.0	25.5	12002	147	197	163	174	171	256	207	254	114
	1000	30.0	200	7.35	25.5	11997	128	229	186	182	194	269	215	268	246
	1010	30.0	200	7.8	25.5	12000	127	230	190	176	192	266	214	267	252
	1020	30.0	200	7.82	25.5	12002	129	232	192	180	196	270	217	271	255
	1035	30.0	200	7.9	25.0	12001	131	236	193	180	197	272	218	272	256
	1040	30.0	200	8.0	25.0	11998	131	234	193	180	198	272	218	273	256
									OPEN	CIRCUIT	A TAP		SECT	10	
	1130	30.0	200	8.1	30.0	7045	127	200	165	149	177	250	196	245	217
	1140	30.0	200	8.8	30.0	7046	128	221	178	160	181	255	202	251	234
	1150	30.0	200	9.0	29.8	7041	130	226	181	164	184	259	205	255	240
	1155	30.0	200	9.0	29.8	7044	130	229	183	166	184	259	206	256	242
	1435	30.0	200	8.89	29.5	7041	131	222	178	163	184	258	206	254	236
	1445	30.0	200	9.0	29.5	7044	132	229	184	167	186	260	207	256	242
	1450	30.0	200	9.0	29.5	7048	130	230	184	167	186	260	206	256	242
	1455	30.0	200	9.0	29.5	7047	131	231	185	166	186	260	207	256	242

LEAR SIEGLER, INC.
OWER EQUIPMENT DIVISION
TAL LABORATORY TEST RECORD

T 6-26-68 TEST LETTER: NO. 000673 TESTED BY WELLS

RE M.P. AIR GAP I.P. AIR GAP COG. ENGR. FEUCHT

PAGE OF

AIR REC'T	STATION DK. LEAD	SPARK PLUG 2.02 LEAD	DK. AIR. *		STATIC INLET PRES.	FLOW MTR PRES.	INLET REC'T PRESSURE "H20	OUTLET REC'T PRESSURE	DK. PRES. "Hg.	FLOW MTR. PRES. CPS	AIR FLOW CIM
205	186	188	128	144	12.3	12.4	9.5	3.15	28.58	261	60.8
227	216	226	124	163	12.6	12.7	9.8	3.3	28.58	263	60.8
225	216	228	130	163	12.6	12.7	9.8	3.3	28.58	263	60.8
227	218	230	132	166	12.6	12.7	9.8	3.3	28.58	262	60.8
244	232	244	136	174	8.4	8.5	6.5	2.15	28.58	213	50.2
246	235	248	138	177	8.4	8.5	6.5	2.15	28.56	212	50.2
248	238	252	140	180	8.45	8.5	6.55	2.15	28.56	212	50.2
248	239	253	142	180	8.45	8.55	6.55	2.15	28.56	213	50.2
264	248	261	144	186	6.1	6.15	4.7	1.55	28.56	177	41.2
265	253	267	146	188	6.1	6.15	4.7	1.55	28.56	178	41.2
268	257	271	148	190	6.1	6.15	4.7	1.55	28.56	177	41.2
269	258	272	149	192	6.1	6.15	4.7	1.55	28.56	179	41.2
254	114	220	132	183	6.1	6.15	4.7	1.7	28.73	186	45.3
268	246	258	147	198	6.1	6.15	4.7	1.7	28.73	169	43.3
267	252	262	148	200	6.1	6.15	4.75	1.7	28.73	169	43.0
271	255	270	147	202	6.1	6.15	4.75	1.7	28.73	170	43.0
272	256	269	149	204	6.1	6.15	4.75	1.7	28.73	170	43.0
273	256	268	150	204	6.1	6.15	4.75	1.7	28.73	170	43.0
SECTION											
245	217	222	124	163	6.5	6.65	4.7	1.55	28.74	291	68.3
251	234	246	134	174	6.5	6.7	4.75	1.55	28.74	291	68.3
255	240	252	137	178	6.55	6.7	4.75	1.55	28.74	291	68.3
256	242	255	139	180	6.55	6.7	4.75	1.54	28.74	291	68.3
254	236	246	132	174	6.55	6.7	4.78	1.55	28.74	292	68.3
256	242	254	138	179	6.55	6.7	4.78	1.55	28.75	292	68.3
256	242	256	140	180	6.55	6.7	4.78	1.55	28.75	291	68.3
256	242	257	140	181	6.55	6.7	4.75	1.55	28.75	291	68.3

Nº 5081
13 120

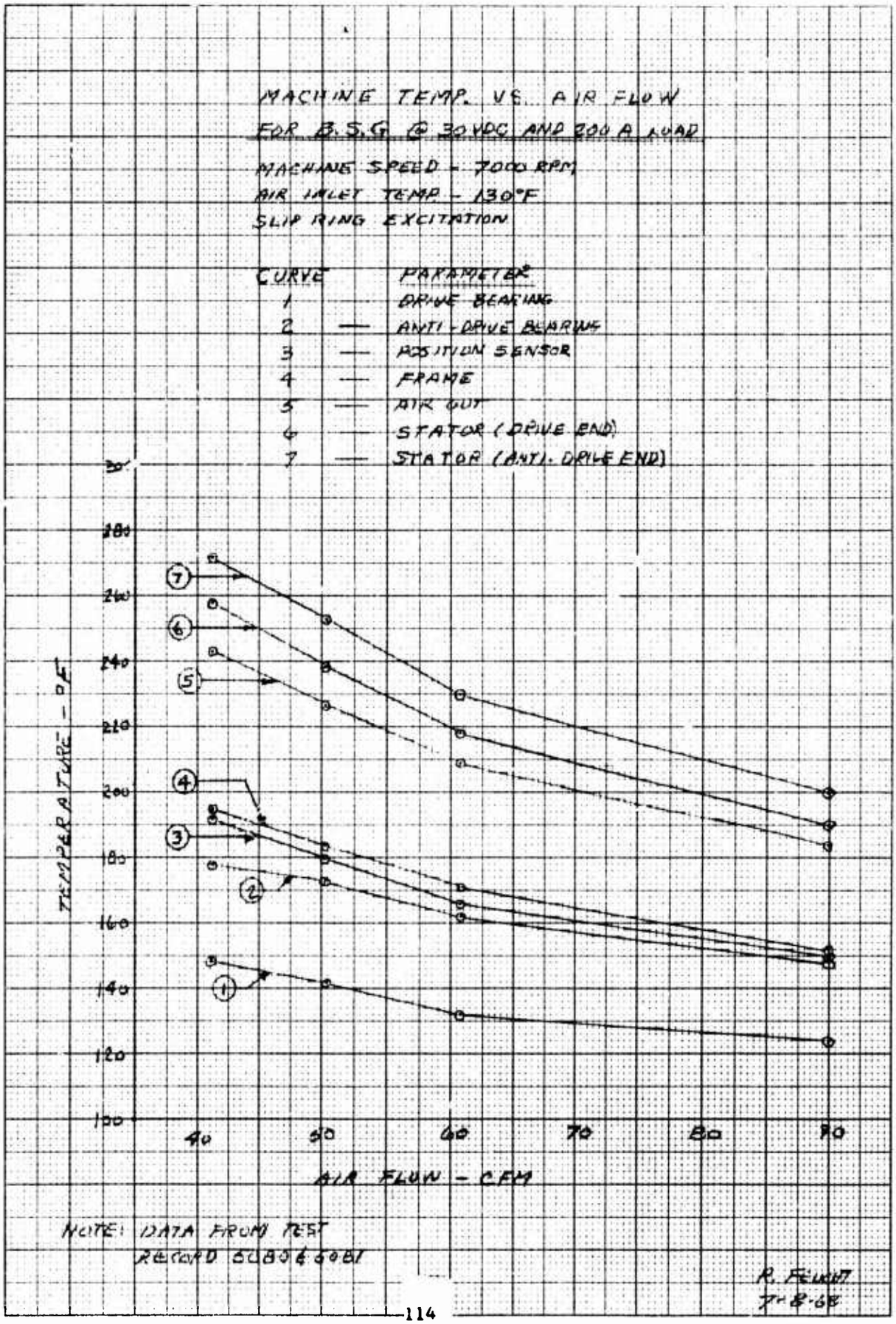
MACHINE TEMP. VS. AIR FLOW
FOR B.S.G @ 30 VDC AND 200 A LOAD
MACHINE SPEED - 7000 RPM
AIR INLET TEMP - 130°F
SLIP RING EXCITATION
CURVE PARAMETER
1 — DRIVE BEARING
2 — ANTI-DRIVE BEARING
3 — POSITION SENSOR
4 — FRAME
5 — AIR OUT
6 — STATOR (DRIVE END)
7 — STATOR (ANTI. DRIVE END)
TEMPERATURE - °F
AIR FLOW - CFM
NOTE: DATA FROM TEST RECORD SLBO & 60BI
R. FLIGHT 7-8-68

Figure 6.111

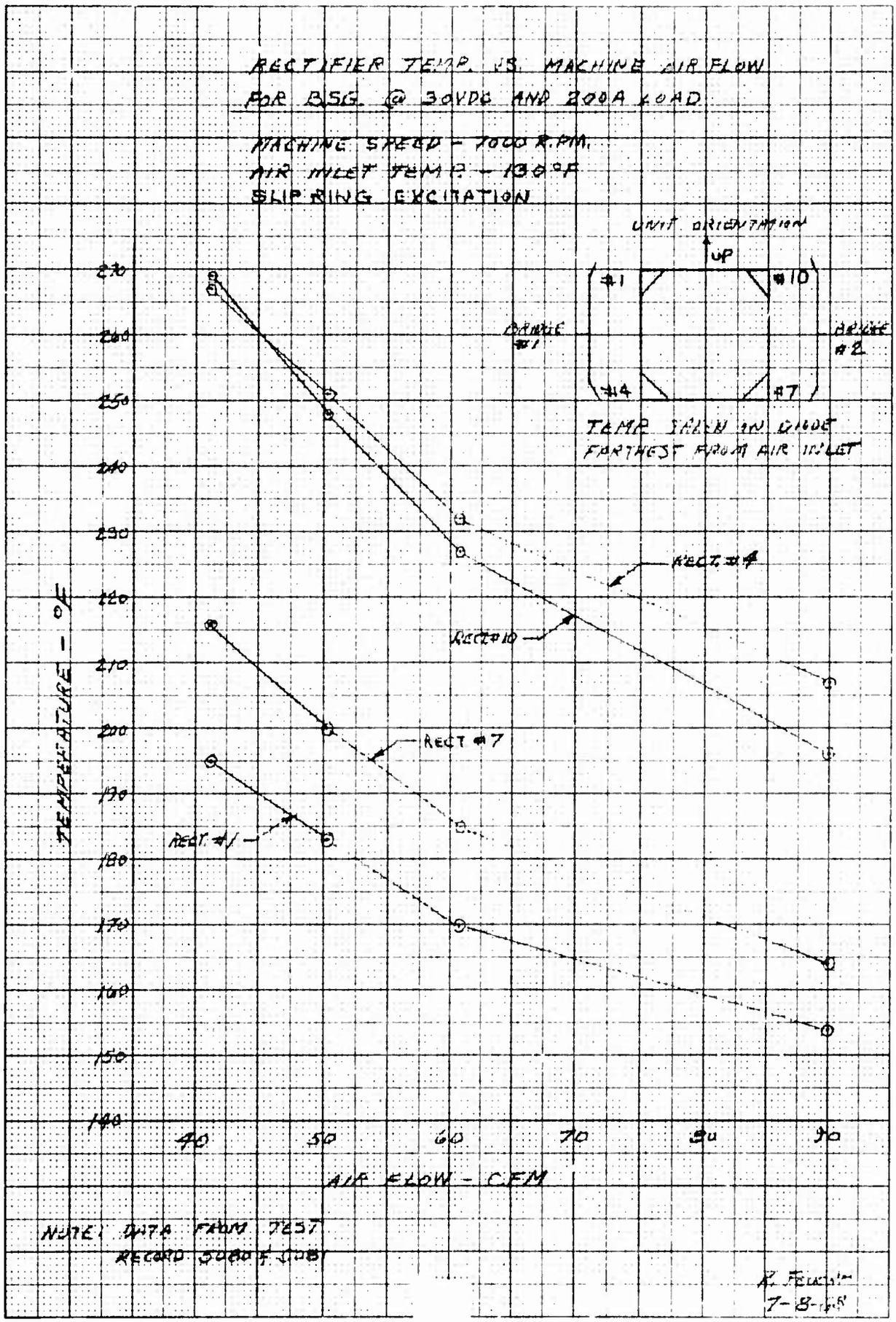

Figure 6.1J

LEAR SIEGLER,
POWER EQUIPMENT
EXPERIMENTAL LABORATO

E.W.O. 54024 MODEL NO. 23068 SERIAL NO. DATE OF TEST 4-17-69

ROTOR NO. STATOR NO. BRUSH GRADE BAR PRESSURE

TITLE

PARA NO.	TIME								AIR	AIR	GEN	RECT	RECT.	RECT.	
DATE	TIME		E_L	I_L		E_F	I_F	SPEED	IN	OUT	FRAME	#1	#4	#7	
			VOLT	AMP		VOLT	AMP	RPM	←						
												MAX. 300	MAX. 300	MAX. 300	
4-17	10 35	START	30.0	200		14.0	31.5	7000	130°	98°	103°	131°	132°	131°	
	10 45		30.0	200		14.08	33.0	7001	130	130	180	179	238	193	
	10 55		30.0	200		14.10	33.5	6998	131	138	190	182	240	195	
	11 05		30.0	200		14.15	33.5	6998	129	212	193	182	239	195	
	11 15		30.0	200		14.15	33.5	6998	130	210	195	183	241	196	
	11 25	STOP	30.0	200		14.15	33.9	6998	130	215	196	183	241	196	
	11 30	START	30.0	200		14.15	33.9	7001	132	223	200	195	256	211	
	11 40		30.0	200		14.15	34.0	7002	131	234	209	202	262	216	
	11 50		30.0	200		14.15	34.0	7002	132	233	208	198	259	213	
	12 00		30.0	200		14.15	34.0	7001	130	233	208	197	257	212	
	12 10	STOP	30.0	200		14.15	34.0	7002	130	233	207	197	257	211	
	12 15	START	30.0	200		14.5	34.0	7001	130	238	208	204	269	222	
	12 25		30.0	200		14.5	34.2	7002	131	243	213	207	270	226	
	12 35		30.0	200		14.5	34.2	6999	132	246	215	208	270	226	
	12 45	STOP	30.0	200		14.15	34.2	7000	130	246	215	207	269	226	
	12 45	START	30.0	200		14.15	34.2	7000	131	248	215	207	273	229	
	12 55		30.0	200		14.15	34.2	7008	130	249	216	209	273	228	
	1 05	STOP	30.0	200		14.18	34.5	7005	132	249	218	207	273	230	
	1 10	START	30.0	200		14.35	25.0	12000	132	249	218	212	272	232	
	1 20		30.0	200		14.4	24.0	11,998	131	252	219	211	273	231	
	1 30		30.0	200		14.38	24.0	12001	131	249	219	209	272	230	
	1 40	STOP	30.0	200		14.38	24.0	12001	130	249	218	210	272.5	230	

START & STOP INDICATED ABOVE REFERS TO CHAM
TOTAL RUNNING TIME = 10:35 AM → 1:40 PM

LEAR SIEGLER, INC.
POWER EQUIPMENT DIVISION
NTAL LABORATORY TEST RECORD

ST 4-17-69 TEST LETTER: NO. TESTED BY GEO. TESLOVICH

RE M.P. AIR GAP I.P. AIR GAP COG. ENGR.

PAGE 1 OF

RECT. #4	RECT #7	RECT #10	STATOR A.D.E	STATOR D.E.	BRG DR.	POS. SEN.	ORF. AIR IN	Q 4	Q 8	STATIC INLET PRE.	FLOW MTR PRE.	INLET RECT. HOUSING	OUTLET RECT. HOUSING	BAR PRE.	AIR FLOW	AIR FLOW
			°F							←	H2O	→		Hg	CPS	CFM
MAX. 300	MAX. 300	MAX. 300	MAX 350°	MAX. 350°	MAX. 325°			MAX 200	MAX. 200							
132°	131°	129°	125°	124°	102°	119°	76°	79°	80°	12.0	12.0	8.5	2.3	28.75	356	
238	193	238	222	214	125	167	76	140	114	12.0	12.0	8.6	2.4	28.75	357	
240	195	230	237	223	133	173	76	140	114	12.1	12.1	8.6	2.45	28.75	356	
239	195	230	240	224	135	174	75	140	113	12.05	12.05	8.60	2.45	28.75	357	
241	196	231	241	225	137	175	76	144	115	12.1	12.1	8.65	2.45	28.75	356	
241	196	230	241	226	137	175	76	144	115	12.05	12.05	8.65	2.45	28.75	356	61
256	211	246	249	237	139	182	75	147	115	8.45	8.50	6.1	1.9	28.75	292	
262	216	252	261	247	143	189	75	148	115	8.40	8.45	6.1	1.8	28.75	291	
259	213	249	261	246	143	188	75	149	115	8.40	8.40	6.1	1.75	28.75	289	
257	212	248	260	245	142	97	75	148	115	8.40	8.40	6.1	1.80	28.75	287	
257	211	247	259	244	142	186	75	146	115	8.35	8.35	6.05	1.75	28.75	287	52
269	222	259	265	252	143	190	75	145	113	6.4	6.45	4.65	1.25	28.75	247	
270	226	261	270	258	145	193	75	144	114	6.45	6.50	4.70	1.25	28.75	248	
270	226	262	273	259	145	194	75	144	115	6.5	6.5	4.70	1.25	28.75	248	
269	226	262	273	260	146	194	75	144	115	6.45	6.5	4.70	1.25	28.75	247	45
273	229	265	274	261	146	195	75	145	115	6.0	6.0	4.35	1.1	28.75	236	
273	228	265	276	263	147	195	75	144	115	6.0	6.0	4.35	1.1	28.75	236	
273	230	266	277	264	147	196	75	144	115	6.0	6.0	4.35	1.1	28.75	237	
																43
272	232	268	276	261	154	204	76	128	109	6.0	6.0	4.35	1.1	28.75	236	
273	231	268	276	261	155	205	76	127	109	6.05	6.05	4.4	1.1	28.75	236	
272	230	267	274	263	153	206	76	127	108	6.0	6.0	4.4	1.1	28.75	236	
272.5	230	267	274	261	155	212	76	130	108	6.0	6.0	4.35	1.1	28.75	237	
											H2O	Hg	BAR PRESS	STD.		
											12.05	.89	29.64	1.07		
TO CHANGE IN AIR FLOW AND OR SPEED											8.45	.625	29.38	1.08		
1:40 PM = 3 HR 5 MIN.											6.40	.472	29.22	1.09		
											6.00	.443	29.19	1.09		

Nº 5326

AIR FLOW VS. STATIC INLET PRESSURE
FOR BSG UNIT WITH CLOSED COMMUTATOR
MACHINE SPEED - 12000 RPM
AIR INLET TEMP 130°F

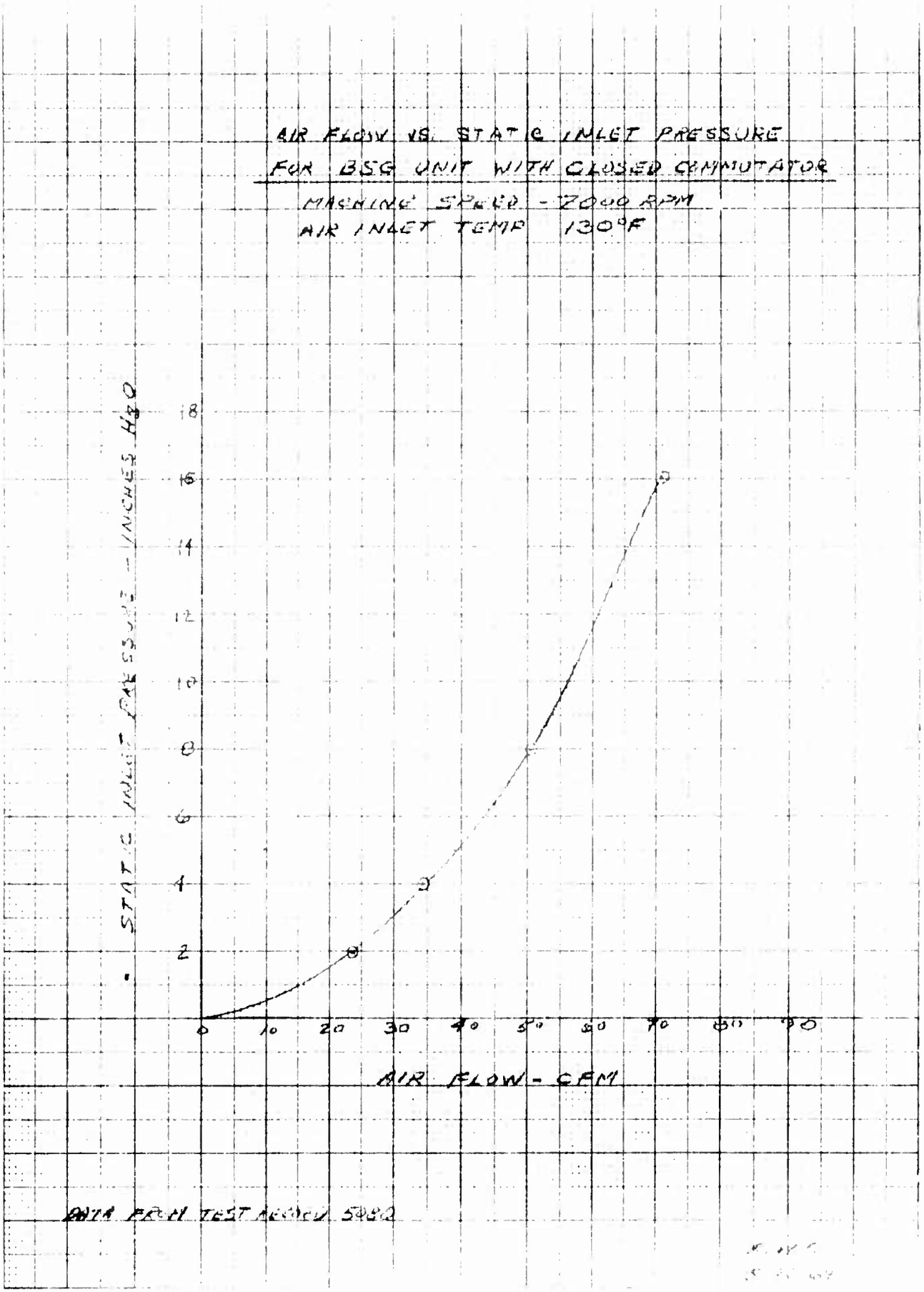

DATA FROM TEST #6004 5960

pressure of 6" of water (the maximum permissible pressure drop stated in MIL-G- 6162(2), the air flow is below the maximum allowable air flow stated in MIL-G-6162(2). A curve of machine temperature versus inlet pressure is shown in Figure 6.1M and indicates values well within the design limits of the machine. The rectifiers' stud temperature versus inlet pressure is shown in Figure 6.1N. It also indicates a reasonable safety margin compared to the maximum allowable stud temperature as indicated by the dotted line. (This dotted line is maximum allowable stud temperature shown by the manufacturer's data for an average current of 33 amps per rectifier and 120 electrical degree conduction, which are well above the conditions at full generator load). Throughout the thermal runs the machine and the breadboarded regulator functioned properly, demonstrating both electrical performance and mechanical integrity. In addition to the thermal runs, photographs were taken of the output ripple and harmonic analysis conducted at 7,000 RPM and 12,000 RPM at full and half load on the unit's output. The photographs of an output ripple at full and half load for two values of filter capacitors are shown in Figures 6.1P and Q, for a machine speed of 7,000 RPM. Figure 6.1R and Figure 6.1S show the output ripple at 12,000 RPM. In each case the output ripple was below maximum allowable ripple of 3 volts peak to peak based on 1.5 volts peak of either polarity from an average DC output. The results of harmonic analysis of an output ripple are shown in Figure 6.1T. On the graph the maximum allowable levels stated in MIL-G- 6162(2) are shown to indicate the

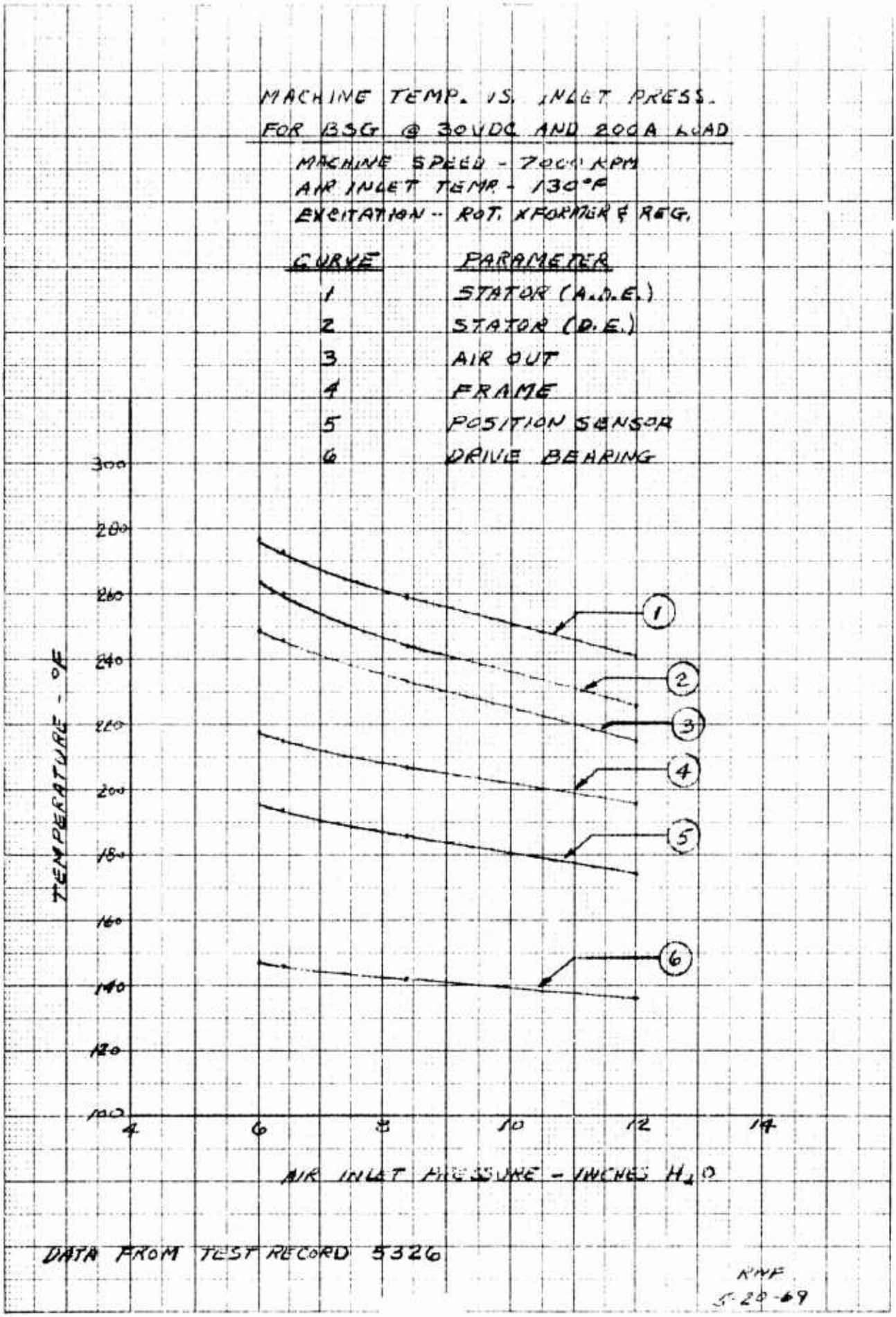

Figure 6.1M

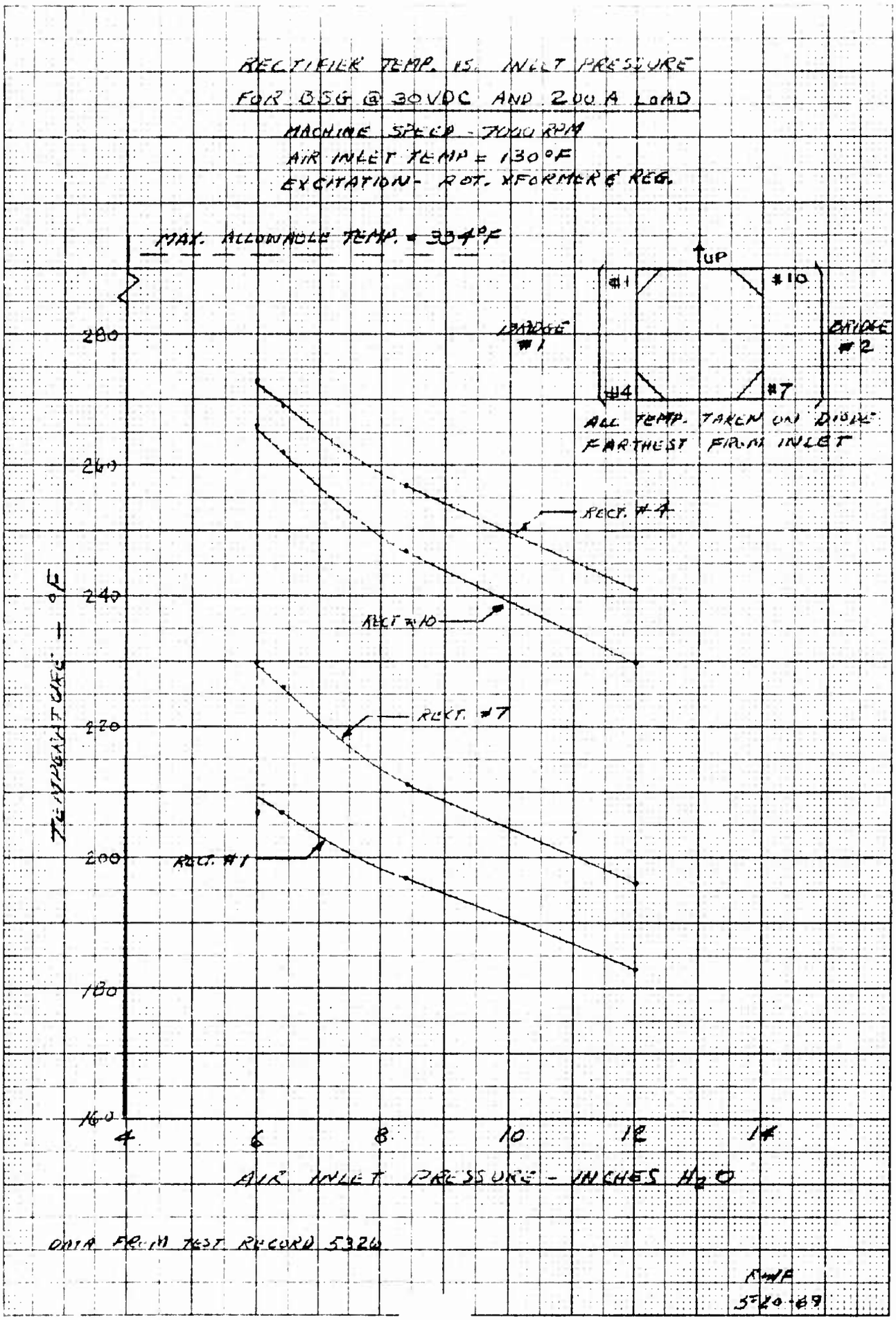
RECTIFIER TEMP. VS. INLET PRESSURE
FOR 85G @ 30VDC AND 200A LOAD
MACHINE SPEED - 7000 RPM
AIR INLET TEMP = 130°F
EXCITATION - ROT. XFORMER REG.
MAX. ALLOWABLE TEMP. = 384°F
UP
#1
#10
#4
#7
BRIDGE #1
BRIDGE #2
ALL TEMP. TAKEN ON DIODE FARTHEST FROM INLET
RECT. #4
RECT #10
RECT #7
RECT. #1
TEMPERATURE - °F
280
260
240
220
200
180
160
4
6
8
10
12
14
AIR INLET PRESSURE - INCHES H2O
DATA FROM TEST RECORD 5326
RMP
5-20-69

Figure 6.1N

OUTPUT RIPPLE VOLTAGE
7000 RPM - 300 MFD FILTER CAPACITOR

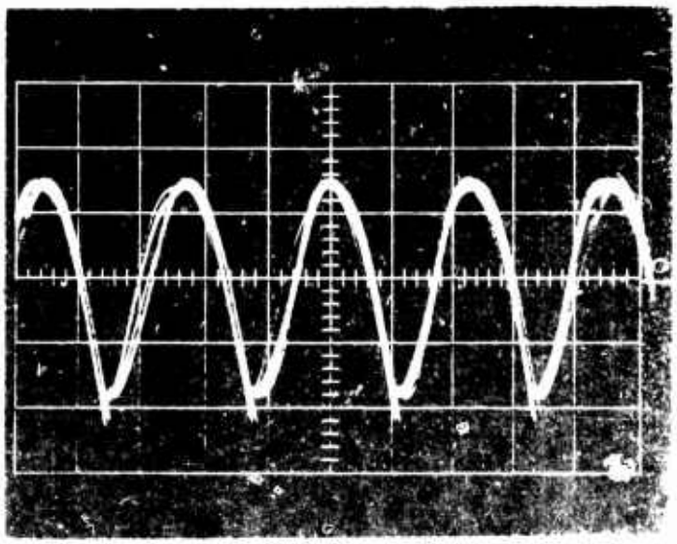

Load V = 30 V.DC
Load I = 100%
Vert. .5V/cm
Horiz. .1 msec/cm

Photo #1

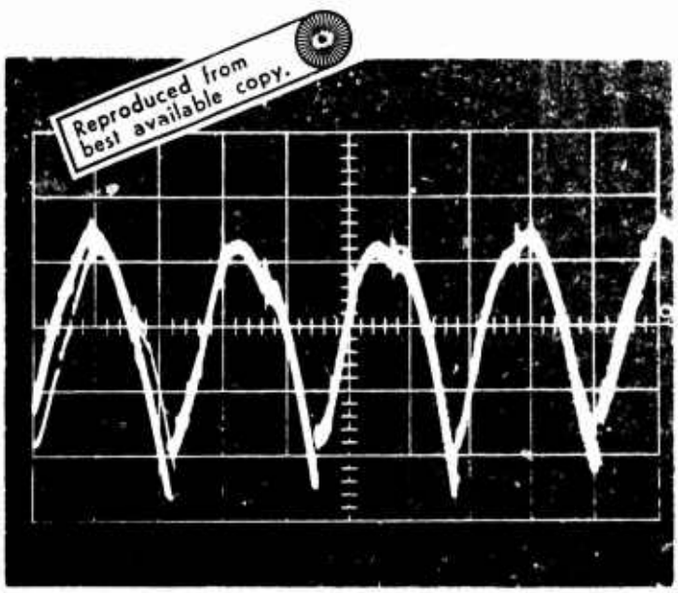

Load V = [illegible]
Load I = [illegible]
Vert. .5V/cm
Horiz. .1 msec/cm

Photo #7

Figure 6.1P

OUTPUT RIPPLE VOLTAGE
7000 RPM - 500 MFD FILTER CAPACITOR

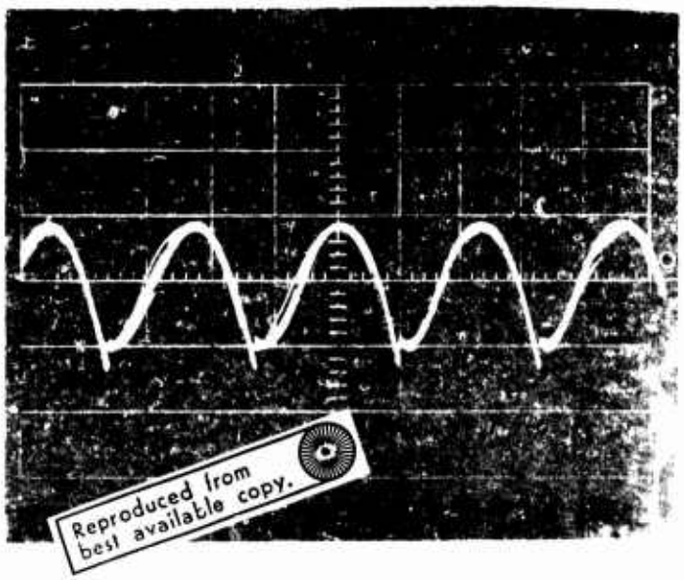

Load V = 30 VDC
Load I = 100A
Vert. .5V cm
Horiz. .1 msec/cm

Photo #2

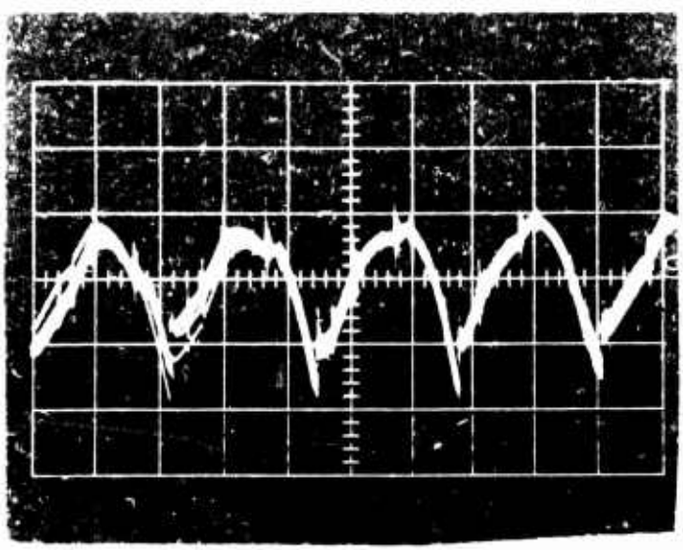

Load V = 30 VDC
Load I = 200A
Vert. .5V/cm
Horiz. .1 msec/cm

Photo #8

Figure 6.10

OUTPUT RIPPLE VOLTAGE
12,000 RPM - 300 MFD FILTER CAPACITOR

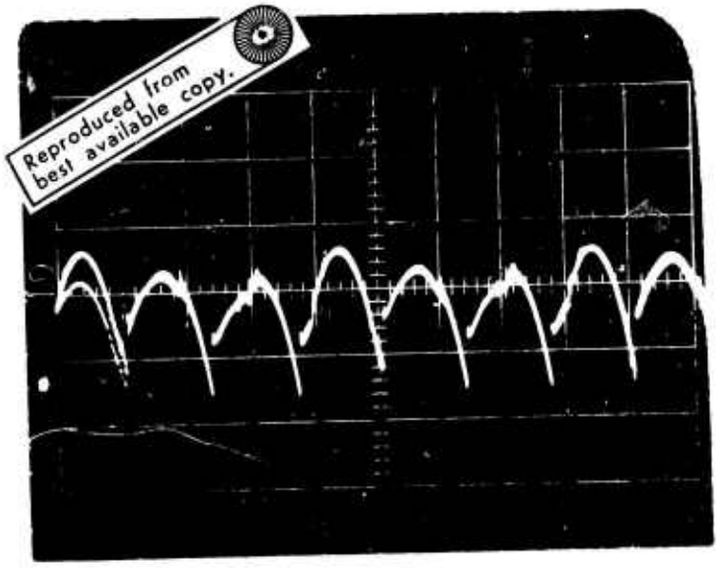

Load V = 30 VDC
Load I = 100A
Vert. .5V/cm
Horiz. .1 msec/cm

Photo #4

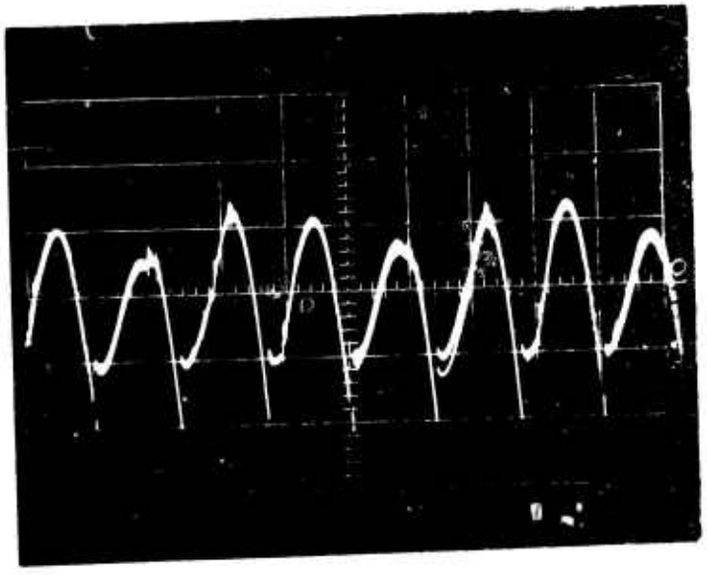

Load V = 30 VDC
Load I = 100A
Vert. .5V/cm
Horiz .1 msec/cm

Photo #5

Figure 6.1R

OUTPUT RIPPLE VOLTAGE
12,000 RPM - 500 MFD FILTER CAPACITOR

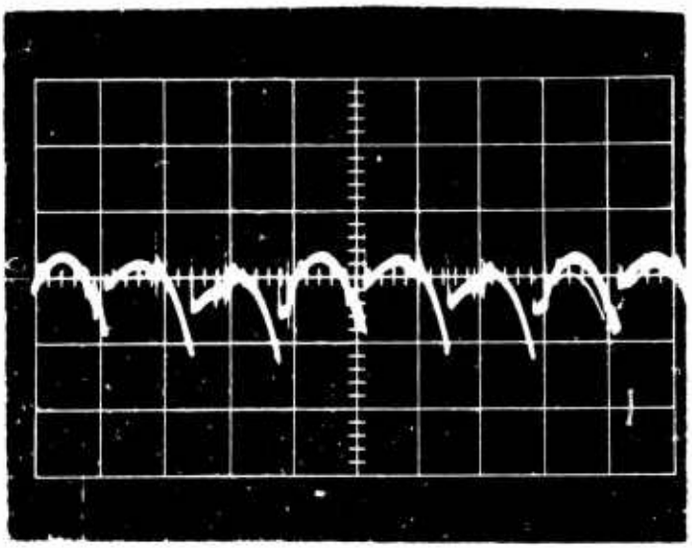

Load V = 30 VDC
Load I = 100A
Vert. .5V/cm
Horiz. .1 msec/cm

Photo #3

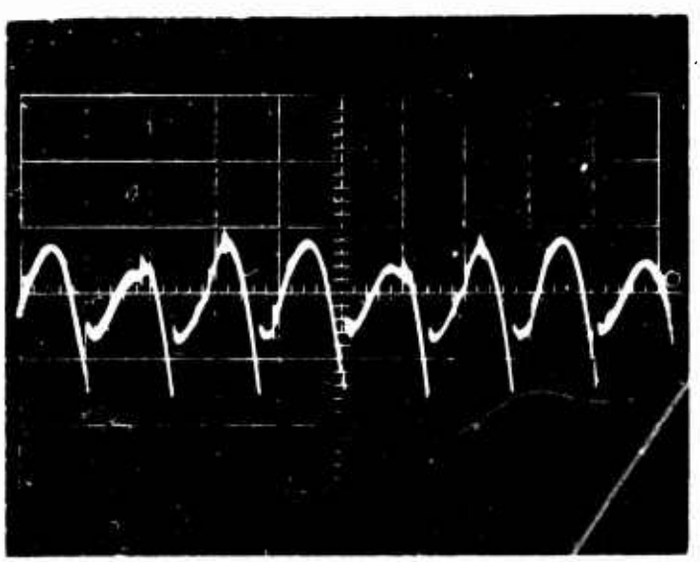

Load V = 30 VDC
Load I = 100A
Vert. .5V/cm
Horiz. .1 msec/cm

Photo #6

Figure 6.1S

KEUFFEL & ESSER CO

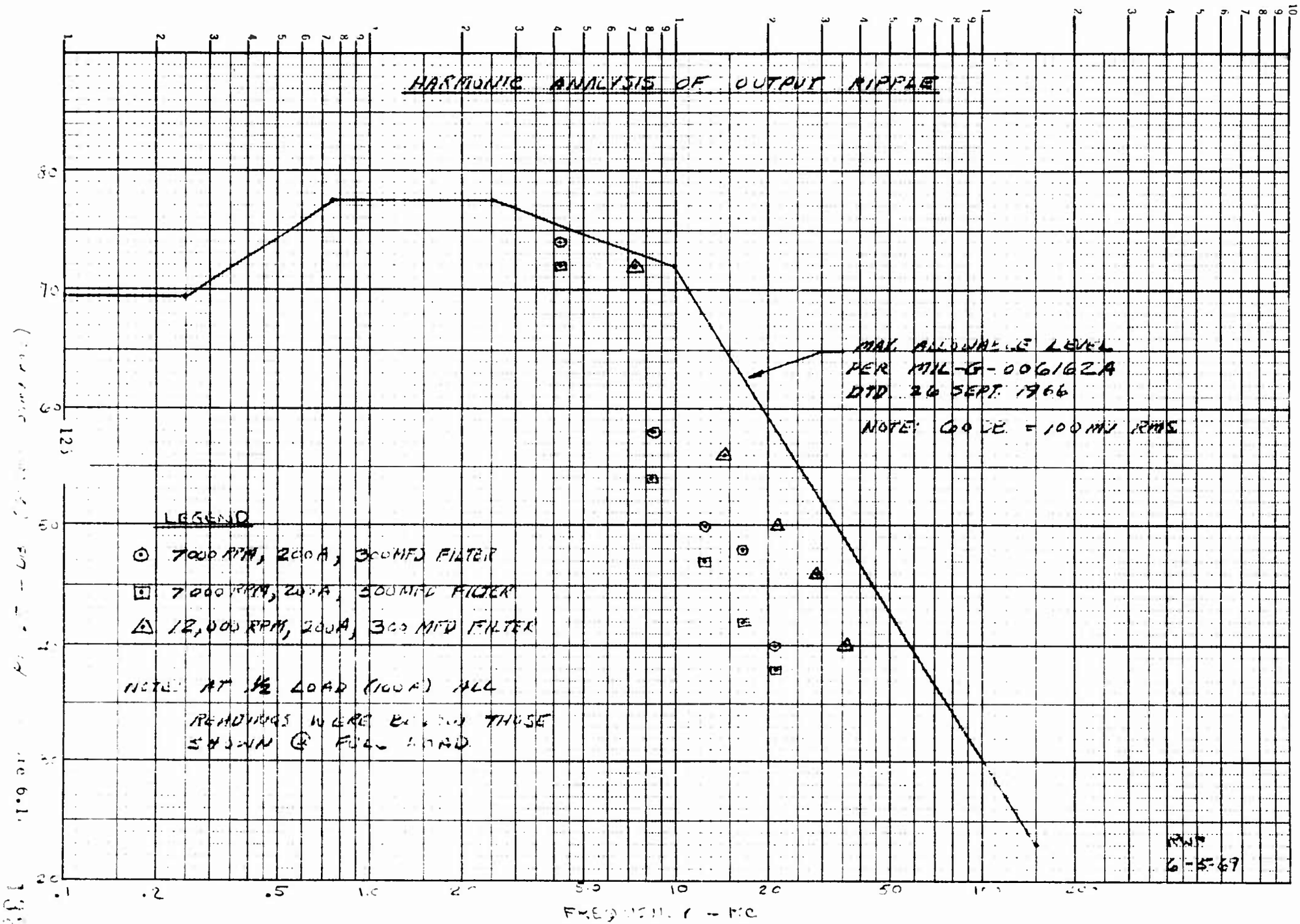

prescribed limits. All these points indicate all values were within the specified requirements for both values of filter capacitors. Based on these results, a 300 microfarad tantalum filter capacitor is sufficient to meet all the output ripple requirements of MIL-G- 6162(2). With these tests and collected data, brushless starter-generator performance as required by the specification was verified.

6.2 Starting Mode

The early tests of this brushless starter-generator in the starting mode were performed using 1/2 of the discrete component commutator. The discrete component solid state commutator was used for the preliminary tests in order to eliminate the possibility of system connection errors. Since the discrete component static commutator had only 100 amp capability, the tests performed were up to this level. The machine was connected to the torque head and inertia load. The discrete component solid state commutator was operated in the closed loop manner with position sensors. This constituted a full operation of a brushless starter-generator in its starting mode. The tests verified logic operation and provided initial data on machine performance. The system was operated up to the current level of 100 amps and the torque of the unit measured at various field excitations. Figure 6.2A illustrates the torque/current relationship of the machine. The tests were repeated with the other set of machine windings and similar results were obtained. These preliminary tests indicated torque levels slightly above those

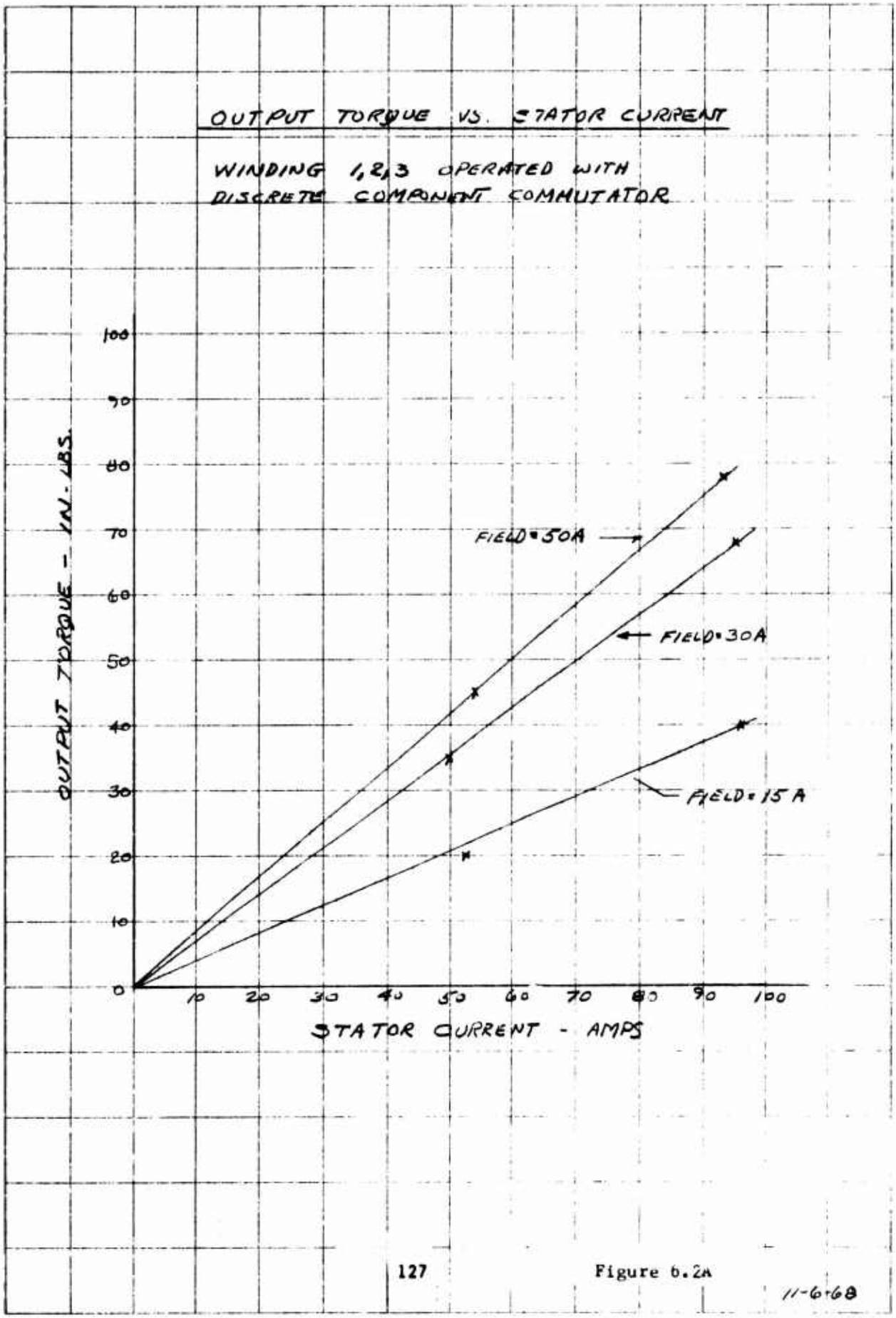

Figure 6.2A

11-6-68

originally predicted. Based on these tests, one can deduct that the full output torque can be achieved when operating at full stator current. Therefore, the tests of discrete component static commutator and the machine confirmed the design for 40 lb/ft. torque at 800 amp input current as specified in Exhibit "A" of the contract. Also, during these tests, the various circuit waveforms were monitored and recorded on photographs to provide complete documentation of circuit operation. The remainder of the starting tests on the system were performed with actual solid state commutator switches assembled on the breadboards. Figure 6.2B shows the arrangement of solid state commutator switches around the periphery of the machine. The machine was coupled to the torque head and the torque head was coupled to the flywheel. The flywheel was the only load used for these tests (Attempts to obtain a better definition of engine load were of no avail. The same is true for the attempts to assign a known jet engine appropriate for this rating of a unit). The test set-up was equipped with automatic, 10 seconds duration, cut-out relays. These relays, after ten seconds of operation, de-energize the system automatically so that any human error would be eliminated in testing the starting torque at high current levels with derated solid state commutator switches. Before the set of starting mode characteristics were obtained by test, the system was pre-tested in various conditions as outlined below:

a) 3-phase, half-wave operation of negative switches with resistive load and signal generator logic sources.

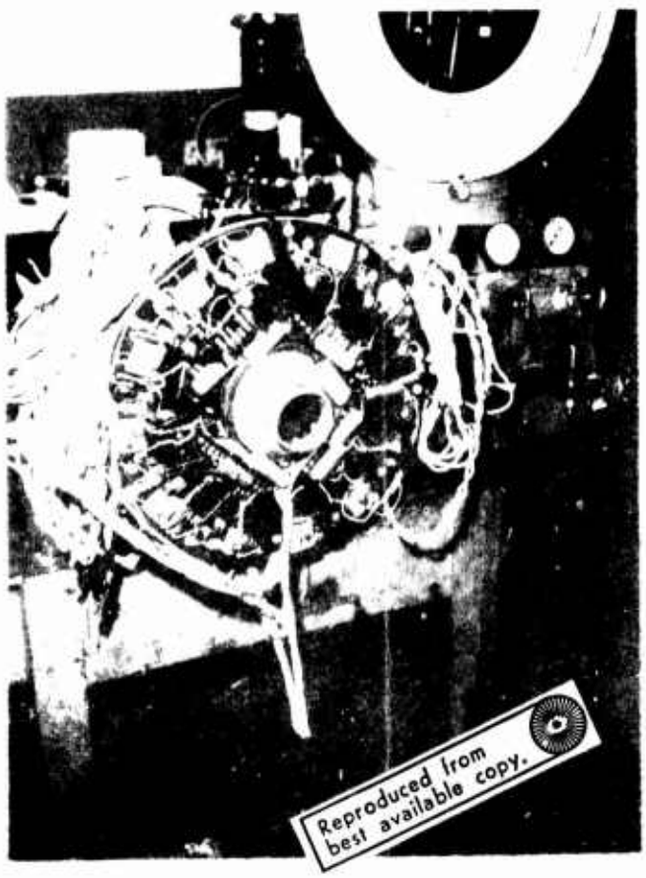

SOLID STATE COMMUTATOR ARRANGEMENT
FOR STARTING TESTS

Figure [illegible]

b) 3-phase, high wave operational positive switches resistive load and signal generator logic source.

c) 3-phase, full-wave operation with resistive load and signal generator source.

d) 3-phase, full-wave operation with the machine and signal generator logic source.

e) 3-phase, full-wave operation with the machine using position sensor output as the logic source. This is the complete closed loop arrangement of the brushless starter-generator.

f) Simultaneous operation of both 3-phase commutator bridges with machine using position sensor source. Again, this is the use of a full commutator with all the feedback loops in operation to utilize the full capabilities of the system considering the limitations imposed by derated commutator switches.

Steps a) through e) were completed on bridge No. 1 up to the current levels up to 300 amps. This current level was chosen since several switches were derated to 334 amps and 300 amps allowed a reasonable safety factor during this evaluation. Tracings taken from photographs of the switch waveforms operating at 300 amps with the machine as shown in Figure 6.20. Note that VCE at turnoff was well within the 80 volt rating of the switches. While operating bridge No. 1, Step e) preliminary torque ratings were obtained for several values of field current. The results of these preliminary tests indicated an

12-3-68

LSI TEST POS. SW. #16

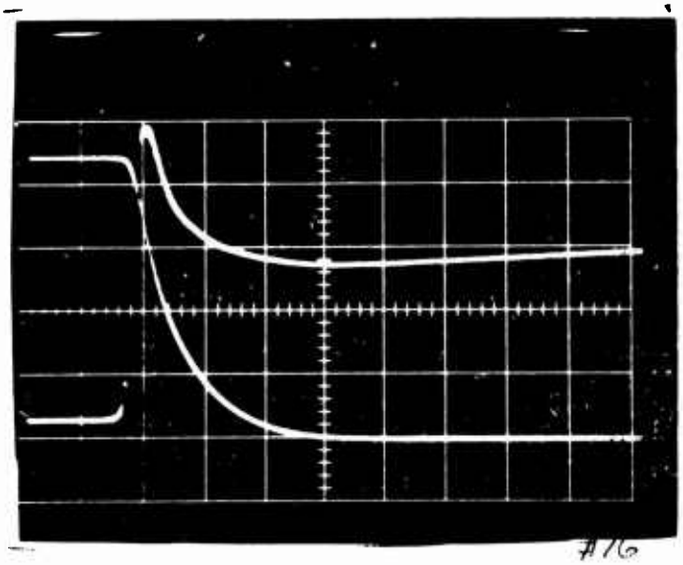

TURN OFF

V_{CE} 10 V/DIV

I_C 62.5 A/DIV

SWEEP 5 μSEC/DIV

SYNC. POS LOGIC SLOPE

300 A LOAD

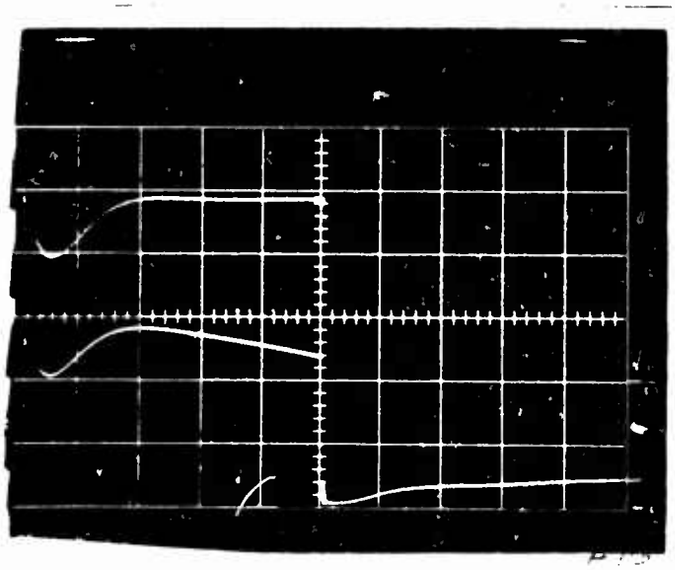

SATURATION VOLTAGE

TOP V_{CE} 1V/DIV

BOT. I_C 125A/DIV

SWEEP [illegible] μSEC/DIV

SYNC. NEG LOGIC SLOPE

300 A LOAD

Figure 6.2C

output torque of 16.7 lb/ft. with 300 amps commutator current and 50 amp field excitation. Extrapolation of these results indicated a torque of 22.3 lb/ft. with result at 400 amp operation with a single bridge. This would result in a total machine torque of both bridges operating at 400 amps each of 1.866 x 22.3 = 41.5 lb/ft. torque. Although these preliminary results indicated a full output torque of 800 amps is feasible, operation at these current levels cannot be achieved with the present commutator switches since several switches are derated. Bridge No. 2, the second half of this solid state commutator, was so evaluated in the same step-by-step manner. During these tests a failure occurred which damaged two solid state commutator switches. Although various corrective actions were taken, the true reason for switch failure cannot be accounted for. This reduced the program to practically no spare switch operation. In order to avoid any future mishaps, the complete system was derated to 400 amps total input current. This meant that the performance achievable from the system is reduced by two. Because spares from RCA were not available, a detailed analysis into the failure mode of these switches was impossible to perform. The risks in continuing this analysis were great and threatened to leave the program without a set of starting mode performance characteristics. Both halves of the starter commutator were connected into the full set of machine windings and tests at 400 amp input current were performed. The oscillograph traces were taken recording the switch performance, the torque produced and speeds achieved. Figures 6.2C, D, E, F and G show the data as taken on the

STARTING MODE PERFORMANCE
(OSCILLOGRAPH TRACE)

Figure 6.2C

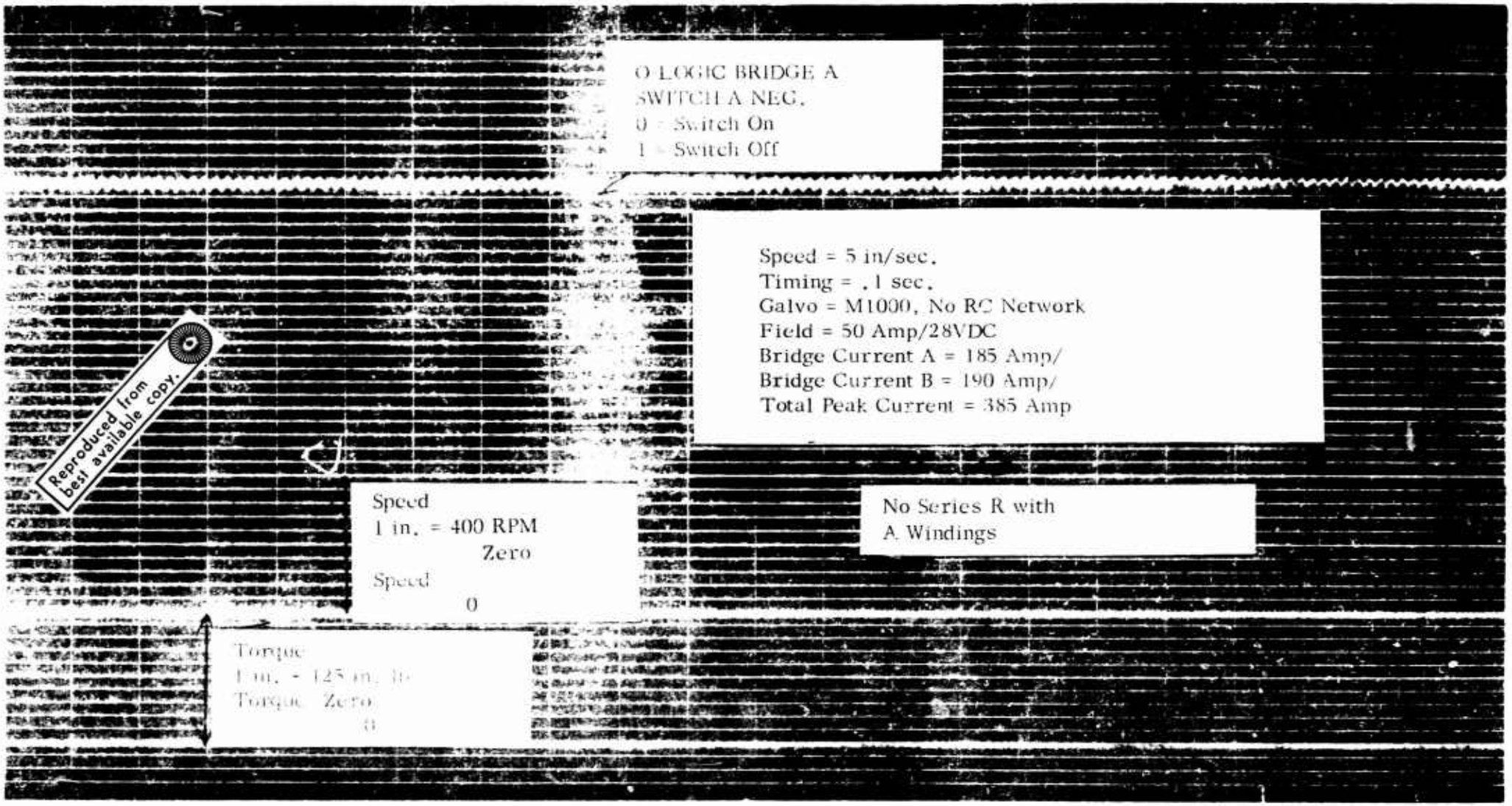
O LOGIC BRIDGE A
SWITCH A NEG.
0 = Switch On
1 = Switch Off
Speed = 5 in/sec.
Timing = .1 sec.
Galvo = M1000, No RC Network
Field = 50 Amp/28VDC
Bridge Current A = 185 Amp/
Bridge Current B = 190 Amp/
Total Peak Current = 385 Amp
Reproduced from best available copy.
Speed
1 in. = 400 RPM
Zero
Speed
0
No Series R with
A Windings
Torque
1 in. = 125 in. lb
Torque Zero
0

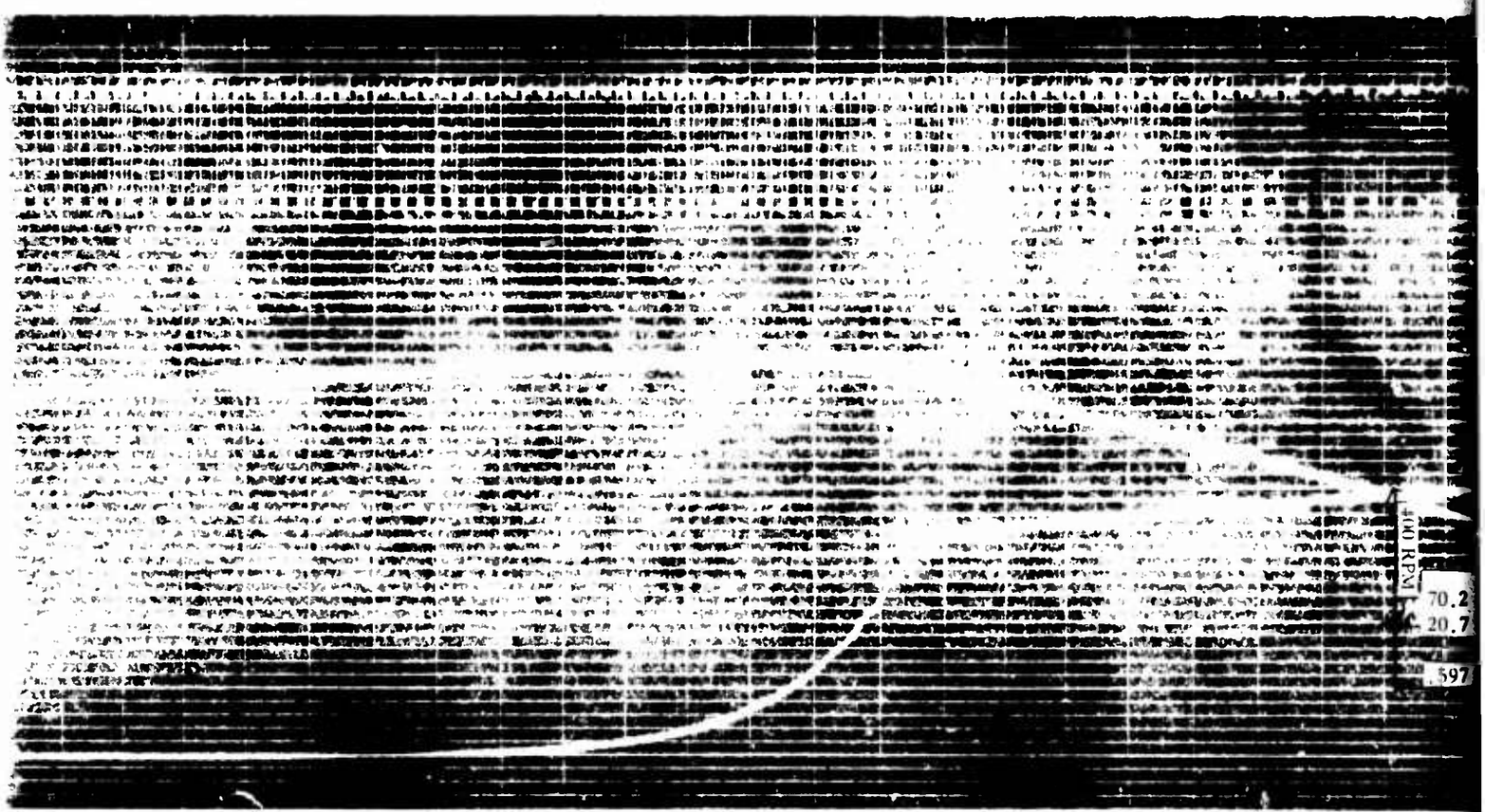

A

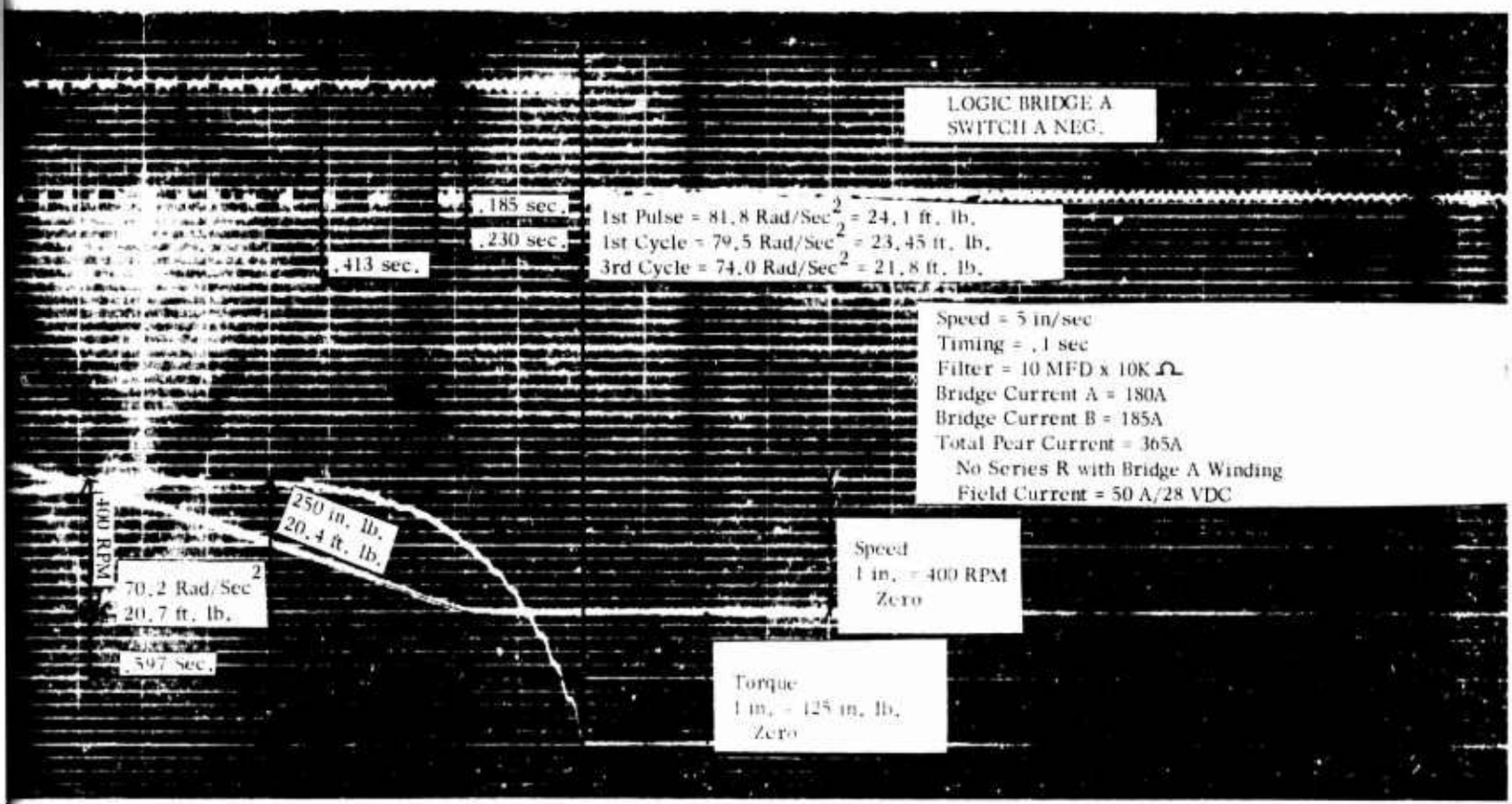
LOGIC BRIDGE A
SWITCH A NEG.
.185 sec.
.230 sec.
.413 sec.
1st Pulse = 81.8 Rad/Sec^2 = 24.1 ft. lb.
1st Cycle = 79.5 Rad/Sec^2 = 23.45 ft. lb.
3rd Cycle = 74.0 Rad/Sec^2 = 21.8 ft. lb.
Speed = 5 in/sec
Timing = .1 sec
Filter = 10 MFD x 10K Ω
Bridge Current A = 180A
Bridge Current B = 185A
Total Pear Current = 365A
No Series R with Bridge A Winding
Field Current = 50 A/28 VDC
400 RPM
250 in. lb.
20.4 ft. lb.
70.2 Rad/Sec^2
20.7 ft. lb.
.597 sec.
Speed
1 in. = 400 RPM
Zero
Torque
1 in. = 125 in. lb.
Zero

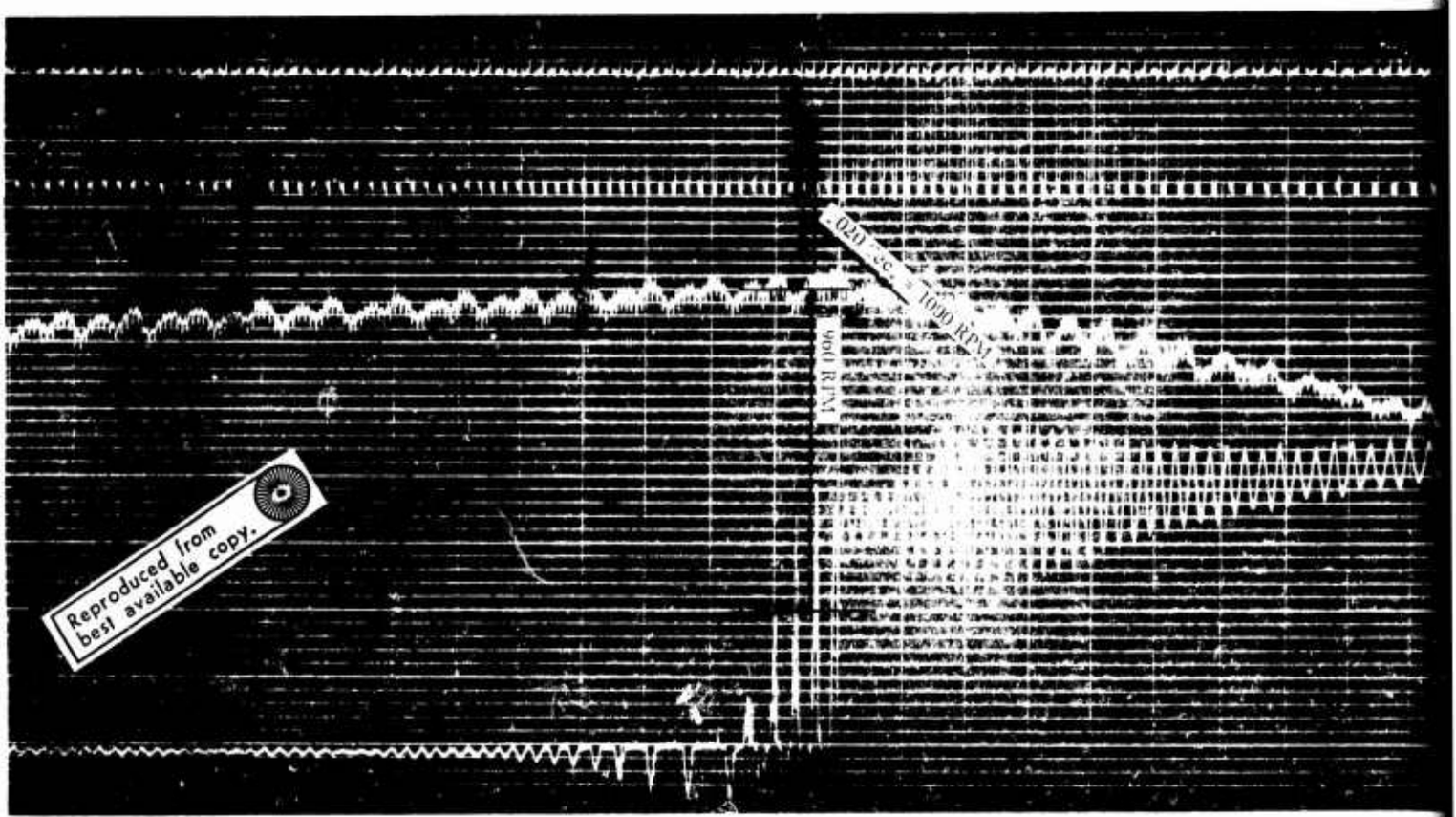

C

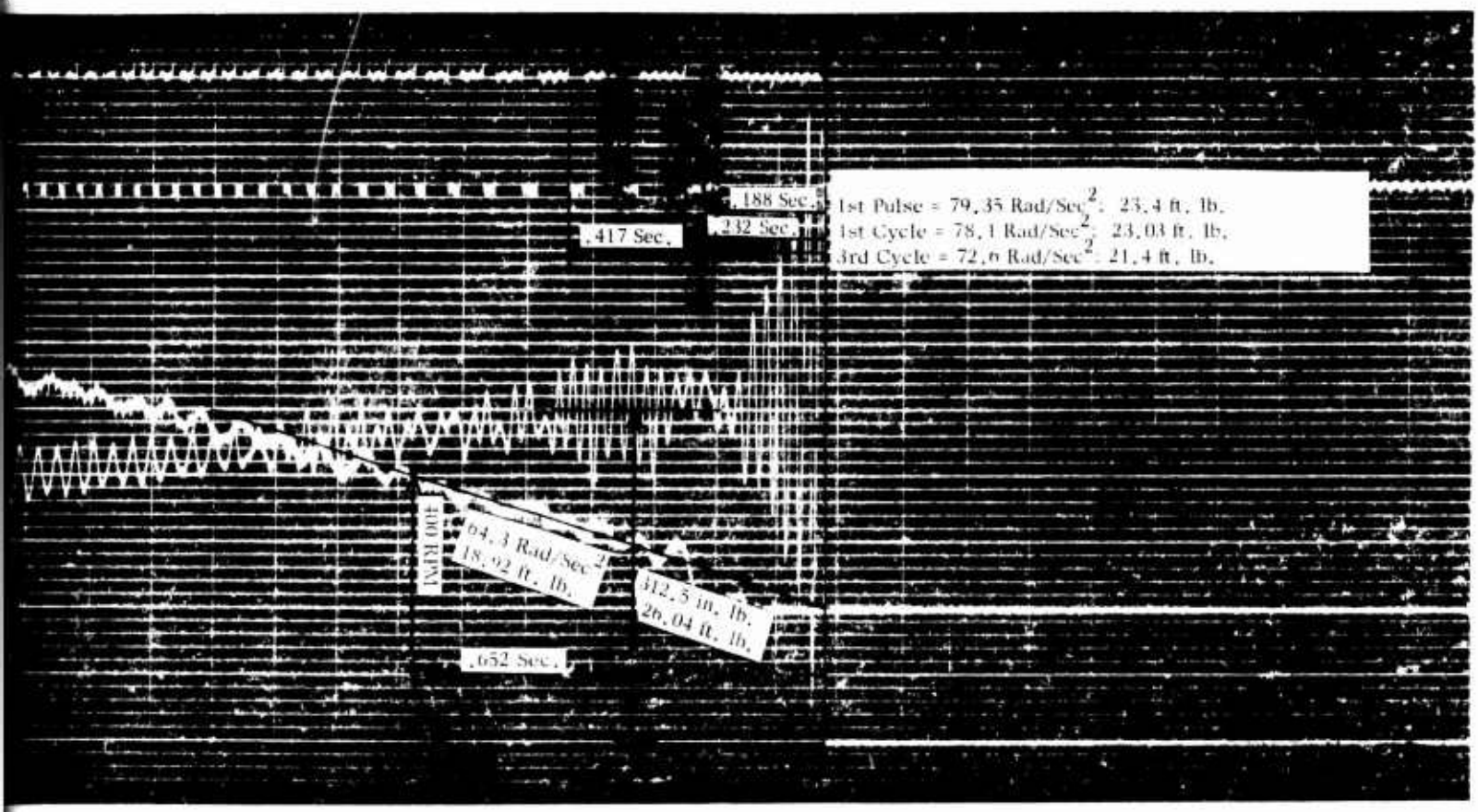
.188 Sec.
.232 Sec.
.417 Sec.
1st Pulse = 79.35 Rad/Sec^2; 23.4 ft. lb.
1st Cycle = 78.1 Rad/Sec^2; 23.03 ft. lb.
3rd Cycle = 72.6 Rad/Sec^2; 21.4 ft. lb.
400 RPM
64.3 Rad/Sec^2
18.92 ft. lb.
412.5 in. lb.
26.04 ft. lb.
.652 Sec.

135

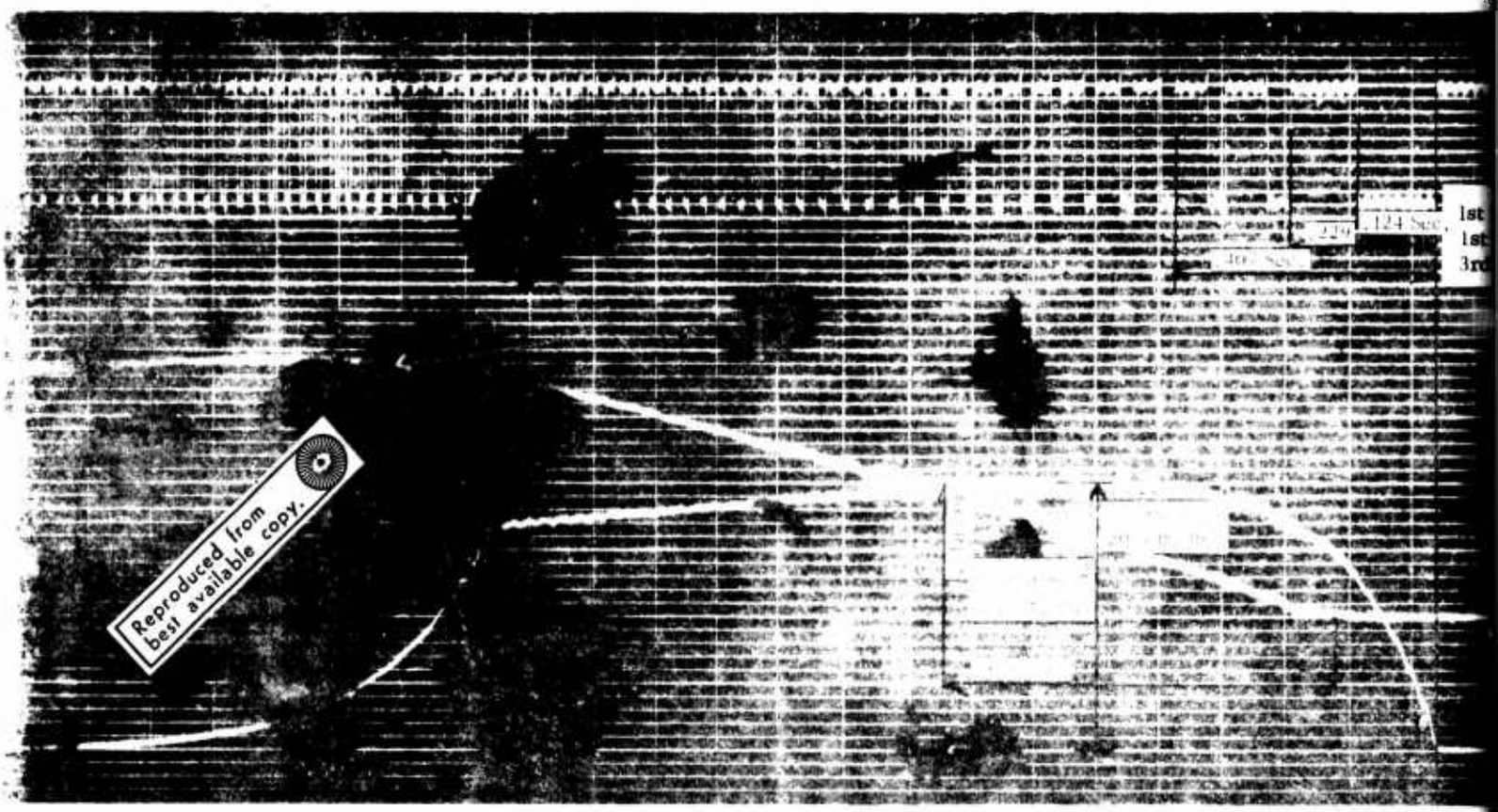

A

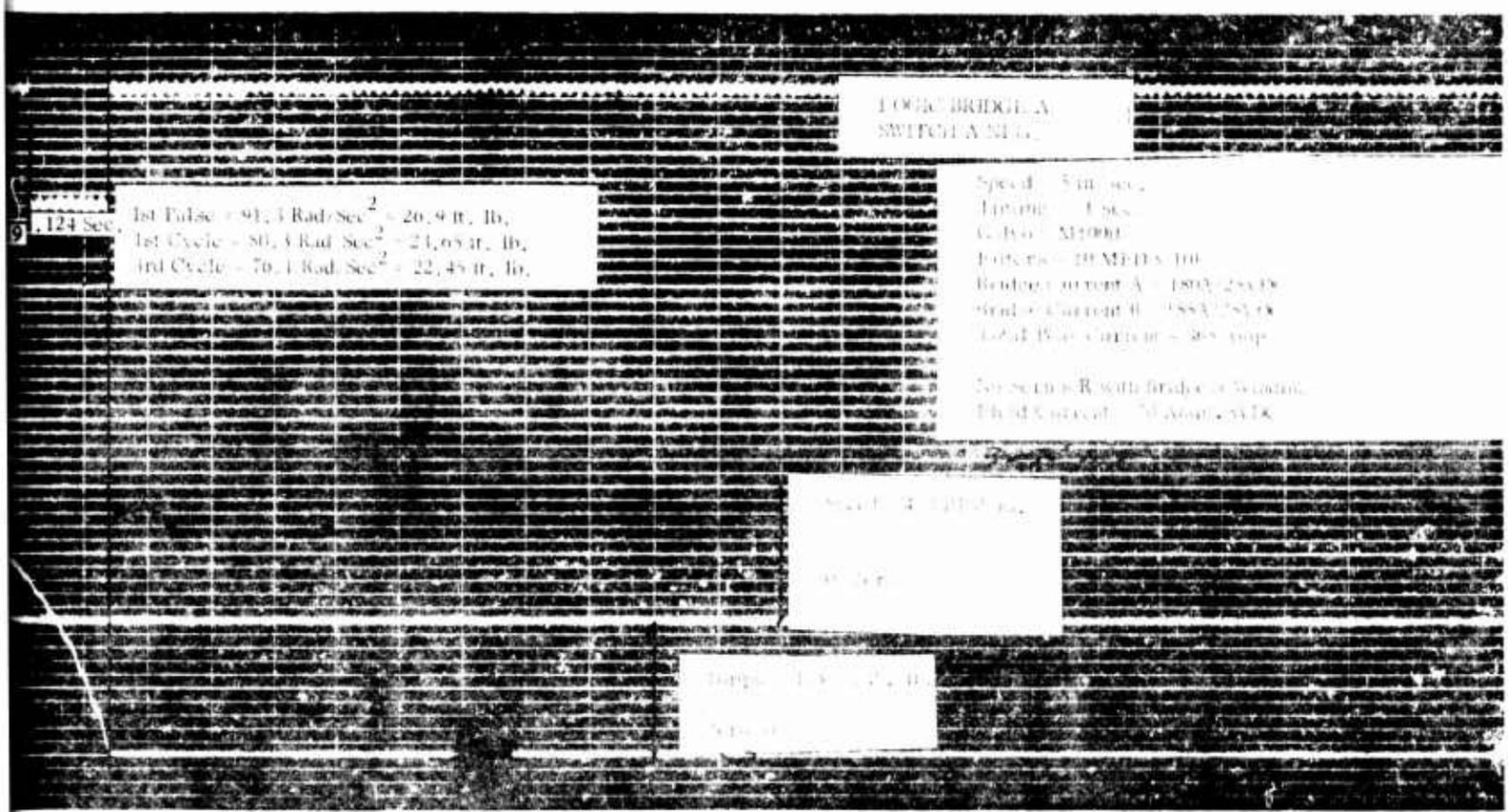
.124 Sec.
1st Pulse = 91.3 Rad/Sec^2 = 20.9 ft. lb.
1st Cycle = 80.3 Rad/Sec^2 = 24,058 ft. lb.
3rd Cycle = 70.1 Rad/Sec^2 = 22,45 ft. lb.

oscillograph. It is important to note that initial torques obtained during these tests reached up to 26.9 lb/ft. During these tests, the one-half of the starting commutator was operating at 180 amp level. The second half at 185 amp level. The total current to the commutator was 365 amps, machine field excitation was at 50 amperes. Since this input is approximately at half the value of the designed magnitude, the produced starting torque is somewhat above the half value as is required by Exhibit "A". Again, this shows that with 800 amp input current the designed torque of 40 lb/ft. can be achieved if the static commutator switches would be capable of handling required input current. Repeated tests were performed with this machine set up in the starting mode to determine possible variations of the initial starting torque due to circumferencial shaft position. Figure 6.2G shows the lowest readings obtainable during the starting mode with the same equipment. These variations were attributed to the torque variation of the machine due to 12 segments of a static commutator switch arrangement. Since the static commutator switches contained a number of deficiencies vs. the specification requirements issued by LSI/PED, Specification #15-100011, the low and elevated temperature tests of a starting mode were not performed since the possibility of total destruction of the solid state commutator existed. In order not to lose this functional hardware (although derated) further activity in testing the starting mode was suspended.

SECTION VII

7.0 CONCLUSIONS AND RECOMMENDATIONS

This brushless starter-generator D&D program was conducted with an end goal of realistic operational hardware procurement. This hardware was designed, procured, assembled and tested. The summary of this program is best expressed by reviewing the results found during the tests of the actual brushless starter-generator hardware.

7.1 Summary of Results During Generating Mode

The brushless Starter-Generator hardware, while operating as a generator, was tested under the actual acceptance test conditions. The rated load of 200 amps at 30 volts DC was produced successfully with AC ripple components not exceeding 1.5 volts peak, as specified by the military electrical specifications. The system was operated in closed loop condition with an AC regulator. During the full system tests, the output voltage regulation was maintained within $\pm$1/2 volt. The operation was also successful at elevated temperatures. A lightweight, small size rotary transformer was developed and tested under the actual operating conditions. This rotary transformer provided a unique means for machine field excitation. All subassemblies of this system were fully checked out and provided safe system performance. Overall generating test results meet the electrical specifications quoted in Exhibit "A".

7.2 Summary of Results Found During Starting Mode

The starting hardware was tested against the inertial load of a flywheel. Actual starting torque measurements closely followed the predicted values obtained during the design period of the brushless starter-generator, indicating the correct design of the machine as a motor. During the starting mode, no external cooling was allowed. Therefore, all heat generated during a simulated or actual engine start was considered to be heat storage in the overall brushless starter-generator hardware. This thermal storage capability was verified within the machine as well as the static commutator. The deficiencies of the solid state commutator switches prevented this program from achieving its full requirements during the starting mode. For example, the static commutator switch deficiency in maximum current handling capability prevented system tests at the full rated input current of 800 amps. Therefore, the maximum possible torque of 40 lb/ft. was not achieved. The switches were operated at 1/2 of their ratings and under these conditions more than 1/2 of the starting torque was exhibited by this hardware. The static commutator switch high saturation voltage is reponsible for increased losses in the commutator switches. These losses prevented the system from repetitive cycling as specified by Exhibit "A". The thermal storage capacity of the commutator was established for a nominal saturation voltage of 3 volts at 400 amps. With each starting cycle the temperature of the static commutator switch

rises 40 centigrade degrees above its ambient condition. During the off-period, the static switch temperature did not go down significantly. Therefore, the next start increased the solid state commutator switch temperature another 40 degrees centigrade and the third start would repeat this again. From this, one can see the reasons why the repeated three-cycle start was not tested with the solid state commutator switches, particularly since spare parts were non-existent. The lack of hermetic sealing in the solid state commutator switches prevented the system from high altitude/low temperature tests. To meet the Exhibit "A" requirements in full, the deficiencies of a static commutator switch must be eliminated. The results obtained during this brushless starter-generator program clearly indicate that more Design and Development is necessary in the area of solid state devices applicable to the solid state commutator required for the brushless starter-generator system. The existing deficiencies of the solid state commutator must be overcome before a fully successful brushless starter-generator can be built. Also, the price of a solid state commutator switch must be reduced to provide a unit that is competitive with brush type starter generators.

DRAWING NO. 23068-9980

STUDS EQUALLY LOCATED ON 7.156 $^{+.003}_{-.000}$ DIA BOLT CIRCLE ⊕.010 DIA.

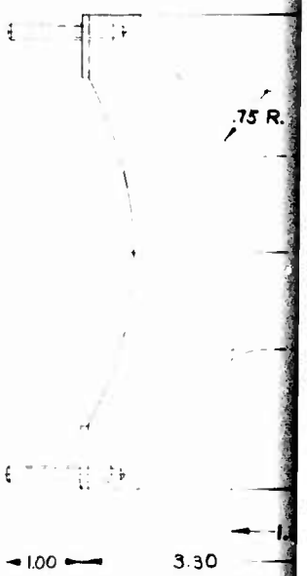

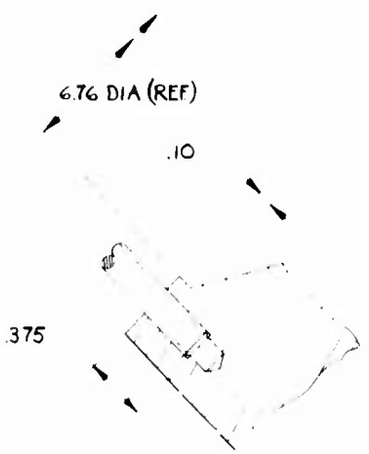

ENLARGED SECTION A-A
2/1 SCALE

⑤ FOUR #10-32 UNF STUDS SHALL BE PROVIDED AS SHOWN, SUITABLY ATTACHED TO STRUCTURE WITH SELF-LOCKING THREAD OR INSERT.

4 COMMUTATOR CONNECTION SHOWN ON LSI/PED DWG. 23068-101

3 PERFORMANCE AND DESIGN OF THE STATIC COMMUTATOR SWITCH SECTORS SHALL COMPLY WITH LSI/PED SPECIFICATION 15-100011

2 SIZE, TYPE AND LOCATION OF ELECTRICAL TERMINALS TO BE COORDINATED WITH LSI/PED.

1 - WEIGHT : 3.5 LBS. MAX.

~~1 - PART MARK PER 16-045005~~

NOTES:

1/1

DRAWING NO	P	E	REVISION
23068-9980			A

REVISIONS				
ZONE	LTR	DESCRIPTION	DATE	APPROVED
	A	REVISED & REDRAWN PER PE. INST.	CDH	

2.156 +.003 -.000 DIA

ELECTRICAL TERMINATIONS TO BE LOCATED ON THIS SURFACE WITHIN THE ENVELOPE. SEE DWG. 23068-9990

.75 R

5.40 SQR. MAX.

270 MAX.

1.80

3.30

2.200 DIA.

GENERATING MODE
RECTIFIER COOLING
PROVISION: AIR ENTERS HERE

UNLESS OTHERWISE SPECIFIED, DIMENSIONS ARE IN INCHES. TOLERANCES ON:
DECIMALS .XX ± .01 XXX ± .005 ANGLES ± 0°30'

DO NOT SCALE THIS DRAWING

MATERIAL

NEXT ASSY	USED ON
FIRST APPLICATION	

DRAWN BY L. SPONTELLI DATE 5-17-67
CHECKED BY DATE
MAT'L APPROVED DATE
PROJECT ENGR V. JANONIS DATE 5-17-67
CONTRACT NO

LEAR SIEGLER, INC / POWER EQUIPMENT DIVISION
CLEVELAND, OHIO 44101

ENVELOPE DRAWING
STATIC COMMUTATOR
PACKAGE

SIZE	CODE IDENT NO	DRAWING NO
D	31435	23068-9980

SCALE 1/1 SHEET 1 OF 1

AF N A CUST. PTI ASSIGNED

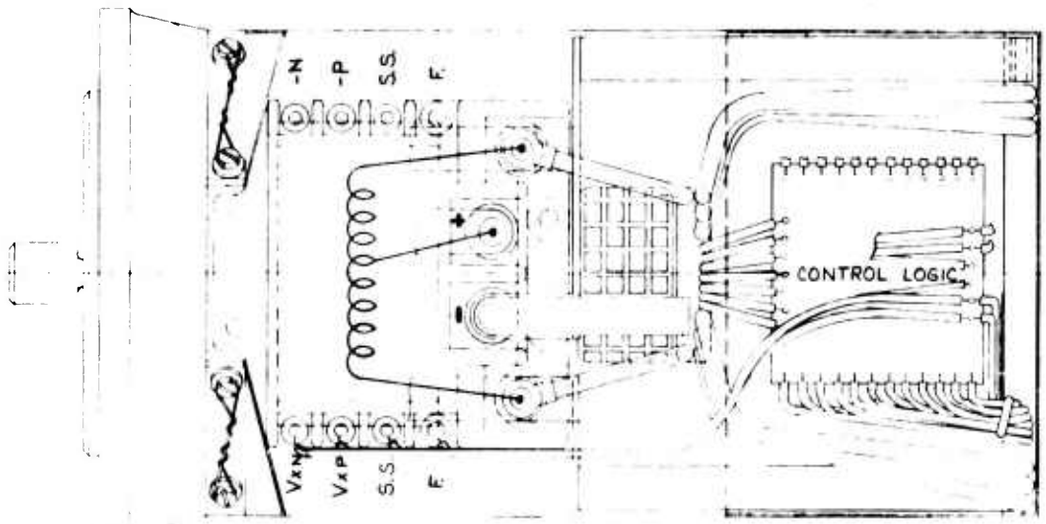

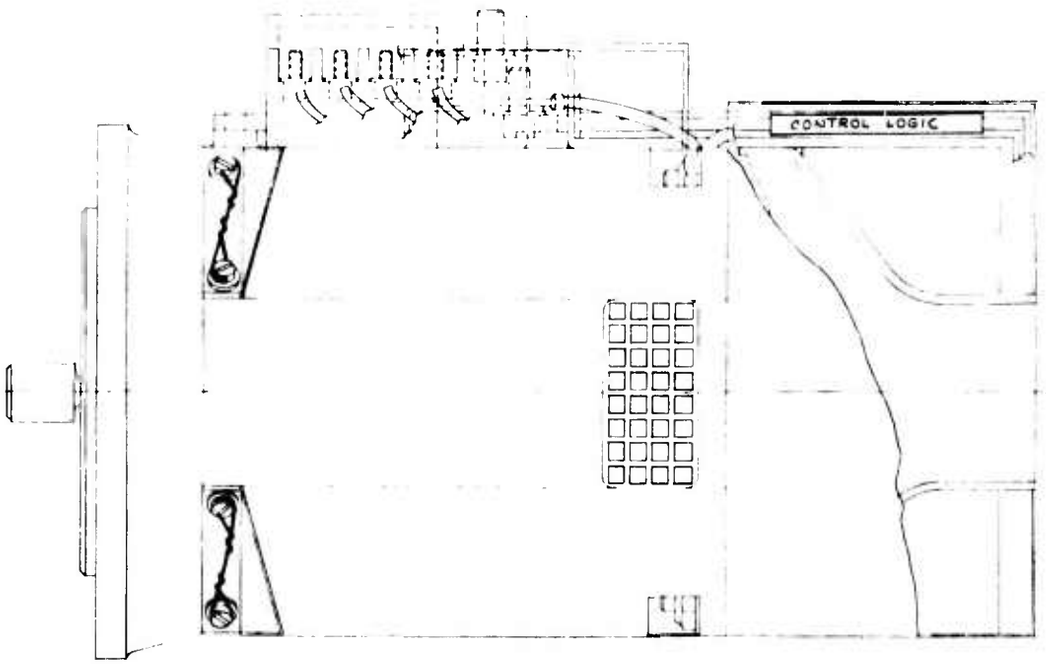

1 - PART MARK PER 16-045005

NOTES:

DRAWING NO	REV LTR
23068-9990	A

REVISIONS				
ZONE	LTR	DESCRIPTION	DATE	APPROVED
	A	REVISED & REDRAWN PER P.E.	CDH	

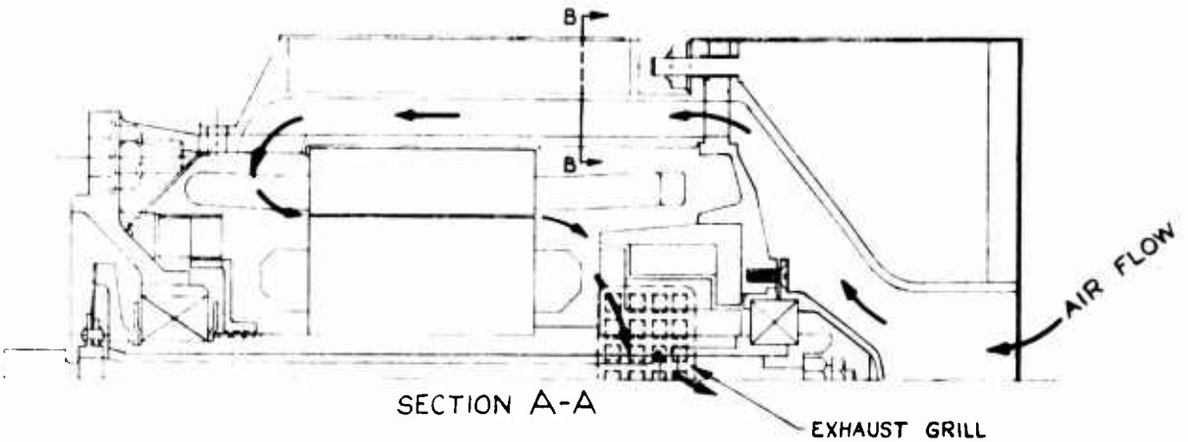

SECTION A-A

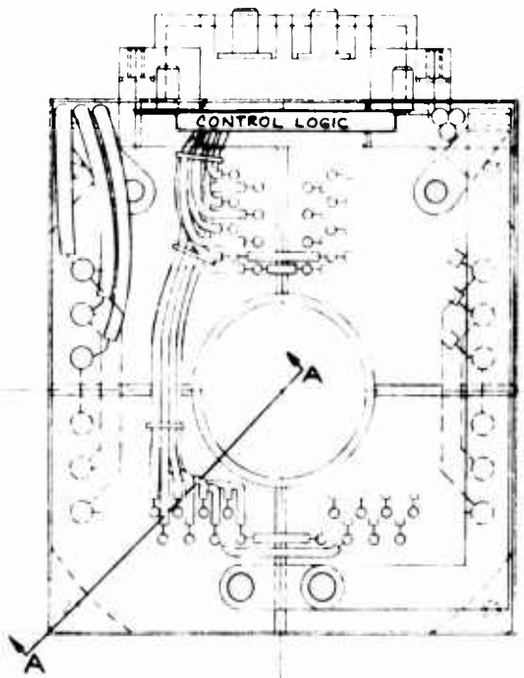

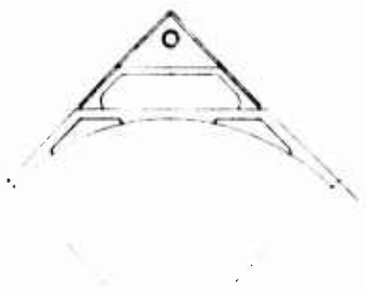

SECTION B-B

UNLESS OTHERWISE SPECIFIED, DIMENSIONS ARE IN INCHES. TOLERANCES ON: DECIMALS .XX ± .01 .XXX ± .005 ANGLES ± 0° 30'	DRAWN BY H. RAAB DATE 5-8-67	LEAR SIEGLER, INC / POWER EQUIPMENT DIVISION CLEVELAND OHIO 44101
DO NOT SCALE THIS DRAWING	CHECKED BY DATE	LAYOUT - BRUSHLESS STARTER-GENERATOR
MATERIAL:	MAT'L APPROVED DATE	
	PROJECT ENGR L. SPONTELLI DATE 5-18-67	SIZE D / CODE IDENT NO 31435 / DRAWING NO 23068-9990
	CONTRACT NO	SCALE 1/4 SHEET 1 OF 1

NEXT ASSY	USED ON
FIRST APPLICATION	

AF N A CUST. PTI ASSIGNED

150

APPENDIX

STATIC COMMUTATOR SWITCH SPECIFICATION

NO. 15-100011

APPENDIX A

LEAR SIEGLER SPECIFICATION NO. 15-100011

EXHIBIT I

Semiconductor Package for Commutation of
Current in Brushless Starter-Generator

Specification No. 15-100011
Original Issue May 17, 1967

TITLE: Semiconductor Package for Commutation of Current in Brushless Starter-Generator

1. SCOPE

1.1 This specification defines requirements of high current semiconductor switches and their integration into an assembly which will provide the function of current commutation in a brushless starter-generator.

2. APPLICABLE DOCUMENTS

2.1 The following item forms a part of this document to the extent specified herein:

SPECIFICATIONS

Military

Mil-G-6162 Amendment, 27 January 1960, Generators 30 Volt Direct Current Aircraft Engine Driven General Specification for

3. REQUIREMENTS

3.1 General:

3.1.1 This document describes the requirements and performance for a lightweight, small volume, solid-state DC current switch. Twelve of these static switches will be assembled to form a brushless commutator for an aircraft starter-generator. Each static switch must be capable of switching 400 amperes into a resistive load when commanded by a drive signal. The drive signal will have the voltage characteristics shown in Figure 1.

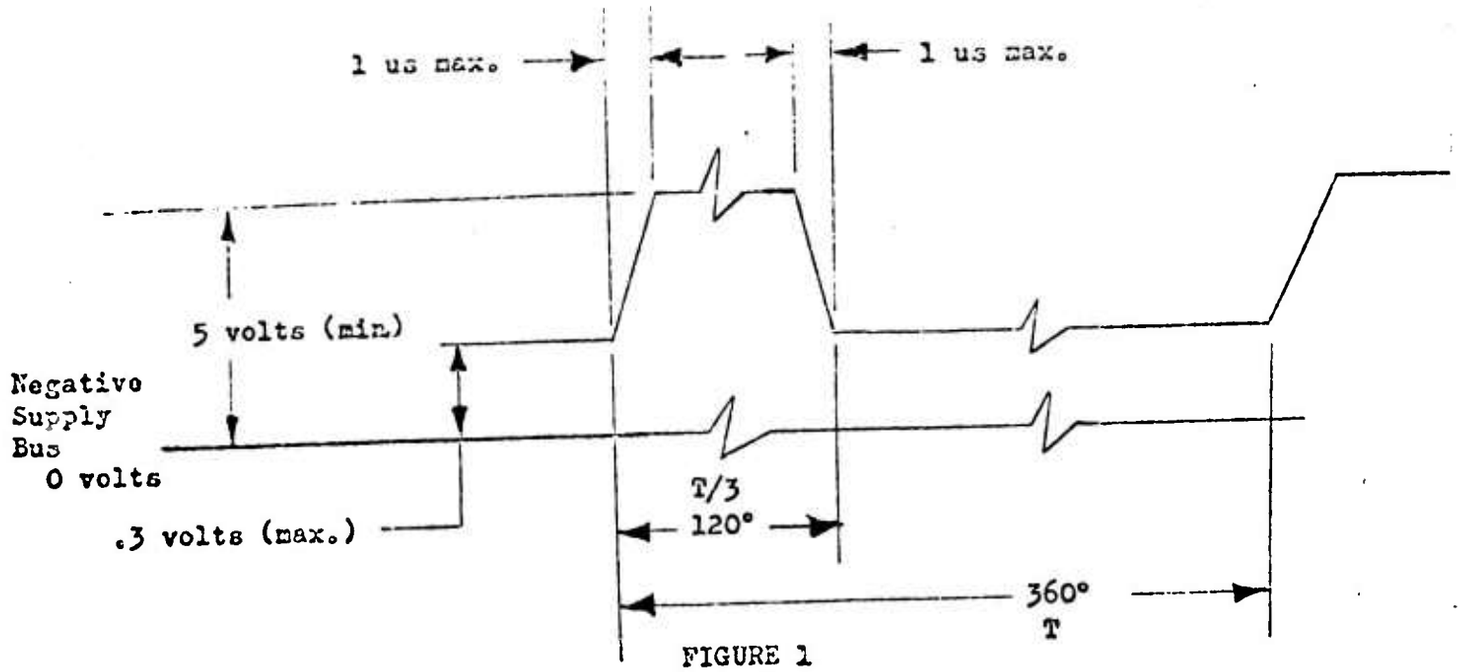

FIGURE 1

The current capacity of the drive signal will be 10 milliamperes maximum.

The output current of the static switch will be in phase with its drive signal. The static switch will operate with a 120 degree duty cycle at a frequency from zero to 200 Hertz. Figure 2 shows the operating frequency vs. time relationship.

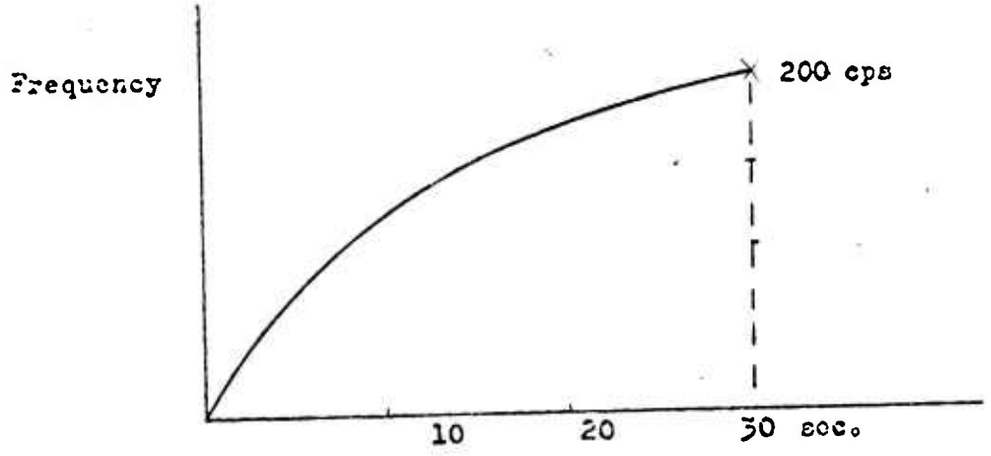

FIGURE 2

The maximum operating frequency of 200 Hertz exists after 30 seconds of operation. The lowest operating frequency will exist during the initial start. First 120° "on" pulse will be completed in .3 second of operation.

The current through the switches will be a maximum of 400 amperes during the initial start, but will decrease with time. Figure 3 shows the switch current vs. time relationship.

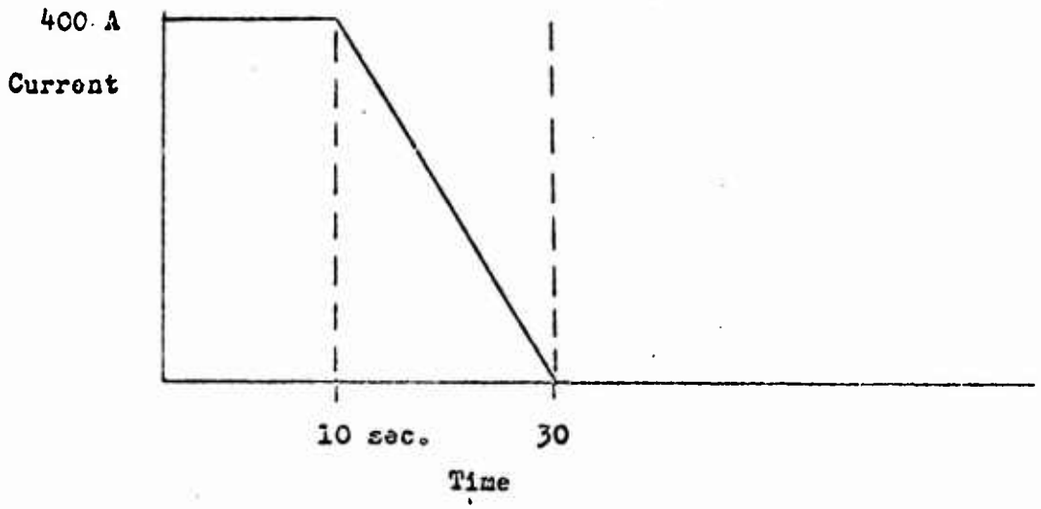

FIGURE 3

The static switch will operate for a maximum of 30 seconds as shown in Figures 2 and 3.

3.2 Positive Static Switch:

The brushless static commutator will consist of twelve static switches. A positive static switch is defined as a solid-state switch that electrically connects the positive side of the power supply and the load. (See Figure 4.) Six positive switches are required, arranged in two sets of three. See Drawing No. 23060-101.

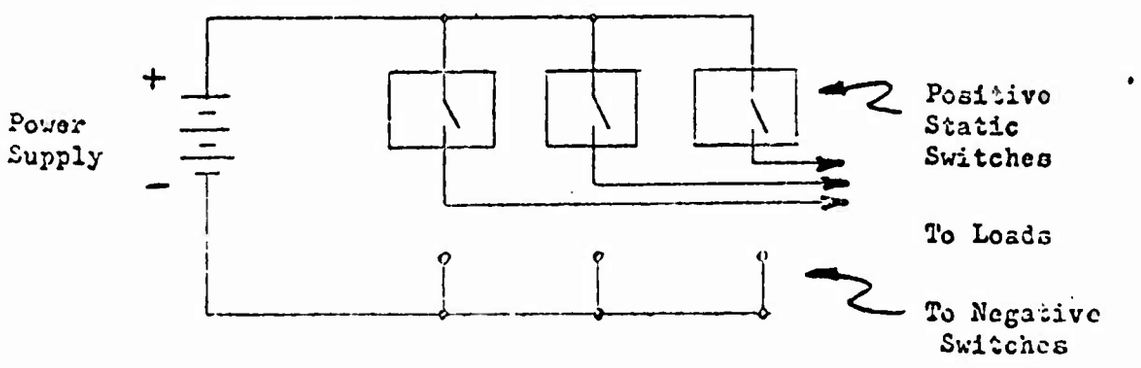

FIGURE 4

156

A PNP solid-state switch is a typical device that meets the requirements of this definition.

3.2.1 The static switch will be driven from the drive signal similar as in Figure 1. Maximum current capability of the drive signal is 10 milliamperes. The minimum number of auxiliary isolated power supplies ~~will be~~ available as shown in ~~Schematic on~~ page 10. The voltage level of these supplies, Vxn,p, ~~is~~ left to vendor's choice, preferably within 6 to 15 VDC.

3.2.2 The output current of the static switch will be 400 amperes peak at 1/3 duty cycle. The output current amplitude vs. time is shown in Figure 3.

3.2.3 The turn-on time, turn-off time, and storage time will be determined by measuring the switch characteristics as shown in Figure 5. Losses associated with these switching times must be compatable with switch thermal rating at full load and maximum operating frequency.

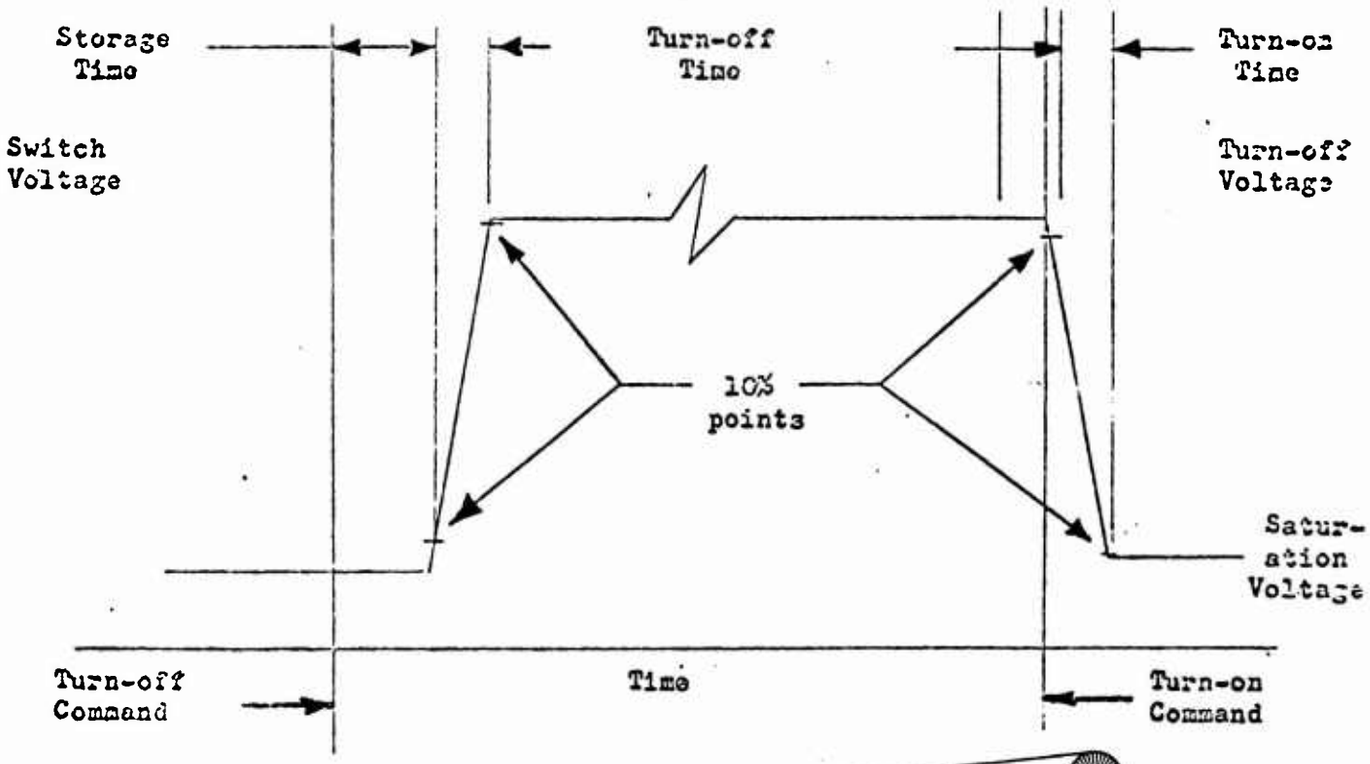

FIGURE 5

3.2.4 The positive static switch will be capable of switching the current shown in Figure 3 at a frequency shown in Figure 1 with a 1/3 duty cycle for a period of time not longer than 30 seconds. The 30 second start cycle shall be repeated 3 times with a two minute wait between starts without failure. No blast air cooling is permitted. The unit shall be stabilized

at 125°F prior to conducting the start test and in an ambient of -65°F during the three consecutive starts.

3.2.5 The static switch will operate from a power source of 30 $^{+3}_{-20}$ volts DC and be capable of sustaining transient overvoltage of 80 volts peak while inoperative.

3.2.6 Commutator Envelope

The commutator envelope is shown on LSi/PED Drawing No. 23068-9980, Rev. A. The commutator is divided into four functional modules or quadrants. Three positive switches form one module or quadrant and are apportioned 1/4 of the envelope. The required electrical interconnections to the machine terminals, rectifiers, and control logic are shown on LSi/PED Drawing No. 23068-101.

The control logic electronics and shaft sensing function will be provided by LSi/PED in a separate package not part of commutator or rectifier envelope.

The commutator shall include the required leads and/or solder terminals for interconnection to the system. LSi/PED Drawing No. 23068-9990, Rev. A, shows the location of typical connections at the inlet air face of the commutator envelope.

3.2.6.1 Connections

(a) Two bus bars are required from the positive halves of the commutator to the choke terminal posts.

(b) One bus bar from the two interconnected negative quadrants to the generator negative terminal posts.

(c) Two solder terminal posts in each quadrant for low current controlled voltage source.

(d) Three terminal posts in each quadrant for interconnection of bridge switches. Three leads will be provided for each positive quadrant for interconnection with their corresponding windings at the machine terminal block. Leads will be provided by LSi/PED for interconnection of stator windings to commutator positive quadrant switches.

(e) Six low current solder terminals in each quadrant for driver input.

A metal shroud will be provided by LSi/PED to protect the terminals and leads which will be routed to the machine terminals, rectifiers, and control logic. It is desirable that the semiconductor circuitry be isolated from the mounting heat sinks to facilitate mounting to common end bell and eliminate insulation between quadrants and shroud.

3.2.6.2 Structural Mounting

The four commutator quadrants shall be joined structurally within the envelope restrictions to form one unit which can be mounted with four No. 10 studs located at the corners of the package shown on LSi/PED Drawing No. 23068-9930, Rev. A. The unit and its mountings shall be designed to withstand the shock and vibration requirements of this specification.

3.2.6.3 Commutator Weight

The total weight of the commutator shall not exceed 3.5 pounds. The total weight of the rectifier assemblies shall not exceed 1.5 pound.

3.3 Negative Static Switch:

The brushless static commutator's six negative static switches are defined as solid-state switches that electrically connect the negative side of the power supply and the load. (See Figure 6.)

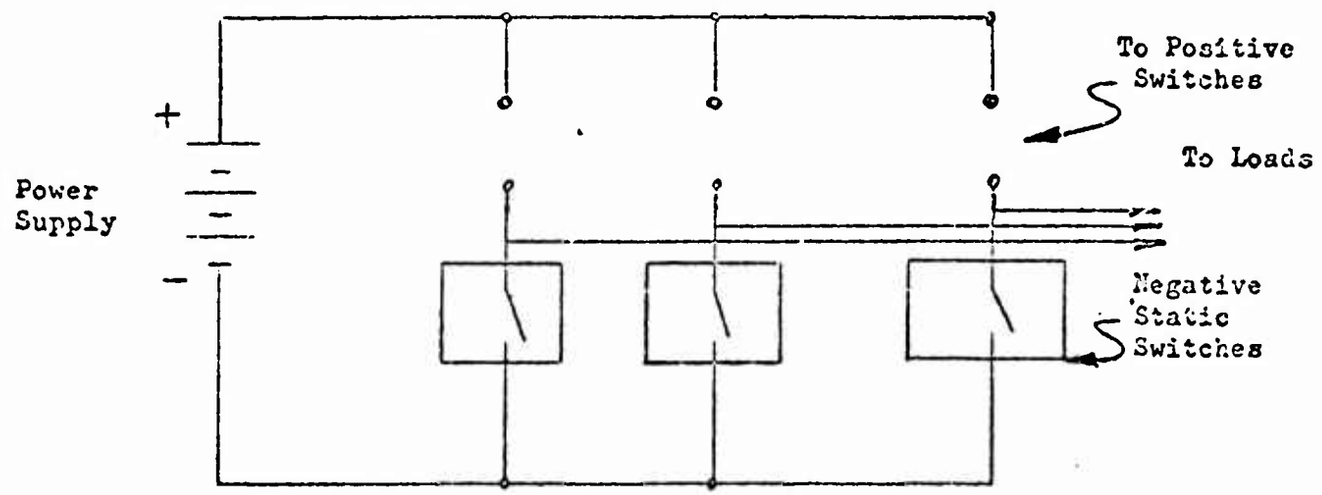

FIGURE 6

An NPN solid-state switch is a typical device that meets the requirements of this definition.

3.3.1 Drive signal same as that in paragraph 3.2.1.

3.3.2 The output current will be the same as that described in paragraph 3.2.2.

3.3.3 Same as paragraph 3.2.3.

3.3.4 The negative static switch will operate as described in paragraph 3.2.4.

3.3.5 The negative static switch will operate from the same power source as described in paragraph 3.2.5.

3.3.6 One set of 3 negative static switches will meet 1/4 of the size and weight requirements of Drawing No. 23068-9980, Rev. A.

3.4 The six positive static switches and the six negative switches when assembled together to form a brushless commutator will meet the size and weight requirements of Drawing No. 23068-9980, Rev. A.

3.5 After the first 30 seconds of operation, the system must function as a generator. Therefore, a diode will be placed electrically in parallel with each positive and negative static switch to form 2 sets of three-phase, full wave rectifiers. The diode will be connected so that the cathode will be at the positive side of each switch. (See Figure 7.)

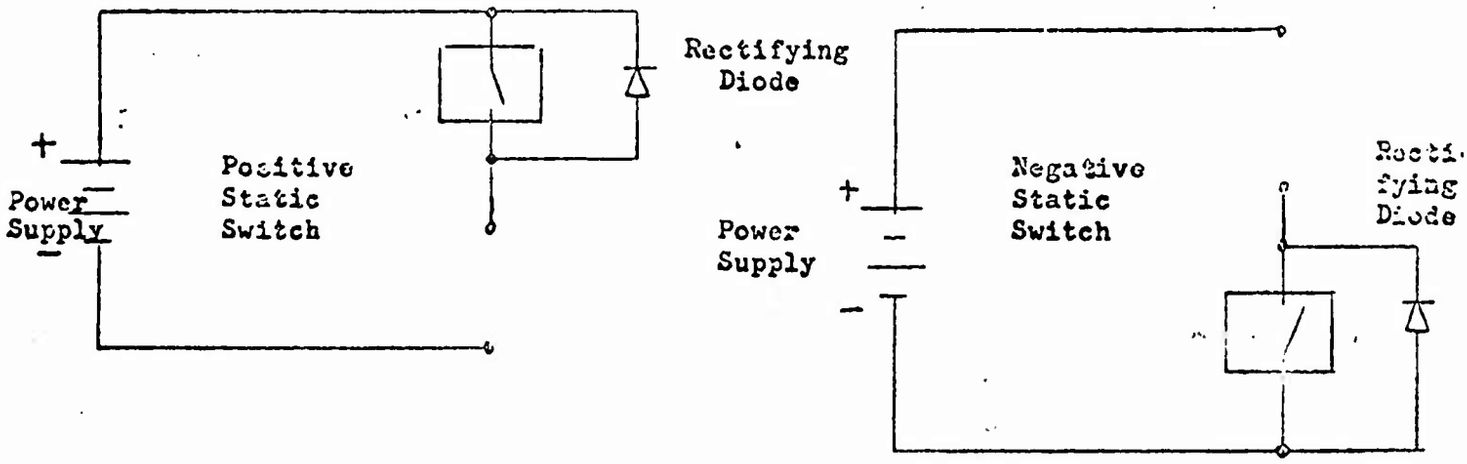

FIGURE 7

3.5.1 The continuous rating of these rectifiers is 33 amperes average, or 58 amperes rms, with sustaining reverse voltage of 80 volts peak. Blast cooling will be provided for diode cooling during generator mode. These rectifiers at 80 volts peak reverse voltage shall exhibit controlled avalanche characteristics.

The generator and rectifiers will be provided a total pressure on the air inlet duct of six inches of H_2O above absolute ambient pressure. The flow of air will vary with inlet air temperature and altitude conditions. Figure 8 shows inlet air temperature vs. altitude. Figure 9 shows maximum air flow vs. altitude permitted for maximum inlet air temperature. Of the six inches of H_2O total pressure available, 2 inches of H_2O has been allotted

for pressure drop from inlet of generator to exhaust from rectifier air passage. The air passage available and path through the brushless starter-generator are shown on LSi/PED Drawing No. 23068-9990, Rev. A.

Performance of the rectifier package will require ground operation of the generator at reduced inlet pressure and flow shown in Figure 9.

3.5.2 Rectifier Mounting

The rectifiers will be mounted in the four corners of the generator envelope on aluminum blocks which will contain air passages for cooling purposes shown on LSi/PED Drawing No. 23068-9990, total weight not to exceed 1.50 pound. The four blocks or modules each contain three rectifiers and four lead terminations for interconnection to machine windings and terminal block.

See envelope drawing 23068-1000 for configuration and lead terminations. For an overall understanding of electrical interconnections see connection diagram 23068-101.

The air flow path through the brushless starter-generator is as follows:

See Drawing No. 23068-9990, Rev. A. Air enters center of commutator envelope through a two inch duct, advances in an annular conical chamber to enter the rectifier cooling passages in the four corners of the generator envelope. After leaving the rectifiers the air enters the generator portion or cavity, reverses direction, and exhausts through four screened parts provided in the anti-drive end of the generator radially outward between rectifier modules. Because the modules will be secured to the generator housing effectively interconnecting them electrically, the rectifiers and electrical circuitry shall be isolated from the mounting base.

3.6 Environment:

The static switch commutator and rectifiers, when mounted in the starter-generator housing, will be capable of operating under all of the following environmental conditions:

A. Ambient Temperature: -65°F to 125°F

B. Altitude: 0 to 50,000 feet

C. Humidity: 0 to 100°

D. Vibration: 20 g's at 80 to 2000 cps

'61

E. Shock: 50 g's

F. Acceleration: 10 g's

The operation of the brushless commutator, when mounted in the housing provided, will not be impaired by salt spray, fungus, sand or dust. These requirements are in accordance with applicable sections of Mil-G-6162.

4. QUALITY ASSURANCE PROVISIONS

4.1 The assembled sector of three positive or negative static switches shall meet all the specification requirements in section 3 of this specification. The necessary tests to verify the switch and rectifier performance to the requirements of section 3 of this specification will be mutually agreed upon and performed by vendor and LSi/PED.

5. PREPARATION FOR DELIVERY

5.1 Delivery of static commutator switches and rectifier modules shall be to LSi/PED Cleveland facility properly packaged for protection during shipment.

6. NOTES

6.1 The attached sketch, "Complementary Transistor Switch Schematic," on page shall be used for illustrative purposes only.

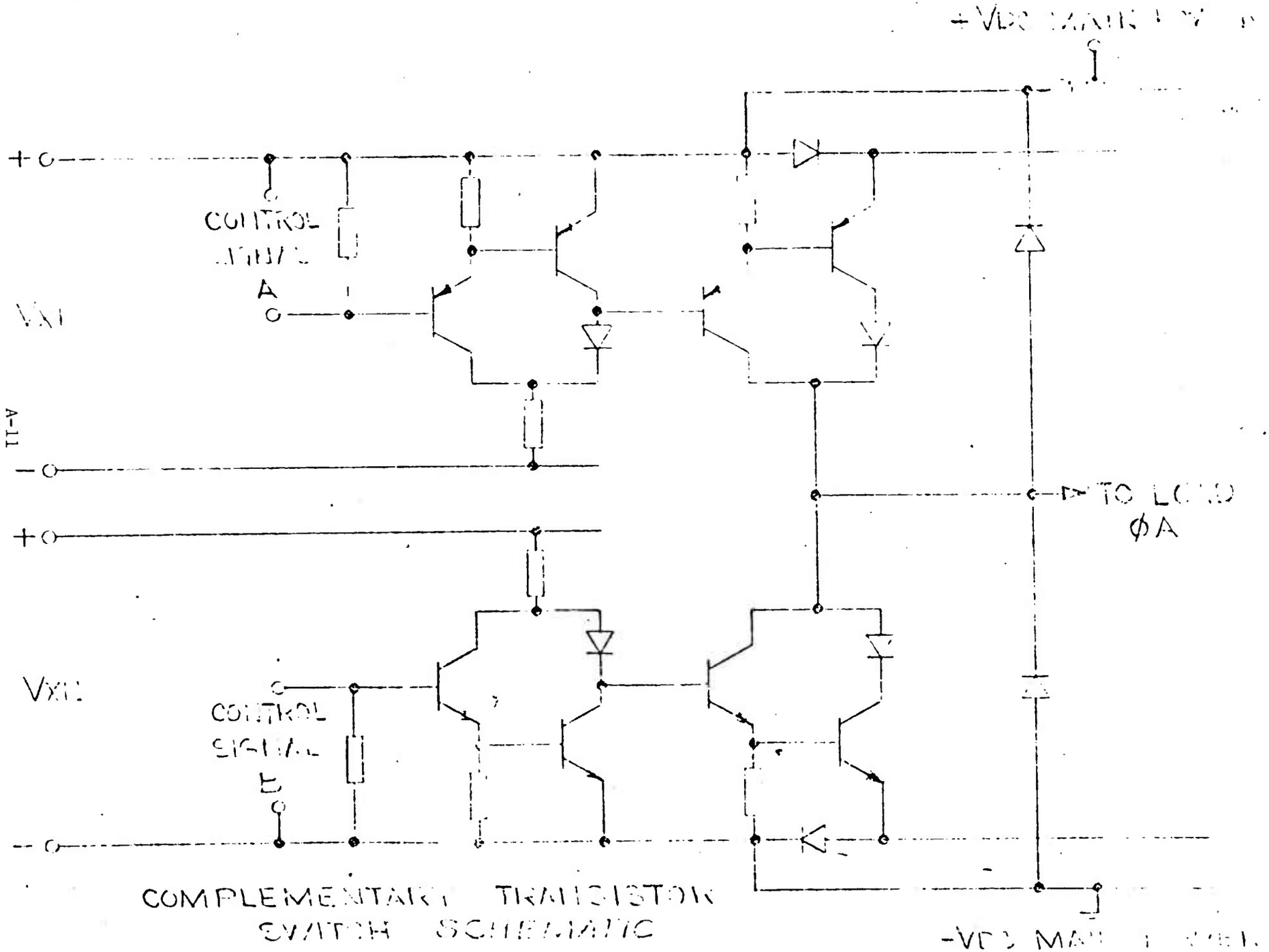

COMPLEMENTARY TRANSISTOR SWITCH SCHEMATIC

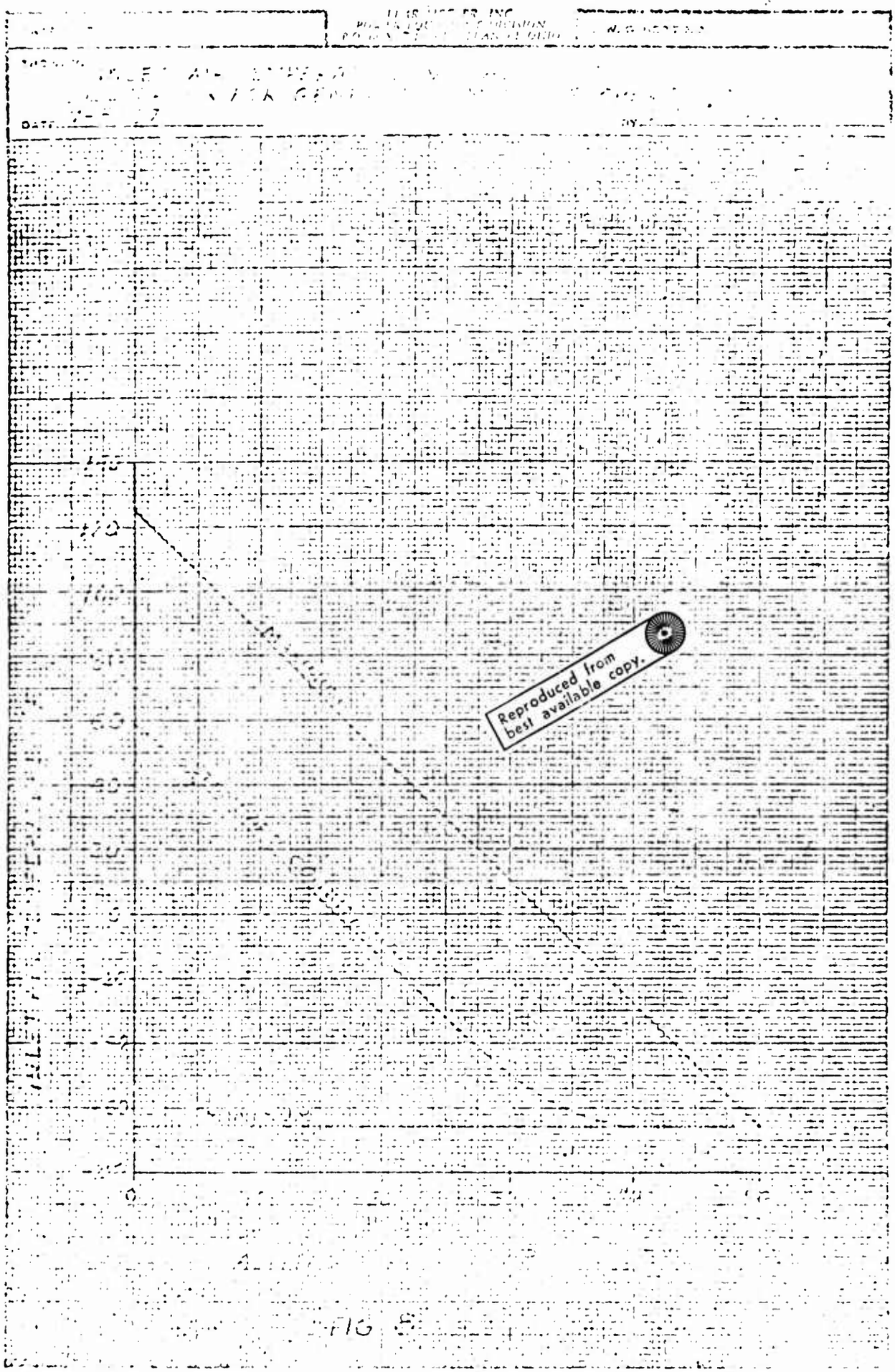
Reproduced from
best available copy.

APPENDIX II

RCA TECHNICAL PROPOSAL

SEMICONDUCTOR PACKAGE

FOR

COMMUTATION OF CURRENT IN BRUSHLESS STARTER-GENERATOR

TABLE OF CONTENTS

TABLE OF CONTENTS (Cont.)

LIST OF ILLUSTRATIONS

SECTION I
INTRODUCTION

RCA is pleased to submit this technical proposal to the Power Equipment Division of Lear Siegler, Inc., in response to its Request for Proposal, for the development of a semiconductor package for commutation of current in a brushless starter-generator. In this program, RCA proposes to develop transistor power switching modules capable of switching 400 amperes per module in a form factor consistent with stringent thermal, volume and weight requirements. Twelve modules, six positive polarity, and six negative polarity, will be used as a brushless commutator for a DC motor for jet engine starting. Four rectifier modules are used to provide full-wave rectification during the generator phase after engine start. The complete switching and rectifying module package is attached directly to the motor-generator and forms part of its external configuration.

The space and weight restrictions rule out the feasibility of using discrete semiconductors to achieve the commutation objective. The RCA approach uses a unique modular concept utilizing novel circuitry, and power transistor chip packaging and interconnecting by using unusual techniques and materials.

RCA has developed substantial competence in the design and manufacture of plastic-encapsulated high-power transistors. RCA has recently announced a broad line of plastic power transistors completing an extensive and successful development. This experience and knowledge will provide technical strength toward solving the difficult encapsulation problems associated with these circuit modules.

One of the major problems in the power transistor industry has been second breakdown. RCA has been a pioneer in non-destructive forward and reverse second break test methods. This capability has enabled RCA to improve, optimize, and fully characterize its power transistors. This technical

capability will provide the background to insure that these circuit modules will operate reliably and free from second breakdown under the stringent motor-generator operating conditions.

SECTION II

TECHNICAL DISCUSSION OF SWITCHING CIRCUITS

2-1. GENERAL DISCUSSION

Positive and negative static switches are direct-coupled transistor circuits that are used to amplify the 5-volt, 10-milliampere drive signal to a level of 400 amperes. There is an attenuator at the input to each switch. The functions of the attenuator are to lower the input signal to the proper level and to minimize the possibility of spurious low-level noise problems from the signals for the adjacent switches.

The static switches employ p-n-p and n-p-n transistors in a direct-coupled configuration to provide maximum gain with a minimum of coupling problems. This configuration of transistor circuit provides the advantage that the only dissipation when the switch is off is due to leakage currents, reducing heating to a minimum.

Transistors have been used throughout the switching circuits to provide rapid switching with the variable-frequency input signal. All transistors are specially selected for low leakage and low saturation characteristics to permit highly reliable operation at elevated temperatures. The device type designations shown in the schematic diagrams of the static switches (Figures 2-1 and 2-2) correspond to similar RCA commercial or developmental types, providing a convenient means of explaining the circuits.

Types 2N4036, 2N3878, 2N5038, and 2N2102 currently are commercially available RCA power transistors. The n-p-n type TA7017 currently is in pilot production in the factory. The p-n-p type TA7279 is in the latter stages of design and will be released for pilot production during mid-third quarter 1967.

The heart of each switch is the type TA7017, which employs the rugged RCA-developed hometaxial-base design. It is a new high-power device that is capable of 300-watt dissipation at 70 amperes. The hometaxial-construction

device was chosen because it has outstanding resistance to forward and reverse second breakdown and low saturation resistance.

The calculations for circuit parameters discussed in the subsequent paragraphs are provided in Appendix B.

2-2. POSITIVE STATIC SWITCH

The positive static switch (Figure 2-1) consists of a three-stage, direct-coupled amplifier. First-stage p-n-p amplifier Q1 is connected in the common-emitter configuration. First-stage current gain is approximately 20. Resistors R1, R8, and R9 form a voltage divider and biasing network for this stage. The collector is direct-connected to the next stage.

The next stage consists of n-p-n transistors Q2 and Q3 connected in the common Darlington configuration. The minimum available current gain of this stage is approximately 400. The output of this stage is applied to the bases of the output stage.

The output stage consists of six identical circuits that are driven in parallel by the second stage. For simplicity, only one of these circuits is shown in Figure 2-1. Because of the method used to interconnect p-n-p transistor Q4 (and Q5 through Q9) and n-p-n transistor Q10 (and Q11 through Q15), Q10 produces the effect of the p-n-p type transistor of the Darlington circuit. This circuit is reliable and has been used in many audio-frequency power amplifiers prior to the development of high-current silicon p-n-p transistors. Since the TA7017 transistor is a 70-ampere device, six output stages (six TA7279 transistors driving six TA7017 transistors) in parallel provide the necessary current-handling properties.

Transistors Q4 and Q10 in the Darlington-type output stage are matched for V_{BE} and $V_{CE}(sat)$ at the collector currents to be used. Matching is required to eliminate the losses associated with local feedback in the output stage.

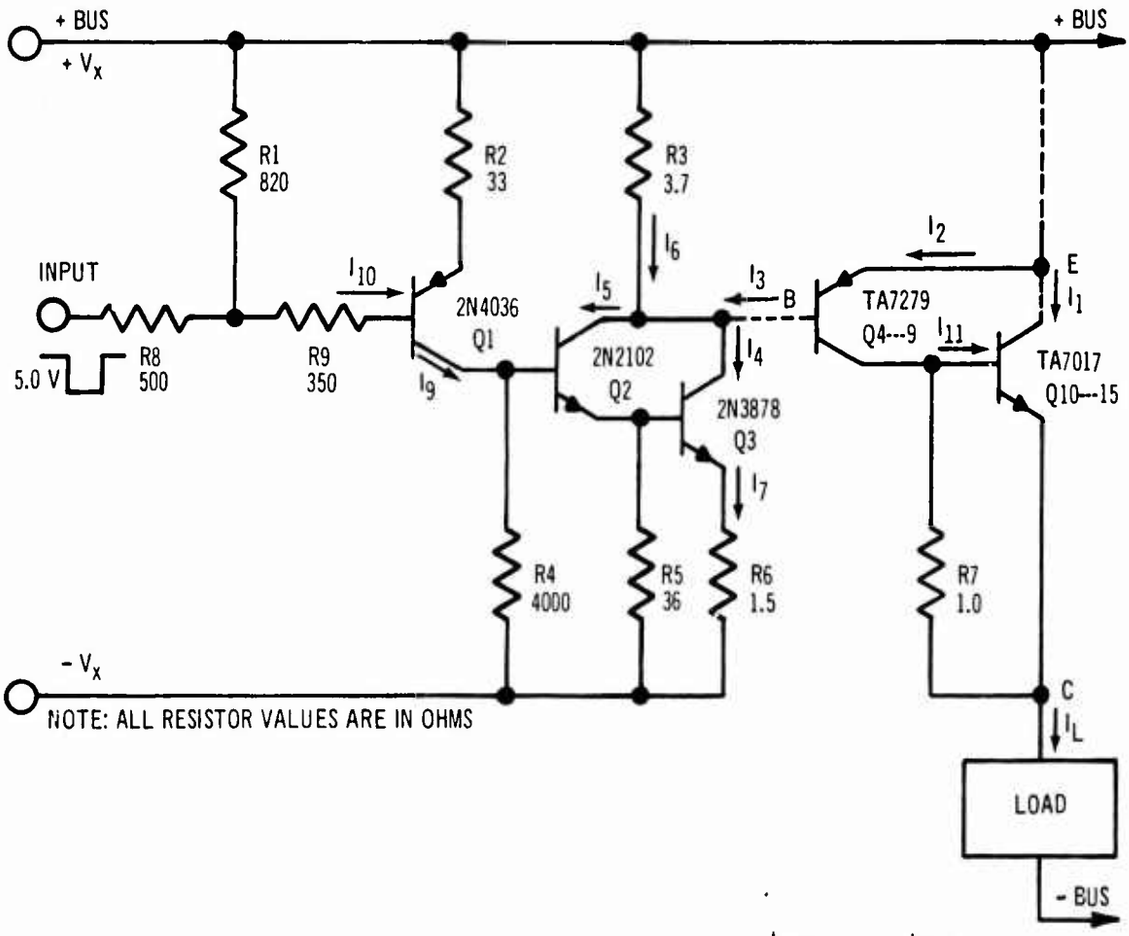

REF DESIG	FAMILY TYPE	QTY PER SWITCH	β MIN	β MAX	$V_{CEM(sat)}$ (VOLTS)	V_{BEM} (VOLTS)	I_{CEO} at 150° C (mA)	I_{CER} at 150° C (mA)
Q1	2N4036	1	20	100	0.65	1.10	0.005	0.010
Q2	2N2102	1	20	100	0.50	1.10	0.005	0.010
Q3	2N3878	1	20	100	2.00	2.00	5.0	10.0
Q4-Q9	TA7279	6	15	100	1.20	2.00	2.5	20.0
Q10-Q15	TA7017	6	8	70	1.20	2.00	10.0	50.0

Figure 2-1. Positive Static Switch

No overall negative feedback was used in the output stage. It was decided to use local feedback at each stage to eliminate phase-shift problems. The negative feedback per stage is calculated using Equation (1):

$$g_{m(FB)} = \frac{g_m}{1 + g_m R_E} \quad \ldots\ldots\ldots\ldots\ldots\ldots\ldots\ldots\ldots\ldots (1)$$

The approximate overall feedback for both positive and negative switches will be approximately 26 dB.

Using the Darlington-type configuration reduces the base current for this combination to approximately 3 amperes. The need for higher-current transistors in the driving stages is eliminated at this current level.

The drive signal is referenced to the positive bus. Negative logic was used in this switch; therefore, a negative-going signal produces a closed-switch condition at the output. Negative logic was selected so that the switch will be open in the absence of a signal, preventing circuit failure due to faulty connections. This configuration also prevents short circuits due to absent signals. A V_x level of -10 volts DC is required with regulation to within 10 percent. This voltage is indicated in the Lear Siegler Request for Proposal and attached Specification 15-100011 (Appendix A) as being available.

2-3. NEGATIVE STATIC SWITCH

The negative static switch (Figure 2-2) is similar to the positive static. The major differences are in the polarity of the power supply, the reference voltage, the input logic, and the output-stage connection.

The input to the negative static switch consists of resistors R4, R5, and R6, which form a network that acts as a signal attenuator and biasing network for n-p-n input transistor Q1. The minimum gain of transistor Q1 is approximately 20. This transistor is in a common-emitter configuration. The collector is connected directly to the second stage.

The second stage consists of p-n-p transistors Q2 and Q3 in a Darlington connection. The Darlington connection is used to obtain high gain and to achieve the objective of very-low power dissipation when the switch is off. The output of the second stage is direct-coupled to the output stage.

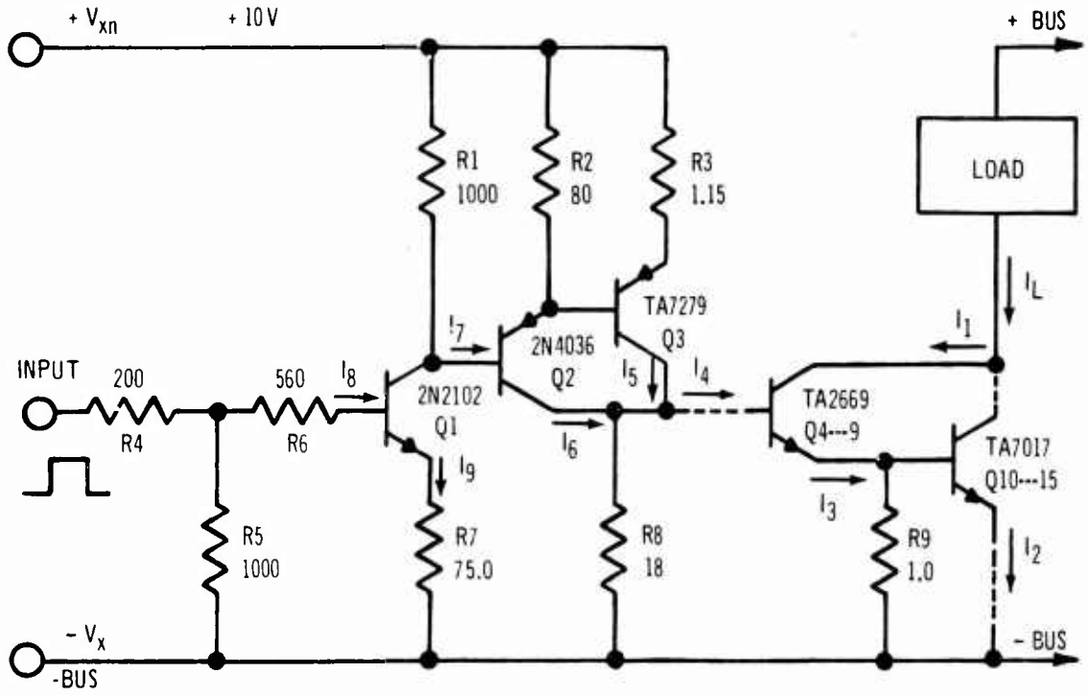

NOTE: ALL RESISTOR VALUES ARE IN OHMS

REF DESIG	FAMILY TYPE	QTY PER SWITCH	β MIN	β MAX	V_{CE}(sat) (VOLTS)	V_{BEM} (VOLTS)	I_{CBO} at 150° C (mA)	I_{CER} at 150° C (mA)
Q1	2N2102	1	20	100	0.50	1.10	0.005	0.010
Q2	2N4036	1	20	100	0.65	1.10	0.005	0.010
Q3	TA7279	1	15	100	1.20	2.00	2.5	20.0
Q4-Q9	TA2669	6	15	100	1.01	2.00	2.5	20.0
Q10-Q15	TA7017	6	8	70	1.20	2.00	10.0	50.0

Figure 2-2. Negative Static Switch

The output stage consists of six identical circuits that are driven in parallel by the second stage. For simplicity, only one of these circuits is shown in Figure 2-2. The Darlington configuration used to interconnect transistor Q4 (and Q5 through Q9) and transistor Q10 (and Q11 through Q15) was selected to achieve maximum gain with a minimum number of transistors. The TA2669-TA7017 combination of transistors was selected to obtain similar switching characteristics and comparable gain performance to the TA7279-TA7017 combination used in the positive static switch (Figure 2-1).

Positive logic was used in this switch; therefore, a positive-going signal produces a closed-switch condition at the output. Positive logic was selected so that the switch will be open in the absence of a signal, preventing circuit failure due to faulty connections. The drive signal is referenced to the negative bus. A V_x level of +10 volts DC is required with regulation to within 10 percent. This voltage is indicated in the Lear Siegler Request for Proposal and attached Specification 15-100011 (Appendix A) as being available.

2-4. BOOSTED DARLINGTON CIRCUIT

The conventional Darlington connections (Figure 2-3) used in the switching circuits can be improved by using additional circuit techniques. The V_{CE} of the output transistor cannot saturate when the transistor is connected in Darlington configuration. This limitation exists because the V_{CE} of the output transistor is the sum of $V_{BE,2}$ and $V_{CE}(sat)_1$. With the TA7017 transistor used in the output stage of the negative static switch, the following parameter values can be used to illustrate switch power dissipation:

$$V_{CE}(sat)_1 = 1.0 \text{ volt}$$

$$V_{CE}(sat)_2 = 1.2 \text{ volts}$$

$$V_{BE,2} = 2.0 \text{ volts}$$

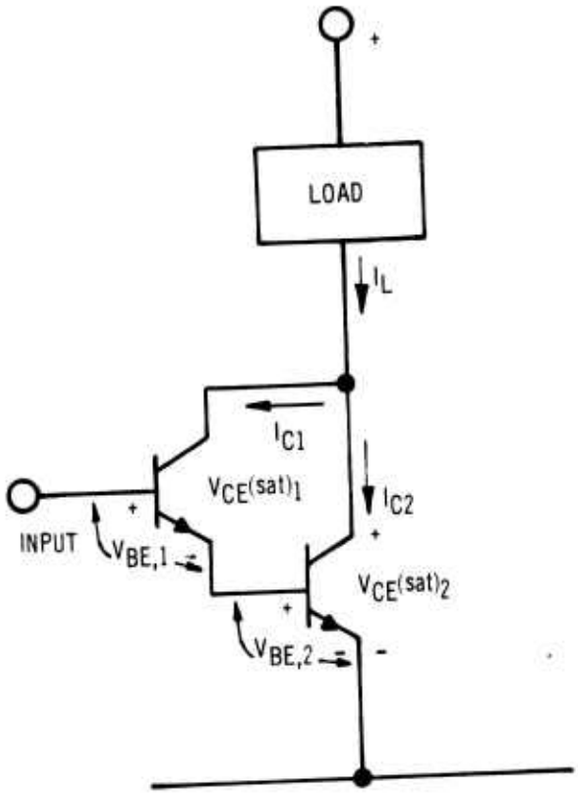

Figure 2-3. Conventional Darlington Amplifier Circuit

Power dissipation, therefore, is $(V_{CE})(I_C)$. Assuming that the switching current is 400 amperes and that $V_{CE} = V_{BE,2} + V_{CE}(sat)_1$, average power is as follows:

$$P_{AV} = D\ V_{CE}\ I_C \quad \ldots\ldots\ldots\ldots\ldots\ldots\ldots\ldots\ldots\ldots\ (2)$$

$$= D \left[(V_{BE,2}) + (V_{CE}(sat)_1)\right] I_C$$

$$= \frac{1}{3}\ (2.0 + 1.2)\ (400)$$

$$= 426 \text{ watts}$$

If output V_{CE} was the $V_{CE}(sat)_2$ of only the output transistor, average power becomes

$$P_{AV} = D\ V_{CE}(sat)_2\ I_C \quad \ldots\ldots\ldots\ldots\ldots\ldots\ldots\ldots\ldots\ (3)$$

$$= \frac{1}{3}\ (1.2)\ (400)$$

$$= 160 \text{ watts}$$

A reduction in power dissipation of approximately 270 watts per switch is realized. There are two methods for achieving this lower dissipation. The first method is to use a circuit other than a Darlington, which results in decreased gain and current-handling ability. The second method is a superior approach using the "boosted Darlington" circuit (Figure 2-4).

The "boosted Darlington" requires the insertion of a voltage (V_x) between the collectors. Voltage V_x must be in the order of 3.0 volts at a 50-ampere current level. This voltage must be isolated for each switch, which requires a power supply with 12 separate supply circuits. The power that must be provided by each one of the 12 power supply circuits is

$$P_{V,x} = \frac{V_{out}\ I_{out}}{\eta} \quad \ldots\ldots\ldots\ldots\ldots\ldots\ldots\ldots\ldots\ (4)$$

$$= \frac{(3)\ (50)}{0.85}$$

$$= 175 \text{ watts}$$

The result of Equation (4) shows a total power saving of 100 watts per switch.

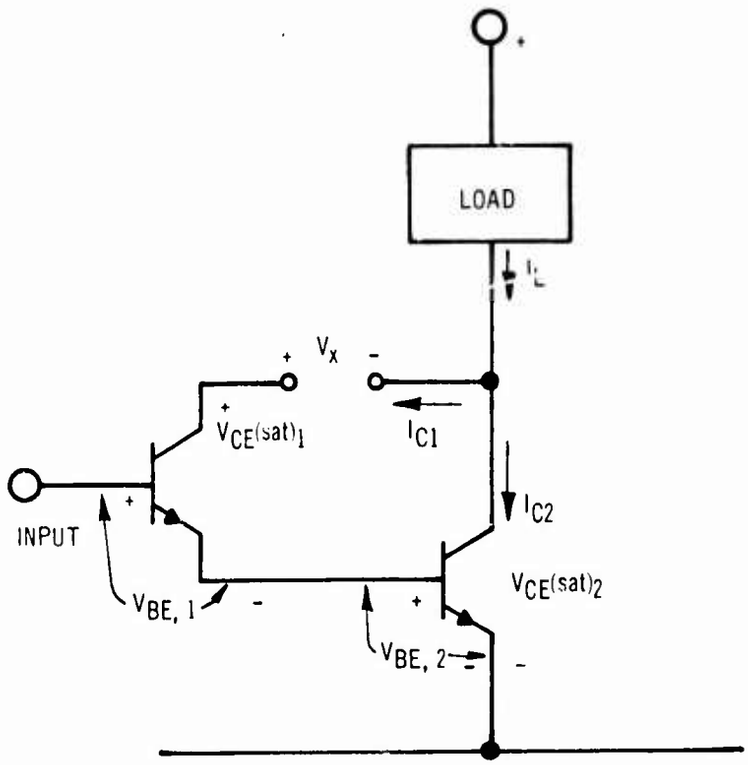

Figure 2-4. Boosted Darlington Amplifier Circuit

It is realized that the 12 voltages must be generated in the peripheral gear, which is located in another part of the system. The supply circuits require wiring that can carry 50 amperes with minimum loss. The real advantage of this approach is that 270 watts of power were removed from the switch chassis. This power reduction should permit a full three starts of the system with an adequate safety factor.

SECTION III

TECHNICAL DISCUSSION OF CIRCUIT PACKAGE CONFIGURATION

3-1. STARTING CYCLE ENERGY ABSORPTION - NORMAL DARLINGTON

The heat absorbing abilities of the most useful materials for heat sinking and structural purposes were calculated and tabulated on the basis that the cooling air during start would be negligible. The number of joules required to produce a temperature rise of $1^{o}C$ was then calculated for the maximum specified weight (5 pounds) for this assembly. The optimum material, aluminum, was then used in a calculation of the temperature rise due to the joules produced during a typical start.

An example of the calculation used to determine rankings for 5-pound heat sinks follows:

$$\text{Aluminum: Joules}/^{o}C = \left(0.225 \frac{\text{Calories}}{\text{gram} - {}^{o}C}\right)\left(4.19 \frac{\text{joules}}{\text{cal}}\right)\left(\frac{10^3 \text{ grams}}{2.2 \text{ lbs}}\right)\left(5 \text{ lbs.}\right)$$

$$= 2150$$

Heat absorption results for 5 pounds of material tested for use in the module mounting plates and commutator assembly structure are tabulated below:

Material	Specific heat (cal/gm)	Space for 5 pounds in in^3	Heat absorption capabilities (joules/^{o}C)
Aluminum	0.225	50	2150
BeO	0.30	50	2850
Copper	0.095	15.6	905
Nickel	0.114	15.6	1085
Titanium	0.112	31	1065

Magnesium was regarded as a fire hazard.

While BeO is the highest ranked material, and though pieces of BeO will be used in each module, aluminum can carry 400 amperes and can become a major part

of the module output circuit. Aluminum is also a logical choice for the rectifier mounting plate and the commutator quadrant assembly framework. Some copper will be needed for stranded cable and so forth, even though it is inferior in this application. However, copper will be a minor component and also its properties will be partially balanced by the superior heat absorption quality of BeO. It will be assumed, therefore, that the heat sink will be equivalent to 5 pounds of aluminum and the heat absorbing capability will be 2150 joules/^{o}C.

Based on the starting conditions of 400 amperes maximum given in Lear Siegler Exhibit 1 (Figure 3), the heat generated in each module can be calculated. As described in Section II, the output portion of the 400-ampere switching module will consist of six RCA TA-7017 chips in parallel driven by six 8A driver chips in parallel, as discussed in Section II. The voltage drop of the circuit in Section II is essentially the V_{BE} of the output circuit plus the $V_{CE(SAT)}$ of the driver. The start-heat generated in each module can then be calculated:

$$Q \text{ joules} = \Big[V_{CE(sat)} \ (I_C) \ (t_{pulse}) + (V_{supply}) \ (I_C) \ (t_{fall} + t_{rise}) \Big] \times (\text{No. of pulses})$$

This calculation is shown in Appendix C: Q = 2130 joules/switch

The total energy in the commutator is 4 times this value plus a 10 percent safety factor: Q_{total} = 55,800 joules/start.

Using this quantity of heat and the heat absorption for the 5-pound aluminum heat sink, the temperature rise for start can now be calculated.

$$\Delta T_{case} = \frac{55{,}800 \text{ joules}}{2150 \text{ joules}/^{o}C}$$

$$\Delta T \approx 26^{o}C$$

Taking the specified ambient temperature of 125^{o}F or 52^{o}C, the temperature of the module assembly will be $52^{o} + 26^{o} = 78^{o}$ at the end of the first start.

The effect of this case-temperature rise on the devices can be calculated as follows: the TA-7017 output units will each pass 67 amperes through a voltage drop of 3.2 volts. The power to be dissipated is P = 67 amperes x 3.2 volts = 220 watts. The standard TA-7017 version is the same 0.380-inch square chip

lead mounted to a molybdenum mounting block brazed to a copper TO-3. Typical thermal resistance values range from 0.25°C/watt to 0.4°C/watt. It is planned to use the same chip and molybdenum block brazed to a copper clad aluminum heat sink for the modular version. A value of 0.4°C/watt will be used for this analysis.

Using the starting power dissipation of 220 watts and a steady state thermal resistance of 0.4°C/watt, a junction temperature rise is calculated:

$$\Delta T_{j-c} = 0.4^{\circ}C/watt \times 220 \text{ watts} = 88^{\circ}C$$

Therefore, at the end of the first start, the devices on the module would momentarily have a junction temperature of

$$T_{case} + \Delta T_{junction\text{-}to\text{-}case} = T_{junction}$$

$$78^{\circ}C + 88^{\circ}C = 166^{\circ}C$$

Taking into account the pulse conditions and the thermal time constants (see Appendix D) the junction temperature is actually 111°C.

Assuming the engine did not start on the first attempt, a 2-minute wait is specified. There may be some small degree of convection cooling during this 2-minute wait but this helpful effect will be neglected in this worst case analysis. The same 55,800 joules will be generated during the second start, heating the 78°C package an additional 26°C to 104°C. The output device junctions will be 36°C above this case temperature, reaching ≈140°C. The second start is still a safe condition.

Assuming the engine does not start on the second attempt and assuming, at this time, that no cooling takes place during the 2-minute wait, the effects of the third start are as follows: the 104°C package will be heated to 104°C + 26°C = 130°C. The output device junctions will then reach a temperature of 130°C + 36°C = 166°C. The third start also appears feasible in these calculations.

3-2. STARTING CYCLE ENERGY ABSORPTION - BOOSTED DARLINGTON

Based on the same specified boundary conditions, but using the "Boosted Darlington" described in Section II, paragraph 2-4, the effects of three starts can also be calculated. It offers an attractive alternative.

The major effect of the "Boosted Darlington" is to reduce the voltage drop in the output stage to the $V_{CE}(sat)$ value of 1.2 volts. This reduces the joules per start, the temperature rise of the package per start, and the ΔT junction-to-case of the device chips. The total commutator joules per start are calculated

$$Q = \left[(V_{CE(sat)})(I_c)(t_p) + (V_{supply})(I_c)(t_{fall})(t_{rise})\right] \left[\text{No. of Pulses}\right]$$

$Q = 22{,}600$ (as shown in Appendix C).

compared to the 51,200 joules of the normal Darlington. The temperature rise of the case now becomes:

$$\Delta T \text{ case} = \frac{22{,}600 \text{ joules}}{2150 \text{ joules}/^{\circ}C}$$

$$\Delta T \text{ case} = 11^{\circ}C \text{ per start}$$

Three starts will only raise the commutator to a temperature of $52^{\circ}C + 33^{\circ}C = 85^{\circ}C$. The power to be dissipated on each output pellet becomes:

$$P = (67 \text{ amperes})\ (1.2 \text{ volts})$$

$$P = 80 \text{ watts}$$

The temperature rise of the junction above the case using the worst case DC condition becomes

$$\Delta T_{j-c} = 80 \text{ watts} \times 0.4^{\circ}C/\text{watt} = 32^{\circ}C$$

Thus, after using the "boosted Darlington" for 3 starts, the calculated maximum junction temperature for the devices will be:

$$T_{j\ max} = 85^{\circ}C + 32^{\circ}C = 117^{\circ}C$$

which is well within the recommended ratings (a very conservative situation). The effects of supplying the necessary biasing currents for the "Boosted

Darlington" will have to be examined from an overall systems viewpoint but it offers a desirable safety factor in the very critical high power semiconductor portion of the equipment.

3-3. COMMUTATOR ASSEMBLY DESIGN

Using the specified boundary conditions of: envelope dimensions, weight, heat absorption needs, and high-current connector terminations, a commutator structure can be designed as shown in Figure 3-1.

Based on the energy absorption calculations which were discussed in paragraph 3-1, aluminum will be the primary material. The 12 individual power switching modules will be arranged radially and will be fastened into electrically insulated slots. Electrical insulation for the module mounting-slots can be a combination of hard anodizing and a protective, thermally-conductive, epoxy resin such as Delta Cote 151 H. These materials will provide reasonable heat transfer out of the modules while electrically isolating the individual modules from the assembly structure. BeO and boron nitride are alternate possibilities for mounting slots that offer electrical isolation and good thermal conduction. The 8 low-current connector terminals and 4 high-current connector terminals will be located on each of the four corners of the assembly. This 12-module structure should be capable of "remove and replace" type maintenance from the termination end of the assembly, providing the shroud is easily removable.

3-4. INDIVIDUAL SWITCHING MODULE

Each of the six positive switches and each of the six negative switches will be physically and electrically interchangeable. However, minor shape variations will prevent mistakingly substituting a positive for a negative switching module if a failure occurs in the field. The basic structure of the individual power switching module will be as shown in Figure 3-2.

The six TA-7017 chips used in the output stage dissipate the most heat and have been dispersed as widely apart as possible.

The mounting plate part of the module will consist of a copper-clad (10% of thickness) aluminum plate. As discussed in Section III, 3-1, the aluminum will

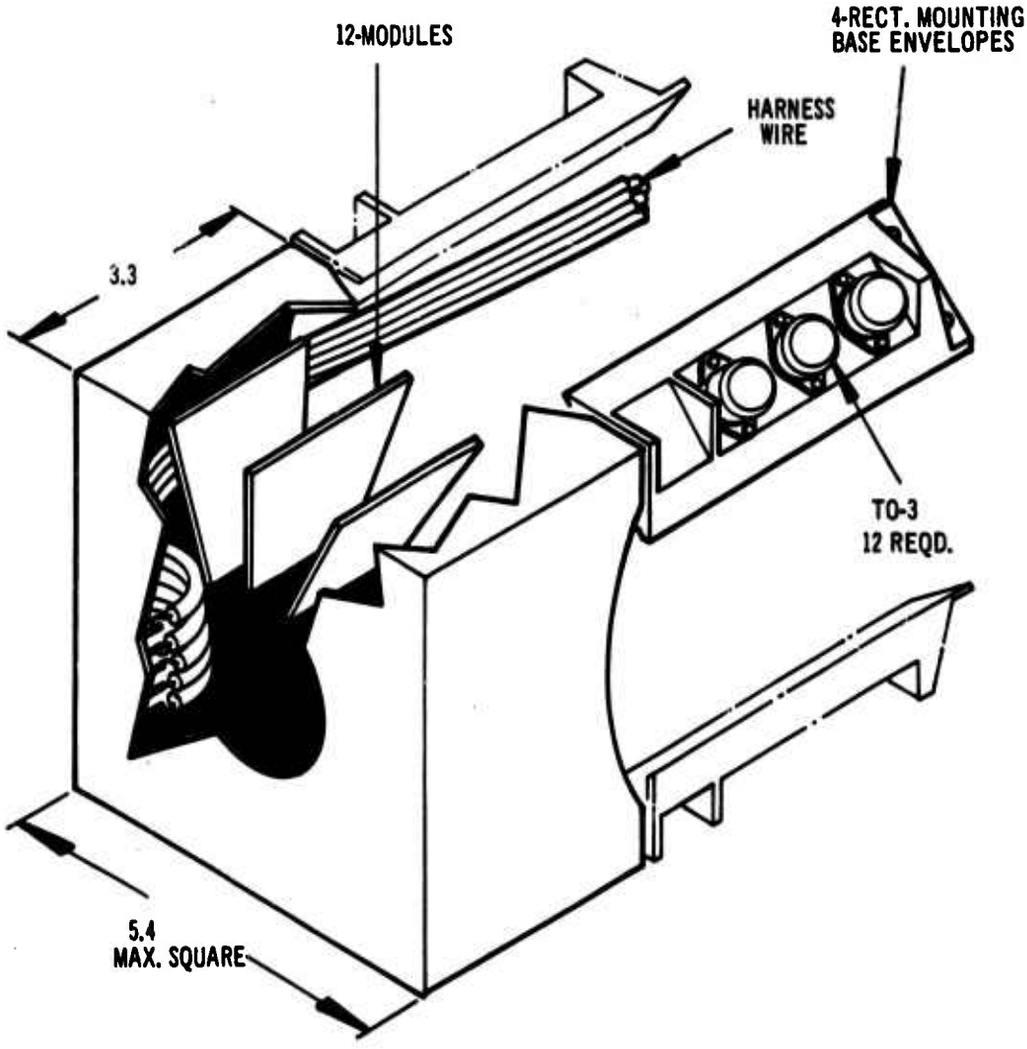

Figure 3-1. Static Commutator Power-Switching Assembly

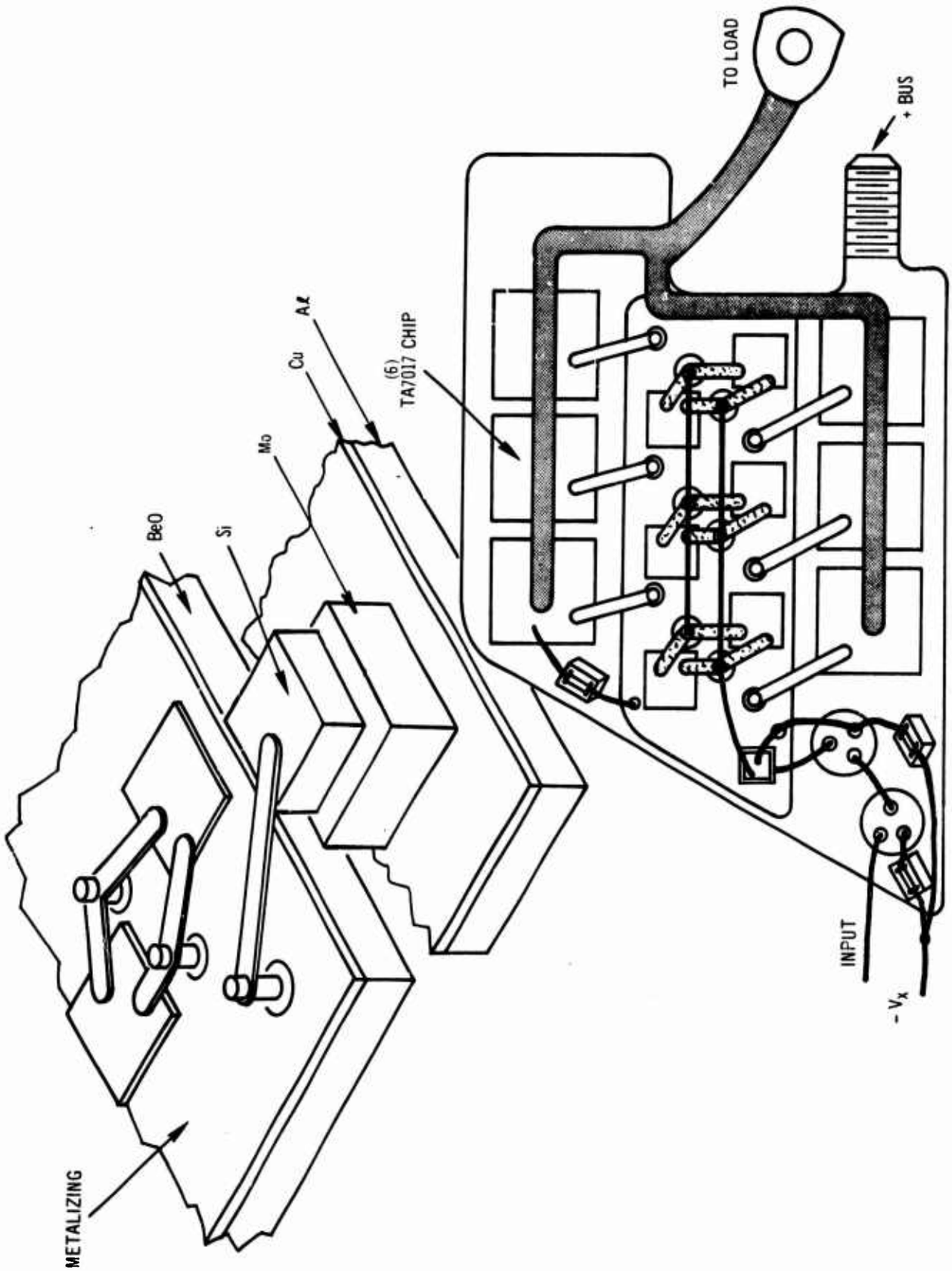

Figure 3-2. Individual Power-Switching Module

absorb the heat produced during the start cycle and act as the conductor for the 400Å collector current. The copper cladding on the aluminum will facilitate brazing the molybdenum blocks and the metalized BeO pieces. The molybdenum blocks are required to match the thermal expansion of the large silicon power TA7017 chips. (The TA7017 is presently the largest number of the RCA hometaxial power transistor family.) The metalized BeO piece will provide electrically isolated mounting for the medium-power driver chips while providing good heat absorption (Section III, 3-1), and good heat transfer to the copper-clad aluminum mounting plate. The pins brazed to various metalized areas on the BeO provide ideal anchor points for soldered clips that will provide interconnection to the emitters, bases, collectors, and thick-film resistors in the circuit. Similar pins brazed to BeO have been used with excellent reliability on RCA power transistors such as the JAN 2N3375. The clips will be similar to those designed into RCA's conventional silicon process power transistors.

Interconnection of chips and thick-film resistors and paralleling of the driver-stage chips can then be accomplished by wiring from pin to pin. The emitter contacts of the output units will be paralleled by soldering a flat-stranded nickel-plated copper strap to each emitter area. This will complete the other half of the 400Å output circuit.

The planar units in the low-level input stages will be packaged in hermetically sealed TO-18 cans and press fit with an insulating sleeve into the aluminum mounting plate. An alternate attaching method would use thermally conductive epoxy to attach the TO-18's to the mounting plate.

When all of the chips and thick-film resistor blocks are soldered into place and electrically checked, the device can then be encapsulated. The first coat will be a silicone junction coating for good electrical characteristics. This will be followed by a thick coating of a flexible silicone resin to provide additional environmental protection and allow the considerable thermal expansion and contraction to take place without additional stresses from the resin. The close fitting finned aluminum cover will be put in place and mechanically staked or swaged Additional resin will be cast or molded into

special holes in the cover and around the electrical termination openings. The completed module will resemble Figure 3-3.

RCA has over a million hours of successful device testing of its new 2N5034 and TA-2911 silicone plastic molded silicon power transistors. The failure rate adjusted to rated conditions from the over-stress test is approximately 0.1 percent per 1000 hours. A similar silicone resin and silicone plastic coating is planned for this power module, which should afford excellent reliability.

These modules will be tested when they are completed and after their assembly into the commutator assembly under the conditions specified in the environmental specification in Lear Siegler Exhibit I.

3-5. RECTIFIER ASSEMBLY DESIGN

The rectifier will be supplied in 4 aluminum mounting blocks or modules. It is planned that each module will contain 3 rectifiers enclosed in individual device envelopes as shown in Figure 3-2.

Modules of suitable material thickness are not to exceed 1.5 pounds for all 4 modules. Each module has the following maximum dimensions and weight restrictions:

a. Maximum weight per module: 0.37 pound
b. Maximum allowable height: Approximately one inch
c. Effective heat sinking and sealing surface area per module: Approximately 3/4 inch x 3-1/2 inches.

Electrically, each rectifier must be capable of a continued average rating of 33 amperes or 58 amperes R.M.S. Also, each rectifier must exhibit controlled avalanche characteristics at 80 volts peak reverse-voltage.

To meet these requirements a device envelope with the dimensions of the TO-3 will be given primary consideration because it appears to best meet the termination configuration, dimensional requirements, and the weight restriction imposed by Lear Siegler drawing No. 23068-1000.

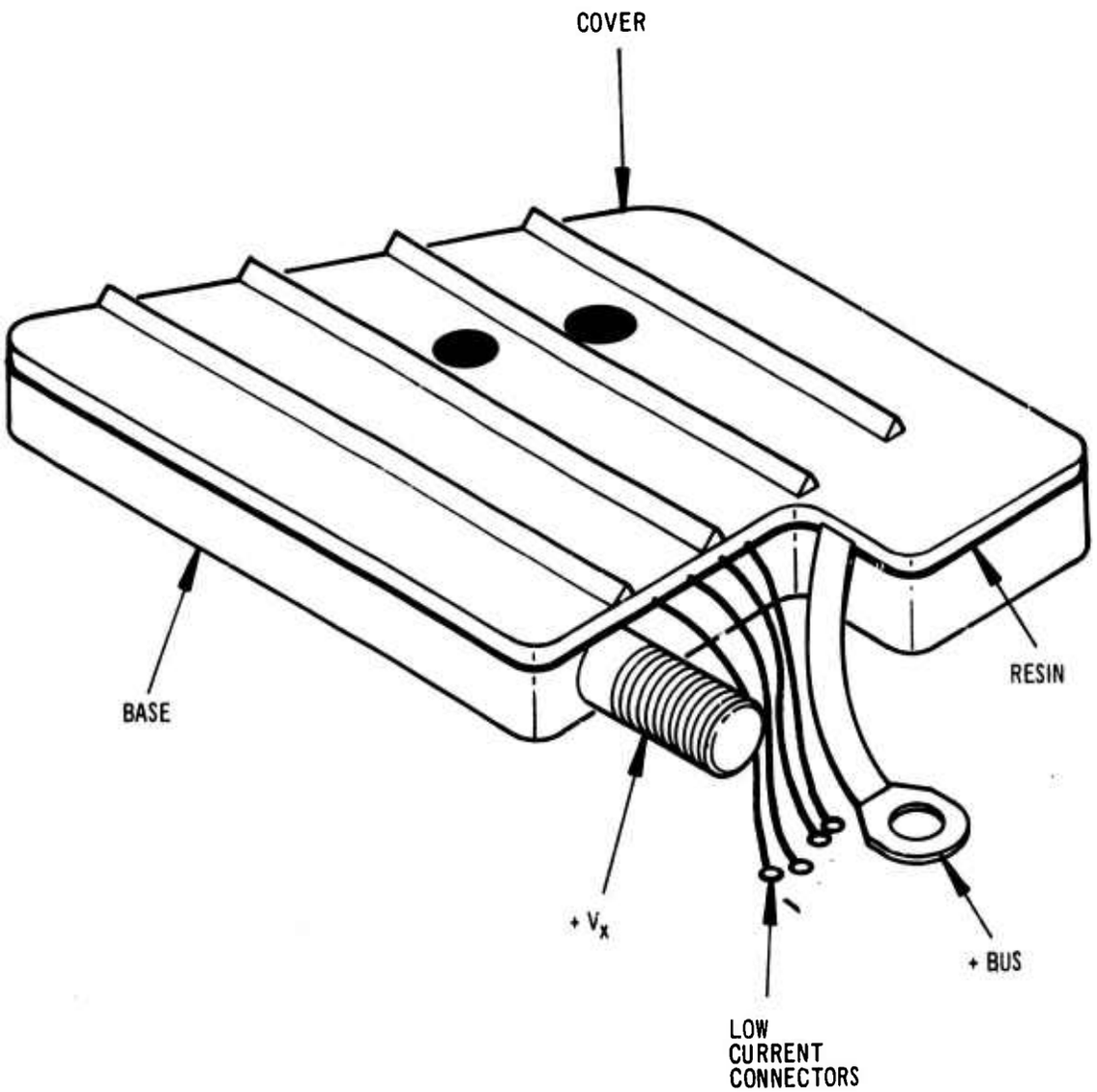

Figure 3-3. Completed Individual Module

In the unlikely event that a 50-watt Zener rectifier (similar to the 1N 2835) cannot meet the established specifications, two alternate approaches can be explored. One alternative involves utilizing a stud package of smaller dimensions than the TO-3. This configuration would use 6 devices per rectifier-module. The other alternative would utilize 3 stud packages per module, but the overall height of these packages would be greater, by approximately 1/2 inch, than the overall height presently permitted by the existing specifications.

These alternatives would be explored only if the original rectifier-package configuration could not meet the stated requirements. Although it is unlikely that either of these approaches would be required, they are indicated as possible choices which could be used by making moderate relaxations in the overall rectifier-module dimension and weight requirements.

SECTION IV

STATEMENT OF WORK

4-1. SPECIFICATIONS

The work will be directed toward designing, building, and delivering two commutator assemblies in accordance with this proposal. Each of these commutator assemblies will consist of 6 positive-switch modules, 6 negative-switch modules, a structure to support each module, 4 rectifier modules and associated wiring. This hardware will comply as closely as possible to the specification of Lear Siegler Inc. as shown in Exhibit I (attached) with the following qualifications:

a. The electrical and environmental performance of the commutator assemblies will be consistent with the best efforts of RCA to achieve the operational requirements of the brushless starter-generator as outlined in Exhibit I.

b. The rectifier portion of the commutator assembly shall be in accordance with paragraph 3-5 of this proposal with particular recognition of the possibility of choosing an alternate approach. Every attempt will be made by RCA to use the TO-3 primary approach to achieve the dimensional requirements of the Commutator assembly.

4-2. WORK SCHEDULE

The proposed work schedule as shown in Figure 4-1 represents the best possible and most realistic assessment of timing-milestones for this program that can be achieved by RCA. It was conceived in full recognition of the urgent need

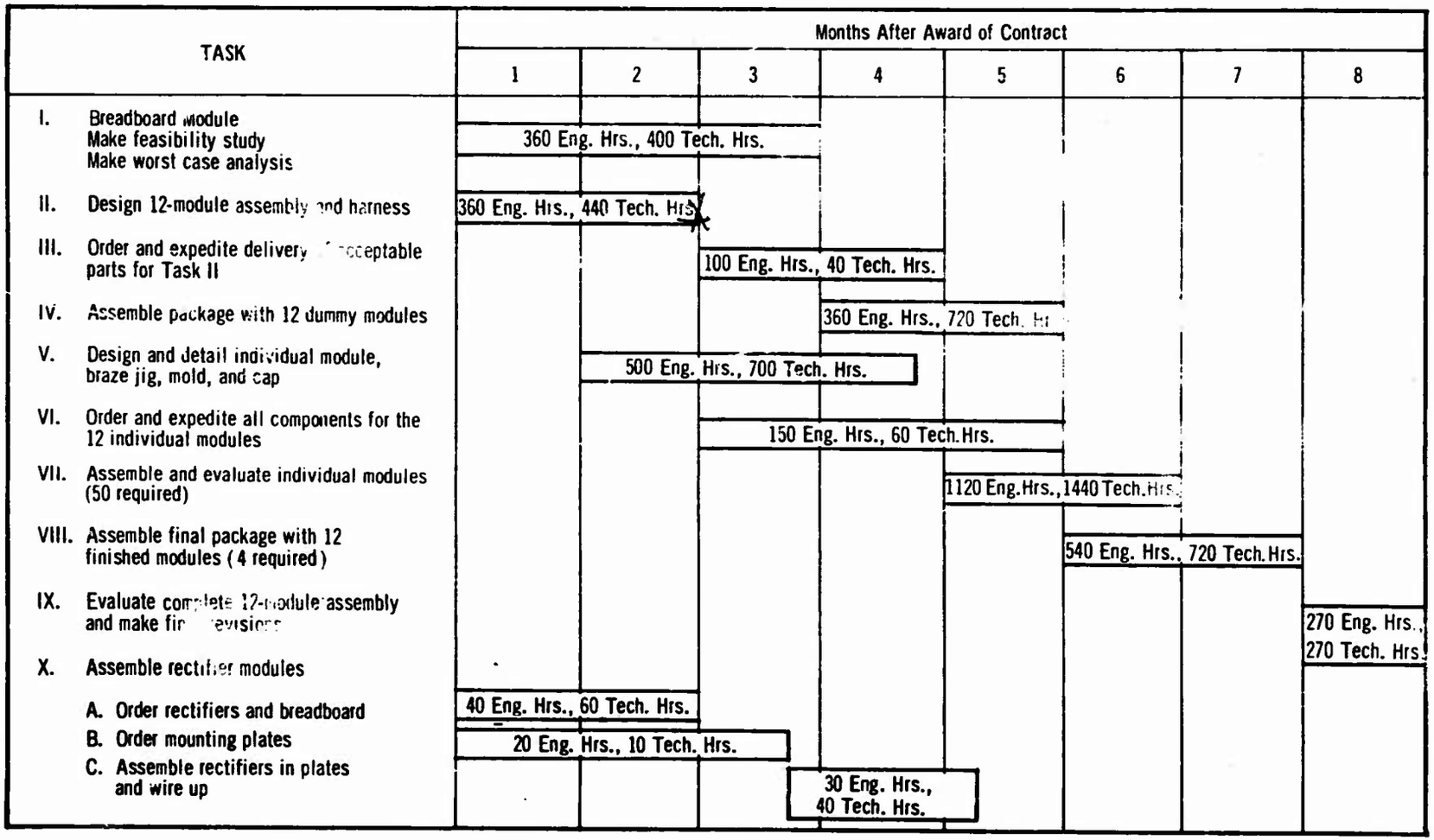

Figure 4-1. Work Schedule

for development of brushless commutator assemblies for Lear Siegler Inc. and consequently reflects the need for developing many phases of this program in parallel.

In view of the stringent timing imposed in this development, RCA has made assumptions on the developmental timing of various phases of this program which do not allow margin for re-design, rework, etc.. Caution should be exercised in assuming the delivery schedule of completed hardware shown as Milestone IX reflects any unusually conservative estimates or built-in margins for major error. RCA has made every attempt to reflect the most realistic possible timing committments consistent with the urgent nature of Lear Siegler's needs.

APPENDIX B

CIRCUIT DESIGN CALCULATIONS

B-1. POSITIVE STATIC SWITCH

Assume T_C maximum = 150°C and V_x is regulated to 10%

$$I_L = I_2 + I_{R,7}$$

If

$$I_2 = (\beta_{10} + 1)\ I_{11}$$

$$I_{R,7} = 0.31 \text{ ampere}$$

$$I_{R,7} = \frac{V_{BE,10} \text{ at } 150^{\circ}C}{R_7}$$

$$R_7 = \frac{0.2}{I_{CER,4} + I_{CBO,10}}$$

$$= \frac{0.2}{21 \times 10^{-3} + 10 \times 10^{-3}}$$

$$= \frac{0.2}{0.031} = 6.5 \text{ ohms per transistor}$$

$$I_{R,7,Fwd} = \frac{V_{BE,10}}{1.0} = \frac{2.0}{6.5}$$

$$= 2.0 \text{ amperes}$$

$$I_L = (\beta_{10} + 1)\ I_{11} + I_{R,7} \quad (I_{R,7} \text{ is negligible})$$

$$400 = (8 + 1)\ I_{11}$$

$$I_{11} = \frac{400}{9} = 45 \text{ amperes}$$

$$I_{11} = (\beta_4)\ (I_3)$$

$$I_3 = \frac{I_{11}}{\beta_4} = \frac{45}{15} = 3.0 \text{ amperes}$$

$$R_3 = \frac{V_{BE,4}}{I_{CBO,4} + I_{CER,3} + I_{CER,2}} \text{ (at } 150^{o}C) = \frac{0.25}{2.5 + 20 + 0.010}$$

$$= \frac{0.2}{23 \times 10^{-3}} = 9.1 \text{ ohms}$$

$$I_6 + I_3 = I_4 + I_5$$

If

$$I_6 = \frac{V_{BE,4}}{R_3} = \frac{2.0}{9.1} = 0.22 \text{ amperes}$$

$$I_5 = (\beta_2)\ (I_8)$$

$$I_4 = (\beta_3)\ (I_{E,2}) = \beta_3\ (\beta_2 + 1)\ I_{B,2}$$

But,

$$I_{E,3} = (\beta_2 + 1)\ I_{B,2}$$

and

$$I_8 = I_{B,2}$$

Then,

$$I_6 + I_3 = (\beta_2)\ (I_8) + \beta_3\ (B_2 + 1)\ I_8$$

$$0.22 + 3.0 = (20)\ (I_8) + (20)\ (20 + 1)\ I_8$$

$$= 440\ I_8$$

$$I_8 = \frac{3.55}{440} = 8.1 \text{ milliamperes}$$

To find R_5,

$$R_5 = \frac{V_{BE,3}}{I_{CBO,3} + I_{CER,2} + \beta_2\ I_{CER,1}} \text{ (at } 150^{o}C)$$

$$= \frac{0.2}{5.0 \times 10^{-3} + 0.010 + (100)(.010)}$$

$$= \frac{0.2}{5.6} = 36 \text{ ohms}$$

$$I_{E,3} = I_{B,2}\,(\beta_2 + 1)(\beta_3 + 1) = 8.1\ (21)(21) = 3.572 \text{ amperes}$$

and

$$I_{E,3} = I_7$$

$$R_6 = \frac{V_x - (V_{CE(sat),2} + V_{BE,3} + V_{BE,4})}{I_7}$$

$$= \frac{10 - (0.5 + 2.0 + 2.0)}{3.572}$$

$$= \frac{10 - 4.5}{3.572} = \frac{5.5}{3.572} = 1.5 \text{ ohms}$$

$$I_{R,5} = \frac{V_{BE,3(on)} + I_7 R_6}{R_5} = \frac{2.0 + 5.5}{36 \text{ ohms}} = \frac{7.5}{36} = 0.21 \text{ ampere}$$

I_8 must be changed to accommodate this current.
If

$$I_{E,2} = I_{B,3} + I_{R,5}$$

$$= \frac{I_{E,3}}{\beta_3 + 1} + I_{R,5}$$

$$= \frac{3.572}{20 + 1} + 0.21$$

$$= 0.17 + 0.21$$

$$= 0.38 \text{ ampere}$$

then

$$I_8 = \frac{I_{E,2}}{(\beta_2 + 1)}$$

$$= \frac{0.38}{21}$$

$$= 0.018 \text{ ampere}$$

$$R_4 = \frac{V_{BE,2} + V_{BE,3}}{I_{CER,1} + I_{CBO,2}} \text{ (at } 150^{\circ}\text{C)} = \frac{0.2 + 0.2}{0.010 + 0.005} = \frac{0.4}{0.015 \times 10^{-3}}$$

$$= 1.0 \text{ kilohm assigned, 23 kilohms permissible.}$$

$$I_{R,4(on)} = \frac{V_{BE,2} + V_{BE,3} + I_7 R_6}{R_4} = \frac{1.1 + 2.0 + (1.5)(3.57)}{1.0}$$

$$= \frac{1.1 + 2.0 + 5.5}{4.0} = \frac{8.5}{1.0} = 8.5 \times 10^{-3} \text{ amperes}$$

$$I_9 = I_8 + I_{R,4(on)}$$

$$= 0.018 + 0.0021$$

$$= 0.0201$$

$$I_{10} = \frac{I_9}{\beta_1} = \frac{20.1 \text{ milliamperes}}{21} = 0.95 \text{ milliamperes}$$

$$I_{R,2} = 21 \text{ milliamperes}$$

$$R_2 = \frac{V_x - (V_{CE(sat),1} + V_{BE,2} + V_{BE,3} + I_7 R_6}{I_{R,2}}$$

$$= \frac{10 - (0.65 + 1.1 + 2.0 + 5.5)}{21}$$

$$= \frac{10 - 9.3}{21} = \frac{0.7}{0.021}$$

$$= 33 \text{ ohms}$$

$I_{10} = 1.0$ milliamperes, but use 2.0 milliamperes.

For the input circuit, assume

$$V_{in} = 5.0 \text{ volts}$$

if

$$V_{R,8} = 2.5 \text{ volts}$$

$$I_{R,8} = 5.0 \text{ milliamperes}$$

then

$$R_8 = \frac{V_{R,8}}{I_{R,8}} = \frac{2.5}{5.0} = 500 \text{ ohms}$$

If

$$V_{R,1} = 2.5 \text{ volts}$$

and

$$I_{R,1} = 3.0 \text{ milliamperes}$$

then

$$R_1 = \frac{2.5}{3.0} = 820 \text{ ohms}$$

If

$$V_{R,9} = 2.5 - (V_{BE,1} + V_{R,2}) = 2.5 - (1.1 + 0.7) = 0.7 \text{ volts}$$

and

$$I_{R,9} = 2.0 \text{ milliamperes}$$

then,

$$R_9 = \frac{0.7}{2.0 \times 10^{-3}} = 350 \text{ ohms}$$

B-2. NEGATIVE STATIC SWITCH

Assume maximum $T_C = 150^oC$ and regulated to 10%

$$I_L = 400 \text{ amperes} = I_1 + I_2$$

If

$$I_1 = \beta_4 I_4$$

$$I_2 = \beta_{10} I_{B,10}$$

$$I_{B,10} = I_3 - I_{R,9}$$

$$I_3 = (\beta_4 + 1) I_4$$

Then,

$$I_L = (\beta_4 I_4) + \beta_{10} (\beta_4 + 1) I_4 - \beta_{10} I_{R,9}$$

$$= (15) I_4 + 8 (16) I_4 - 16$$

$$= (143) I_4 - 16 = 400 \text{ amperes}$$

$$I_4 = \frac{416}{143} = 2.9 \text{ amperes}$$

and

$$I_1 = (\beta_4) (I_4) = (15) (2.9) = 43.5 \text{ amperes}$$

$$I_3 = (\beta_4 + 1) (I_4) = (16) (2.9) = 46.5 \text{ amperes}$$

$$I_{B,10} = I_3 - I_{R,9} = 46.5 - 2.0 = 44.5 \text{ amperes}$$

$$I_2 = \beta_{10} (I_{B,10}) = 8 (44.5) = 356 \text{ amperes}$$

$$R_9 = \frac{V_{BE,10}}{6I_{CER,4} + 6I_{CBO,10}} \quad (\text{at } 150^oC)$$

$$= \frac{0.2}{6(20) \times 10^{-3} + 6(10) (10^{-3})}$$

$$= \frac{0.2}{0.180} \approx = 1.0 \text{ ohm}$$

$$I_{R,9(on)} = \frac{V_{BE,10(on)}}{R_9}$$

$$= \frac{2.0}{1.0} = 2.0 \text{ amperes}$$

Now,

$$R_8 = \frac{V_{BE,4} + V_{BE,10}}{I_{CER,2} + I_{CER,3} + I_{CBO,4}} \text{ (at } 150^{\circ}\text{C)}$$

$$= \frac{0.20 + 0.20}{0.01 + 20 + 2.5} = \frac{0.4}{22.5}$$

$$= 18 \text{ ohms}$$

$$I_{R,8(on)} = \frac{V_{BE,4} + V_{BE,10}}{R_8} = \frac{2.0 + 2.0}{18} = \frac{4.0}{18}$$

$$= 0.225 \text{ ampere}$$

$$I_5 + I_6 = I_4 + I_{R,8} = 2.9 + 0.225 = 3.125 \text{ amperes}$$

If

$$I_5 = \beta_3 I_{E,2}$$

$$I_{E,2} = (\beta_2 + 1) I_7$$

$$I_6 = \beta_2 I_7$$

Then,

$$\beta_3 (\beta_2 + 1) I_7 + \beta_2 I_7 = I_4 + I_{R,8}$$

$$(15) (20 + 1) I_7 + (20) I_7 = 3.125$$

$$335 I_7 = 3.125$$

and:

$$I_7 = \frac{3.125}{335} = 9.35 \text{ milliamperes}$$

Now for R_3

$$V_{B,3} = V_x - (V_{CE(sat),3} + V_{BE,4} + V_{BE,10})$$

$$= 10 - (1.20 + 2.0 + 2.0) = 10 - 5.2$$

$$= 4.8 \text{ volts}$$

$$R_2 = \frac{V_{BE,3 \text{ at } 150^oC}}{I_{CBO,3} + I_{CER,2}} \quad (\text{at } 150^oC) = \frac{0.2}{2.5 + 0.01} = \frac{0.2}{2.5}$$

$$= 80 \text{ ohms}$$

$$I_{R,2(on)} = \frac{V_{BE,3} + V_{R,3}}{R_2} = \frac{2.0 + 4.8}{80} = \frac{6.8}{80}$$

$$= 85 \text{ milliamperes}$$

$$I_{E,2} = (\beta + 1)\ I_{B,2} = (21)\ (9.35)$$

$$= 196 \text{ milliamperes}$$

But,

$$I_{E,2} = I_{E,2} + I_{R,2(on)} = 196 + 85$$

$$= 281 \text{ milliamperes}$$

Now,

$$I_{B,2} = \frac{I_{E,2}}{B_2 + 1} = \frac{281}{21}$$

$$= 13.4 \text{ milliamperes}$$

$$I_{E,3} = (\beta + 1)\ (I_{E,2}) = (20 + 1)(196) = (21)(196)$$

$$= 4.116 \text{ amperes}$$

$$R_3 = \frac{V_{R,3}}{I_{E,3}} = \frac{4.8}{4.116}$$

$$= 1.15 \text{ ohms}$$

$$I_{C,1} = I_{R,1} + I_7$$

$$R_1 = \frac{V_{BE,2} + V_{BE,3}}{I_{CER,1} + I_{CBO,2}} \quad \text{(at } 150^{\circ}C\text{)}$$

$$= \frac{0.2 + 0.2}{0.01 + 0.05} = \frac{0.4}{0.015}$$

= 26 kilohms, use 1.0 kilohm

$$I_{R,1(on)} = \frac{V_{BE,2} + V_{BE,3} + V_{R,3}}{R_1} = \frac{(1.1 + 2.0 + 4.8)}{1000} = \frac{7.9}{1000}$$

= 8.0 milliamperes

$I_{C,1}$ = 8.0 + 13.4

= 21.4 milliamperes

$$I_8 = \frac{I_{C,1}}{\beta} = \frac{21.4}{20}$$

= 1.05 milliamperes

$I_{E,1} = (\beta + 1)(I_8) = (21)(1.05)$

= 22 milliamperes

For R_7,

$V_{R,7} = V_{CC} - (V_{CE(sat),1} + V_{BE,2} + V_{BE,3} + V_{R,3})$

= 10 - (0.5 + 1.1 + 2.0 + 4.8) = 10 - 8.4

= 1.6 volts

$$R_7 = \frac{V_{R,7}}{I_{E,1}} = \frac{1.6}{22.0}$$

= 75 ohms

$I_{R,4} = I_{R,6} + I_{R,5}$

= 5.0 milliamperes

Assume 1.0 volts across R_4, then,

$$R_4 = \frac{V_{R,4}}{I_{R,4}} = \frac{1.0}{5 \times 10^{-3}}$$

= 200 ohms

If

$$V_{R,5} = V_{signal} - V_{R,4} = 5.0 - 1.0$$

$$= 4.0 \text{ volts}$$

$$I_{R,5} = 3.0 \text{ milliamperes}$$

Then,

$$R_5 = \frac{V_{R,5}}{I_{R,5}} = \frac{4.0}{3.0}$$

$$= 1.33 \text{ kilohms}$$

and

$$V_{R,6} = 4.0 - (V_{BE,1} + V_{R,2})$$

$$= 4.0 - (1.1 + 1.6)$$

$$= 1.3 \text{ volts}$$

If

$$I_{R,6} = 2.0 \text{ milliamperes}$$

then,

$$R_6 = \frac{V_{B,6}}{I_{R,6}} = \frac{1.3}{2.0}$$

$$= 560 \text{ ohms}$$

APPENDIX C

CALCULATION OF POWER AND ENERGY

C-1. ASSUMPTIONS

1. Use six-step graphical analysis (see Figure C-1).
2. Assume 4 switches are on at one time.
3. Calculations are based on a single switch basis.
4. Assume 33% "on" time.
5. Period is equal to 3 times the pulse width.
6. Pulse width read from log plot assuming a linear plot from 300 milliseconds to 1.7 milliseconds.

The terms are defined as follows:

$V_{CE(sat)}$ = output stage collector-to-emitter voltage in the "on" state.

I_c = output stage current that is equal to load current.

t_p = pulse width of the current.

V_{cc} = supply voltage = 30 volts.

t_f = transistor fall time = 25 μs

t_r = transistor rise time = 25 μs

No. Pulses = number of pulses in a 5 second period.

The energy per switch is

$$Q = \left[(V_{CE(sat)})(I_c)(t_p) + (V_{cc})(I_c) \times (t_f + t_r)\right] \left(\text{No. Pulses}\right)$$

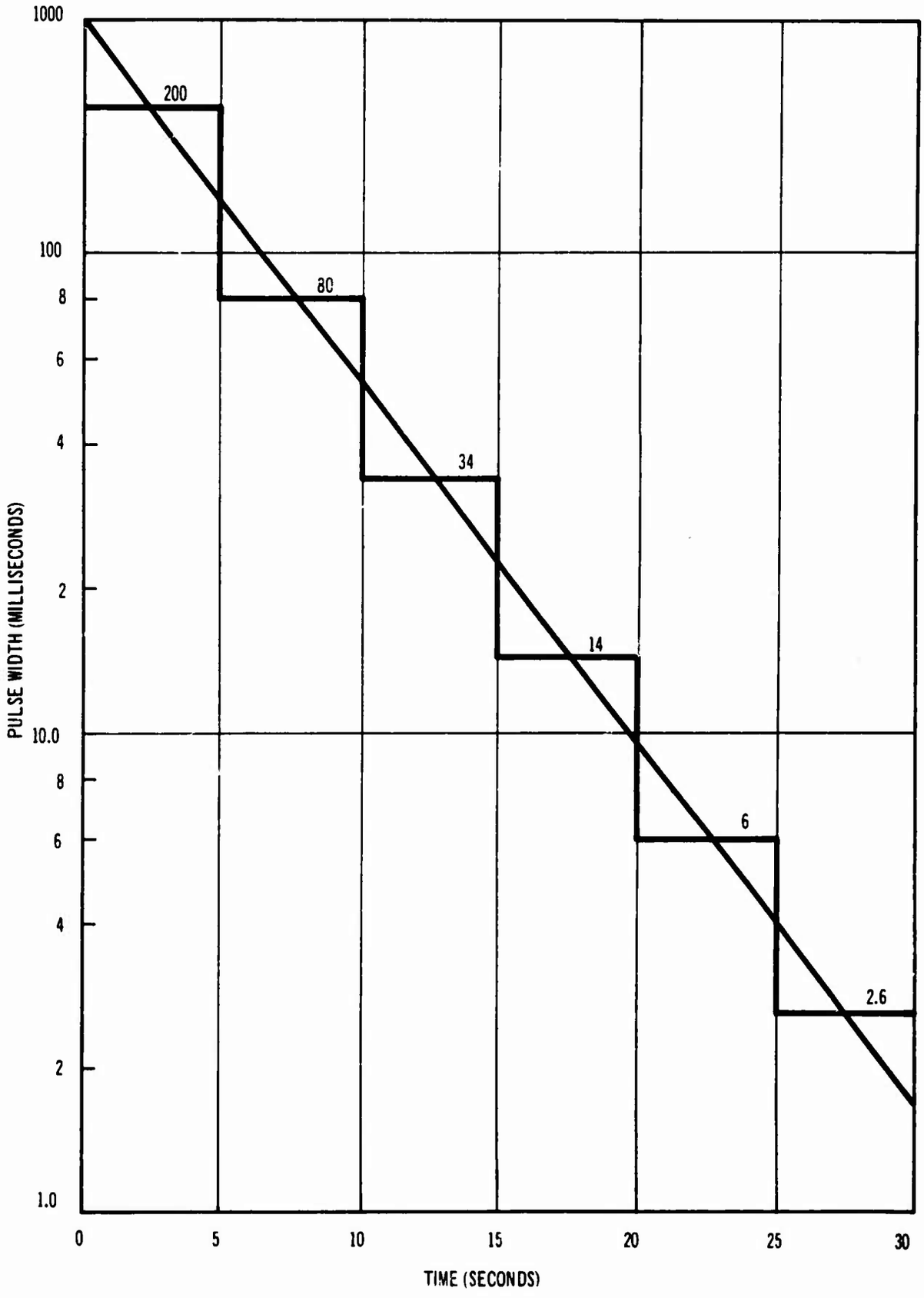

Figure C-1. Pulse Width vs Time of Output Stage

Sample calculation for first step

$$Q = \left[(3.2)(400)(200 \times 10^{-3}) + (30)(400)(50 \times 10^{-6})\right] \quad 8.3$$

$$= \left[(1280)(200 \times 10^{-3}) + (12000)(50 \times 10^{-6})\right] \quad 8.3$$

$$= (256 + 0.6) \quad 8.3$$

$$= 2129.78 \text{ joules/switch}$$

The six-step integration is shown in Table C-I.

Total energy in commutator for Normal Darlington

$$Q = (\text{Energy/Switch}) (\text{No. of switches}) (\text{safety factor})$$

$$= (12{,}682 \text{ joules}) (4) (1.1)$$

$$Q \text{ Total} = 55{,}800 \text{ joules}$$

The Boosted Darlington energy per switch may be calculated using the above equations with a $V_{CE(sat)}$ of 1.2 volts. See Table C-II for the six-step integration.

$$Q = 5151 \text{ joules/switch}$$

The total energy in the commutator for the Boosted Darlington is

$$Q = (\text{Energy/Switch})(\text{No. of switches}) (\text{safety factor})$$

$$= (5151 \text{ joules}) (4) (1.1)$$

$$= 22{,}600 \text{ joules/start}$$

The current is assumed to be constant at 400 amperes for the full 30-second period. This is pessimistic assumption.

TABLE C-I. NORMAL DARLINGTON ENERGY CALCULATION RESULTS

Quantum Period	Pulse Width (ms)	Period (ms)	f (c/s)	No. of Pulses	t_{on} (ms)	t_{off} (ms)	Switching Energy (Joules)	Power Pulse Energy (Joules)	Total Energy (Joules)
1	200	600	1.66	8.3	200	400	5.0	2124.8	2129.8
2	80	[illegible]	4.0	21	80	160	11.6	2150	2161.6
3	34	[illegible]	10.0	50	34	68	30	2175	2205
4	14	50	20	100	14	28	60	1750	1810
5	6	20	50	250	6	12	150	1850	2000
6	2.6	8	125	625	2.6	5.2	375	2000	2375
Total							632	12,050	12,682

TABLE C-II. BOOSTED DARLINGTON ENERGY CALCULATION RESULTS

Quantum Period	Pulse Width (ms)	Period (ms)	f (c/s)	No. of Pulses	t_{on} (ms)	t_{off} (ms)	Switching Energy (Joules)	Power Pulse Energy (Joules)	Total Energy (Joules)
1	200	600	1.66	8.3	200	400	5.0	796	801
2	80	240	4.0	21	80	160	11.6	807	819
3	34	100	10.0	50	34	68	30	815	845
4	14	50	20	100	14	28	60	656	716
5	6	20	50	250	6	12	150	695	845
6	2.6	8	125	625	2.6	5.2	375	750	1125
Total							631.6	4,519	5,151

APPENDIX D

TRANSIENT THERMAL RESISTANCE

D-1. CALCULATION

The thermal resistances and capacitances of the various assembled parts of the output units used to compute the thermal RC or thermal time constant are listed below.

	R_{th} °C/W	C_{th} Watt-sec/°C	RC Thermal in milliseconds
Silicon chip	2.88×10^{-2}	2.5×10^{-3}	0.072
Lead	2.14×10^{-2}	3.5×10^{-3}	0.074
Molybdenum	1.5×10^{-1}	2.9×10^{-1}	43.0
Aluminum (adjacent to molybdenum)	1.05×10^{-1}	2.06	210.0

The thermal time constants may be compared to the on and off times occurring toward the end of the start cycle, i.e., t_{on} = 2.6 milliseconds, t_{off} = 5.2 milliseconds.

These times are significant in that the silicon chip and the lead will be modulated by the short pulses, but the molybdenum block and aluminum will be thermally charging and achieving a steady state.

The lumped thermal resistance of the molybdenum and aluminum, though calculated at 0.25°C/W, will be set at 0.35°C/W to allow for real device variations. The effective pulse power for the molybdenum and aluminum is one third of the 220 watts or 73 watts. The ΔT rise will be 75 W x 0.35°C/W = 26°C. The time constants of the silicon chip and lead are short compared to the pulse. The ΔT is then calculated on full power:

$$\Delta T = 220 \text{ W} \times 0.05^{\circ}\text{C/W} = 11^{\circ}\text{C}$$

The total ΔT junction-to-case is $36^{\circ}C$. The junction temperature is then

$$T_{case} + \Delta T_{j-C} = T_{junction}$$

$$75^{\circ}C + 36^{\circ}C = 111^{\circ}C$$

APPENDIX III

RCA FINAL REPORT

SEMICONDUCTOR HYBRID ARRAY

FOR

COMMUTATION OF CURRENT IN BRUSHLESS STARTER-GENERATOR

SEMICONDUCTOR HYBRID ARRAY FOR COMMUTATION OF CURRENT IN BRUSHLESS STARTER-GENERATOR

Final Report
MARCH 1969

Prepared by

D.M. Baugher, H.R. Meisel, and J. Rivera
RCA ELECTRONIC COMPONENTS
Somerville, New Jersey

For

LEAR SIEGLER, INC.
Power Equipment Division
Cleveland, Ohio

FOREWORD

The work covered by this report was sponsored jointly by Lear Siegler, Inc. and by RCA. Lear Siegler sponsorship was defined by their Purchase Order No. 74453 under Air Force Contract AF33(615)-3625. The design followed the guidelines established in Lear Siegler Specification No. 15-100011, dated May 17, 1967.

TABLE OF CONTENTS

TABLE OF CONTENTS (Cont.)

LIST OF ILLUSTRATIONS

LIST OF TABLES

SECTION I
INTRODUCTION

The need for a lightweight, compact array of twelve 400-ampere transistorized switches led to this program for the design and fabrication of high-current power hybrid modules. The 12-module array produced for this program is part of an electronic commutator for a DC motor; the array replaces the present mechanical brush and commutator parts.

A hybrid integrated power module design was chosen after it was determined that conventionally packaged discrete transistor assemblies could not meet the prescribed weight and volume limitations of the system. The contract specified a maximum weight of 5 pounds and a configuration that would fit within a special shape of 75 cubic inches. Each module was required to switch 400 amperes from an input signal of 10 milliamperes; to block 80-volt transient peaks in the "off" state; and to absorb the 1.2 kilowatts dissipated on the basis of a one-third duty cycle for a specified short period of operation.

SECTION II
TECHNICAL DISCUSSION

A. GENERAL INFORMATION

The module array developed for this contract contains two groups of six transistorized switch modules, a total of 12 switch modules. Figure 1 shows the switch array with two switch modules removed. Each module group contains three positive switch modules and three negative switch modules. Figure 2 is the block diagram of one module group; windings L1 through L3 represent the load, i.e., the starter motor windings. The other six switch modules of the array are identical but are operated 30 degrees out of phase with those of Figure 2. Each module is basically a switching amplifier, the output stages of which contains "composite" or paralleled multiple chips. The switch modules operate with a 120-degree (one-third) duty cycle at frequencies from DC to 200 hertz. Figure 3 shows variations in frequency response as a function of time.

Input signals to switches A, B, and C (Figure 2) are referenced to the positive bus; these switches are termed positive switches. Input signals to switches D, E, and F are referenced to the common bus; those switches are termed negative switches. The type of signal and the current-carrying requirements are such that the positive switch must have pnp action and the negative switch npn action.

B. CIRCUIT DESIGN

1. AC SIMULATION

By opening and closing in proper sequence the pairs of switches shown in Figure 2, current flows in a controlled manner through Y-connected load windings L1 through L3. Windings L1 and L2 pass current in one direction with switches A and E closed and in the opposite direction with switches B and D closed. A polyphase AC output is produced, therefore, from a DC supply.

02835P

Figure 1. Module Array with Two Switch Modules Removed

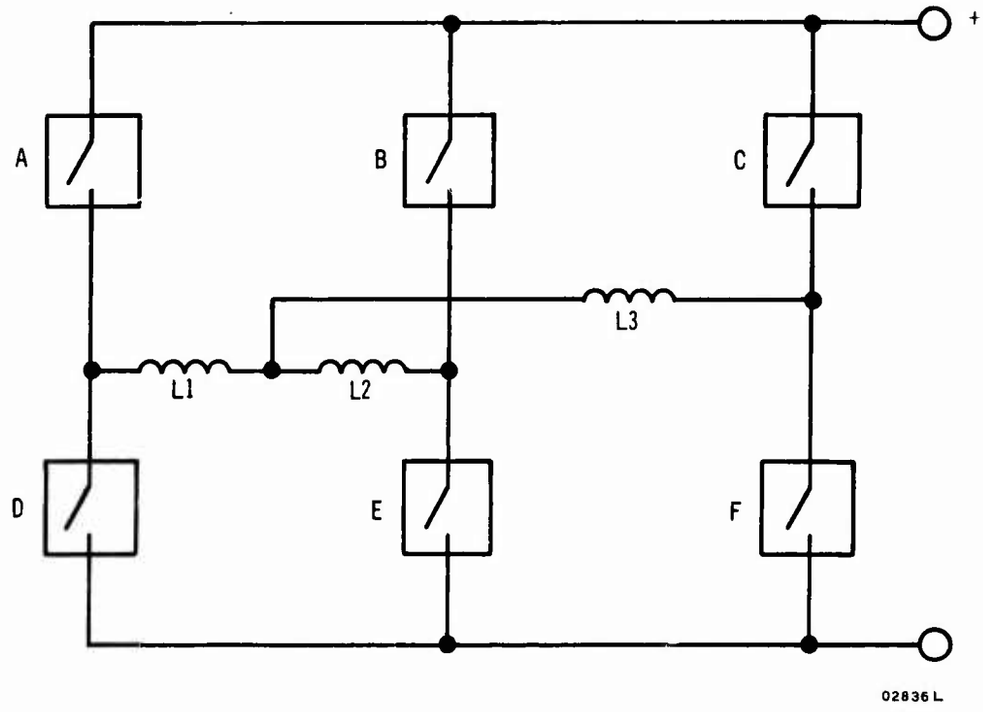

Figure 2. Module Group, Block Diagram

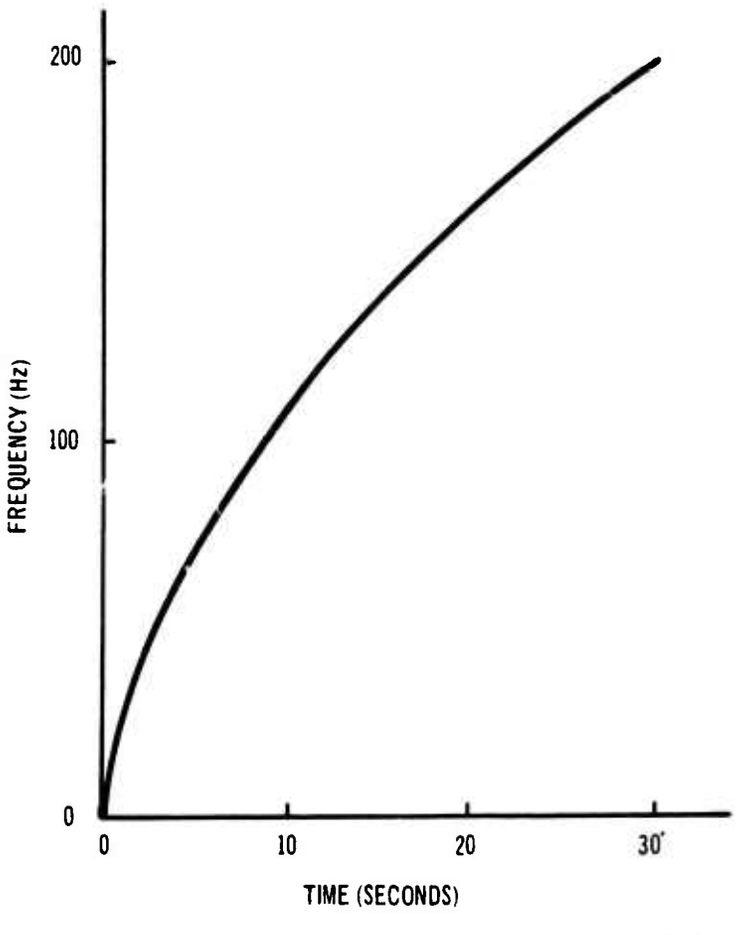

Figure 3. Variation of Switch Operating Frequencies As Function of Time

Properly synchronized input signals to the 400-ampere power switches are supplied by the Lear Siegler logic system. The signal level to the switches is specified as 5 volts minimum for an "on" current of 10 milliamperes. The switches are on for one-third of the period and off for two-thirds; they must be capable of DC operation for 0.3 second at the initiation of operation and capable of operating at 200 hertz at the end of an operating cycle.

2. CIRCUIT CONSIDERATIONS

The circuit used in each switch is similar to a quasi-complementary audio-amplifier output stage in which high-current pnp action is required. An output stage of this type is shown in Figure 4; it makes use of a pnp and npn Darlington-configured output to simulate the action of a high-current, high-gain, pnp transistor. The switch circuit makes use of the recently developed transistor type 2N5575, a 70-ampere, 60-volt, npn, silicon transistor. The 400-ampere current level is achieved by paralleling the 2N5575 transistor chips. Because the transistor chips are matched electrically, current sharing is assured.

The general configuration of the switches was made as symmetrical as possible to keep the losses and operation of each switch as similar as possible. Both positive and negative switches may be divided into three sections: a predriver, a Darlington driver, and a Darlington output. Dissipation was kept at a minimum by designing so that all transistors are on during the one-third period when the switch is on and off during the two-thirds period when the switch is off. Each switch has a resistive-divider network at the input, which reduces the "off" signal level presented to the input transistor and ensures that the switch remains off with a maximum "off" input level as high as 0.3 volt. Some additional noise immunity also is provided, because the switches are packed very closely.

A secondary supply is used to minimize both driver-level variations due to power-supply variations and noise at the input generated by the operation of the other switches. If a single supply was used, the resistors and transistors would suffer excess dissipation with a high supply voltage, because the circuit operates at low supply voltages. The secondary supply

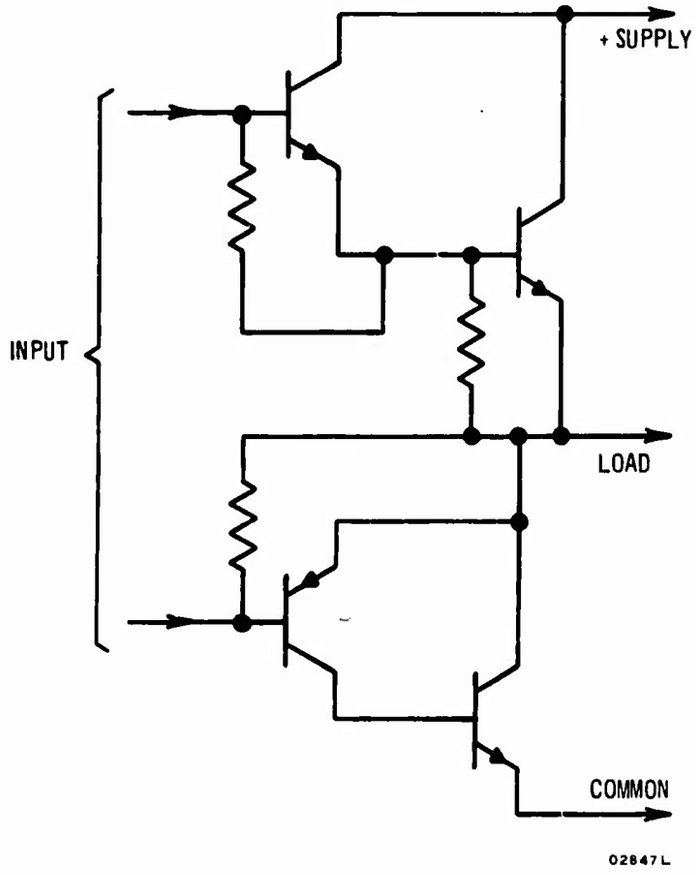

Figure 4. Quasi-Complementary Output Stage

also permits isolation of low-level circuits from transients that accompany the main supply voltage. For reliable operation, a regulated 10-volt supply, accurate to ±10 percent, is used as the secondary supply. Secondary supply current varies with system conditions; nominal current is about 10 amperes, worst-case current is 16 amperes. Supply current is drawn only when a switch is on. Because three switches are on during one-third of each period, current drawn from the secondary supply remains reasonably constant. Another design constraint dictates that an 80-volt transient be sustained for certain time periods. This requirement is met by ensuring that the V_{CER} of the output and driver transistors is above the 80-volt level. While fulfillment of this requirement necessitates a premium voltage as well as a high current selection, it is important to reduce heat during the off period by preventing the transistors from being driven into the sustaining breakdown region.

3. POSITIVE-SWITCH DESIGN

The positive switch shown in Figure 5 was designed with a pnp predriver direct-coupled to an npn Darlington-driver pair, which, in turn, are direct-coupled to a pnp and npn quasi-Darlington output stage. The circuit makes use of direct coupling because it is a system requirement and because it minimizes phase-shift and switching problems. Hybrid construction problems also are reduced, because capacitors are eliminated. The pnp and npn quasi-Darlington output of the switches has been used in high-quality, high-power audio amplifiers with excellent reliability. The five-transistor stages can provide a minimum current gain of 720,000.

A third supply capable of providing reverse bias for "turn-off drive" was not available for use in this application. This additional design constraint dictated the use of medium-frequency transistors throughout the switch except for the paralleled output transistors. Because of the high second-breakdown capability of the hometaxial (single-diffused) transistor structure, it was decided to use this type of transistor in the output stage as an additional precaution in handling the high currents. Hometaxial construction produces a rugged, low-frequency device; its use as the output transistor makes it the only limiting device in determining the switching speed.

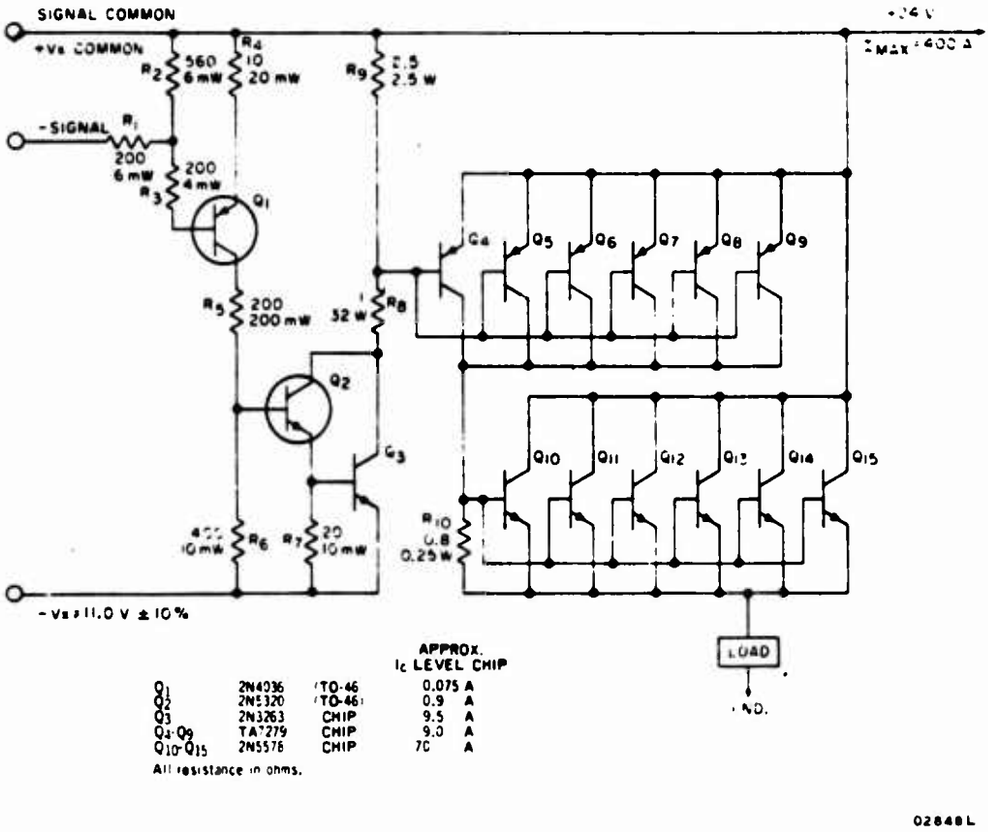

Figure 5. Positive Switch, Schematic Diagram

Resistors connect the base of each transistor stage to the appropriate emitter and provide a turn-off current path and a shunt path for leakage currents. This shunt path prevents the switch from being turned on by the leakage currents even at elevated temperatures.

4. CHIP PARALLELING

To meet the 400-ampere requirement, the output Darlington in the positive-switch circuit is constructed of six parallel RCA Dev. Type TA7279 transistors that drive six parallel 2N5575 transistors. The TA7279 transistors are 8-ampere pnp types; the 2N5575 transistors are 70-ampere npn types. To parallel transistors and at the same time assure good current sharing requires either matching to tight limits or using some additional external components such as ballast resistors. Because of space and power-dissipation limitations of the 400-ampere switch design, a matched chip was chosen even though it required extra testing and parts grouping. The transistors in each set are grouped tightly for V_{BE} and $V_{CE}(sat)$ at their highest operating-current level; in addition, at the high current levels used in this circuit, there is a self-compensation effect that aids sharing. The V_{BE} for a given collector current increases with temperature at high current levels, instead of decreasing with temperature as it does at low current levels. The current level in the output transistor is high enough so that this effect may be used to improve the degree of sharing. At the current level involved, any transistor carrying more than its share of current will heat rapidly and thereby increase the V_{BE} required to sustain its current. Because all of the transistors are operated in parallel, this action, in effect, will increase the V_{BE} applied to the other transistors and force them to carry more of the current.

The thick-film power resistors on alumina substrate are bonded to the heat sinks and are designed with a maximum power density of 100 watts per square inch. This power density was determined from thermal-resistance measurements and by the thick-film vendor's recommendation of a 150°C maximum operating temperature. Temperature coefficients of various resistor materials were taken into account in the circuit design.

5. NEGATIVE SWITCH

The negative switch shown in Figure 6, which was designed in the same manner as the positive switch, acts like a high-gain, high-current, npn transistor. It consists of an npn input transistor and a pnp Darlington-pair driver stage with two RCA Dev Type TA7279 chips paralleled to handle the driver output current level. The output Darlington stage consists of three paralleled 2N3265 20-ampere npn chips driving six paralleled 2N5575 70-ampere npn transistors.

6. CALCULATIONS

Both positive and negative switches were designed with the aid of a computer and a simple transistor model to minimize routine calculations in evaluating component changes and device-characteristic variations. Because components and devices were to be used in a saturated switching application, only h_{FE}, leakage currents, V_{BE}, and $V_{CE}(sat)$ were used. By tabulating variations in these parameters and using the information in a subroutine, the effects on switch operation of variations in component and device parameters were predicted quickly. Working breadboards of both positive and negative switch circuits were built and were checked out before complete module fabrication was begun.

C. SWITCH-MODULE PERFORMANCE

RCA delivered switch modules to Lear Siegler as follows: November 1968, modules 8, 11, 16, 51, 52, and 71; January 1969, modules 50 and 62; 5 February 1969, modules 70, 11 (repaired), and 71 (repaired); 18 February 1969, modules 6, 12, 19, 64, 65, and 100. Power-test data for these modules are shown in Table I, which also identifies each module as a positive switch (+) or a negative switch (-).

Modules 11, 16, and 71 were returned to RCA for analysis and repair. The power resistors were replaced in modules 11 and 71, and the modules were reshipped to Lear Siegler. It was found that module 16 could not be repaired; therefore, it was scrapped (see Monthly Technical Report 16 dated February 7, 1969).

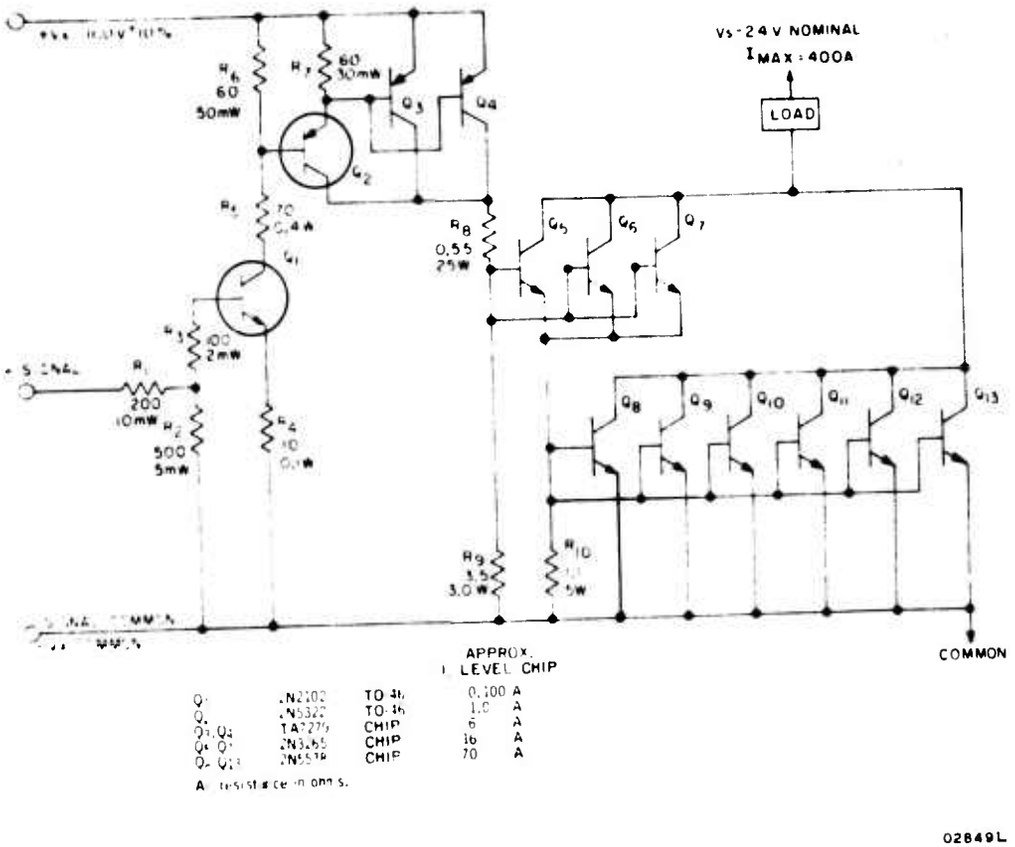

Figure 6. Negative Switch, Schematic Diagram

TABLE I. SWITCH MODULES, POWER-TEST DATA

Module	Polarity (+)	Polarity (-)	Functioning Output Transistors	Functioning Driver Transistors	Power Test Data: Current (A)	Power Test Data: Duty Cycle (%)	Power Test Data: Time (Minutes)
6	✓		6	7	400	10	1
8	✓		6	6	300	10	1
11 (before repair)	✓		6	5	200	10	1
11 (after repair)	✓		6	5	200	10	1
12	✓		6	6	400	10	0.5
16	✓		6	5	300	10	1
19	✓		6	7	400	10	1
50*		✓	5	3	250	10	1
51		✓	6	3	400	10	1
52		✓	6	3	400	10	1
62*		✓	6	3	250	10	1
64		✓	6	3	400	10	1
65		✓	6	3	400	10	1
70		✓	6	3	400	10	1
71 (before repair)		✓	6	3	400	10	1
71 (after repair)		✓	6	3	400	10	0.5
100	✓		5	7	300	10	1

*Modules 50 and 62 were subjected also to a short test at 400 amperes.

A "perfect" positive switch contained six functioning driver transistors and six output transistors. A "perfect" negative switch contained three drivers transistors and six output transistors. An additional driver building block was incorporated into positive modules 6, 12, 19, and 100.

In addition to the power-test data shown in Table I, the following measured values were typical for the switch modules:

a. Switching at 400 amperes: storage time, 10 microseconds; fall time, 12 microseconds

b. V_{CE}(sat): 3 volts at 400 amperes

c. Output-circuit leakage current: less than 20 milliamperes at 80 volts

D. DESIGN FABRICATION

1. MODULE HEAT SINK

After exploring a number of possible configurations and materials, aluminum was chosen as the optimum material for the module heat sink. Machinability provided to be an important factor, because close packing was necessary. Under the design limits imposed, a wedge-shaped heat sink (Figure 7) provided the best combination of compactness, heat absorption, symmetrical thermal response, and maximum internal mounting surface for the components.

2. BUILDING-BLOCK CONCEPT

It was planned originally to attach the semiconductor chips directly to the molybdenum and beryllia pads, which were prebrazed to the module heat sink. Although several early negative switches were made successfully in this manner, in-process yields (especially of the positive switch) led to the building-block concept. This concept was used to make all positive switches and most of the negative switches.

Building blocks are complete functioning transistors on the smallest possible substrate that is compatible with chip size, terminal pins, and

02838P

Figure 7. Module Heat Sink

thermal-resistance needs. These building blocks are not hermetic, but they have a protective resin on the chip. Dual-purpose terminal pins are used for clip-mounting the chip to the substrate and for module circuit-interconnect terminals. Grounded-collector building blocks use a copper or molybdenum substrate with emitter and base pins brazed to ceramic buttons for isolation. Isolated-collector building blocks use alumina or beryllia, depending upon the power requirement.

The building block approach has the following basic features:

a. All building blocks are processed optimally and independently of the common module substrate.

b. All building blocks are tested individually before attachment to the modules to minimize rejects.

c. Units can be matched closely, both electrically and for paralleling requirements.

d. An inventory of building blocks can be established, simplifying logistics and reducing lead time for both assembly and new designs.

e. Building blocks solve the assembly problem of chips with different metallurgical mounting systems, such as gold for some chips and solder on nickel plate for other chips.

Building blocks have an advantage under the following conditions:

a. The yield per chip factored by the number of chips indicates an uneconomic composite yield.

b. Close electrical matching is needed.

c. Removal or repair is needed.

3. OUTPUT-TRANSISTOR BUILDING BLOCKS

Only a limited fraction of the standard 2N5775 population met the module needs. Chips were screened for 80-volt V_{CER} minimum and were pulse

tested at 70 amperes for beta, V_{BE}, and V_{CE}. After device chips have been mounted to a special molybdenum-on-copper building block and have undergone surface treatment, they are retested for the original parameters plus an additional key power-transistor test, the power-rating test (PRT). During this test, the device is pulsed with a voltage-current product that takes the device to safe-area-of-operation limits. This screening test, which was developed for the standard power-device line and extended to include high-power building blocks, has correlated very well with module performance. Units passing these postmount tests are encapsulated and are inventoried in V_{BE} groups for module assembly. Units needing further processing are recycled until they are satisfactory for encapsulation or are scrapped. An output-unit building block is shown in Figure 8.

4. DRIVER TRANSISTOR

The same basic process is used for the driver and the output transistor building blocks, but different substrates are used for isolation and for minimum use of real estate. A grounded-collector 2N3265 20-ampere npn driver is shown in Figure 9. An isolated-collector TA7279 8-ampere pnp driver is shown in Figure 10.

5. TRANSISTOR ASSEMBLY

After the output and driver transistor building blocks have been attached to the main module heat sink by a high-tin-content solder, they are given another electrical check before they are interconnected. The yield at this point has been very high; however, a decision can be made whether to replace a defective building block or simply not to interconnect it. A U-shaped copper emitter-interconnect strap, which is soldered to the six emitter connectors, carries the 400-ampere current to the external terminal lug with negligible losses. The 400-ampere collector current is carried by the body of the switch. The exterior of the module is isolated doubly by anodizing and epoxy coating. Except for the output stage, most of the interconnect ribbons are welded to the flat tops of the terminal pins on the building blocks.

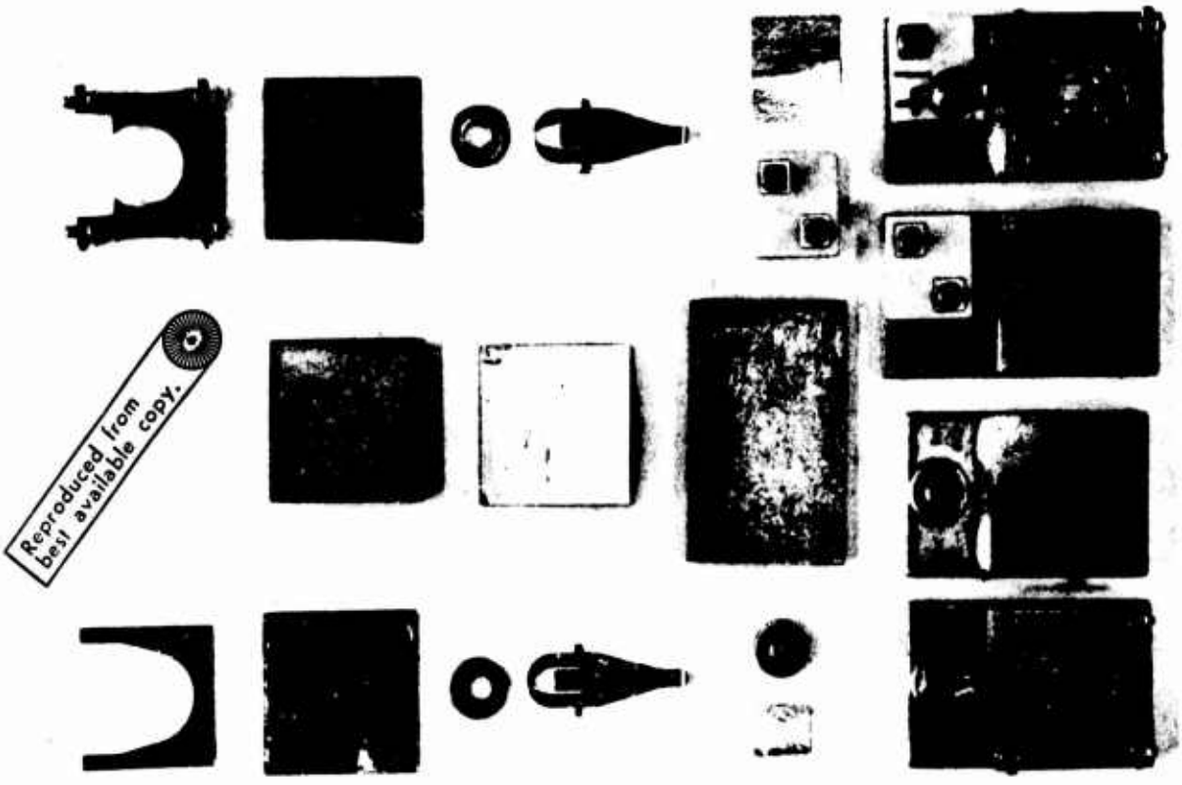

02839P

Figure 8. Output-Transistor Building Block and Component Parts

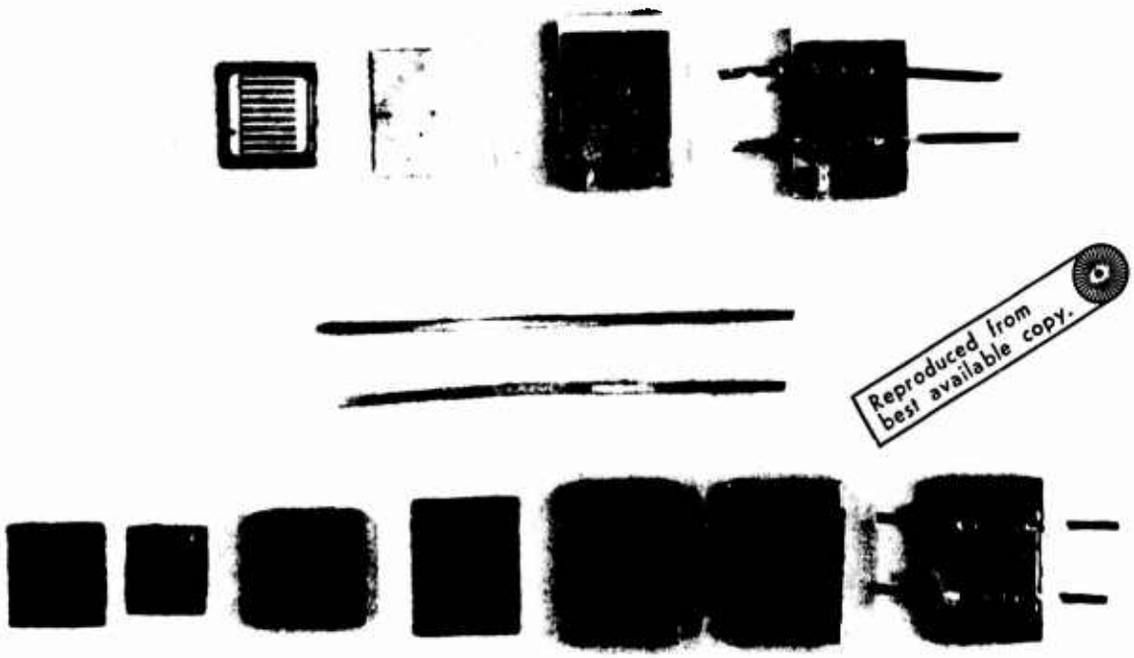

02840P

Figure 9. 2N3265 Chip Building Blocks, Isolated (Upper) and Grounded (Lower) Versions

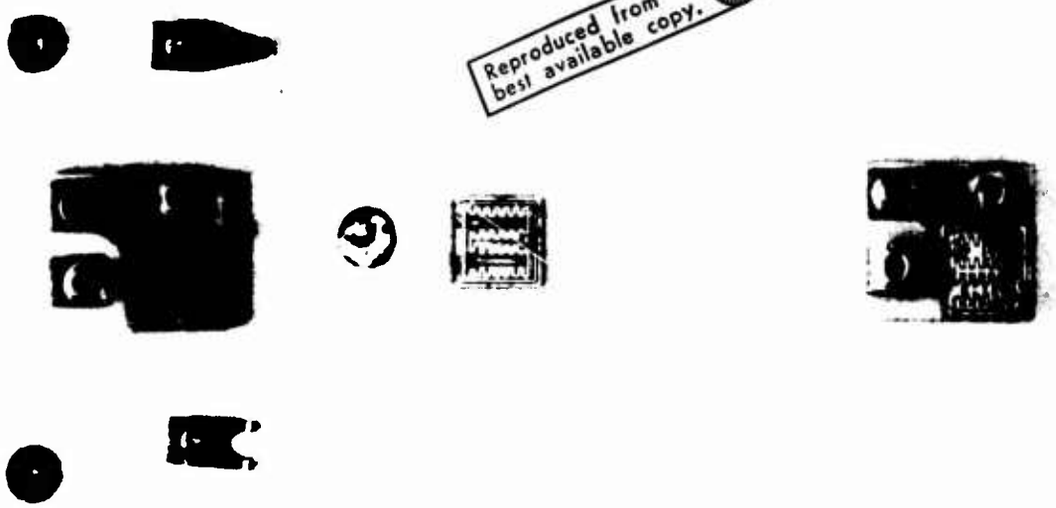

02841P

Figure 10. Isolated Collector TA7279 PNP Building Block

6. EVALUATION OF RESISTOR NETWORK AND POWER RESISTOR

Thick-film resistors on alumina were checked on a 100-percent basis for resistance and were checked on a sampling basis, on separate test substrates, for power-handling capability. Resistor substrates then were attached to the heat sink with a highly filled epoxy and were interconnected into the switch circuit. The two input transistors were fabricated in TO-46 packages and were soldered to the input resistor-conductor substrate.

Power resistors and input network subassemblies are shown in Figure 11. The space required for these small units in the power module was relatively insignificant and allowed focusing development effort on the power chip building blocks.

7. SWITCH MODULE ASSEMBLY

A fully assembled switch module is shown in Figure 12. The philosophy used in assembly was to ensure that only good transistor chips were made into building blocks and that only good building blocks were attached to the module heat sink and interconnected.

After completing the interconnects and applying a final resin coating, the module is checked electrically. An anodized cap is attached, and electrical performance is rechecked.

Except for the output stage, most of the interconnect ribbons are welded to the flat tops of the terminal pins on the building blocks.

E. ELECTRICAL TESTS

Typical test results for a positive switch are described in subsequent paragraphs. Test results for a negative switch are similar, but lower values of $V_{CE}(on)$ were obtained.

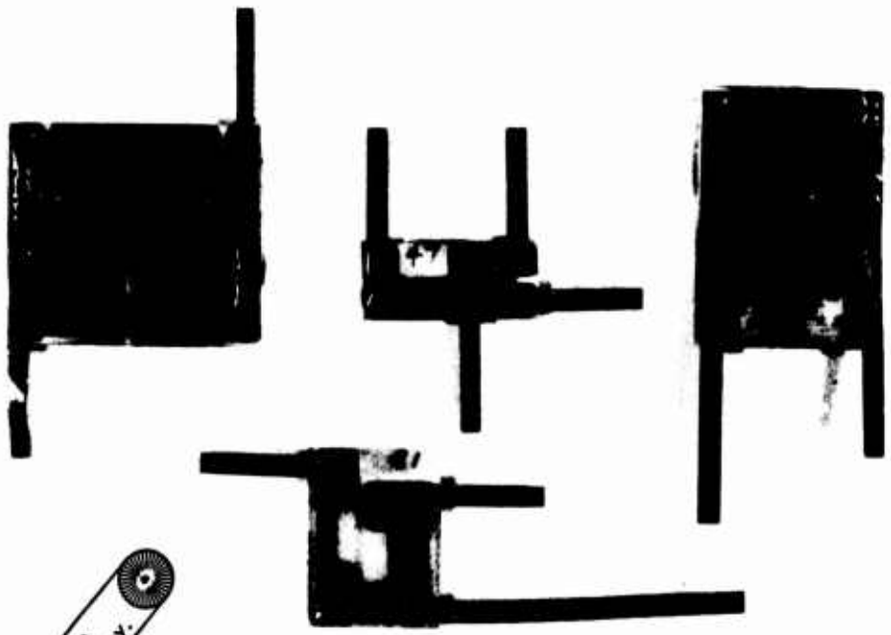

QA. THICK-FILM POWER RESISTORS ON ALUMINA

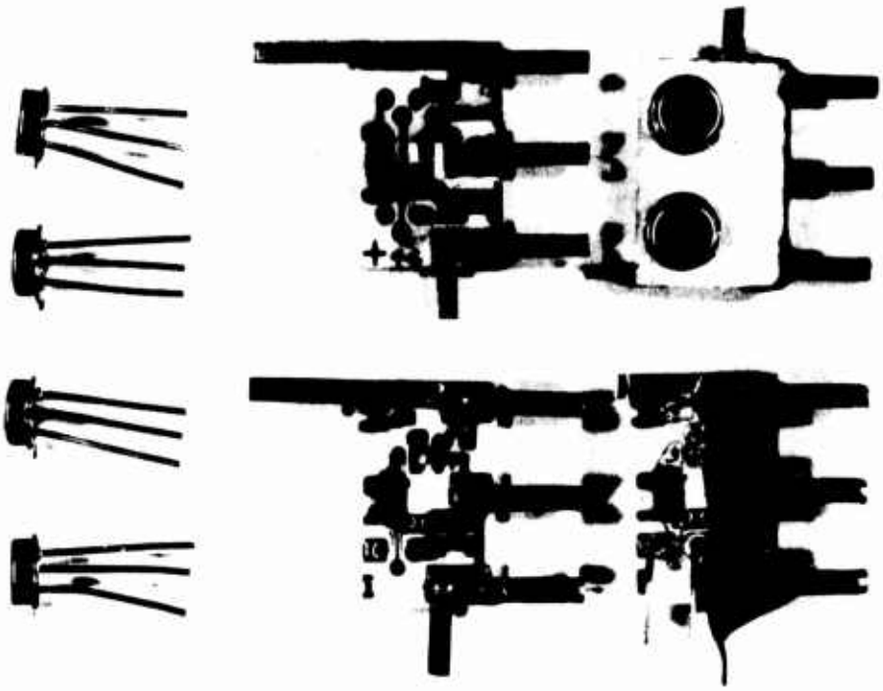

B. INPUT NETWORK AND INPUT-STAGE TRANSISTORS IN TO-46 PACKAGE

02842P

Figure 11. Power Resistors and Input Network Subassemblies

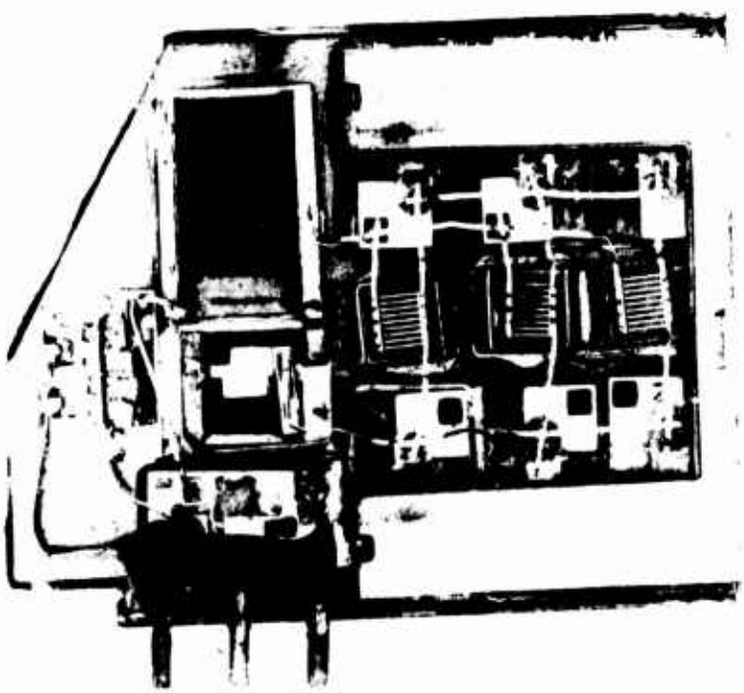

02843P

Figure 12. Fully Assembled Module

The leakage of the switch is about 20 milliamperes at 100°C and with 100 volts across the output terminals. The leakage is about 0.02 milliampere across the drive supply terminals at 100°C and with 20 volts supplied. This leakage represents an "off" dissipation of about 0.4 watt, which meets the design goal of low "off" dissipation. These leakages were measured with the input terminals open. Figure 13 shows waveforms of $V_{CE}(on)$ and I_c during an "on" pulse. The I_c is 400 amperes near the end of the pulse, and $V_{CE}(on)$ is 3.1 volts. These values indicate a peak module dissipation of 1240 watts during the "on" cycle; average power dissipation would be 410 watts on the basis of a one-third duty cycle. The waveforms in Figure 13 were obtained at shorter duty cycles so that the equipment could be adjusted during long-term operation. These switches were tested also, for short periods, at a one-third duty cycle. Values of voltage and current were obtained under conditions similar to those described for thermal analysis, Paragraph II.E. The value of $V_{CE}(on)$ obtained is the value that would be expected with the output Darlington chips sharing current equally.

Switching times were well within the design goals, even without reverse or turnoff drive. The waveforms of Figure 14, which were obtained with the oscilloscope triggered by the trailing edge of the input pulse, show storage and fall times of 10 microseconds and 16 microseconds, respectively. Because switching dissipation losses are a function of switching time, these reasonably short switching times help to minimize dissipation and heating. The waveform of Figure 15 shows the load current rise time, which depends upon circuit inductance. Because circuit inductance limits current rise time, dissipation due to the turn-on time of the switch can be neglected. These acceptable switching speeds confirmed the original design philosophy: using medium-frequency transistors in the lower level stages in which second-breakdown problems would be minimal; and using slower, more rugged, wide-basewidth hometaxial devices only in the output stage. Total switching time is virtually the same as that of the output chips and is well within the design goals.

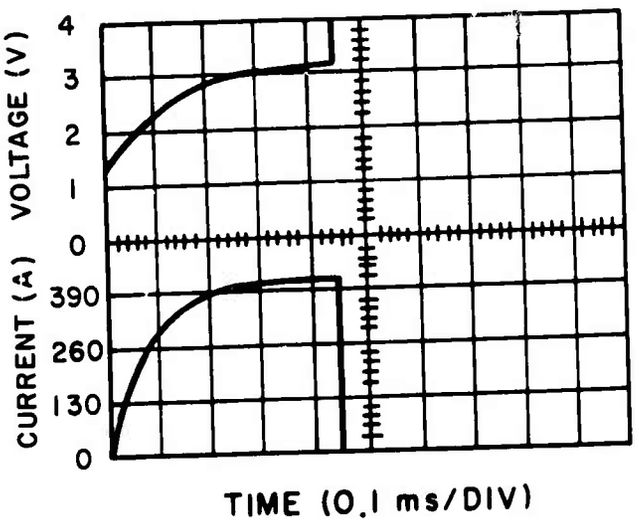

Figure 13. $V_{CE(on)}$ and I_C During "On" Pulse

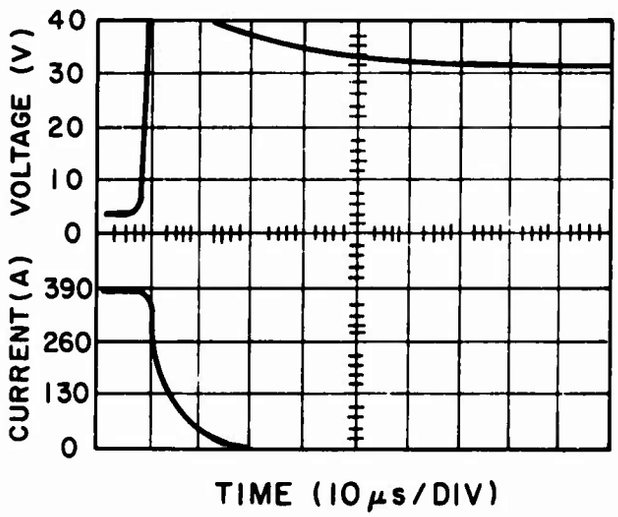

.02845L

Figure 14. Storage and Fall Times for Typical Switch Module

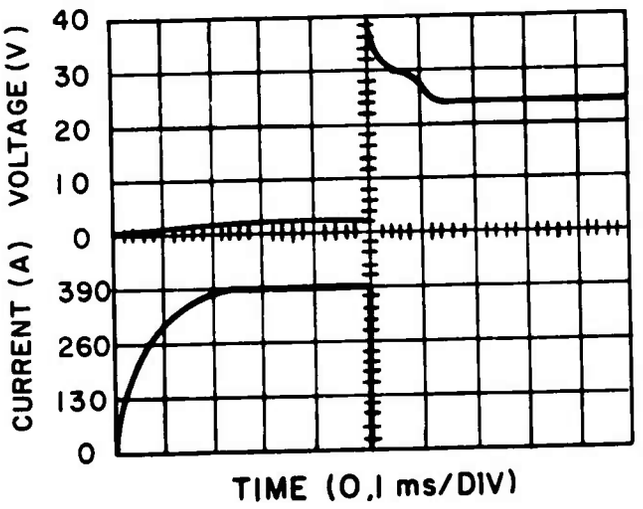

Figure 15. Rise Time of Current in Switch

944

F. THERMAL TESTS

The heat sinks of individual switch modules have the maximum allowable mass of aluminum. Most of the heat energy is absorbed by individual module heat sinks, with only a small amount of heat transferred to the retainer ring and from switch to switch. Although all switches were monitored for unusually high temperatures and for temperature rises during high-current testing, positive switch module 12 was subjected to a special thermal test. The switch was encapsulated but was not capped, and the module was tested while it was resting upon a thermally insulated surface. The conditions of the test were as follows:

a. I_c = 300 amperes

b. $V_{CE}(on)$ = 3.0 volts

c. On time = 1.7 milliseconds

d. Duty cycle = one-third (5-millisecond repetition rate)

Temperature probes were placed at three points on the module: on the emitter strap, directly above the output chip; on the copper plate, near the molybdenum block; and on the aluminum heat sink, near the copper plate. Temperatures initially and after 15 and 30 seconds of operation are shown in Table II.

TABLE II. SPECIAL THERMAL TEST RESULTS

Probe Location	Temperature (^{o}C) 0 Seconds	15 Seconds	30 Seconds
Emitter strap	32	76	113
Copper plate	32	70	105
Aluminum heat sink	32	67	103

The amount of heat energy (HE) in joules dissipated during this test is the product of power in watts and the time, 30 seconds. Dissipated power is

the sum of the saturation losses and the bias supply dissipation. Total heat energy dissipated during the test cycle, therefore, is as follows:

$$HE = \left[\frac{(300 \times 3) + (10 \times 10)}{3}\right] \times 30 \text{ joules} = 10{,}000 \text{ joules}$$

The average energy dissipated by the switches in the modules is 400 amperes x 3.0 volts x 20 seconds = 8650 joules. The dissipation during the special thermal test was slightly more severe than the average switch module dissipation.

Values of thermal resistance, thermal capacitance, and thermal time constant were calculated for the output-chip mounting. The values are shown in Table III.

TABLE III. CALCULATED THERMAL VALUES FOR OUTPUT-CHIP MOUNTING

Part	Thermal Resistance ($^{o}C/W$)	Thermal Capacitance (Joules/^{o}C)	Thermal Time Constant (ms)
Silicon chip	2.88×10^{-2}	2.5×10^{-3}	0.072
Lead solder	2.14×10^{-2}	3.5×10^{-3}	0.074
Molybdenum block	1.5×10^{-1}	2.9×10^{-1}	43.0
Copper plate	2.2×10^{-2}	4.1×10^{-1}	9.0
Aluminum heat sink (region adjacent to device)	1.05×10^{-1}	2.06	210.0

Instantaneous power per output chip is

$$P_{instant} = \frac{300 \times 3}{6} = 150 \text{ watts}$$

Average power is one-third of the instantaneous power or 50 watts.

Because the thermal time constants of the silicon chip and the lead solder are shorter than the "on" pulse, values of instantaneous power will be used

to calculate chip temperature. Because the thermal time constant of the molybdenum block is longer than the period of the "on" pulse, values of average power will be used. Chip temperature, therefore, is

$$T_{junction}(peak) = P_{instant}\ (\theta_{Si} + \theta_{Pb}) + P(av)\ (\theta_{Mo}) + T_{Cu}$$

$$= 150\ (0.03 + 0.02) + 50\ (0.15) + 113$$

$$= 128^{o}C$$

where

θ_{Si} = thermal resistance of silicon

θ_{Pb} = thermal resistance of lead

θ_{Mo} = thermal resistance of molybdenum

If the heat sink had been at the worst-case ambient of $52^{o}C$, instantaneous peak temperature would have been $20^{o}C$ higher or $148^{o}C$. This temperature is a safe operating junction temperature; therefore, one operating cycle appeared feasible.

SECTION III
CONCLUSIONS

The work performed on this program demonstrated that a lightweight, compact hybrid switch can be built that is capable of switching 400 amperes with good switching speed and with a blocking voltage of 80 volts. Parallel output and driver stages combined with the building-block concept provide a reasonable fabrication approach. Thermal analysis and measured data indicate that heat sinking and heat removal must be improved to provide a full three-start capability.

SECTION IV
RECOMMENDATIONS

RCA has invested substantial engineering effort over the past several years in the design and development of high-power hybrid modules. Based upon this effort and the experience gained while working on these switches and upon a better understanding of the electrical and thermal behaviors of these modules and components, RCA has proposed to Lear Siegler a new module design that will satisfy fully the requirement for three consecutive starts and will provide a more suitable design for economic manufacture.

The proposed design has eight output-transistor chips, instead of six chips, and has power-sharing diodes in series with the output collectors. These additional components will reduce the dissipation in each output transistor by more than 50 percent. These two changes are the major changes necessary to obtain three-start capability.

Additional clearances between the building blocks in the module and an improved interconnect scheme will make the modules easier to assemble and repair, thus leading to a minimum number of rejects. This new arrangement, however, requires additional volume. The proposed design also makes maximum use of parts that are common to RCA commercial power hybrid module programs. Use of these parts will lead to lower costs due to purchasing savings at the higher volume.

In summary, the experience gained in making the present modules has enabled RCA to project a second-generation design of considerably improved performance. The major improvements are as follows: two additional output chips; incorporation of power-sharing diodes; and a building block layout and an interconnect arrangement that are more suitable for manufacture.

8.4 BIBLIOGRAPHY

"Principles of Inverter Circuits", B. D. Bedford & Hoft, R. G., New York, John Wiley & Sons, 1964.

"High Voltage Brushless DC Torpedo Propulsion Motor", V. Janonis, IEEE Transactions, March 1966.

Brushless Starter-Generator Quarterly Reports, #1 through #12, Lear Siegler, Inc., Power Equipment Division, Cleveland, Ohio

"The Fundamental Theory of Arc Converters", Kissik, London Chapman & Hall, Ltd., 1939.

"Rectifier Circuits" by Johannes Schaefer, New York, John Wiley & Sons, 1965.